

DESIGN ISSUES IN THE STANCE PHASE  
CONTROL OF ABOVE-KNEE PROSTHESES

by

Jeffrey Llevret Stein

B.S. University of Massachusetts  
(1973)

S.B. Massachusetts Institute of Technology  
(1976)

S.M. Massachusetts Institute of Technology  
(1976)

Submitted to the Department of Mechanical Engineering  
in partial fulfillment of the requirements for the degree of

Doctor of Philosophy

at the

Massachusetts Institute of Technology

January 1983

Copyright Massachusetts Institute of Technology

Signature of Author Jeffrey Llevret Stein  
Department of Mechanical Engineering  
January 7, 1983

Certified by Woodie C. Flowers  
Professor Woodie C. Flowers  
Thesis Supervisor

Accepted by \_\_\_\_\_  
Chairman, Department Committee  
on Graduate Studies

-2-

DESIGN ISSUES IN THE STANCE PHASE CONTROL OF  
ABOVE-KNEE PROSTHESES

by

JEFFREY L. STEIN

Submitted to the Department of Mechanical Engineering  
on January 7, 1983, in partial fulfillment of the  
requirements for the Degree of Doctor of Philosophy in  
Mechanical Engineering

ABSTRACT

Improving the mobility of above-knee (A/K) amputees requires improving the performance of currently available prostheses. The determination of the design and control issues affecting the mechanics of the A/K amputee gait during the stance phase of level walking is the focus of this thesis.

The three-dimensional gait mechanics, which are presented in terms of the kinematics and dynamics of the leg segments in the sagittal plane on the prosthetic side were measured under two stance phase conditions. In the first set of trials, the amputee used a prosthesis with a conventional knee controller that allowed the amputee to keep the knee joint in full extension during the stance phase. In the second set of trials, the prosthetic knee during stance echoed the modified kinematics of the amputee's sound (intact) knee that had been recorded during the previous sound stance phase.

All trials were conducted on a laboratory restricted, person-interactive, computer controlled, prosthesis simulator system. The global kinematics of the prosthesis were recorded by a Selspot system which measured the three-dimensional position of infrared emitting diodes attached to the prosthesis. The foot/floor interaction forces were measured with a forceplate.

Analysis and interpretation of the data was augmented by developing simplified two-dimensional kinematic and dynamic designer gait models. Major results include: 1) providing normal knee kinematics to the prosthesis does not produce normal hip displacements (i.e. eliminate vaulting) but does reduce the amount of work done by the hip; 2) SACH foot design strongly affects the mechanics of gait; 3) knee controller design and SACH foot design are mutually interdependent; 4) hip torque is not responsible for propulsion; 5) designer gait modeling and simulation is a very valuable additional tool to the prosthesis designer.

Thesis Supervisor: Woodie C. Flowers  
Title: Professor of Mechanical Engineering

-3-

Doctoral Committee

Dr. Woodie C. Flowers (Chairman)  
Associate Professor of Mechanical Engineering  
MIT

Dr. Neville Hogan  
Assistant Professor of Mechanical Engineering  
MIT

Dr. Robert W. Mann  
Whitaker Professor of Biomedical Engineering and  
Professor of Mechanical Engineering  
MIT

Dr. Henry M. Paynter  
Professor of Mechanical Engineering  
MIT

## Acknowledgements

Thomas Edison must have had graduate life at MIT in mind when he described creativity as 1% inspiration, 99% perspiration. Fortunately, during my eight and one-half year tenure, I met many people who helped me wipe my brow while guiding my search for inspiration.

To my thesis supervisor, Professor Woodie Flowers, who provided unending intellectual, moral and financial support, there is no thank you that is adequate. I can only hope that I have as much to offer my students.

To my thesis committee member, Professor Neville Hogan, an extended thank you for responding far beyond the call of duty. Our start-in-the-afternoon-end-in-the-very-late-evening meetings were as helpful as they were unbelievable. Your intellectual leadership and moral support will always be appreciated.

To my other thesis committee members, Professors Robert Mann and Hank Paynter, an appreciative thank you for your interest and insights that kept me from spending even more years at MIT.

To Steve Cornell, for being a cooperative and tireless subject in all the locomotion trials, a warm thanks.

To Mark Marich, prosthetist, Children's Hospital, thank you for providing a willing clinical ear.

I would also like to thank:

Professor Warren Rohsenow for opening the door for me eight and one-half years ago.

Doctors Joe Mansour and Shelly Simon of the Children's Hospital Gait Lab for providing the initial gait data that got this whole thesis started in its final direction.

Roger McCarthy for making the Qualifying Exams seem relatively easy after his rehearsal sessions for the orals.

Pat Tan for making footswitches that worked!

Zvi Ladin for his many perceptive questions and friendship.

Cary Abul-Haj for providing never ending entertainment on the mezzanine.

Bill Murray for providing insights into microprocessor applications and hockey subtleties.

Knee Group Members Chris Cullen, Ed Glassman, Paul Tyra, Mike Shepley, Don Grimes and G.P. Lavoie for providing good friendship, good knee talk and good group spirit.

Katja Mamalakis, for pushing the cart with a smile.

Laboratory director, Maureen Hayes, for being there in the right way at the right time.

The countless other people around the large lab and in the Department whom I have met in the last eight and one-half years. It is you who provided the needed perspective on the MIT experience.

Finally and clearly no lastly, to Karen, for surviving the last year of this work. And to my entire family, who have always been a bottomless source of love and support.

This research was performed in the Eric P and Evelyn E. Newman Laboratory for Biomechanics and Human Rehabilitation and funded by NSF Grant Number ECS-8023193 and a DuPont University Science and Engineering Grant.

Dedication

The thesis is dedicated to my father,

Lloyd E. Stein





II-4	Dynamic Designer Gait Models.....	56
II-4.1	Introduction.....	56
II-4.2	Dynamic Designer Gait Models.....	61
Chapter III -	Experiment Work.....	63
III-1	Introduction.....	63
III-2	Person-Interactive Prosthesis Simulation.....	63
III-2.1	Introduction.....	63
III-2.2	The Electrohydraulic Simulator System.....	64
III-2.3	Implementation of Control Strategies.....	67
III-3	Telemetered Real-time ACquisition of Kinematics.....	71
	(TRACK)	
III-3.1	Introduction.....	71
III-3.2	Measuring the Three-Dimensional Kinematics....	71
III-3.3	Measuring the Foot/Floor Interaction Forces...	74
III-4	Data Acquisition.....	76
III-4.1	General Requirements and Implementation.....	76
III-5	Data Processing.....	79
III-5.1	General Requirements.....	79
III-5.2	Digital Filtering.....	80
III-6	Calibration.....	82
III-6.1	General Requirements.....	82
III-6.2	Electrohydraulic Simulator System	
	Calibration.....	82
III-6.3	Overall System Accuracy - Confidence Limits...	87
III-7	Procedures.....	88
III-8	Subject.....	89
Chapter IV -	Results.....	90
IV-1	Data Format.....	90
IV-2	Kinematics.....	92
IV-2.1	Overall Kinematics.....	92
IV-2.2	Prosthetic Knee Angle.....	92
IV-2.3	Prosthetic Shank Angle.....	97
IV-2.4	Foot Placement Timing.....	101
IV-2.5	Center of Pressure.....	106

- IV-2.6 Thigh (socket) Angle.....110
- IV-2.7 Hip Displacement.....113
  - IV-2.7.1 Forward Displacement.....113
  - IV-2.7.2 Vertical Displacement.....116
- IV-2.8 Hip Velocity.....125
  - IV-2.8.1 Forward Velocity.....125
  - IV-2.8.2 Vertical Velocity.....127
- IV-2.9 Kinematics Summary.....129
- IV-3 Dynamics and Power.....130
  - IV-3.1 Prosthetic Knee Torque and Power.....130
  - IV-3.2 Hip Torque and Power.....138
  - IV-3.3 Foot/Floor Reaction Forces.....143
    - IV-3.3.1 Vertical Reaction Force.....143
    - IV-3.3.2 Anterior/Posterior Reaction Force....146
  - IV-3.4 Stump Loading.....150
  - IV-3.5 Sound Leg Forces.....153
    - IV-3.5.1 Vertical Sound Leg Forces.....153
    - IV-3.5.2 Anterior/Posterior Sound Leg Forces..155
- Chapter V - Interpretive Gait Modeling and Simulation.....158
  - V-1 Introduction.....158
  - V-2 Role of SACH Foot.....159
    - V-2.1 Kinematics of Prosthetic Heel Roll.....160
    - V-2.2 Rigid Model of SACH Foot.....162
    - V-2.3 SACH Foot Heel Stiffness.....166
  - V-3 Dynamic Simulation of Gait.....169
    - V-3.1 Introduction.....169
    - V-3.2 Dynamic Simulation of Heel Compression.....171
    - V-3.3 Dynamic Simulation of the Prosthetic Stance Phase - Latching Spring Model.....177
      - V-3.3.1 Results Simulation.....181
  - V-4 Propulsion.....185
    - V-4.1 Introduction.....185
    - V-4.2 Propulsion Tests and Results.....185

Chapter VI - Conclusions.....	189
VI-1 Knee Control Versus SACH Foot Design.....	189
VI-2 Person-Interactive Simulation.....	191
VI-3 Hip Torque.....	192
VI-4 Designer Gait Modeling and Simulation.....	192
REFERENCES.....	193
APPENDICES.....	202
APPENDIX 1 - Designer Gait Models.....	202
1.1 Cam geometry of the SACH foot.....	202
1.2 Equations of Motion for Model #1.....	209
1.3 Equations of Motion for Model #2 and Latching Spring Model.....	214
APPENDIX 2 - SACH Foot Heel Testing.....	224
APPENDIX 3 - Inverse Dynamic Model Parameters.....	227
APPENDIX 4 - LED Array.....	229
APPENDIX 5 - Sign Convention of Gait Data.....	231
APPENDIX 6 - Data File Nomenclature.....	233
APPENDIX 7 - Data Acquisition and Processing Parameters.....	234
APPENDIX 8 - Low Pass Filter Program Listing.....	235
APPENDIX 9 - Control and Data Acquisition Program Listing.....	244

## List of Figures

I-1	The Design Approach.....	25
II-1	Sequential Gait Parameters.....	28
II-2	Right Knee Moment, Angle and Power of Four Normal Subjects [10].....	30
II-3	Right Ankle Moment, Angle and Power of Four Normal Subjects [10].....	31
II-4	Right Hip Moment, Angle and Power of Four Normal Subjects [10].....	32
II-5	Typical Above-Knee Prosthesis.....	35
II-6	Stance Stability Resulting from Alignment and Hyper- Extension Stops.....	36
II-7	SACH Foot.....	38
II-8	Knee Parameters. A/K Prosthesis Versus Normal.....	41
II-9	Damping Function.....	46
II-10	Inertia Segments of Amputee/Prosthesis.....	51
II-11	Stump/Socket Interface.....	53
II-12	Model Kinematics and Dynamics.....	57
II-13	Dynamic Estimator Equations.....	58
III-1	Person Interactive Simulator.....	65
III-2	The Electrohydraulic A/K Prosthesis.....	66
III-3	Computer Interface.....	68
III-4	Parameter and Control Events Per Cycle.....	69
III-5	Photograph of Electrohydraulic Prosthesis As Used in This Study.....	73
III-6	Instrumentation and Data Collection.....	75
III-7	The Tool.....	77
III-8	Shank Load Cell and Knee Torque Calibration.....	83
III-9	Heel and Toe Footswitches.....	85

IV-1 A Typical Relative Rotation of the Saggital Plane  
of the Prosthetic Shank With Respect to the  
Plane of Progression. Run JL2024..... 91

IV-2 Joint Trajectories (Straight Knee)..... 93

IV-3 Joint Trajectories (Flexible Knee)..... 94

IV-4 Typical Prosthetic Knee Angle Trajectories  
During Stance. A Comparison of ME vs CL Stance  
Phase Knee Controllers. Run JL1494 vs JL1427..... 95

IV-5 A Sample of Prosthetic Knee Angle Trajectories  
During Stance. A Comparison of ME vs CL Stance  
Phase Knee Controllers..... 96

IV-6 Typical Prosthetic Shank Angle Trajectories  
During Stance. A Comparison of ME vs CL Stance  
Phase Knee Controllers. Run #JL1427 vs JL2022..... 98

IV-7 A Sample of Prosthetic Shank Angle Trajectories  
During Stance. A Comparison of ME vs CL Stance  
Phase Knee Controllers..... 99

IV-8 The Initiation and Termination of the ME Stance  
Phase Controller.....100

IV-9 Typical Timing of Prosthetic and Sound Foot  
Placement During Stance. A Comparison of  
ME vs CL Stance Phase Knee Controllers.  
Run JL1427 vs. JL2022.....102

IV-10 A Sample of Prosthetic Foot Placement Timings  
During Stance. A Comparison of ME vs CL Stance  
Phase Knee Controllers.....103

IV-11 A Sample of Sound Foot Placement Timings During  
Stance. A Comparison of ME vs CL Stance Phase  
Knee Controllers.....104

IV-12 A Typical Prosthetic Footswitch Pattern as a  
Function Shank Angle. A Comparison of ME vs CL  
Stance Phase Knee Controllers. Run #JL1497 vs JL1494.....105

IV-13 A Typical Center of Pressure Trajectory. A  
Comparison of ME vs CL Stance Phase Knee Controllers.  
Run JL1427 vs JL2022.....107

IV-14 A Typical Center of Pressure vs Shank Angle.  
A Comparison of ME vs CL Stance Phase Knee Controllers.  
Run #JL1427 vs JL2022.....108

IV-15	A Sample of Center of Pressure vs Shank Angles. A Comparison of ME vs CL Stance Phase Knee Controllers.....	109
IV-16	Typical Thigh (socket) Angle Trajectories in Stance. A Comparison of ME vs CL Stance Phase Controllers. Run JL2024 vs JE2624.....	111
IV-17	A Sample of Thigh (socket) Angle Trajectories in Stance. A Comparison of ME vs CL Stance Phase Knee Controllers.....	112
IV-18	Typical Forward Hip Displacement Trajectories During Stance. A Comparison of ME vs CL Stance Phase Knee Controllers. Run #JL1427 vs JL2022.....	114
IV-19	A Sample of Forward Hip Displacement Trajectories During Stance. A Comparison of ME vs CL Stance Phase Knee Controllers.....	115
IV-20	Typical Vertical Hip Displacement Trajectories During Stance. A Comparison of ME vs CL Stance Phase Knee Controllers. Run JL1427 vs JL1494.....	117
IV-21	A Sample of Vertical Hip Trajectories During Stance. A Comparison of ME vs CL Stance Phase Knee Controllers.....	118
IV-22	Typical Vertical Displacement of the Prosthetic Knee Joint as a Function of Shank Angle During Stance. A Comparison of ME vs CL Stance Phase Knee Controller. Run #JL1427 vs JL1494.....	121
IV-23	Hip Height Question.....	123
IV-24	Typical Vertical Hip Displacements vs Shank Angle During Stance. A Comparison of ME vs CL Stance Phase Knee Controllers. Run JL1427 vs JL1494.....	124
IV-25	A Sample of Forward Hip Velocities During Stance. A Comparison of ME vs CL Stance Phase Knee Controllers....	126
IV-26	A Sample of Vertical Hip Velocities During Stance. A Comparison of ME vs CL Stance Phase Knee Controllers....	128
IV-27	Typical Prosthetic Knee Torque Trajectories as Measured by TRACK During Stance. A Comparison of ME vs CL Stance Phase Knee Controllers. Run #JL2004 vs JL1494.....	131
IV-28	A Sample of Prosthetic Knee Torque Trajectories as Measured by TRACK During Stance. A Comparison of ME vs CL Stance Phase Knee Controllers.....	132

IV-29 Typical Prosthetic Knee Power Trajectory as Measured by TRACK During Stance. A Comparison of ME vs CL Stance Phase Knee Controllers. Run #JL1497 vs JL1494.....133

IV-30 A Sample of Prosthetic Knee Power Trajectories as Measured by TRACK During Stance. A Comparison of ME vs CL Stance Phase Knee Controllers.....134

IV-31 The Typical Kinematic Relationship That Exists Between Forward Hip, Knee, and Center of Pressure Position During Stance Under CL Control. Run JL2022.....135

IV-32 The Typical Kinematic Relationship That Exists Between Forward Hip, Knee, and Center of Pressure Position During Stance Under ME Control. Run JL2024.....136

IV-33 Typical Hip Torque Profiles on the Prosthetic Side During Stance. A Comparison of ME vs CL Stance Phase Controllers. Run JL1427 vs JL1494.....139

IV-34 A Sample of Hip Torque Profiles on the Prosthetic Side During Stance. A Comparison of ME vs CL Stance Phase Controllers.....140

IV-35 A Sample of Hip Power Profiles on the Prosthetic Side During Stance. A Comparison of ME vs CL Stance Phase Knee Controllers.....141

IV-36 Typical Vertical Foot/floor Reaction Trajectories. A Comparison of ME vs CL Stance Phase Knee Controller. Runs JL1427 vs JL2022.....144

IV-37 A Sample of Vertical Foot/floor Reaction Trajectories. A Comparison of ME vs CL Stance Phase Knee Controllers....145

IV-38 Typical A/P Foot/floor Reaction Trajectories. A Comparison of ME vs CL Stance Phase Knee Controllers. Runs JL1427 vs JL2022.....147

IV-39 A Sample of A/P Reaction Force Trajectories. A Comparison of ME vs CL Stance Phase Knee Controllers.....148

IV-40 Typical Vertical Foot/floor Reaction Forces as a Function of Thigh Angle. A Comparison of ME vs CL Stance Phase Knee Controller. Run JL1427 VS JL2022.....151

IV-41 A Sample of Axial Loads on the Stump at the Knee as a Function of Thigh Angle During Stance. A Comparison of ME vs CL Stance Phase Knee Controllers.....152

IV-42 A Sample of Sound Leg Vertical Forces Applied at the Hip on the Prosthetic Side. A Comparison of ME vs CL Stance Phase Knee Controllers.....154

IV-43 A Sample of Sound Leg A/P Forces Applied at the Hip on the Prosthetic Side. A Comparison of ME vs CL Stance Phase Knee Controllers.....156

V-1 A Typical ELL Trajectory During Stance with a CL Stance Phase Controller. Run #JL1494.....161

V-2 Kinematics of the SACH Foot.....163

V-3 Fitting Three Straight Lines to the Center of Pressure vs Shank Angle Data.....164

V-4 SACH Foot Rigid Cam Profile.....165

V-5 The ELL Versus Shank Angle. A Comparison of the Rigid SACH Foot Model to Data Produced by CL Stance Phase Controller.....167

V-6 Measured SACH Heel Stiffness as a Function of Shank Angle.....168

V-7 Predicted SACH Heel Deflection from Vertical Reaction Load Data as a Function of Shank Angle. Run #JL1494.....170

V-8 Compliant Heel-Pivot Model.....172

V-9 Compliant Heel-Cam Foot Model.....174

V-10 Hip Displacements and Velocities During Heel Compression. A Comparison of Model #2 Versus Data.....176

V-11 Hip Displacements and Velocities During Heel Compression. A Comparison of Model #1 Versus Data.....178

V-12 Heel Compression.....179

V-13 Hip Displacement and Velocities During the Stance Phase of Level Walking with a CL Stance Phase Knee Controller. A Comparison of the Latching Spring Model Versus Data.....182

V-14 Demonstrating the Effect that the Hip Torque and Sound Leg Forces Have on Propulsion.....186

V-15 The Relative Magnitude of the Terms in the Equation of Motion of the Spring Latch Model.....188

A-1.1 Kinematics of The SACH Foot.....203



A-1.2	SACH Foot Kinematics.....	205
A-1.3	Model #1 - Details.....	210
A-1.4	Compliant Inverted Pendulum with Cam.....	216
A-1.5	Rigid Inverted Pendulum with Cam.....	218
A-2.1	SACH Foot Heel Stiffness Testing.....	225
A-4.1	Infra-Red LED Array.....	230
A-5.1	Sign Convention.....	232

## List of Tables

IV-1	Four Kinematic Factors Affecting Vertical Hip Displacements.....	120
V-1	Propulsion Testing.....	185
A-2.1	Heel Stiffnes Values as a Function of Shank Angle.....	224

## List of Symbols and Definitions

- A/P** Anterior/posterior
- Anterior is the front of the body or the positive direction travel.
- Posterior is the back of the body or the negative direction of travel.
- ATDC** After top dead center - any position or angle of body after the shank angle has past vertical
- BTDC** Before top dead center - any position or angle of body before the shank angle reaches vertical
- c.g.** Center of Gravity
- CL** Conventional Lockup - conventional stance phase knee controller requiring the amputee to actively maintain the prosthetic knee joint in full hyperextension from PHC to SHC
- ELL** Effective leg length, the length of an imaginary leg connecting the hip joint on the prosthetic side to the center of pressure of the foot/floor interaction forces
- Gait cycle** - Heel contact to heel contact of the same leg
- Knee break** - instant in time when prosthetic knee angle starts to flex to prepare for the swing phase
- LED** Infra-red light emitting diode
- ME** Modified Echo - stance phase controller in which the modified position trajectory from the amputee's sound (intact) leg is used as a reference position for the prosthetic knee to follow from PHC to SHC
- PFF** Prosthetic footflat - anytime when prosthetic heel and toe are on the ground
- PHC** Prosthetic heel contact - instant of contact
- PHO** Prosthetic heel off - instant of loss of contact signifies end of PFF
- PHR** Prosthetic Heel roll - time after PHC and before PTC
- PTO** Prosthetic toe off - instant of loss of contact, signifies end of prosthetic stance

PTR      Prosthetic toe roll - time after PFF and before PTO

SACH  
foot      Common type of prosthetic unit used to simulate  
            ankle and foot function

SACH      Solid Ankle Cushioned Heel

SHC      Sound heel contact - instant of contact, signifies  
            end of single support prosthetic stance

Step      Heel contact of one leg to heel contact of the  
            other leg

STO      Sound toe off - instant of loss of contact, signifies  
            start of single support prosthetic stance

## I INTRODUCTION

Human biped locomotion is simply the act of transporting ourselves from one location to another. The comfort, ease, efficiency, adaptability and transparency of this process to humans is a result of millions of years of evolution (good design). The psychological, sociological and economic implications of losing even some of this capability can be enormous. Therefore, effort to design the "best" prosthesis is demanded.

The difficulty, however, of replacing missing human locomotor parts with prosthetic ones has been clearly demonstrated. The human locomotor system is, amongst other things, an engineering marvel. Biochemical fuels are readily stored and retrieved with great speed and in large quantities. The biomechanical actuators (muscles) are powerful yet lightweight. The organic sensors are pervasive and redundant. The central and peripheral nervous system is an individualized, and robust controller. The entire locomotor system is extremely flexible and reliable allowing the normal human to optimize the variable of his choosing when moving from one location to another. Designing a prosthetic leg, that will effectively interface with this system, is the *raison d'être* for this thesis.

### I-1 Statement of Problem

Unilateral, above-knee (A/K) amputees are currently fitted with a prosthesis that improves their reduced locomotor capabilities but still results in gait that is fatiguing, non-cosmetic, not adaptable to changing topology, not individualized, detrimental to their stump, and potentially unsafe.

This is particularly true during the prosthetic stance (support) phase. A/K prostheses contain no active elements, therefore, normal stance phase knee and ankle function are not possible. The amputee is concerned with knee stability during stance and this is achieved by the amputee maintaining the knee in the full hyperextended position by "appropriate" placement of his body, action of his sound leg and activation of his hip muscles on the prosthetic side. This fixed knee angle stability constraint during stance is not normal and requires compensatory behavior of the amputee. Stance phase controller design is inadequate.

### I-2 Statement of Purpose

The purpose of this thesis is to determine the important issues affecting the design and control of A/K prostheses during the stance phase of level walking. These issues are to be determined from a quantitative study of the mechanics of gait and clinical observations with the perspective of improving the design of specific elements of the current prosthesis system.

### I-3 Statement of Approach

The design and control of A/K prostheses extends back for hundreds of years. During that time, while some major changes in the function of A/K prostheses have occurred little change in the "cut and try" design process has occurred. After World War II, an accelerated effort to understand

human biped gait, both normal and abnormal, was undertaken in this country. Much of this work was centered at the University of California at Berkeley under the National Research Council, an advisory committee to the Veterans Administration. This provided a much needed data base to improve on the "cut and try" design process. However, the limitation of designing a specific prosthesis to perform a specific function remained. Any new control or design idea required building a new and different prosthesis. This is, of course, time consuming, expensive and makes evaluation of different designs more difficult.

In the 1970's, with the advent of readily accessible and inexpensive digital technology, the idea of using a computer to control the prosthesis came to fruition (Cvetinovic et al [28], Kato et al [71], Radcliffe et al [100], Moskowitz [86], Dyck et al [36], Flowers [43,44]). This allowed the designer to change the behavior of the prosthetic leg by simply altering the control algorithm program.

Flowers [43] in 1972 and Grimes [54] in 1979, exploited this idea and developed the most sophisticated prosthesis to date. Combining a powerful lightweight actuator with a digital computer, they produced a prosthesis simulator which could be programmed to mimic any currently available prosthesis as well as generate an almost endless list of new ones (see Chapter III-2). While this person-interactive approach improved the design process by accelerating the rate of trying out different knee controller designs, it still did not explicitly change the "cut and try" design approach.

The approach of this thesis in determining the design issues in the stance phase control of A/K prosthesis, is to combine person-interactive simulation with a gait analysis system (inverse dynamics model) and dynamic designer gait models. This design process is illustrated in Figure I-1. The right side of this figure represents the "build one try one" approach. The left side represents the person-interactive simulation process which allows ideas generated on the right side to be implemented directly without building new hardware. This thesis attempts to expand the design process by bridging the person-interactive simulation trials with the new knee controller designs by providing a quantitative flow of information.

The inverse dynamics model is the classical approach to calculating the forces and torques across the joints based on the measured kinematics of the body segments, segment properties, and foot/floor interaction forces (see Chapter II-3). The designer gait model is a dynamic (or kinematic) representation of the amputee prosthesis system which contains explicit representation of detailed parts of the prosthesis. Simulation of the designer model yields information of the specific behavior or contribution of the modeled effect. This added information allows the designer to determine the effect of a new design and provide a basis for future designs.

This thesis will specifically investigate the similarities in and differences between an amputee's stance phase level walking gait when the knee is controlled in the following two ways: 1) conventional control (CL) in which the amputee maintains the prosthetic knee joint in full





hyperextension from prosthetic heel contact (PHC) to knee break (swing phase preparation); 2) modified echo (ME) control in which the modified position trajectory from the amputee's second (intact) leg is used as a reference position for the prosthetic knee to follow. The investigation will include the use of a three dimensional gait analysis system to generate the gait data to be analyzed, and the development of designer gait models to aid in the data interpretation process.

#### I-4 Summary of the Remaining Chapters

The thesis organization is intended to emphasize the process that leads up to the development of the designer gait models. This process is presented as follows. Chapter II provides background on normal gait, A/K gait with a conventional prosthesis, and details of the ME stance phase knee controller. Also details of the inverse dynamic model and a discussion of the designer model concept are provided. Chapter III provides details of the prosthesis simulator, gait analysis system and the rest of the experimental details. Chapter IV contains the gait data comparing the two stance phase knee controllers used in this study. The kinematic data is presented first followed by the dynamic gait results. Chapter V develops the designer gait models in light of the results presented in Chapter IV. Results of the models are presented and discussed. Finally, Chapter VI discusses the implications of the gait results and usefulness of the designer gait models. Note, all the details of the experimental process and equations for the dynamic designer models are included in the appendices.

## II BACKGROUND

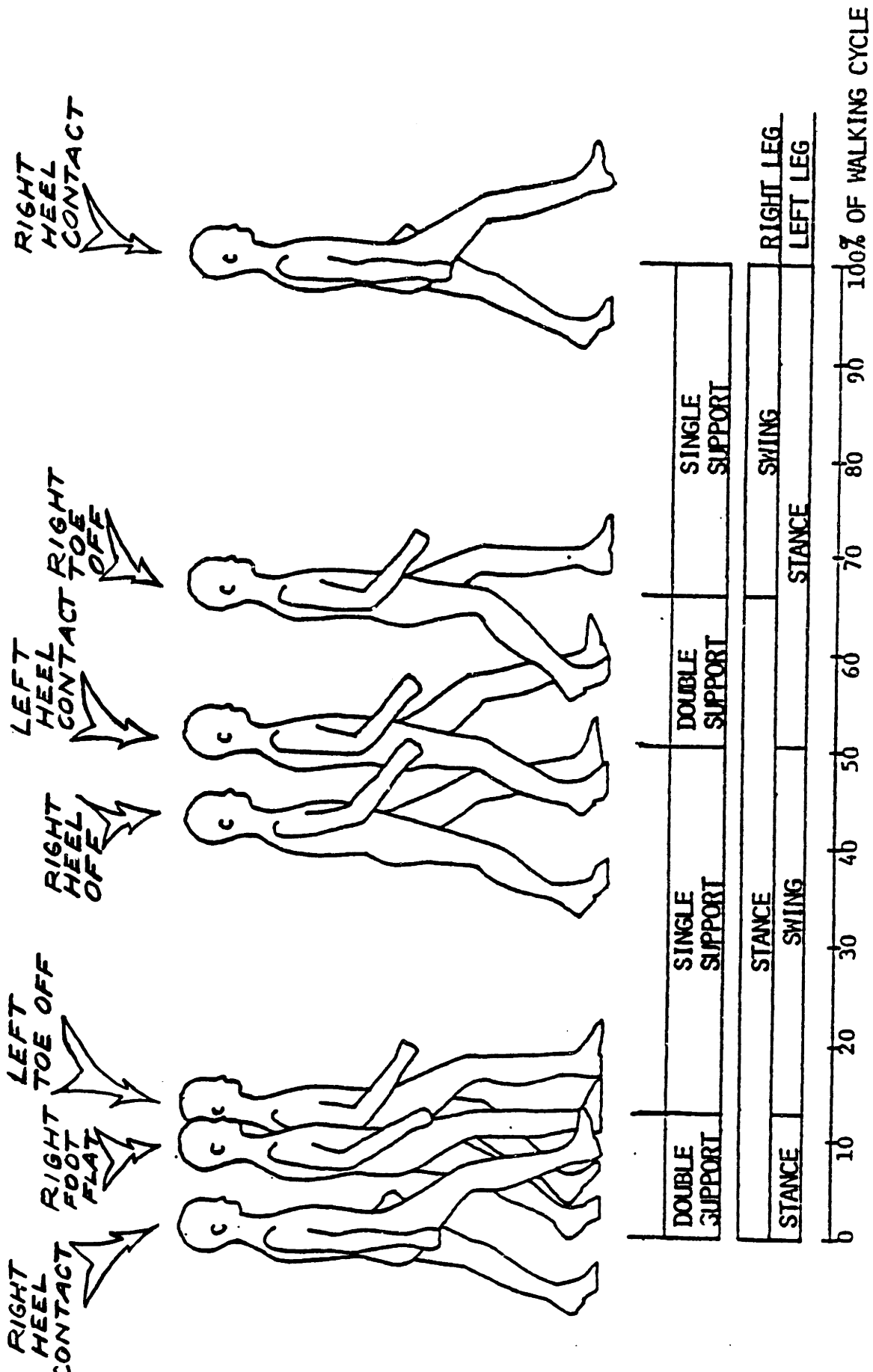
### II-1 Human Gait

This thesis is concerned with the design and control of A/K prostheses during the stance phase of level walking. In order to design prostheses, a sound understanding of both A/K and normal gait must be acquired. It should be stressed, however, that optimum control of an A/K prosthesis is not when "normal gait" is produced. Clearly additional constraints such as cost, reliability, technical feasibility and ease of use makes the optimizing function for the best A/K gait different than for normals.

The large number of books and articles that have been written just about normal gait is a tribute to its complexity. Many in-depth gait studies on the mechanics and energy of walking [10,11,12,13,14,27,37,38,40,47,63,87,94,95,104,110,111,115,120] have helped establish a foundation to the understanding of normal and pathological gait. A very brief description of normal gait follows and the reader is encouraged to explore the cited references.

#### II-1.1 Normal gait

The general terminology applied to gait is shown in Figure II-1. The gait cycle is defined as from heel contact to heel contact of the same leg while one step is from heel contact of one leg to heel contact of the other. During the gait cycle each leg goes through alternating roles of providing support to the body (stance phase) and being lifted and swung



SEQUENTIAL GAIT PARAMETERS  
FIGURE II-1

through to prepare for the next stance phase. The non-support time is called the swing phase. For level walking, overlap occurs between the stance phase of one leg and stance phase of the other. This is called the double support phase. The start of the stance phase is defined by heel contact (HC) of either leg and is terminated at toe off (TO) of the same leg. During the stance phase, the foot progresses from HC to TO in the following way. HC is followed by heel roll (HR) as the foot rotates forward, HR is terminated by toe contact (TC) which begins a new phase called foot flat (FF). FF is terminated by heel off (HO) which defines the beginning of toe roll (TR). TR ends at TO, the end of stance for that leg. These abbreviations are usually preceded by the letter R or L for right or left leg or by the letter P or S for the prosthetic or sound leg. As an example, PHC is prosthetic heel contact (see list of symbols).

As the body moves forward during normal level walking, it is both suspended and propelled forward by the legs. The suspensory action is provided by the load bearing leg from HC to opposite leg HC, and the propulsion is thought to be provided by the leg in TR ("push off") and HR ("catch").

Figures II-2, II-3, and II-4 show the performance of the knee, ankle, and hip of four normal subjects during level walking beginning at HC (a method for measuring this type of data will be discussed in Chapter II-3). AT HC, the knee flexes and the ankle plantar flexes absorbing energy. This reduces the loading on the leg. During foot flat the body moves over the stationary foot and because the tibia advancement is controlled by the calf muscle, the knee extends without supplying much (if any) power while

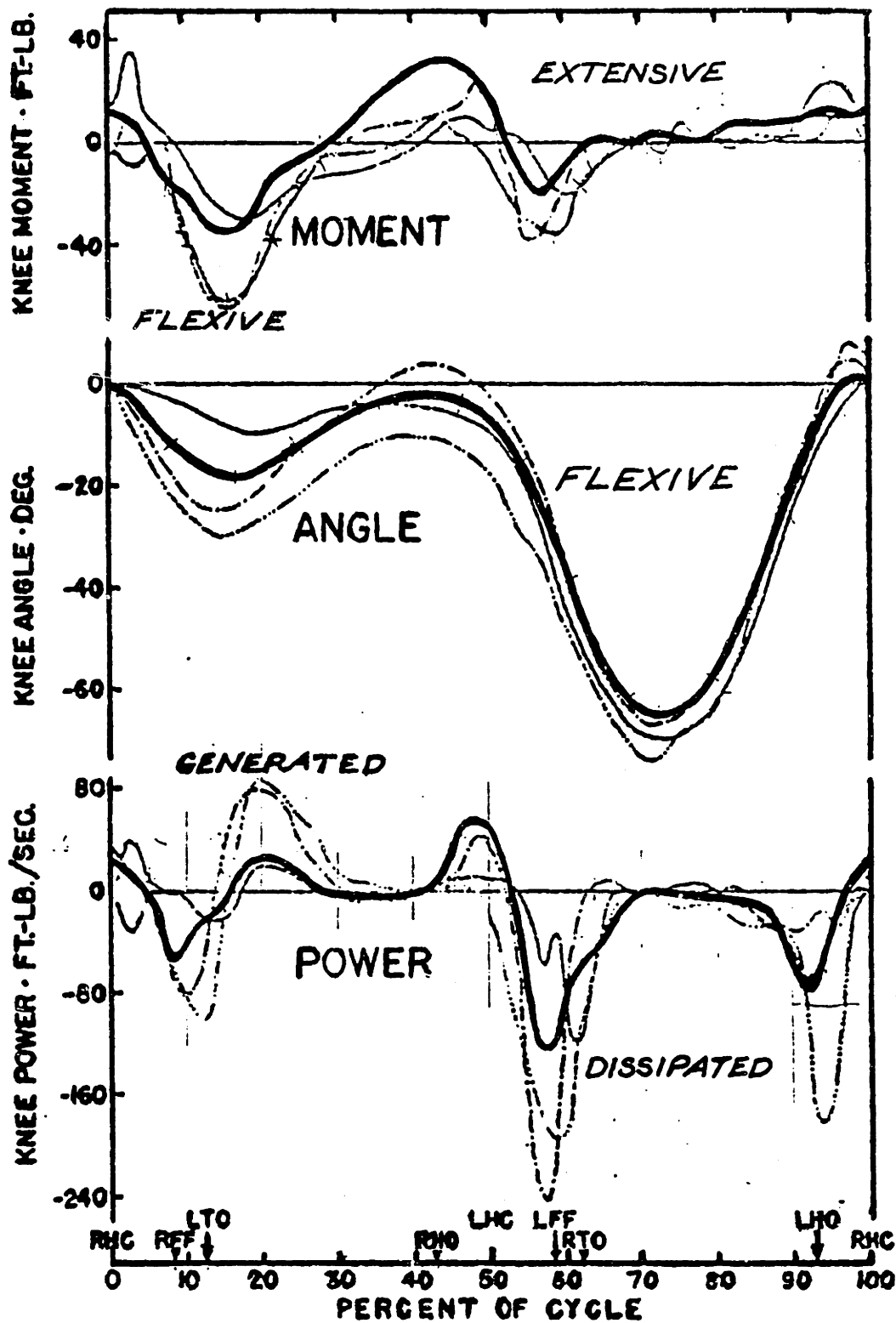


FIGURE II-2

Right knee moment, angle, and power of four normal subjects [10].

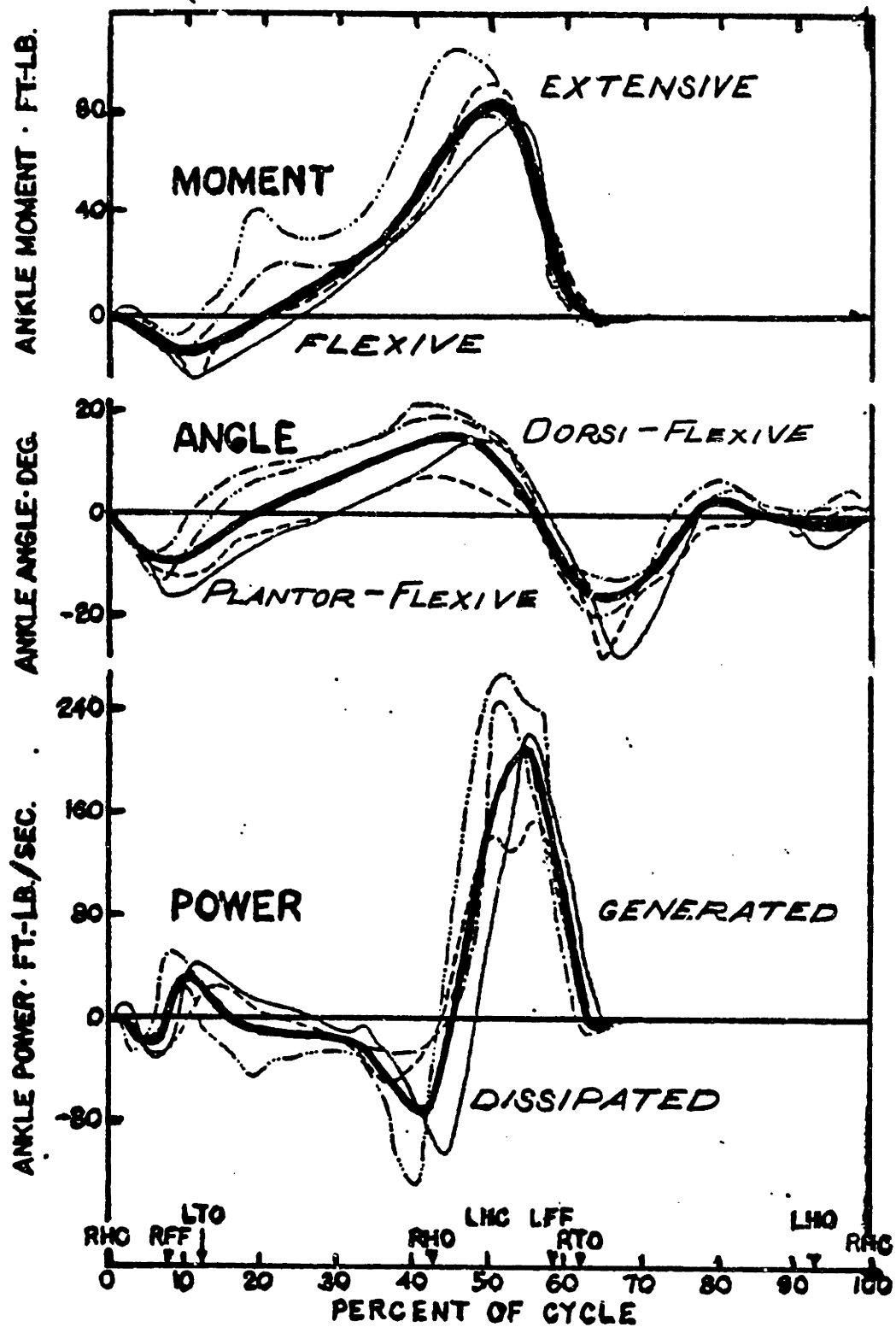


FIGURE II-3

Right ankle moment, angle and power of four normal subjects [10].

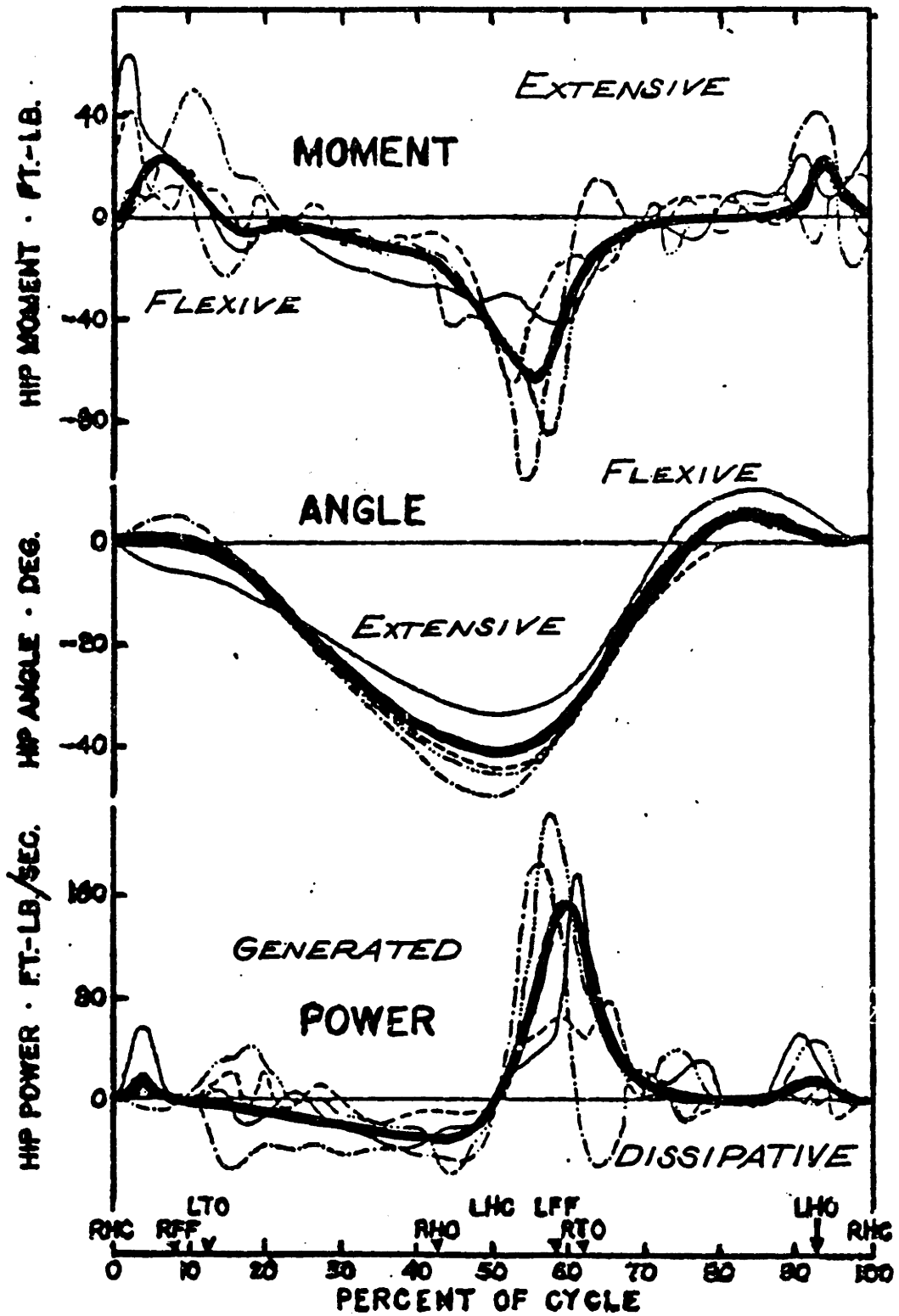


FIGURE II-4

Right hip moment, angle and power of four normal subjects [10].



the ankle dorsiflexes, absorbing energy as tibia does progresses forward. During TR the body falls forward and the knee continues to re-extend. As opposite leg HC occurs the hip torque becomes flexive, causing the thigh to flex and the knee to passively flex as the load is transferred to the opposite leg. The ankle actively plantar flexes pushing the body up and forward on to the opposite leg.

The swing leg is controlled by the hip torque. The leg is initially lifted, hip flexes to 20 degrees and the knee to 60 degrees. The leg is then pulled through by the active hip flexion and the knee extends as it follows the thigh, responding like a damped pendulum (always dissipating power). Ankle is dorsiflexed to insure toe clearance. Knee is fully extended by the end of swing to initiate heel contact (start of stance).

## II-1.2 Conventional above-knee prostheses

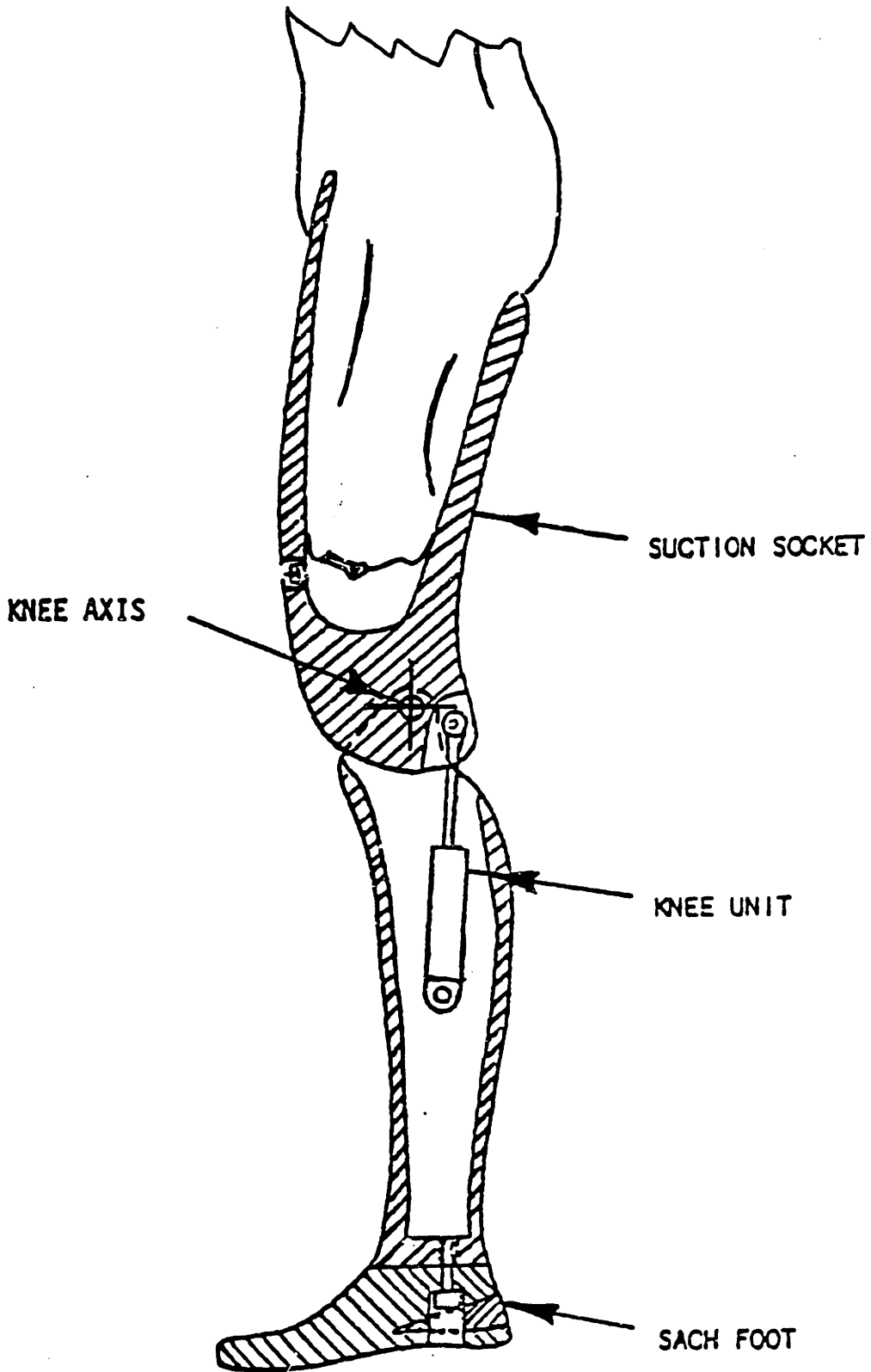
A/K prostheses have been under intensive development for the last thirty-five years. As a result, the number of currently available A/K prostheses is large. In a "Survey of Knee Mechanisms for Artificial Legs", [70] 149 different types of knee mechanisms are listed. While this list includes research prototypes as well as some of the commercially available units, it is clear that a wide selection is available.

However, despite this wide selection, compared to normal knee function, all of these units are functionally very simple. They all try to provide stability during stance, cosmesis during swing as well as comfort throughout the gait cycle. The mechanisms must be durable and reliable. Providing stability in stance (stance phase control) and a

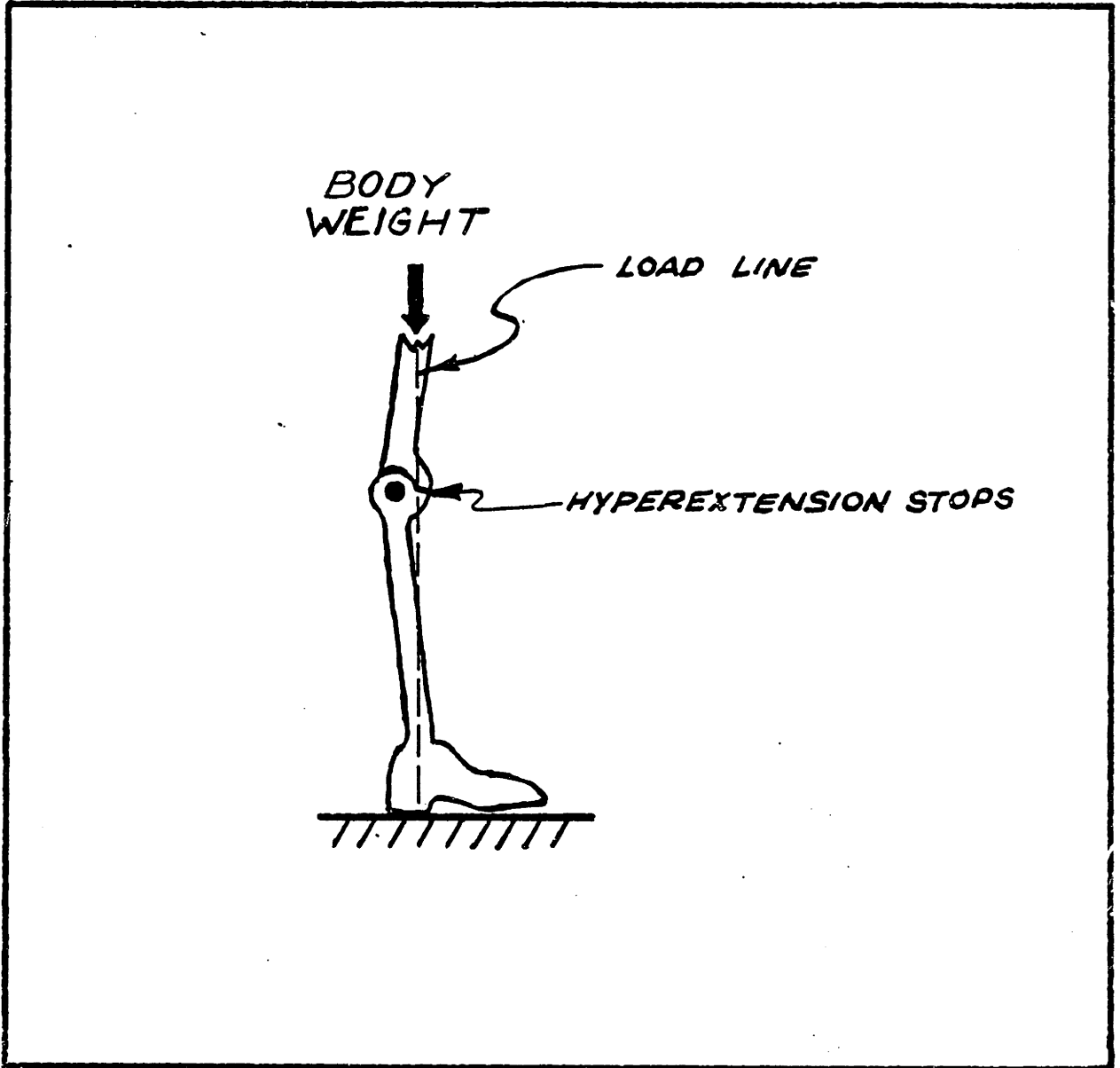
duplication of normal level walking, knee kinematics during swing (swing phase control) is generally considered as fundamental.

Figure II-5 depicts a typical conventional A/K prosthesis. It is attached to the amputee by means of a pelvic belt (not shown) holding his stump into the socket and/or the suction produced by the custom fitted suction socket. The socket rotates about a single axis (knee joint) with respect to the shank. The relative motion is controlled by the knee unit. The ankle and foot are included as one unit called the SACH (Solid Ankle Cushioned Heel) foot. While other ankle and foot mechanisms are available, they are not widely used. The knee unit as shown in Figure II-5 is a passive device in all commercially available A/K prostheses. This means that energy can be absorbed or dissipated at the knee joint but cannot be generated. As shown in Figure II-2, the normal knee during the swing phase of level walking acts like a damper. Therefore, during the swing phase, the knee unit controls the motion of the shank by dissipating energy input into the system through the hip. The knee unit is, therefore, often called a swing phase control unit and while they vary in sophistication (and price) the intended function is to mimic the swing phase knee kinematics of normal level walking.

During the stance phase, the conventional prosthesis is held against its mechanical hyperextension stops by appropriate action of the amputee's hip muscles and placement of his body c.g. (see Figure II-6). The prosthesis designer can control the "amount" of stability by adjusting the anterior/posterior (A/P) position of the knee axis relative to the load line. There are also some A/K prostheses with polycentric knee linkages



*TYPICAL ABOVE-KNEE PROTHESIS*  
*FIGURE II-5*



STANCE STABILITY  
RESULTING FROM  
ALIGNMENT AND HYPEREXTENSION  
STOPS

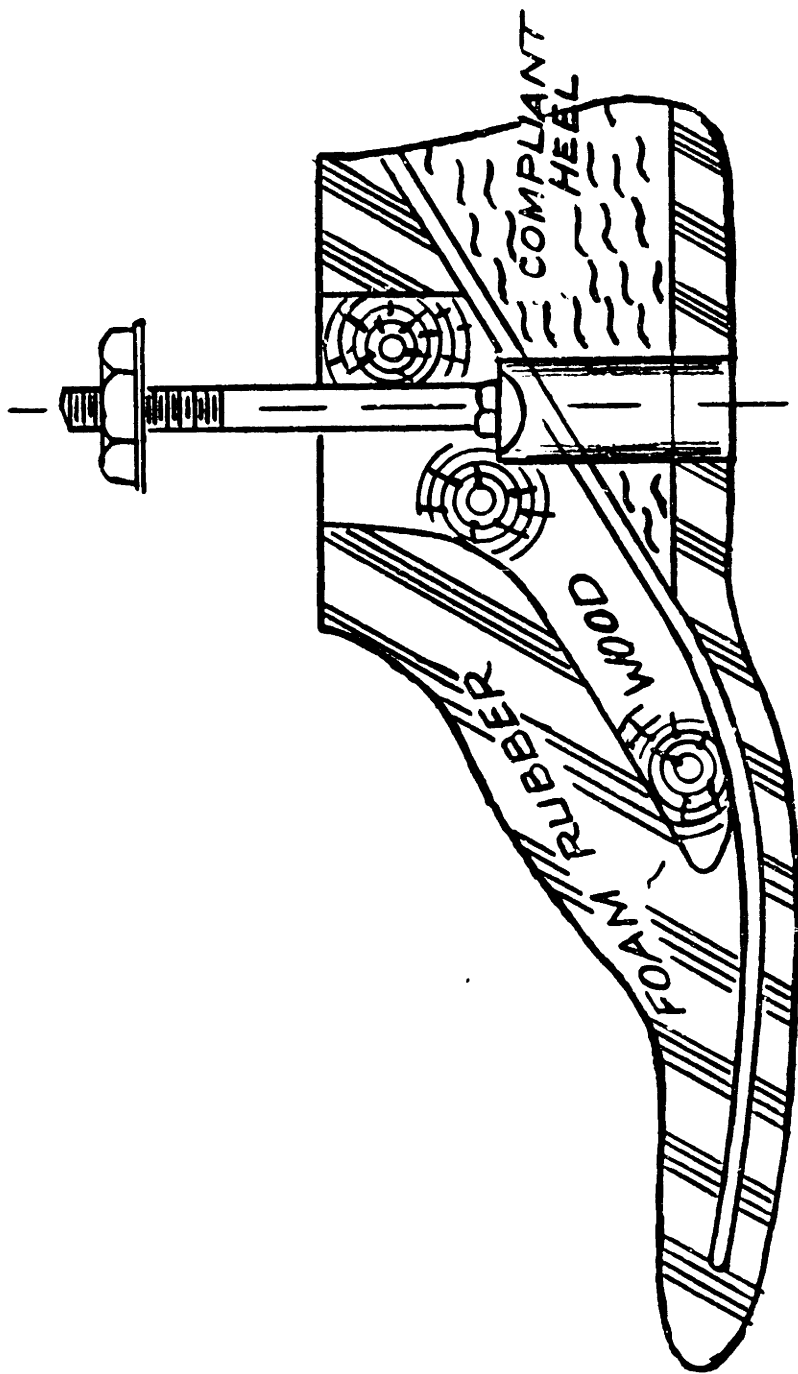
FIGURE II-6

that give the amputee more control over maintaining the knee in the full extension. Thus, the conventional prosthesis remains fully extended during the stance phase up to SHC. After SHC, the knee is allowed to flex as the load is being transferred to the sound leg.

Stance phase performance with a conventional prosthesis is also affected by the SACH foot. The SACH foot shown in Figure II-7 is "principally designed to provide motion in the anteroposterior plane in simulation of plantar flexion and dorsiflexion of the ankle and extension of the toe" [108]. Therefore, at PHC, the SACH heel provides some energy absorption that the normal ankle (plantar flexion) and knee flexion give. During PTR the SACH toe section helps control shank advancement by resisting (simulated dorsiflexion) bending. The overall system stability can also be controlled by SACH foot A/P alignment. Anterior movement will tend to stabilize the knee at PHC, but will make toe break more difficult [81]. Finally, stance phase performance is affected by SACH heel and toe break stiffness (they are made as soft, regular and firm). For example, stiff toe break makes the prosthesis more stable during PTR but, therefore, more difficult to generate knee break at SHC.

### II-1.3 Above-Knee amputee gait

Gait patterns for A/K amputees have been studied by many researchers [6,12,27,37,38,63,64,98,104,110,120]. One common problem that exists in interpreting the results is that pathological locomotion patterns are as numerous as the disorders that cause them. Despite this, useful general observations have been made concerning A/K level walking gait. These



"SOLID ANKLE - CUSHION HEEL"  
SACH FOOT  
FIGURE II-7



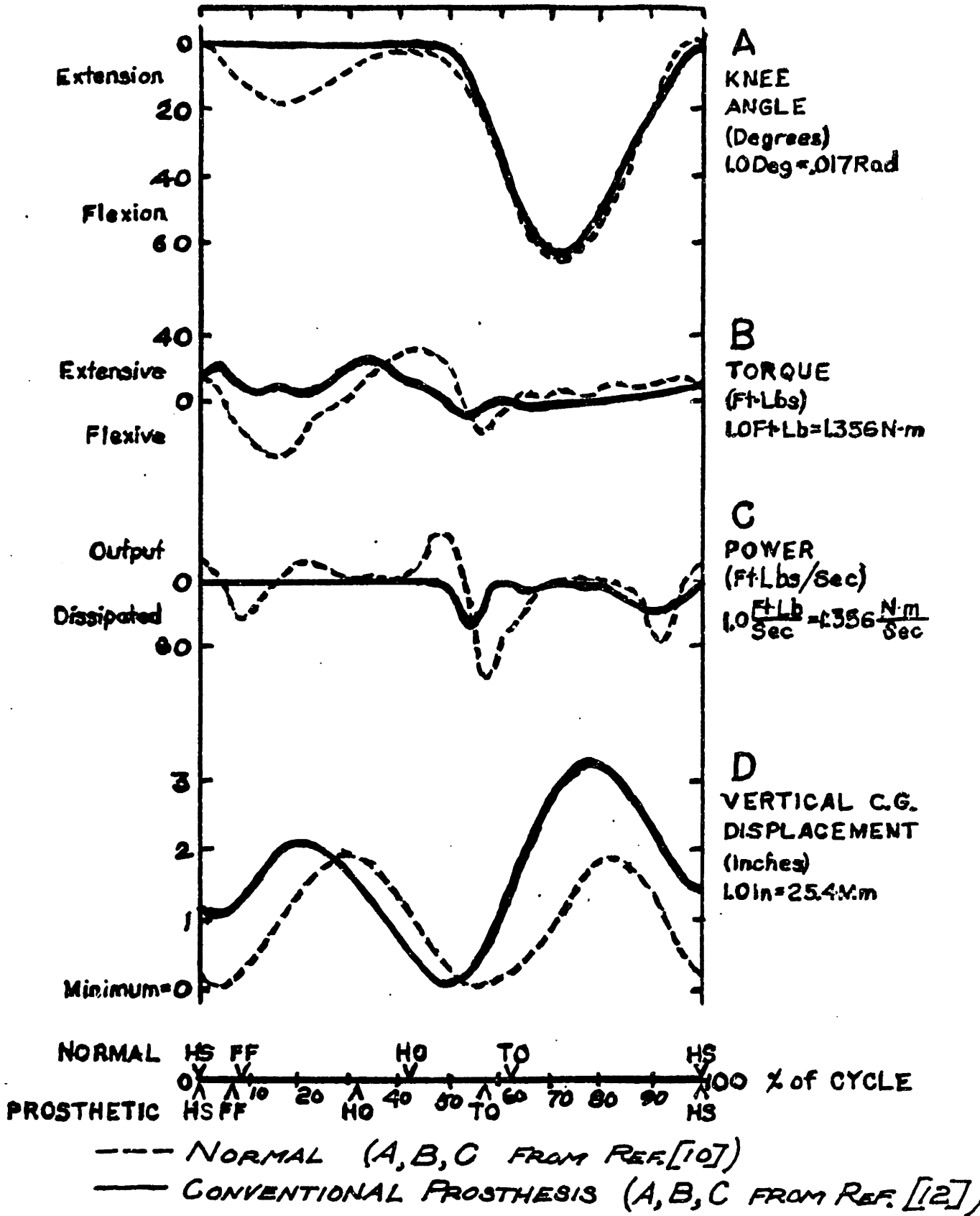
b. Sound leg stance is longer (65%) and swing phase is shorter (35%) than normal [54].

Typical knee parameters for a level walking cycle are shown in Figure II-8 comparing A/K gait to normal gait. Differences between gaits is clearly shown. At PHC the amputee applies an extensive torque at his hip to keep the prosthetic knee torque extensive and thus keep the knee at full extension through the entire stance phase (up to knee break). The knee remains at full extension as opposed to normals who flex and re-extend the knee. This action requires an active (powered) knee joint as shown in the power profile for normals. Since conventional A/K prostheses are passive, the amputee must keep the prosthetic knee fully extended in order to have a stable support during stance. The hip torque goes flexive causing the knee torque to go flexive at SHC. This results in knee break and thus prepares the prosthesis for the swing phase. During swing, normal and prosthetic knee kinematics can be quite similar even though the c.g. excursion is higher for the A/K case in order to insure toe clearance. Also, note that power flow at the knee is dissipative for both normals and A/K amputees.

In summary, while falling considerably short of normal leg function, A/K prostheses do provide amputees with a great deal of mobility. This mobility, however, is a result of a gait pattern which is:

1. fatiguing
2. detrimental to the stump due to stump/socket forces





KNEE PARAMETERS  
(A/K PROSTHESIS VERSUS NORMAL; REF. [54])

FIGURE II-B

3. non-cosmetic
4. potentially unsafe
5. not adaptable to changing topology.

It is important to note that four out of the five above mentioned gait pattern problems are exclusively stance phase problems. It is therefore the aim of this thesis to study to determine the important design issues relevant to the stance phase control of A/K prostheses.

## II-2 Stance Phase Knee Controllers

### II-2.1 Background

Level walking stance phase control of current commercially available A/K prostheses currently consists of properly aligning the socket and SACH foot with respect to the knee axis as previously discussed in section 1.2 of this chapter. Many attempts to improve the functionality of A/K prostheses during the stance phase of level walking have been tried and in some cases marketed. These design can be divided into these categories:

1. Standard alignment dependent knee stability mechanisms
2. Polycentric knee mechanisms
3. Voluntary and involuntary passive knee locking and/or knee yielding under load
4. Active knee mechanism allowing knee flexion

and re-extension under load.

Category 1 stance phase knee controllers were discussed in section 1.2. They represent the most commonly used stance phase knee controller.

Category 2 stance phase knee controllers exist in several commercially available units such as the Dyna-Plex O.H.C. Polycentric Knee Disarticulation Prosthesis as well as research units such as the UCB-4Bar and 6 Bar prostheses [70]. These units move the center of rotation closer to the hip, when the leg is in full extension. This gives the amputee better control over keeping the prosthesis in full extension and initiating knee break.

Category 3 stance phase knee controllers are more in the development stages [70], however, commercial units such as the Henschke-Mauch Hydraulic Swing-N-Stance Knee Control do allow controlled yield in early stance if the amputee keeps unit in hyperextension for .1 seconds after PHC.

Category 4, flex-extend action of the knee during stance, is the most closely related to normal knee function. Essentially only two research groups have clinically explored this type of knee control. One group is the developers of the Bouncy Knee [41,42,67] in the Bioengineering Center at the University College, London. Used in conjunction with the Blatchford Stabilized Knee, the Bouncy Knee provides a range of possible maximum knee flexion angles of up to 14 degrees [75] during stance dependent on spring stiffness used. Current clinical trials indicate improved symmetry of gait but that further improvements in symmetry would

result if the knee flex rate were controlled to be more natural. The unit deflects too slowly after PHC and re-extends too quickly from max flexion. The second group is the researchers this author is affiliated with, the MIT Knee Group. Using the MIT Knee Simulator Grimes [54] implemented a stance phase knee control strategy which commanded the prosthetic knee to follow a modified position trajectory recorded one half cycle earlier from the sound (intact) knee. Since the simulator is an active device, this trajectory can be followed exactly. Laboratory trials have produced very positive results.

The purpose of this thesis is to explore the general design issues in the stance phase control of A/K prostheses. Therefore, a control strategy from categories 1 and 4, the most common type as well as the most "natural" like stance phase knee controller were selected for testing. These stance phase control strategies represent the basic to the most sophisticated. This large difference in control strategies will help determine the boundaries within which future stance phase knee controllers can be developed.

## II-2.2 Stance phase control strategies tested

### II-2.2.1 Introduction

The details of the control strategies used in this study will be described in this section. The controller from category 1 is simply a "hydraulic like" swing phase control strategy combined with a "hold in full extension" or conventional (CL) stance phase controller. The controller from category 4 is the Modified Echo (ME) approach of Grimes

[54] combined with the same swing phase controller from category 1. The ME controller was chosen over the Bouncy Knee because at this time, the Modified Echo approach produces more natural knee kinematics. Both the CL and the ME controllers were implemented on the MIT, person-interactive simulator system.

#### II-2.2.2 Conventional control

The conventional knee controller has two regions over which the amputee uses two different control strategies.

From PHC to SHC the amputee holds the conventional prosthesis against the hyperextension stops as described previously in II-1.3. After SHC which corresponds to knee break, the amputee swings the leg by imparting energy through his stump. The knee is always controlled to be a damped pendulum. The damping scheme used is identical to the one used by Grimes [54]. The damping is an angle dependent velocity squared damper of the form:

$$\text{Damping Torque} = B(\Theta) * \text{ABS}(W) * (W)$$

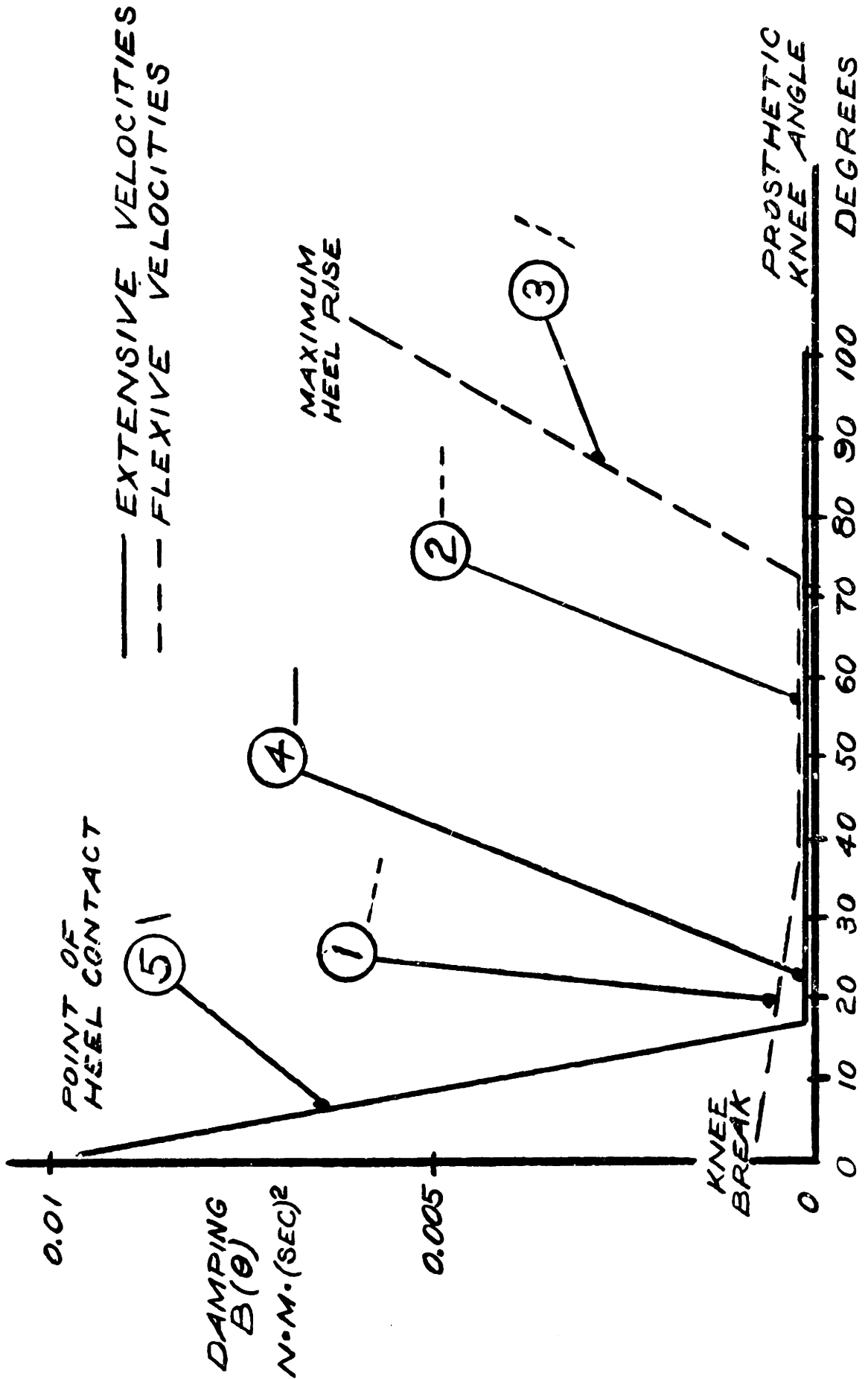
where  $\Theta$  is the knee angle

$W$  is the knee angular velocity.

ABS is the absolute value function

The damping function,  $B(\Theta)$  is shown in Figure II-9. The swing phase damping is divided into five regions as marked in Figure II-9. The damping in the five regions controls

1. buckling during the end of stance,



DAMPING FUNCTION

FIGURE II-9

2. toe off at end of stance,
3. excessive heel rise past 75 degrees,
4. initiation of swing through,
5. impact at full extension.

"Once tuned, these damping coefficients effectively control the prosthesis to duplicate the kinematics of the normal knee during the swing phase of level walking" [Grimes [54] pg. 63].

#### II-2.2.3 Modified echo control

This control scheme was developed by Grimes and implemented here with only slight technical changes by the author. For complete details see reference [54].

Modified echo control is implemented from PHC to SHC. During this time, the knee angle of the prosthesis follows a trajectory which was modified from the trajectory recorded from the sound (intact) knee during the previous sound stance phase. From SHC to PHC the prosthesis is controlled as a damped pendulum exactly as described for the CL controller. The approach is called modified echo control because the sound knee profile must be adjusted so it approximates a normal knee trajectory. There are two reasons why the sound knee trajectory must be modified: 1) "The sound knee of an A/K amputee flexes more during the stance phase of level walking than the knee of a normal" (Grimes [54] pg. 58), and 2) "The maximum flexion during the stance phase for a normal knee varies as a function of cadence" (Grimes [54] pg. 58). Thus, the sound knee profile is multiplied by a gain factor which is chosen so that the

maximum knee flexion angle of the modified sound trajectory matches the maximum flexion knee angle for a normal knee at the existing cadence. Cadence is determined from the time of one step, PHC to PHC.

In summary, two stance phase knee controllers are to be tested; 1) is a conventional controller (swing and stance) 2) is a modified echo controller which is designed to produce normal kinematics of the prosthetic knee during the stance phase. The swing phase is the same for both controllers. It is assumed that the ME controller will produce the following results:

1. provide the prosthesis with normal knee kinematics (as shown by Grimes [54]),
2. reduce vaulting,
3. improve gait symmetry,
4. reduce loading on the stump.

## II-3 Biomechanics: Measuring Human Gait

### II-3.1 Introduction

Human motion has been a subject that has fascinated many individuals. As early as the 19th century, human motion data have been collected and published. Since that time, the method of quantifying gait data has remained essentially unchanged; only the tools have become more sophisticated.



For obvious reasons, measuring human motion (and the associated forces) must be done by measuring only the external motion and forces acting on the body. This information when combined with the inertial and geometric properties of the body segments of interest can be used to calculate the net force and moment vectors that must have been present to produce the recorded kinematics. This "Inverse Dynamics Model" does not provide any information about the individual muscles, tendons, etc.; it does accurately reflect the net mechanics (or biomechanics) of the gait process.

## II-3.2 Inverse dynamics model

### II-3.2.1 Assumptions

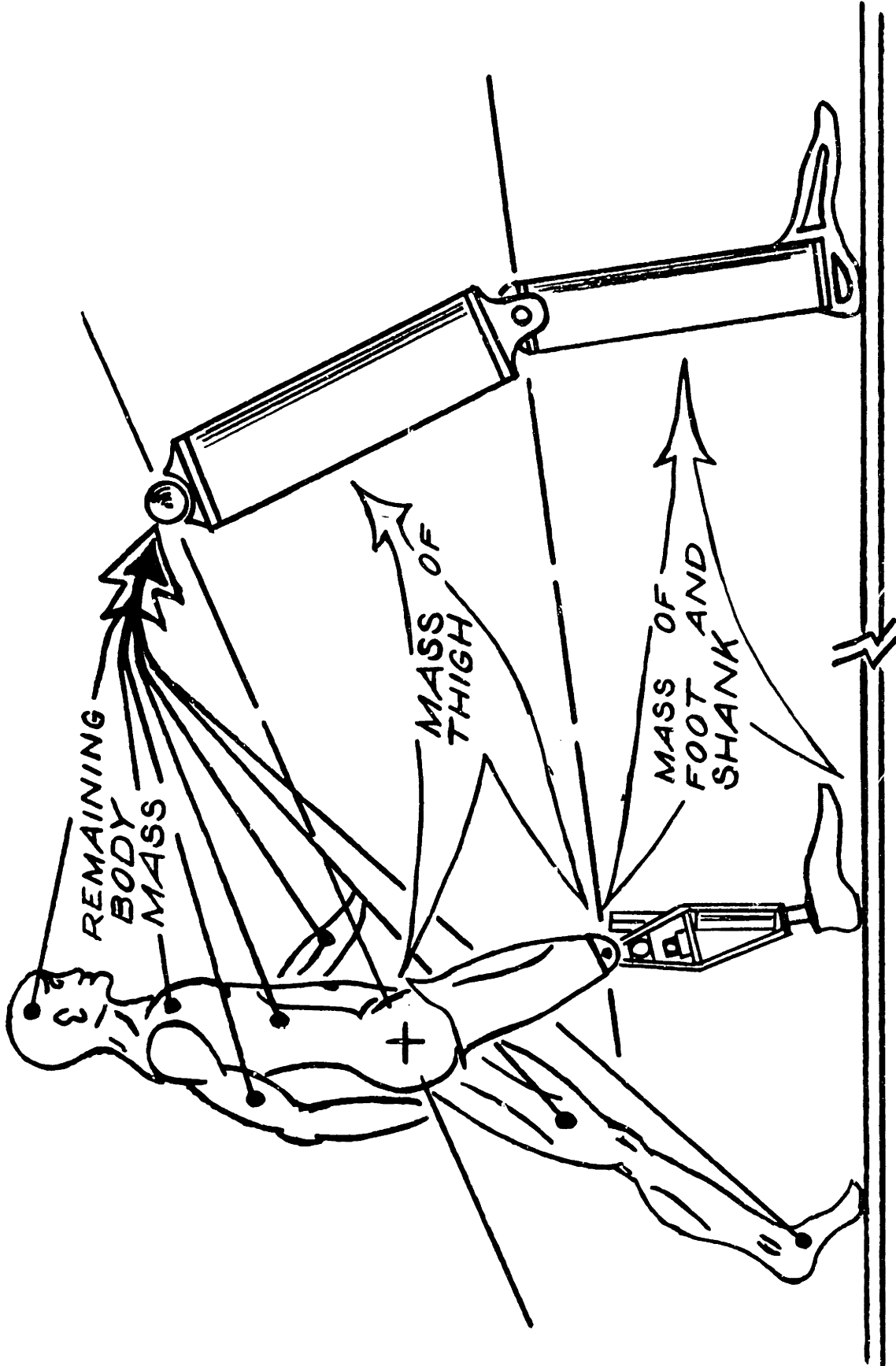
In practice there are many assumptions or estimates that have to be made in generating the 3-dimensional body mechanics. Some of these include:

- 1) Certainty of being able to segmentize the body into individual inertias (rigid bodies).
- 2) Certainty of measuring the movement of the segment due to soft tissue motion with respect to the skeleton.
- 3) Certainty in measuring or estimating inertia and geometry of the segment.
- 4) Knowledge of the frequency content of the measurement noise.

These assumptions will be discussed in reference to the particular measurement task of this thesis.

**Assumption 1. Certainty in selecting body inertia segments.**

In this thesis, the concern is with the dynamics of the lower limbs. In particular, the dynamics of the prosthetic leg. Figure II-10 illustrates the way in which the inertias of the amputee/prosthesis system are assumed to be distributed. This is similar to the assumptions of other researchers [11,12,47] except for two considerations. 1) The shank and SACH foot are not separated as two individual masses. This does not reduce the ability to predict ankle torques nor does it affect calculation of knee forces if the inertia of the moving parts of the SACH foot are small relative to the shank inertia, and/or if the relative kinematics of the SACH foot are small compared to shank kinematics or other effects like static loading of the body c.g. [12]. Bresler et al [12], showed that the energy level of the SACH foot during stance is negligible compared to other body segments. This means that reasonable results will be produced by neglecting the SACH foot as an independent inertia. 2) The body is considered to be a point mass acting at the hip on the prosthesis side. This assumes the entire effect of the rest of the body on the prosthesis is a point mass equal to the body mass plus an external force. The purpose for making this assumption is to calculate this external force. This force is assumed to represent the sound leg's effect at the hip on the prosthesis side. Since the dominant energy of the upper body is the energy of translation (the energy of rotation is less than 1% percent of



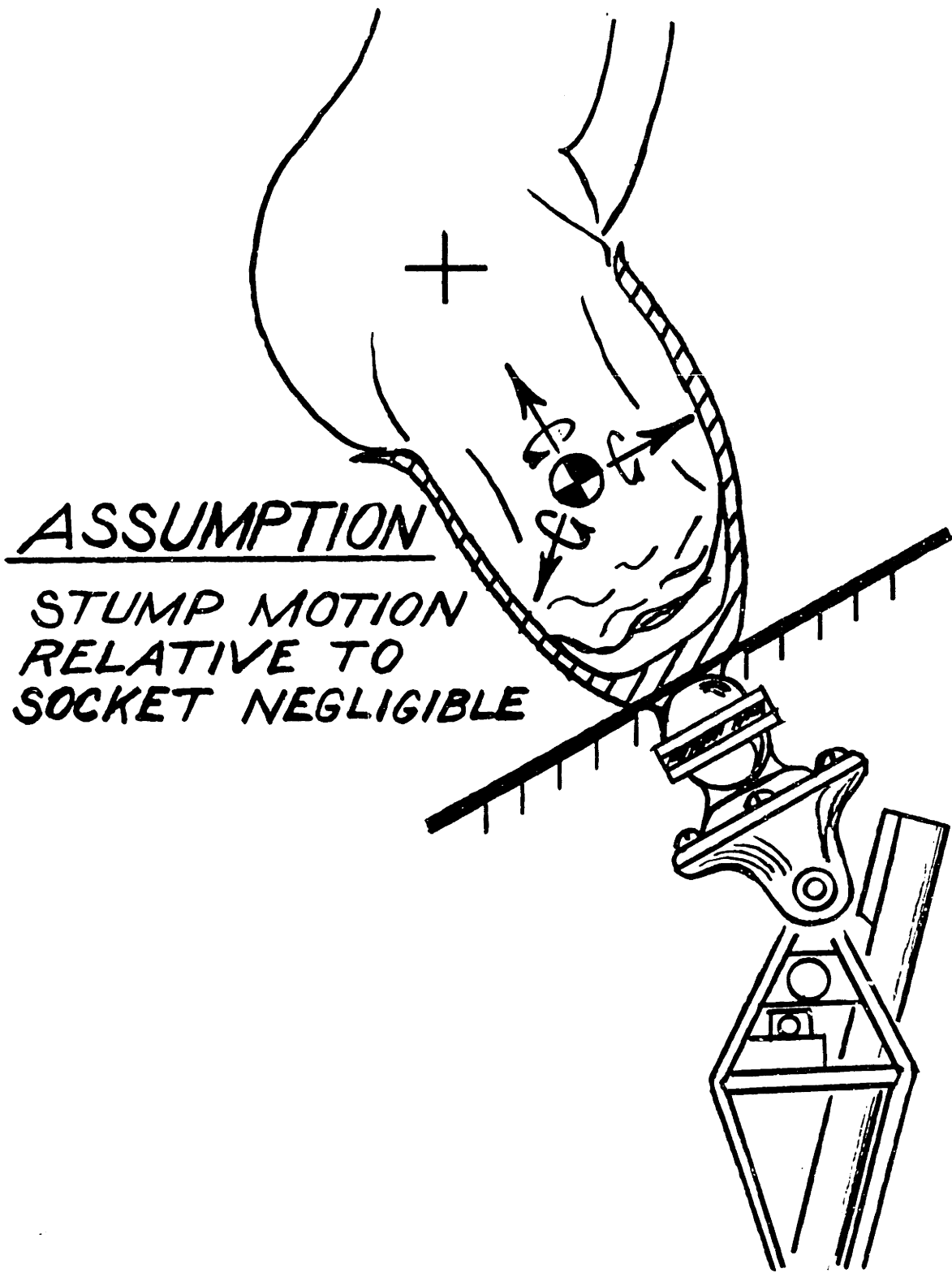
AMPUTEE SUBJECT (STANCE PHASE)

MASS ELEMENT-DYNAMIC MODEL

INERTIA SEGMENTS OF AMPUTEE-PROTHESIS  
 FIGURE II-10

the energy of translation for normals (Zarraugh [120] pg 113), this assumption should be reasonable. It should be carefully noted that this assumption has no affect on the calculation of forces and torques at the hip and below.

Another uncertainty exists in assuming a rigid link from the hip to the prosthetic knee. Figure II-10 shows the stump/socket "inertia" as one rigid element. As Figure II-11 illustrates there is a possibility of the femur moving relative to the socket. To date, this movement has not been measured dynamically during the walking cycle, so the amount of movement is an unknown and assumed unimportant for this study. Other researchers while clearly acknowledging the importance of a good fitting socket have also neglected this movement. Appoldt et al [6] have measured stump/socket slip to be less than 1/16" and occuring mostly at the end of the stump. This, of course, still does not reveal the motion of the femur with respect to the socket. Finally, since this motion is so difficult to measure, as a prosthesis designer, it is unlikely that this information will be used in feedback control strategies.



**STUMP-SOCKET INTERFACE**  
**FIGURE II-11**

Assumption 2: Certainty due to soft tissue motion with respect to skeleton.

As will be discussed in Chapter III, the "markers" used to measure shank and thigh kinematics were firmly attached to the prosthesis. There is no soft tissue interface uncertainty in this study. Since no "marker" is placed on the pelvis or femur, the assumption is that knowing the kinematics of the socket is a sufficiently accurate representation of the hip. This again refers to the assumption of no relative movement of the stump with respect to the socket.

Assumption 3. Certainty in measuring the inertia and geometry of the segments.

Measuring the inertia of body segments can be a difficult problem. Researchers such as Braune et al [9], Contini [20], Dempster [32], Drillis et al [35] and Winter [115] have developed general correlations between body dimensions. As examples: whole body density and body segment densities; whole body volume and body segment volumes; segment center of mass location and total length of segment; and radius of gyration of body segments and the body inertias. While this is not a comprehensive list, it is adequate for determining the model's inertias, specifically the thigh inertia. It should be noted that the thigh refers to the stump plus the socket and the turntable platform at the top of the prosthesis. While the amputee's "thigh" is different than the standard thigh used in the segment studies, the differences were neglected. The shank inertia is more easily measured since it is a piece of hardware which can be removed from the amputee and measured very accurately. The body mass is also easily estimated after the thigh and shank mass are known. It is simply

the total body mass minus the mass of the thigh (stump/socket) and shank.

Because this thesis is concerned with stance phase mechanics the uncertainty in segment inertia estimation can be very high without affecting the certainty of the results. This is due to the almost negligible rotational energy of the thigh and shank during stance [12]. Even the translational energy of the thigh and shank is low with respect to the energy of the body mass. The parameters used in this study are contained in Appendix 3.

Assumption 4. Knowledge of frequency content of gait information and measurement noise.

In his doctoral thesis [5], Antonsson provides an analysis of the frequency content of normal gait and the motion measurement system used in this thesis. Other researchers such as Cappazzo et al [13], Lesh et al [74], and Winter et al [119] have also worked on this problem. Gait data frequency content below 5-12 Hz is generally accepted an adequate representation of the gait process. This is particularly true during prosthetic stance where, except for heel contact, the process is quasi-static, gravity dominated or sound leg force dominated (inertia effects of the leg are small) activity (see Chapter V-4). Heel contact forces can have frequency content up to 20 Hz but is generally below 10 Hz for normal level walking [5]. Since a sample frequency of 157.5 Hz was used with subsequent low pass filtering between 5-20 Hz, it is assumed that the data recorded accurately reflects the actual gait mechanics.

### II-3.2.2 Dynamic estimation of joint force and torques

The mass element model in Figure II-10 is shown in free body diagram form in Figure II-12. The knee and hip joint forces and torques as well as the sound leg forces can be calculated given the following information:

1. Forceplate forces and torques
2. Shank and thigh kinematics
3. Shank and thigh c.g. locations, masses  
and inertias
4. Body mass

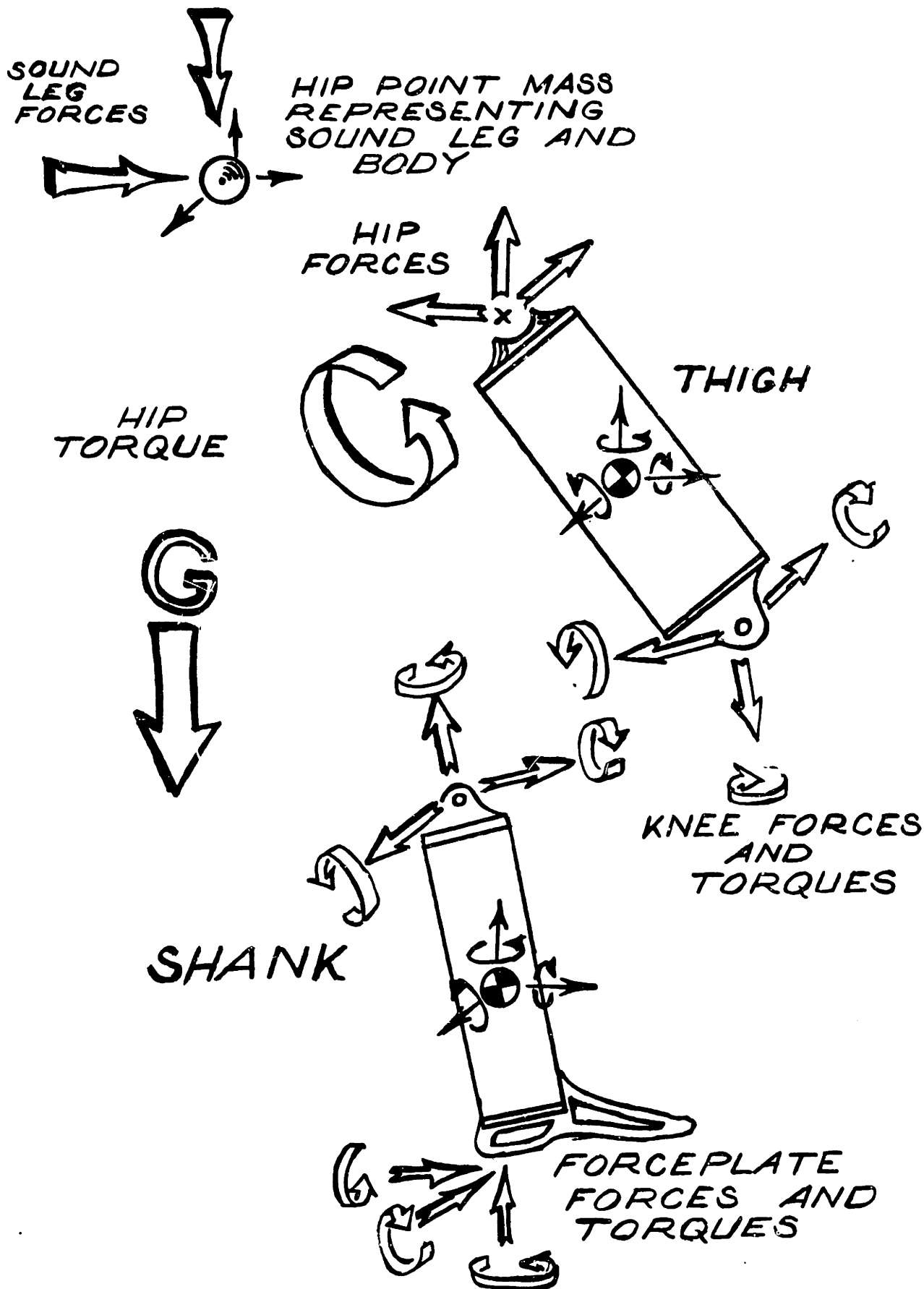
and using Newton's laws of motion. Given that each link has only two points of application of external forces on the segment then the proximal end forces and torques of the segment can be calculated from the given distal forces and torques. The negative proximal forces of the shank (knee force) become the distal force for the next link. Thus the calculation is started with the most distal link (shank) and proceeds proximally. Figure II-13 contains the dynamic estimator equations.

## II-4 Dynamic Designer Gait Models

### II-4.1 Introduction

The inverse dynamics model approach does not always explicitly answer questions that a designer might ask. For instance, the recorded kinematics of the shank is a result of all the external forces and all of the energy storage and dissipating elements, and all of the geometric constraints interacting. The designer may ask what is the contribution of





MODEL KINEMATICS AND DYNAMICS

FIGURE II-12

$$\sum \text{Forces} = F_p + mg - ma + F_d = 0$$

$$\sum \text{Moments} = T_p - I\dot{w} - w \times Iw + F_p \times r_p + T_d + F_d \times r_d = 0$$

Where:

$m$  = the segment mass

$I$  = the segment inertia tensor

$g$  = the global gravity vector

$a$  = the global acceleration vector

$\dot{w}$  = the global angular acceleration vector

$w$  = the global angular velocity vector

$F_p$  = the proximal force vector

$F_d$  = the distal force vector

$T_p$  = the proximal torque vector

$T_d$  = the distal torque vector

$r_p$  = the vector from the BCS origin to the point of application of the proximal force

$r_d$  = the vector from the BCS origin to the point of application of the distal force

$\times$  = the vector cross product operator

## *DYNAMIC ESTIMATION EQUATIONS*

*FIGURE II-13*

the SACH heel spring to the hip torque or hip trajectory. Large? Small? No effect? The inverse dynamics model alone cannot answer that question.

A dynamic model with an explicit representation of the heel spring could answer that question, where a dynamic model is defined as a mathematical model representing the kinematic and energy storage and dissipating elements of a system plus the external inputs and the initial values of all the states in the model. The answer would be generated by integrating the equations from the known initial conditions under the influence of the external inputs. Unfortunately, this has not been successfully done to date.

The main problem with using dynamic models is determining the inputs. The inputs represent the amputee's intent, they are generally measurable but not predictable. For example, if the inverse dynamics model in Figure II-10 were used as a dynamics model then the hip torque and sound leg forces would have to be known a priori in order to calculate the kinematics (not the other way as is done with an inverse dynamics model). It is possible to measure the hip torque and sound leg forces once and assume that they do not change as, say, the knee controller or leg alignment changes. This, however, seems unlikely given the amount of fine control humans have over their limbs. The appropriate inputs for the dynamic model remains an unanswered question.

Even with its difficulties, several researchers have studied human gait with simple dynamic models. Morawaski [85], Hemami et al [58], McGhee et al [77] tried to establish the feedback control laws necessary

to make the models follow published gait data. Mochon [33], Cavagna et al [14], Siegler et al [106] all assumed the inputs are zero (i.e. walking is ballistic). Mochon using an inverted pendulum model demonstrated some correlation with published data on walking speed and step length during the stance phase of level walking for normals. Cavagna also using an inverted pendulum model showed that the energy to lift the body c.g. and to increase its forward speed is related to the total mechanical energy involved in raising a mass over a rigid pendulum at intermediate walking speeds. Siegler using a compliant and damped inverted pendulum predicted the joint kinematics in the saggital plane as well as foot/floor interaction forces for both normals and A/K amputees. While all of these studies provided valuable information related to normal and A/K gait, the quality of agreement would not be sufficient to predict, for example, the effect of heel stiffness on forward velocity or even more importantly. the effect of the sound leg on the forward velocity (an effect demonstrated from an energy perspective by Bresler and Berry [10] for normals and Bresler, Radcliffe and Berry [12] for A/K amputees).

An alternate approach was used by Rahmani [102] in 1979. Rahmani's work provided some useful insights into normal level walking by using an interpretive modeling approach. He combined the dynamic model with results of an inverse dynamic model. For example, by employing increasingly complicated linkage models, and driving the models with forceplate data, and by constraining some of the models joints to follow published data he was able to predict ankle knee and hip joint forces and torques for normals, and show how different assumptions concerning foot

geometry, limb lengths, and body mass affect the model's predictions. While his method of using experimental data for constraining certain parts of the dynamic model seemed non-physical and somewhat arbitrary, his results seemed to justify his means.

#### II-4.2 Dynamic designer gait models

The dynamic designer gait model approach is similar to the interpretive modeling approach of Rahmani, except that the inputs taken from an inverse dynamics model represent the causally correct physical and biomechanical inputs. The dynamic designer gait model's structure is related to the physical elements of the prosthesis. The inputs are the forces and torques the amputee generates while using the prosthesis. The inputs used in this thesis are

- 1) the sagittal plane hip torque,
- 2) the vertical sound leg force,
- 3) the horizontal sound leg force.

These are all shown in Figure II-12 and represent along with the initial conditions, the inverse dynamics model's crossover with the designer gait model.

The physical structure of the designer model will be developed in Chapter V after the results of the inverse dynamics model in Chapter IV have been discussed. This is necessary since the model structure is motivated by the physical insight gained from the gait data.

In summary, the designer gait model provides an additional tool for the designer to interpret the gait mechanics data in light of specific prosthetic leg design requirements.

### III EXPERIMENTAL WORK

#### III-1 Introduction

The main task of the experimental work was to collect gait data using a Selspot-based gait acquisition system known as TRACK while an A/K amputee used the MIT knee simulator prosthesis in the Mobility Facility of the Eric P. and Evelyn E. Newman Laboratory for Biomechanics and Human Rehabilitation Laboratory for Biomechanics and Human Rehabilitation. The laboratory is 60' x 30' x 15' high with a Kistler Forceplate located approximately half way down a 60' walkway. Two sets of trials were run. 1) The simulator was controlled to simulate a conventional prosthesis. 2) The simulator during prosthetic stance was controlled to follow a modified knee trajectory recorded from the sound knee during the previous sound stance phase. The swing phase controller was identical to the one used in set number 1. This experimental setup required two mini-computers running synchronously. One recorded the global 3-Dimensional kinematics and foot/floor forces, while the other controlled the prosthesis simulator and recorded data from its transducers.

#### III-2 Person-Interactive Prosthesis Simulation

##### III-2.1 Introduction

As was discussed in Chapter I, person-interactive simulation is a method employed for simulating prosthetic knee controllers with the complex inputs required to run the simulation coming from the amputee. Person-interactive simulation is, at least in this case, an A/K amputee wearing a general purpose prosthesis which can be controlled by a digital

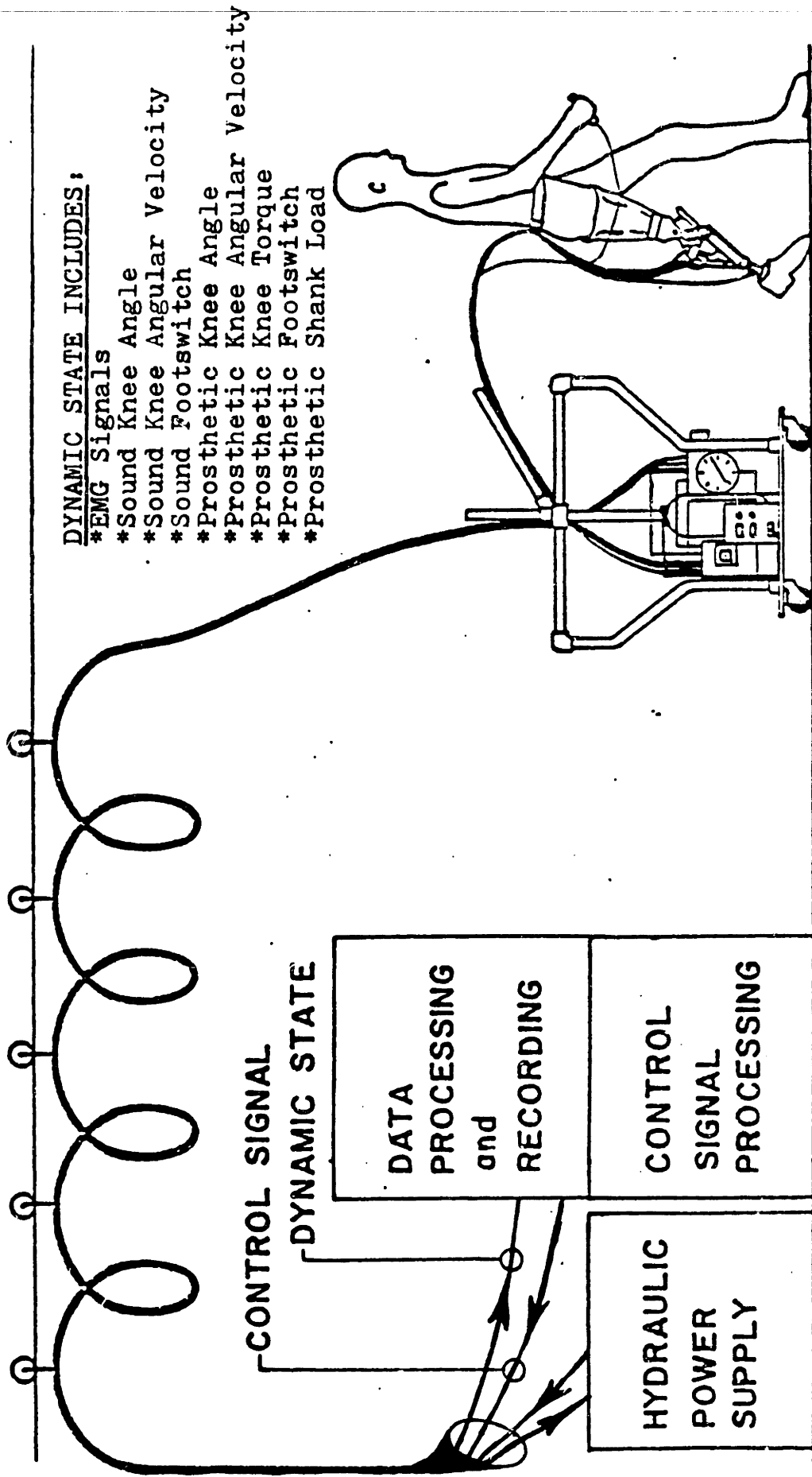
(or analog) computer to simulate almost any prosthesis that is available or a novel controller that a prosthesis designer wishes to test. It is not necessary to build new hardware for each new control scheme, it is only necessary to change the computer control program.

### III-2.2 The Electrohydraulic Simulator System

The A/K prosthesis simulator system used in this study is shown in Figure III-1. This system was developed by Flowers [43,44] and was updated by Grimes [54] (these references contain a complete description of the system). The actual prosthesis is shown in Figure III-2. Movement of the shank about the socket is controlled by a high performance servo valve which controls the flow of 1000 psi hydraulic fluid through an actuating ram. This movement (knee angle) is recorded by a position potentiometer and the net torque developed by the ram and external loads about the knee axis is measured by a load cell and a DCDT.

Control of the prosthesis is accomplished by feeding back the torque and/or the position signal to the servo valve. With torque feedback, the prosthesis behaves like a viscous damper. With position feedback the prosthesis behaves like a spring. If the position feedback is subtracted from a reference position then the leg will follow the reference signal still retaining its spring characteristics. If the gain on the error between the reference signal and the position signal is "large" then the leg will follow the reference signal with essentially no lag and high stiffness. This is called a position follower control.





PERSON INTERACTIVE SIMULATOR  
FIGURE III-1

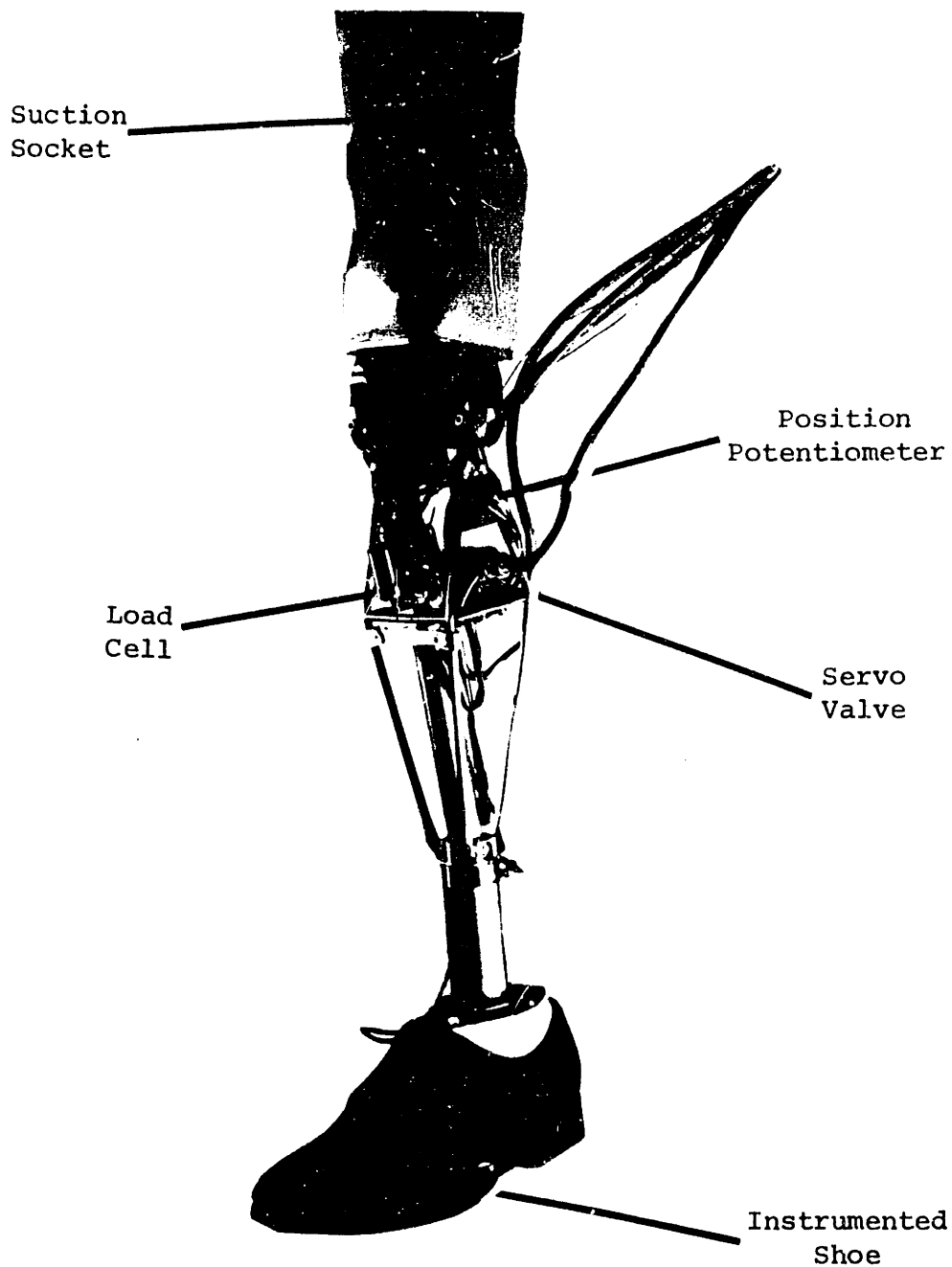


FIGURE III-2

The Electrohydraulic A/K Prosthesis

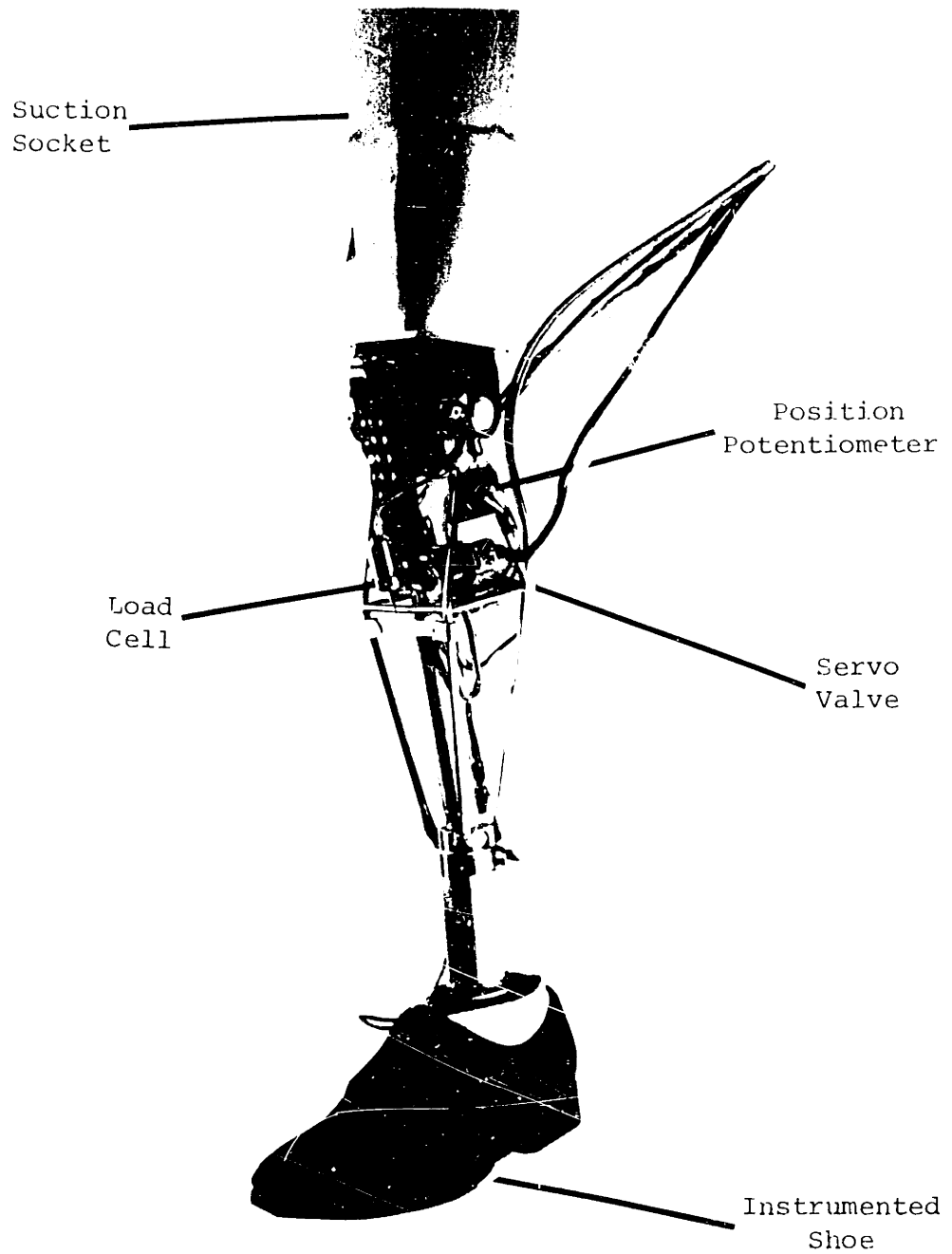


FIGURE III-2

The Electrohydraulic A/K Prosthesis

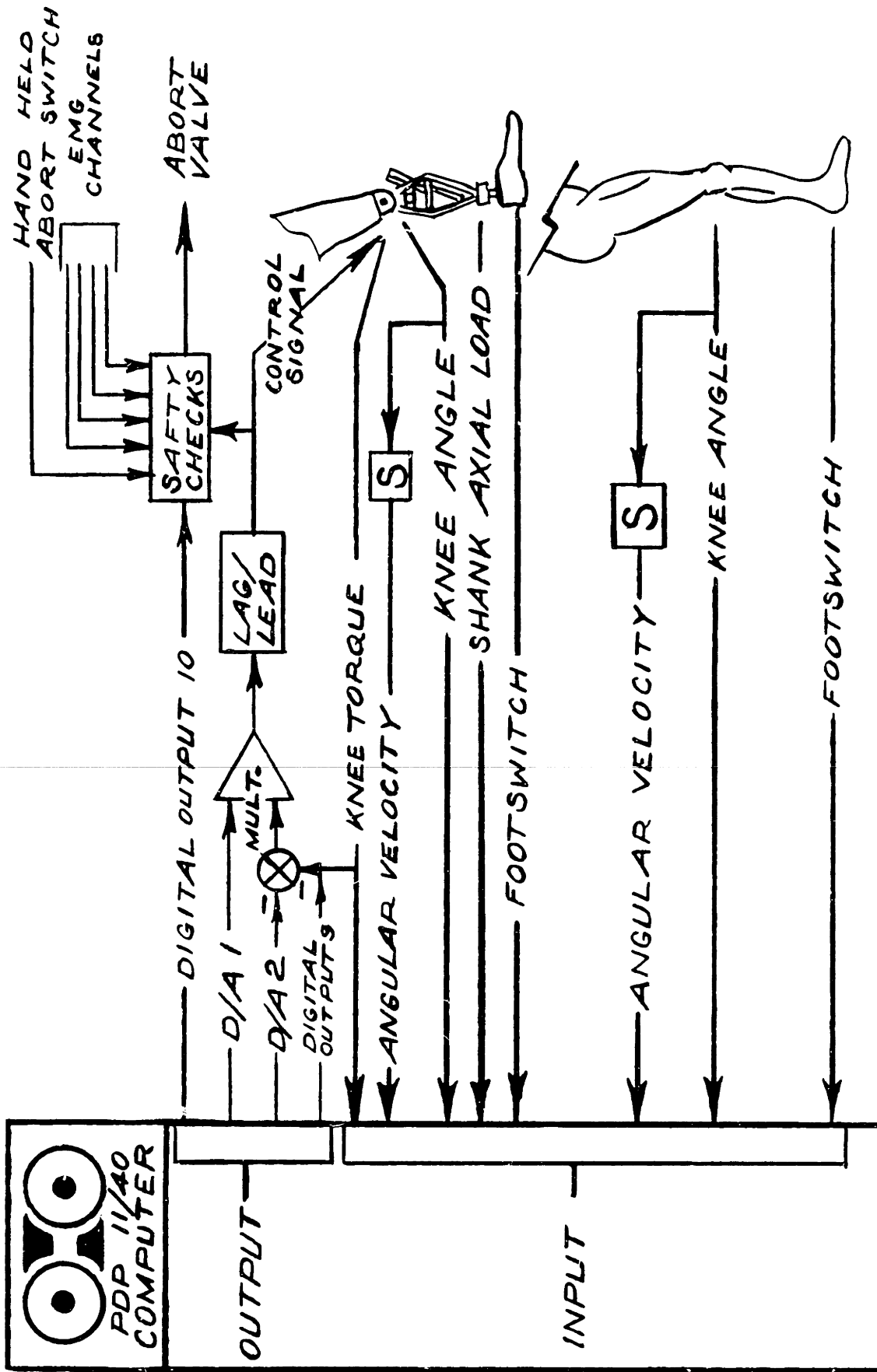
In the complete system the position and torque signal are fed back through a Digital Equipment Corporation PDP11/40 computer. The interface is shown in Figure III-3. Other signals that are available include:

1. angular velocity of prosthetic knee,
2. angle of sound leg knee (recorded by a goniometer attached to amputee leg),
3. angular velocity of the sound leg knee,
4. heel and toe switches on both feet,
5. the load in the shank of prosthesis  
(transducer not shown in Figure III-2),
6. safety check signals.

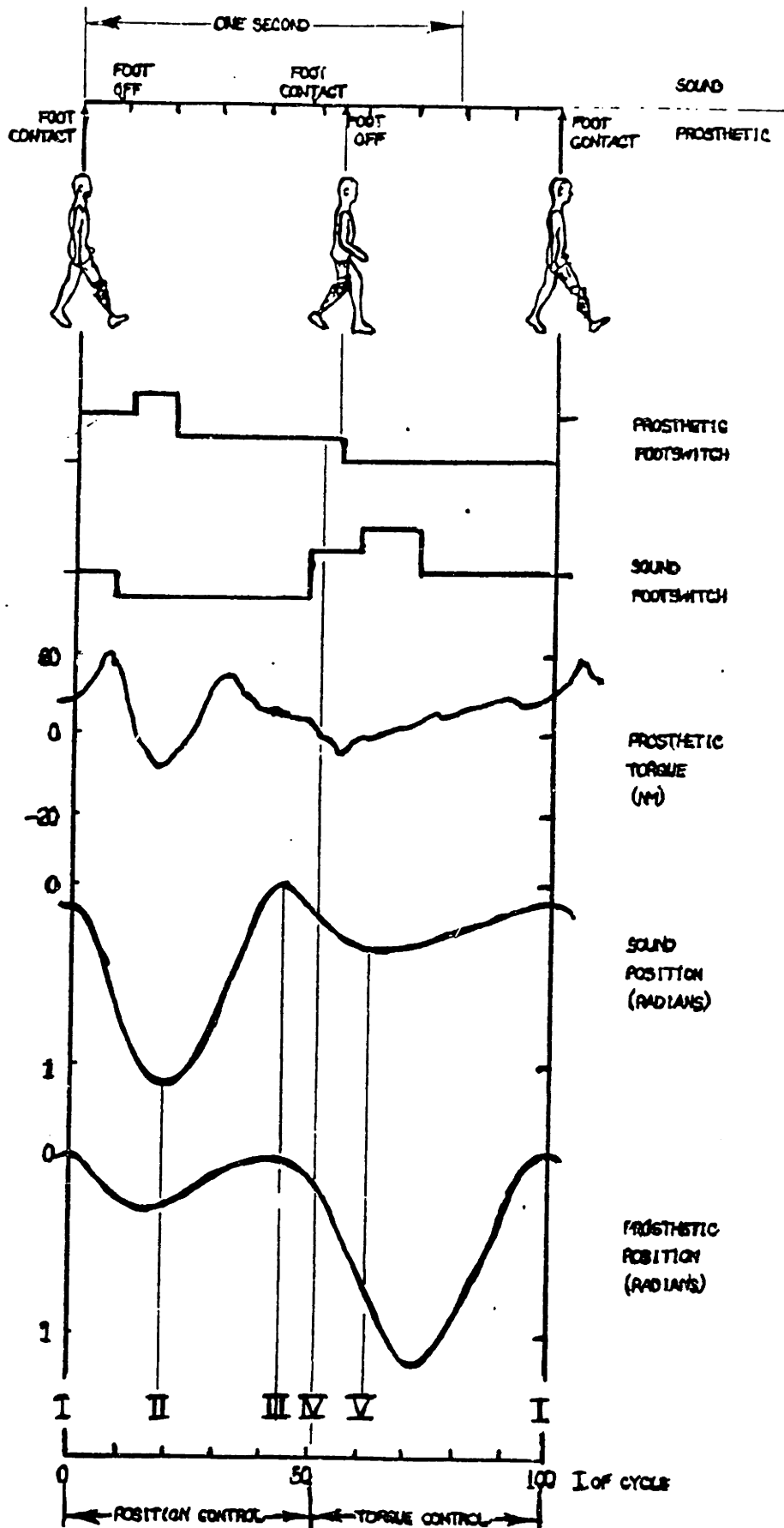
The angular velocity and angular position of the prosthetic knee is used to modulate the gain of the torque loop to give velocity square damping as a function of knee angle as described in Chapter II-2.2.2. This information alone is enough to control the simulator to simulate a conventional A/K prosthesis [54]. The other signals in the list are required to implement modified echo control during the stance phase.

### III-2.3 Implementation of control strategies

Modified echo control was implemented in the following way. At PHC (I in Figure III-4), as measured by the shank load cell, the position control loop on the simulator is closed and the torque loop open. Also cadence is measured and used to modify the sound knee profile, the initial condition of the modified trajectory is then matched to the current position of the simulator. The prosthesis then follows the modified sound knee trajectory. Storage of the sound leg trajectory that the prosthesis



COMPUTER INTERFACE  
 FIGURE III-3



PARAMETER AND CONTROL EVENTS PER CYCLE [54]

FIGURE III-4

is currently following is stopped when the sound knee reaches maximum flexion during swing (II Figure III-4). Storage of the sound profile for the next prosthetic stance phase is started when the sound knee reaches maximum extension right before SHC (III in Figure III-4). Just after SHC when the prosthesis torque becomes flexive the position loop is opened and the torque loop is closed. Modified echo control has ended and conventional damper control has started (IV in Figure III-4). The damping function shown in Figure II-9 is now implemented. From SHC to PTO the damping function in this section marked 1 in Figure II-9 is used. After PTO the damping function in the section marked 2 is used. At approximately this time, the sound leg is reaching maximum knee flexion during stance. This value is stored and used in the calculation of the next scaling factor for modifying the currently being stored sound profile (V in Figure II-9). The section marked 3 is used after 75 degrees of prosthetic knee flexion to prevent excessive heel rise. Sections 4 and 5 are used on swing through with the damping function corresponding to 5 being used within 18 degrees of full extension. At PHC the cycle is complete and restarts. This control routine provides smooth transitions between stance and swing control. Results are presented in Chapter IV.

### III-3 Telemetered Real-time ACquisition of Kinematics (TRACK)

#### III-3.1 Introduction

The inverse dynamics model, discussed in Chapter II-3.2, required as input the kinematics of the individual mass segments and the forces acting on the most distal segment. Measuring these kinematics and forces is the purpose of this section.

The system used in this study to record the three-dimensional kinematics and foot/floor interaction forces is called TRACK. This system was developed principally by Antonsson and Conati [4,5,19] in the Newman Laboratory at MIT. The system can be divided into three main sections that include:

- 1) Hardware for measuring kinematics
- 2) Hardware for measuring forces
- 3) Software for collecting and storing all the data.

In this study the Track systems role was expanded to work synchronously with the person-interactive prosthesis simulator system. In this section the hardware will be discussed. The software will be discussed in Chapter III-4.

#### III-3.2 Measuring the three-dimensional kinematics

The hardware for measuring the 3-dimensional kinematics is a Selspot I system (Selcom AB, Goteborg, Sweden). The system used, has a pair of cameras with lateral-photo-effect diodes (detector plates) at their focal planes. These detectors are sensitive to infra-red light, and (with the aid of some additional electronic equipment) produce a digitized signal



representing the "x,y" location of the centroid of the infra-red light incident on the detector plates surfaces. With two cameras producing four pieces of information (x,y location on each detector plate) the three-dimensional location of the origin of the infra light can be determined. The infra-red light spot on the detector plates comes from an infra-red light emitting diode (LED). If at least 3 LEDs are mounted on a rigid surface or surfaces such that the LEDs are not colinear then the three-dimensional position and rotation of a coordinate system attached to the LED array can be determined.

In this study a planar array of 14 LEDs was securely fastened to the shank of the prosthesis (see Appendix 4 for details on the array construction). A lightweight shroud was placed between the array and the prosthesis to prevent any infra-red light from reflecting off the surfaces of the prosthesis (see Figure III-5).

A large planar array containing 14 LEDs (instead of the required minimum of three) was used to improve the accuracy and reliability of the system. The accuracy is improved because calculating the rotation matrix can be done more accurately if the LEDs are far apart with respect to the positional resolution of the Selspot system. The reliability was improved due to the following. At the start of each sampling period the LEDs are turned on, in a predetermined sequence. Each LED remains on for 50 microseconds with a 50 microseconds delay between LEDs. During the time that the LED is on, and if for any reason (object blocking path of light, a stray reflection etc.) the measured 3-dimensional location of any of the 14 LEDs is out of position with respect to the relative position of the other 13 LEDs, then the information from that LED is discarded for that

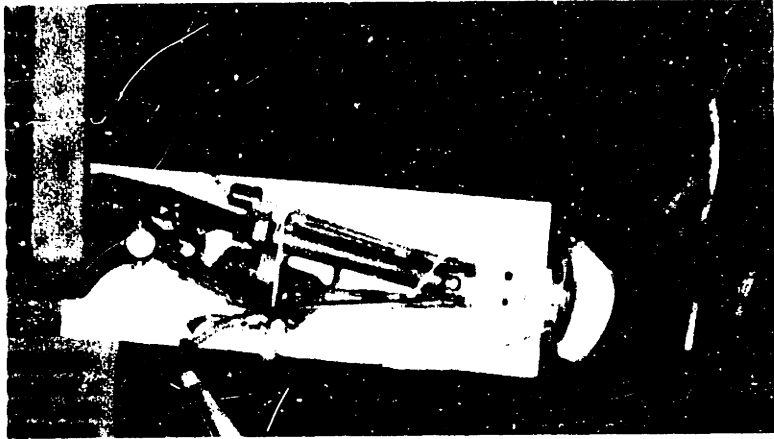
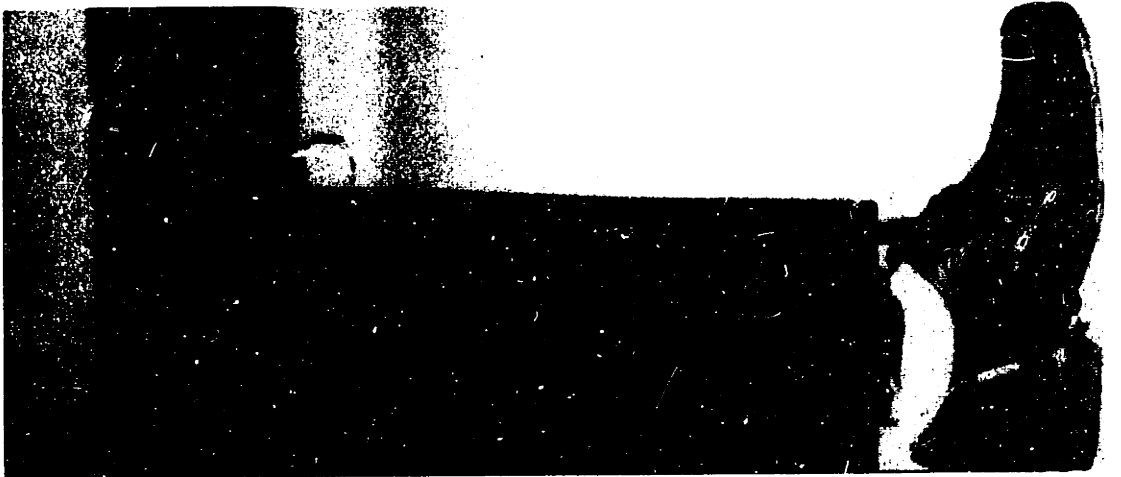


FIGURE III-5

Photograph of Electrohydraulic Prosthesis as Used in This Study.

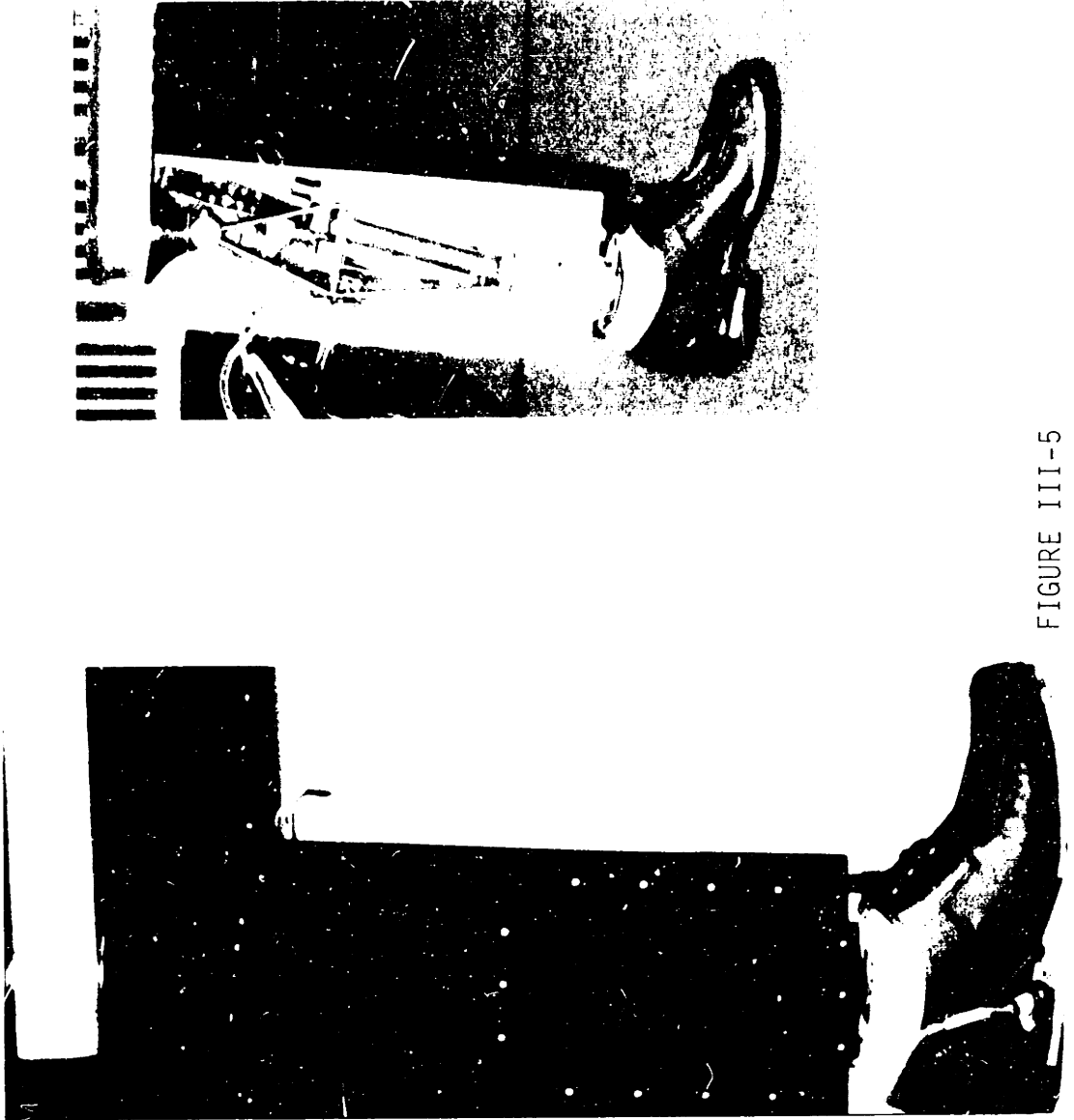


FIGURE III-5

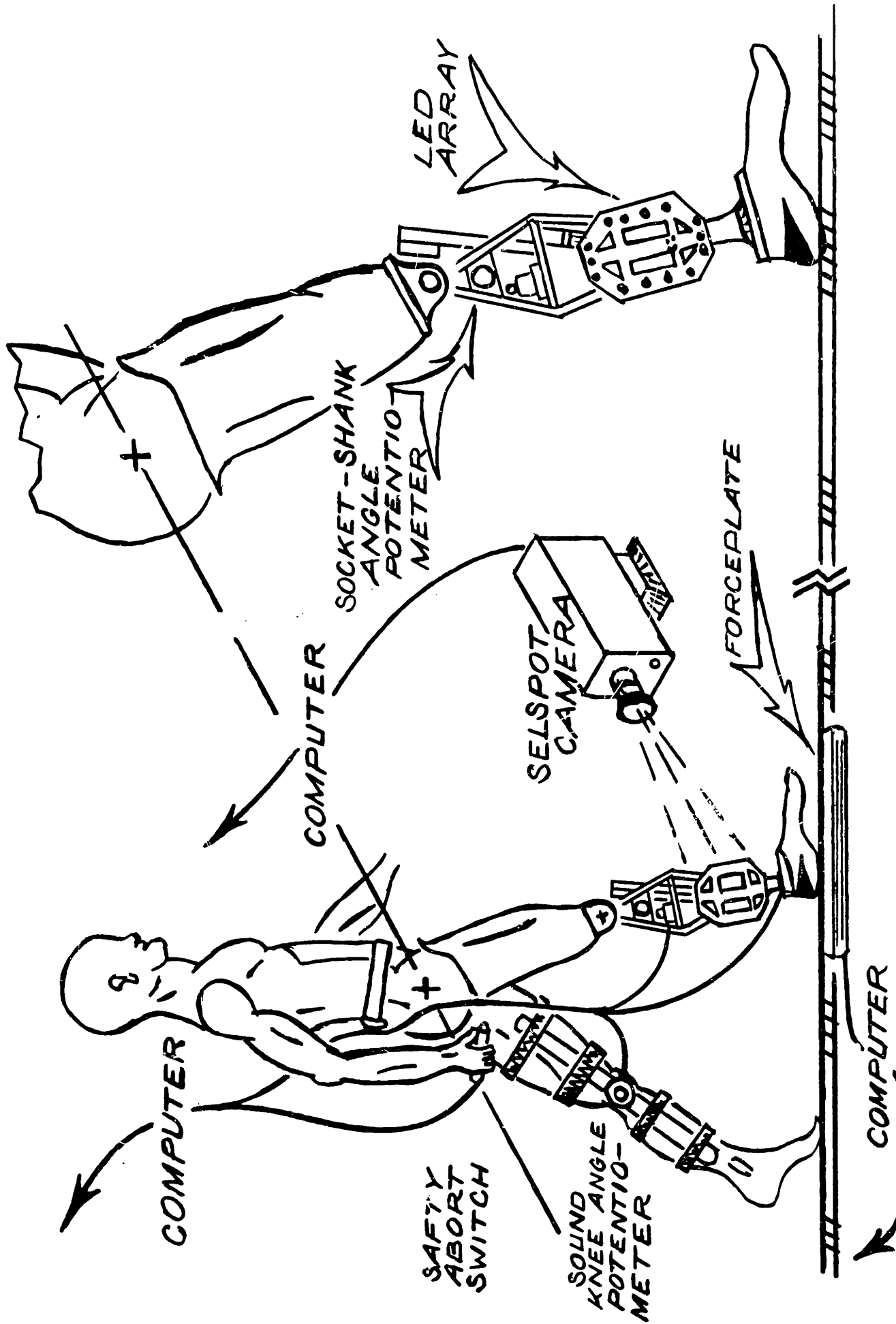
Photograph of Electrohydraulic Prosthesis as Used in This Study.

sampling period. This "checking" process which is part of the TRACK software continues until all the LEDs which do not stay within a user selectable tolerance are discarded. Clearly, the chance of having the minimum of three good LEDs is improved by having a large number of LEDs in an array.

The inverse dynamics model requires the kinematics of all the independent mass segments shown in Figure II-12. This means that the kinematics of the shank and thigh must be measured. A second LED array could have been placed on the socket but the prosthesis has a position potentiometer measuring knee angle as explained in Section 2.2 of this chapter. Since the socket and shank are geometrically constrained to rotate in the same plane, the complete three-dimensional kinematics can be recorded using one LED array on the shank and the position potentiometer at the knee (see Figure III-6). It should be noted that with this method of measuring the kinematics any motion that might exist between the hip and the socket will not be measured.

### III-3.3 Measuring the foot/floor interaction forces

The hardware used to measure the foot/floor interaction forces required for the inverse dynamics model is a Kistler 9281A, multi-component force sensing platform (forceplate) (Kistler Instrument AG Winterthur, Switzerland). The forceplate was mounted flush with the surrounding floor surface [5] approximately 25 feet from the start of the 60 foot walkway. The forceplate measures: force in three orthogonal directions, position of the net center of force on the platform's surface, and the torque about an axis perpendicular to the surface of the



INSTRUMENTATION AND DATA COLLECTION  
 FIGURE III-6

forceplate. The natural frequency of the forceplate is above 1.0 KHz according to the manufacturer's specifications.

### III-4 Data Acquisition

#### III-4.1 General requirements and implementation

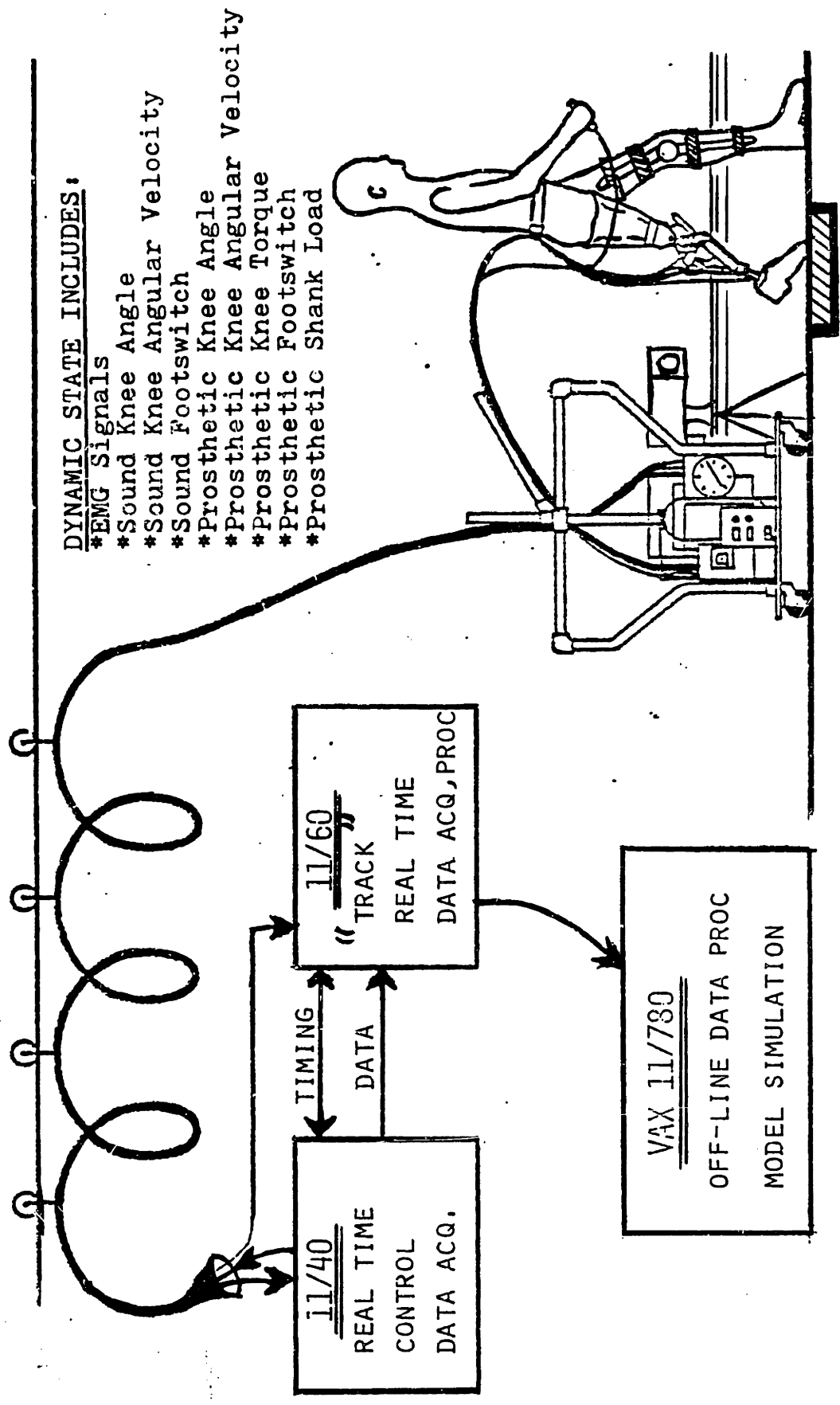
The complete data acquisition system is shown in Figure III-7. From a software design point of view, the following specification needed to be satisfied:

On a Digital Equipment Corporation PDP11/40 -

- 1) control the electro hydraulic simulator implementing the ME and CL controller;
- 2) while the simulator is being controlled on command from an external source record 8 channels of A/D information for at least one complete gait cycle;
- 3) while the simulator continues to be used, save this data under a user selectable filename.

On a Digital Equipment Corporation PDP11/60 -

- 1) record all Selspot produced kinematic data for at least one gait cycle;
- 2) synchronously record all the forceplate data for one prosthetic stance phase;
- 3) send out flags to PDP11/40 to start and stop recording



DYNAMIC STATE INCLUDES:

- \*EMG Signals
- \*Sound Knee Angle
- \*Sound Knee Angular Velocity
- \*Sound Footswitch
- \*Prosthetic Knee Angle
- \*Prosthetic Knee Angular Velocity
- \*Prosthetic Knee Torque
- \*Prosthetic Footswitch
- \*Prosthetic Shank Load

"THE TOOL"  
FIGURE III-7

- the data from the simulator system  
synchronously with the Selspot systems;
- 4) save data under the same filename  
as used on the 11/40.

To meet the requirements specified for the PDP11/40 a FORTRAN program called STANCE was written. This program will allow the user to select at the beginning of a trial, either the ME or CL control. The program will continuously control the simulator while simultaneously recording (upon command from the 11/60) the eight channels of D/A information available from the simulator's transducers (see Figure III-3). After the data stream is terminated by the 11/60, the user can select a filename and brief description of the data trial, and the data will be saved on disk without interruption of the control algorithms. A listing of program STANCE is in Appendix 9.

The requirements for the 11/60 as stated above were met by a large set of existing programs collectively known as TRACK3 (track version III). Written by Antonsson [5] they provide all the user selectability and performance stated above. See reference for a description and listing of those programs.

A sampling frequency of approximately 150 Hz was used for both controlling the simulator and collecting data with the track systems. The actual sampling frequency was 157.5 Hz which is the nearest sampling frequency to 150 Hz that the selspot hardware could implement.



## III-5 Data Processing

### III-5.1 General requirements

At the end of a data acquisition run the simulator and track data are stored in raw form on their respective computer systems. A data processing software system was written to perform the following:

On the 11/40 -

- 1) convert raw simulator data to standard form and send file to the 11/60

On the 11/60 -

- 1) convert raw TRACK data into three-dimensional position and rotation of the shank and foot/floor interaction forces;
- 2) filter simulator and TRACK data;
- 3) determine velocity and acceleration from position data;
- 4) combine data from each systems and calculate the joint forces and torque using the inverse dynamics model and send a copy of the results to the VAX11/782;
- 5) plot the results.

On the VAX11/782 -

- 1) combine inverse dynamic model data

with designer gait model and

run simulation

## 2) plot results

The software used was written in FORTRAN or assembly code. The programs to convert the raw TRACK data are part of the TRACK III system and can be found in reference [5]. Except for the differentiation and filter routines, details of the rest of the software are omitted due to their lack of general applicability.

The digital differentiation routines used to calculate the derivatives of the kinematic TRACK data and the simulator knee angle data were calculated using a five-point Lagrangian technique for equally spaced (with respect to the independent variable i.e. time) points (see Antonsson [4]).

### III-5.2 Digital filtering

A digital low pass filter was used in the study to filter the position data before it was differentiated to produce velocity and acceleration information. Because differentiation is a "noise" amplifier, it is particularly important that the filter remove all unwanted noise without corrupting the gait data in its passband. (The noise is presumed to have a frequency content spectrum that does not overlap the desired gait data). This is a particular problem with one cycle of gait which is a short transient stream of data because, in addition to filtering the high frequency noise, the filter can ring, corrupting the data around the cutoff frequency of the filter. It is important to design the filter in both the frequency and time domains. For example, the ubiquitous

Butterworth filter (especially high order versions) have excellent frequency response characteristics. They are exceptionally flat in the passband right up to the desired cutoff frequency and have a sharp roll off thereafter. However, the transient response (settling time) of the Butterworth filters, especially for higher order versions, is poor [8].

A third order filter was designed by using "Dynamic Response Plots and Design Charts for Third-Order Linear Systems" by Meyfarth [82]. This reference provided a method for calculating the coefficients of a constant coefficients, linear, 3rd order differential equation as a function of the desired step and frequency responses. Coefficients were chosen to give the "optimum" fast rise and short settling times. The filter was then implemented directly in a difference equation. (This was possible due to the sampling frequency being approximately 10 times the filter cutoff frequency.) The data was filtered both forwards and backwards in time to remove the phase shift introduced by the filter. This also has the effect of making the filter 6th order. A program FLTAUT implementing this filter is listed in Appendix 8. The filter was named the Stein filter.

As a bench mark of performance the unit step response of the Stein filter was compared to the Butterworth filter. While this is not a definitive test, it does shed some light on the improvement, if any, the Stein filter has in the time domain. Using a 10 Hz cutoff frequency for both filters, the rise time (time to get from 0% to 90% of the way to the first crossing (or final value)), the settling time (time to get within 2% of the final value) and the percent overshoot were compared. The rise time of the Butterworth filter was 30 percent shorter, however, the Stein filter settled out 55 percent sooner and had 95 percent less overshoot.

Overall by judiciously selecting the cutoff frequency, better performance was obtained with the Stein filter on the actual data.

### III-6 Calibration

#### III-6.1 General requirements

There are two measurement systems used in this study. They include:

- 1) the TRACK system;
- 2) the prosthesis simulator system.

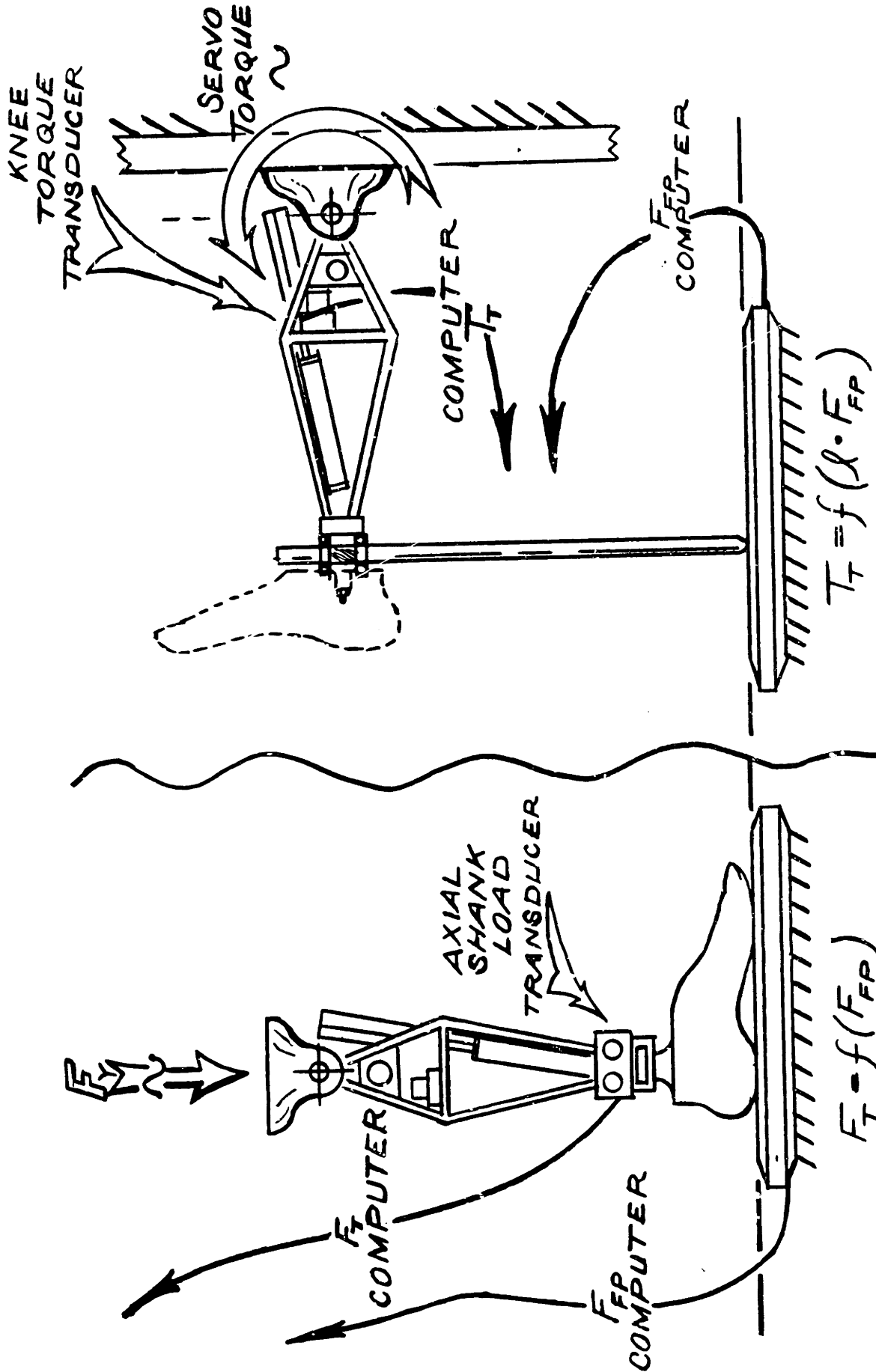
The TRACK system was calibrated by Antonsson [5] and shown to have 1 mm positional accuracy and 1.2 degree rotational accuracy. The forceplate manufacturer claims a .3 percent accuracy throughout the load range of the platform. The values were accepted as being correct. The prosthesis simulator, however, has several transducers which required calibration.

#### III-6.2 Electrohydraulic simulator system calibration

The simulator has three transducers which required calibration. They included:

- 1) the knee torque transducer,
- 2) the shank load transducer,
- 3) the knee angle position potentiometers.

The knee torque and shank load transducers were calibrated against the forceplate. The shank load cell was calibrated by simply pushing it against the forceplate while holding it vertical. The contact with the forceplate was through a ball bearing. The Selspot system monitored the actual angle of the leg (see Figure III-8). The load was dynamically



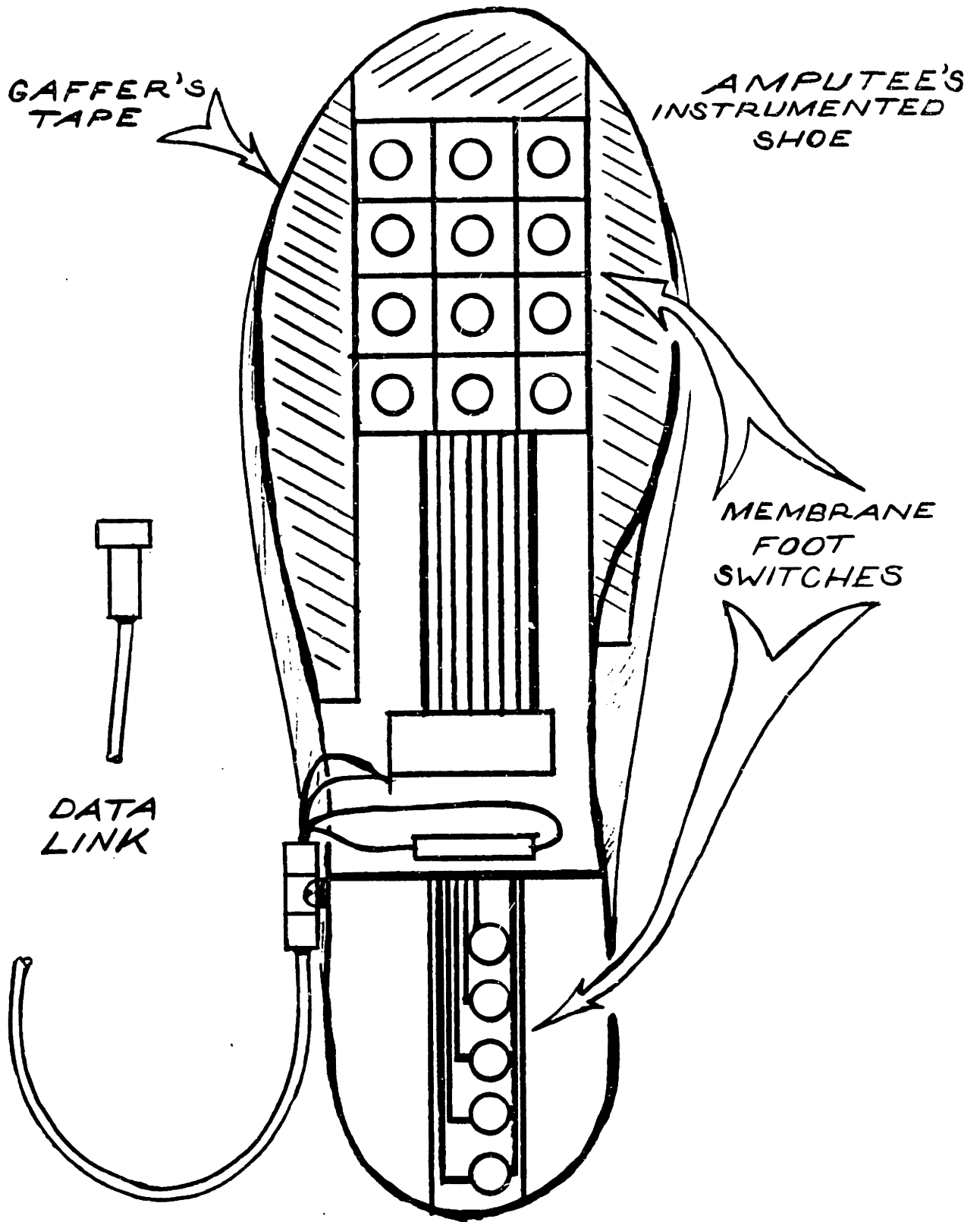
SHANK LOAD CELL AND KNEE TORQUE CALIBRATION  
FIGURE III-8

varied during the sampling period of 2 seconds. The shank load cells output was then compared to TRACK's calculation of shank load (forceplate plus static angle correction). The load cell was within 1% of the forceplate. However, when this procedure was repeated, replacing the ball bearing with a SACH foot the moments generated in the shank caused the shank load cell to give unacceptable results. Therefore, the shank load cell was only used in this study to determine PHC.

The knee torque transducer was calibrated in a similar manner but with the configuration shown in Figure III-8. In this case, the dynamic load was applied by the simulator system pushing itself against the forceplate. The forceplate load was then compared to the knee torque transducer divided by the moment arm. This produced agreement to within 3 percent over the normal range of knee torques.

The knee angle potentiometers on the sound leg goniometer and in the simulator were calibrated in two ways. First, a carpenter's square was used to find a position calibration factor based on two points, zero degrees and 90 degrees. Second, the simulator was only rotated through 90 degrees in front of the Selspot cameras. The angles were equivalent to within 1 degree over the entire range.

The footswitches used on the soles of the shoes were membrane switches manufactured by Molex. Two different patterns of cells were used as shown in Figure III-9. A one by five array of cells was used on the heel to try to get as close to the back of the heel as possible. A four by three array was used on the toe of the shoe to cover as much area as possible. The cells in any one switch are connected in parallel, so only



HEEL AND TOE FOOTSWITCHES  
FIGURE III-9

one cell needs to be closed to indicate heel or toe contact.

The fact that the switches are located at discrete location on the foot means that there is a delay between when actual HC occurs and when the heel footswitch closes. This is similarly true for T0. As a result of this, the shank load cell was used to indicate PHC and PTO to the ME control algorithm. The prosthetic footswitches were only used to indicate PFF. The sound footswitch, however, had to be used for the ME controller. It was calibrated by having a normal walk across the forceplate and compare the forceplate output to the footswitch closings. The delay between sound heel contact and the second cell in the heel array closing was approximately 30 milliseconds (the first cell failed (the only failure) in the first week of calibration and a replacement could not be obtained). The delay between footswitch indicated ST0 and actual ST0 was 50 milliseconds, even greater than for the heel switch and had a lot more variability depending how the subject actually rolled off the shoe. In fact, the subject could be instructed to "linger" on his toe at T0 and cause the switch to open and reclose causing errors in predicting ST0 of over 100 milliseconds. This was also observed in the amputee trials. The sound switch although used (and successfully) in the ME control scheme (ME controller is not concerned about ST0) should not be considered as an indicator of ST0. ST0 can be estimated from the sound leg forces (see Chapter IV-3.5).



### III-6.3 Overall system accuracy - confidence limits

The accuracy of the track system in estimating joint forces and torques depends on a large number of events some of which have already been discussed with respect to the inverse dynamics model in Chapter II-3.2. Antonsson attempted to determine the errors in estimating joint forces and torques with TRACK [5]. His upper bound estimates of hip joint force and torque errors, however, are much too conservative to apply to this work for several reasons: 1) there are no soft tissue interfaces affecting the LED arrays, and 2) this study is for the stance phase only and therefore the gravity load term (forceplate) dominates (Zarragh [120]), for example, the calculation of the vertical force at the hip. No attempt is made to redo Antonsson's analysis. His calibration of the Selspot system and those done in this thesis clearly indicate that the major contribution to uncertainty is the noise level associated with twice differentiated position data (accelerations). Since this thesis is concerned with determining the design issues associated stance phase control by testing (comparing) two controllers, then if the results produce two distinct noisy patterns which do not overlap, and each are related to a particular controller, then those patterns are significantly different. It is on this basis, combined with the high degree of confidence in the calibration of the individual components, that allows the results in Chapters 4 and 5 to be reliable and useful.

### III-7 Procedures

One subject was tested over a six month period in the Mobility Facility of the Eric P. and Evelyn E. Newman Laboratory for Biomechanics and Human Rehabilitation in the Mechanical Engineering Department at MIT. A total of 17 experimental sessions each lasting 1 1/2 to 3 hours were conducted. A duplicate of the amputee's everyday SACH foot was used with the simulator (Otto Bock, Pedilan Soft heel, Size 11) and the amputee's prosthesis alignment was also duplicated on the simulator. The first four months were exclusively testing the CL controller and data acquisition system but over the last two months both controllers were used. The subject was asked to walk at a comfortable pace and was given as much time to get comfortable as he felt was needed before data was taken or the ME controller activated. The subject was asked for comments concerning the system's performance throughout the experimental session. If a request was made adjustments were made accordingly. The subject paced off his own distance from the forceplate. A total of four strides occurred by the time the subject reached the general area of the plate. Strip chart recordings of knee angle indicated that the subject was in steady state after three strides. The forceplate location while generally known by the subject was not easily seen and therefore often missed. This behavior was rewarded so that no special effort would be made to step directly on the plate. The subject was generally unaware of which trials were data collecting trials.

### III-8 Subject

The subject who participated in this study is a left, unilateral A/K amputee with no other health complications. He is a 26 year old male, 5'7" tall, weighs 150 pounds with his prosthesis on, and has been an amputee since age 12. He wears a prosthesis with a Mauch S-N-S knee unit and an Otto Bock, SACH foot with a soft heel. He is an active person and a good walker.

## IV RESULTS

### IV-1 Data Format

In order to maximize clarity, and unless otherwise noted, all figures containing gait mechanics are presented in a consistent format. The abscissa is either actual time in seconds or time as a percentage of the total time, where total time is the time of the prosthetic stance phase. Time equal zero seconds or percent corresponds to PHC and time equal to maximum time shown or 100 percent is PTO. Since all the data is for one amputee with a left side amputation, all plots are for the left or prosthetic leg. Torques and angular kinematics are shown in the body coordinate systems, i.e. sagittal plane, while forces and translational kinematics are in the global coordinate system, i.e. the average plane of progression. These planes, in general, do not differ greatly but as seen in Figure IV-1 may be rotated with respect to one another about a vertical axis by as much as 15 degrees. The sign convention is flexion is positive. Forward displacement is defined as zero at the location of PHC. Vertical displacement is zero at the floor (see Appendix 5). All figures are either the average of all the trials, data from one trial that is considered typical or a large sample the plots to show data scatter. A run number is shown with a figure containing a typical run. The run number is defined in Appendix 6. Unless otherwise stated, the values quoted in reference to a Figure containing samples of several runs represent approximate averages of all the runs displayed. All variables are in the MKS system of units except for angular displacement which is in degrees.

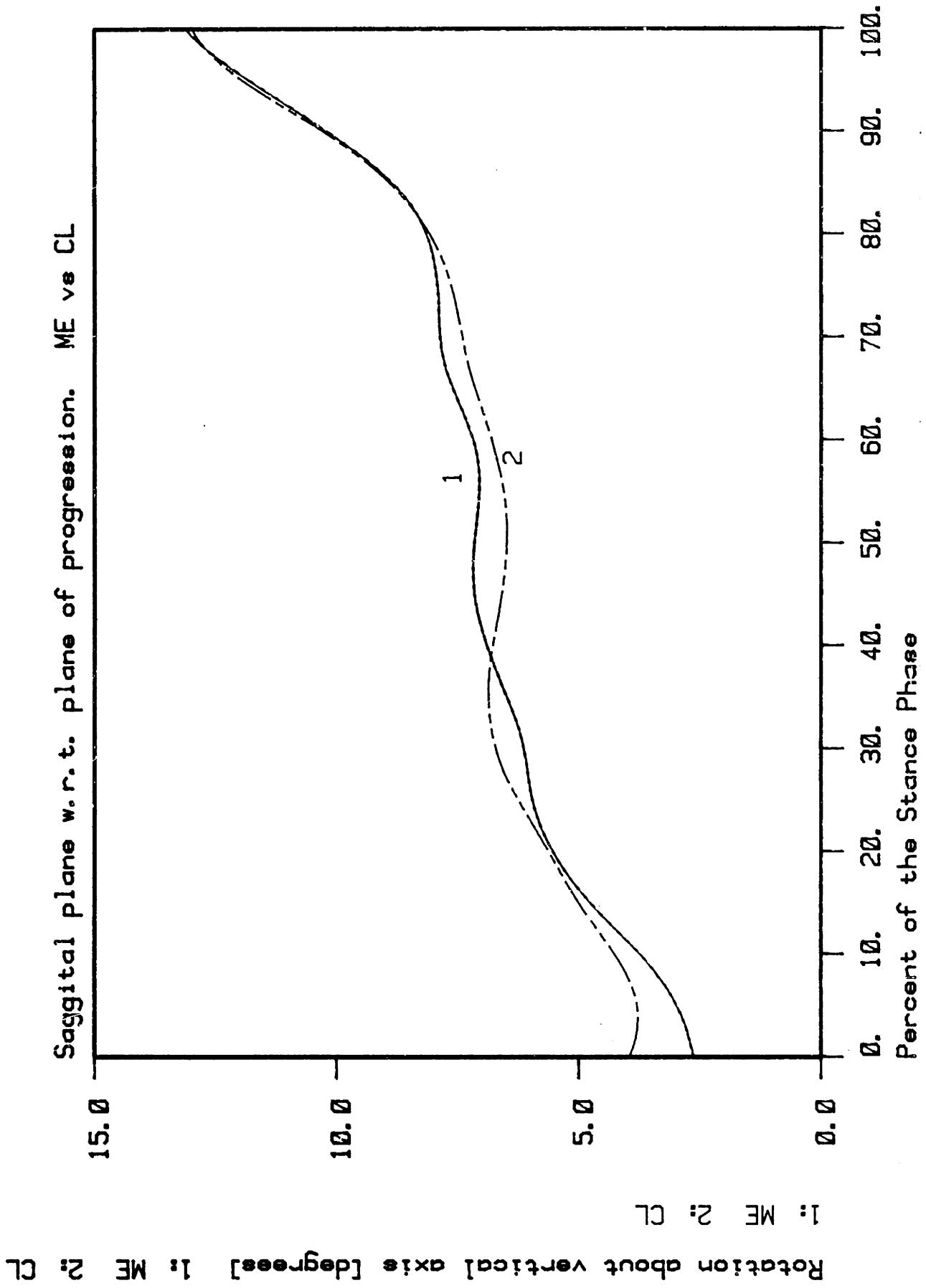


FIGURE IV-1

A Typical Relative Rotation of the Sagittal Plane of the Prosthetic Shank with Respect to the Plane of Progression. Run JL2024.

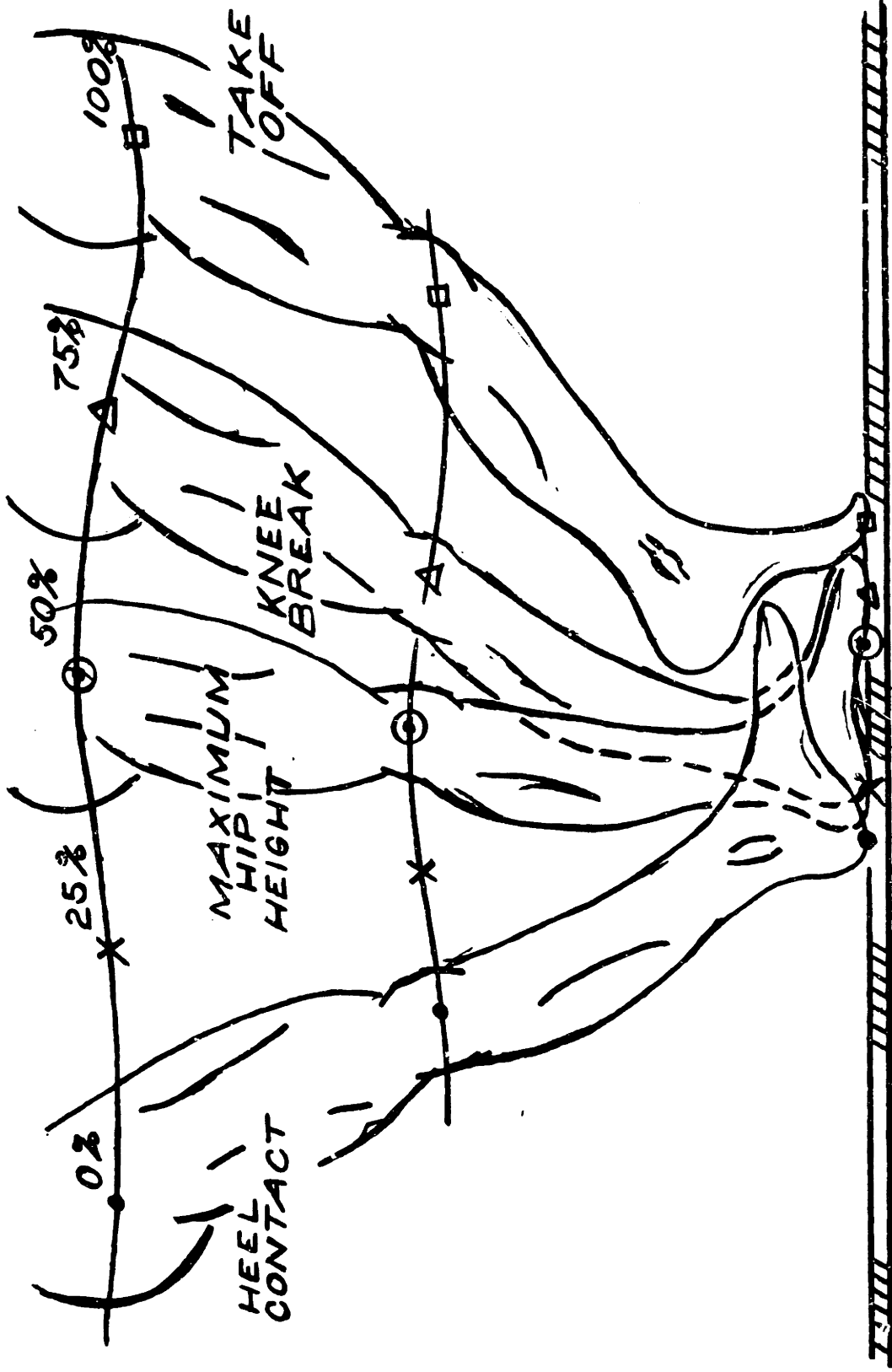
## IV-2 Kinematics

### IV-2.1 Overall kinematics - Figures IV-2 and IV-3

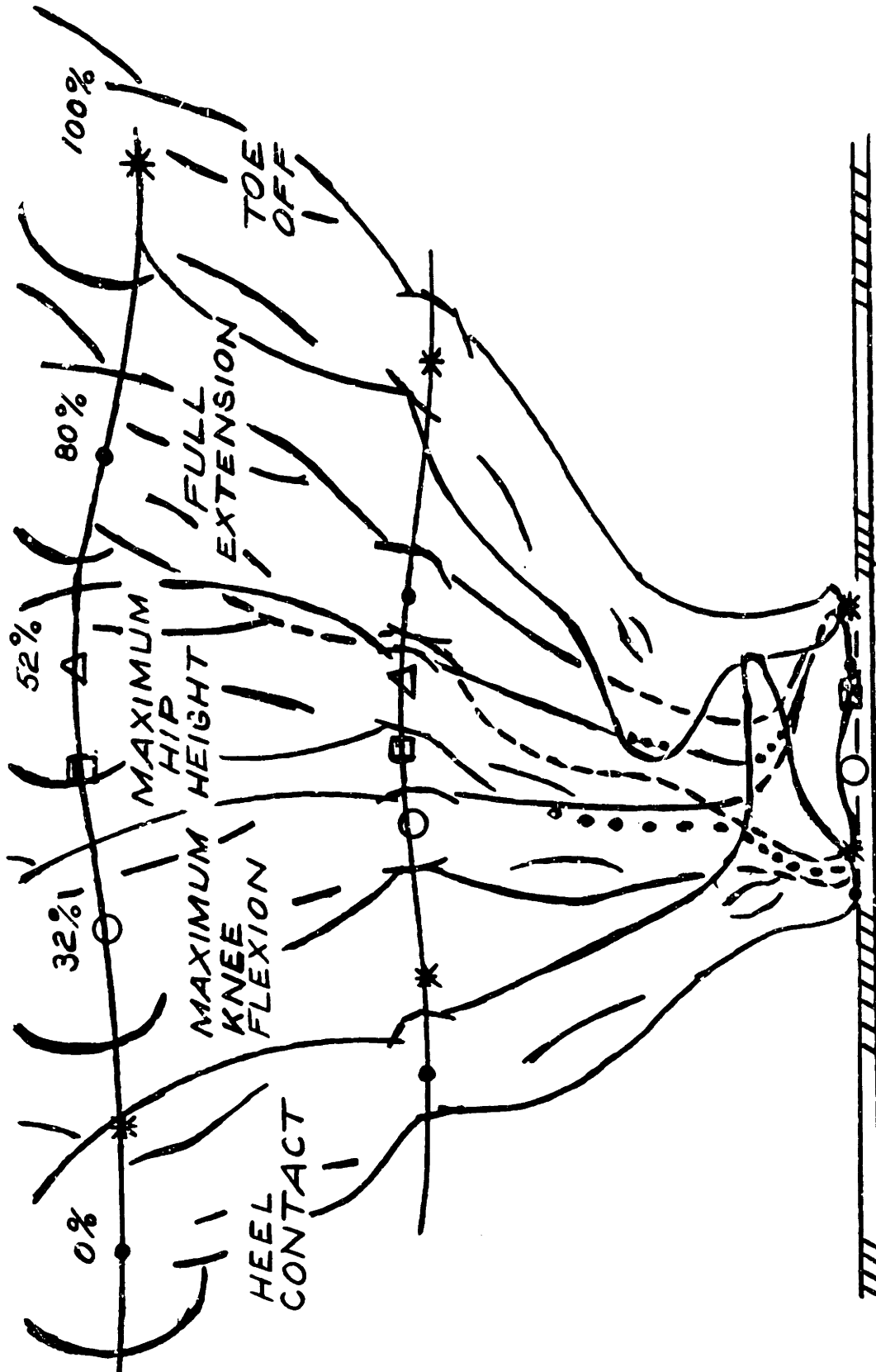
A representation of the prosthetic leg motion during the stance phase of level walking for the CL and ME stance phase knee controllers is presented in Figures IV-2 and IV-3 respectively. The leg sketches were generated by drawing the general outline of the leg around the known positions of the hip and knee joints, and the foot's center of pressure as a percent of the stance phase. Since all this kinematic information and more will be presented separately in the following sections, no description of the kinematics of the gait process will be given here. Instead the reader is encouraged to refer to these sketches often during the following detailed descriptions to help conceptualize the entire prosthetic leg kinematics during the stance phase of level walking.

### IV-2.2 Prosthetic knee angle - Figures IV-4 and IV-5

If implementation of the controllers is successful then by definition the prosthetic knee angle trajectories will be different. Under CL control, knee angle plots show that the knee joint is in full extension 5 percent after PHC and remains there until knee break occurs at SHC. Under ME control, the prosthetic knee angle equals the CL case at PHC (3 degrees flexion). In the first 5 percent of stance the knee angle extends to a maximum of 1 degree. Then starts to flex reaching a maximum of 14 degrees at 33 percent. The knee then extends to within 5 degrees of full extension at SHC. At SHC the ME controller changes into a CL controller and the knee begins to flex in a manner similar to the trials using the CL controller exclusively, reaching approximately 30 degrees of knee flexion



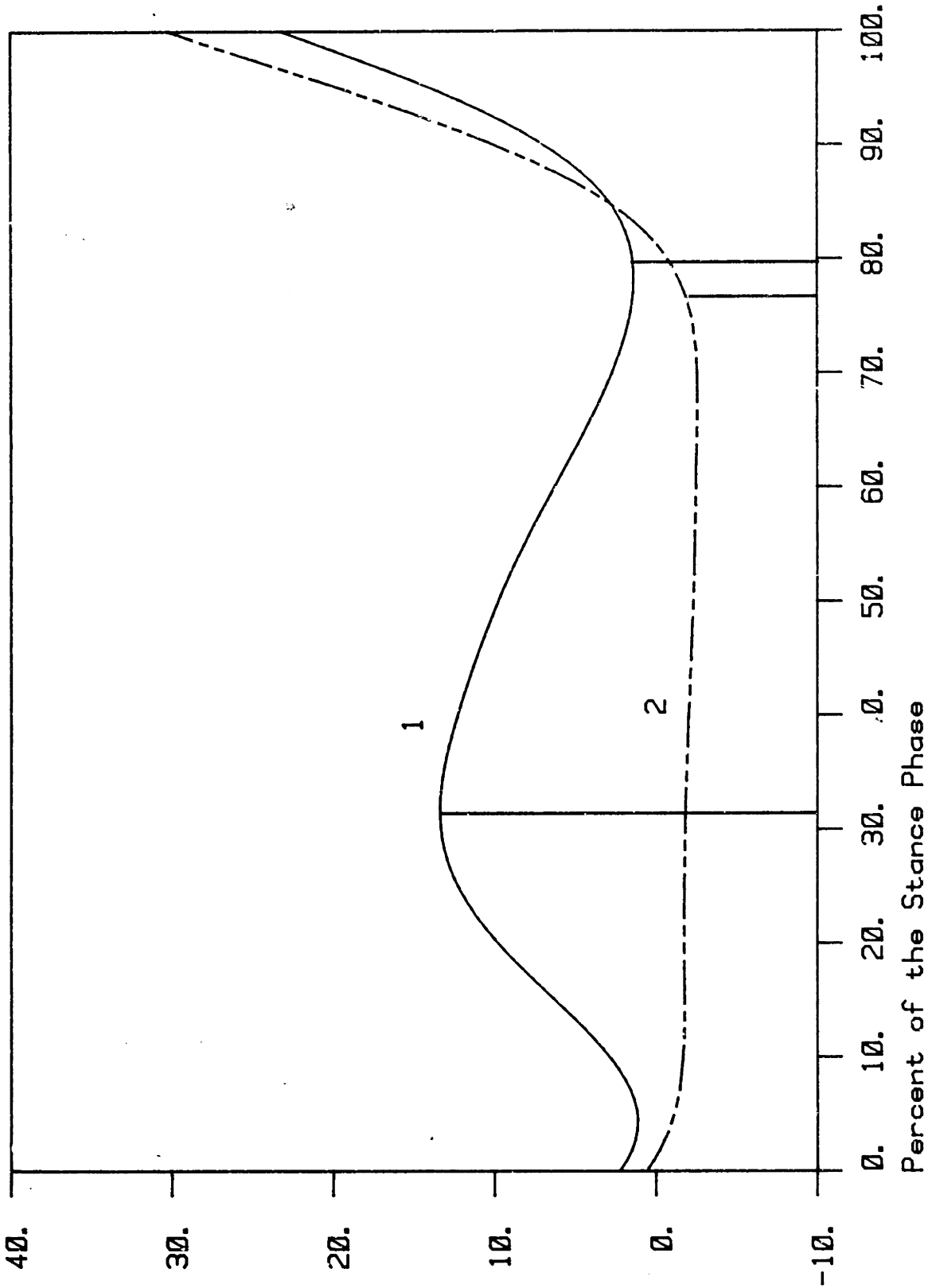
JOINT TRAJECTORIES  
 (STRAIGHT KNEE)  
 FIGURE IV - 2



JOINT TRAJECTORIES  
(FLEXIBLE KNEE)  
FIGURE IV-3



A comparison of prosthetic knee angles. ME vs CL JL1427.94



Knee Angle [degrees] 1: ME 2: CL

FIGURE IV-4

Typical Prosthetic Knee Angle Trajectories During Stance. A Comparison of ME vs CL Stance Phase Knee Controllers. Run JL1494 vs JL1427

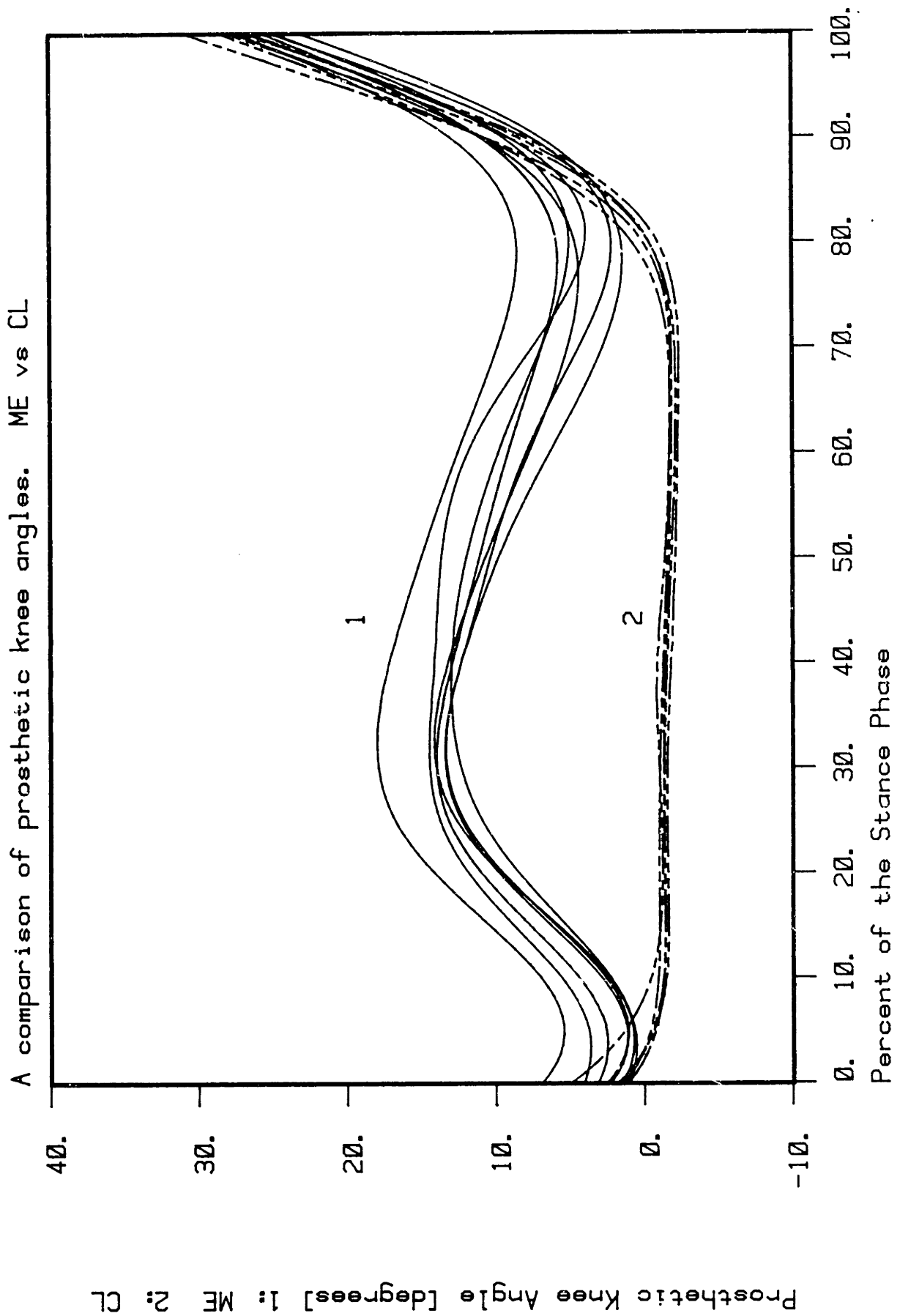


FIGURE IV-5

A Sample of Prosthetic Knee Angle Trajectories During Stance. A Comparison of ME vs CL Stance Phase Knee Controllers

at PTO. The data scatter between trials is very small for the CL controller partly because the amputee has years of experience with it. The ME controller shows more scatter partly from lack of experience but also because there is no hard geometric constraint being set for the sound knee which is, of course, setting up the trajectory for the prosthetic knee to follow.

#### IV-2.3 Prosthetic shank angle - Figures IV-6 and IV-7

The ME and CL knee controllers have the same initial condition on shank angle trajectories (20 degrees at PHC) but diverge after that up until knee break (approximately 80 percent) where they reconverge, exiting stance at the same value.

Under CL control the angular velocity is relatively constant producing a linear change in shank angle with time up to knee break (78 percent). After knee break a more rapid forward rotation produces a second steeper shank angle slope. Under ME control active knee flexion after PHC causes the shank to rotate forward more rapidly than under CL control, producing a maximum lead angle of 6 degrees at around maximum knee flexion. As the knee extends the shank angular velocity slows down converging with the CL case at SHC and remaining converged through PTO. The fact that the two control schemes converge in terms of shank angle after SHC is related to, but not guaranteed by the fact that, the ME controller changes to a CL controller at SHC (see Figure IV-8).

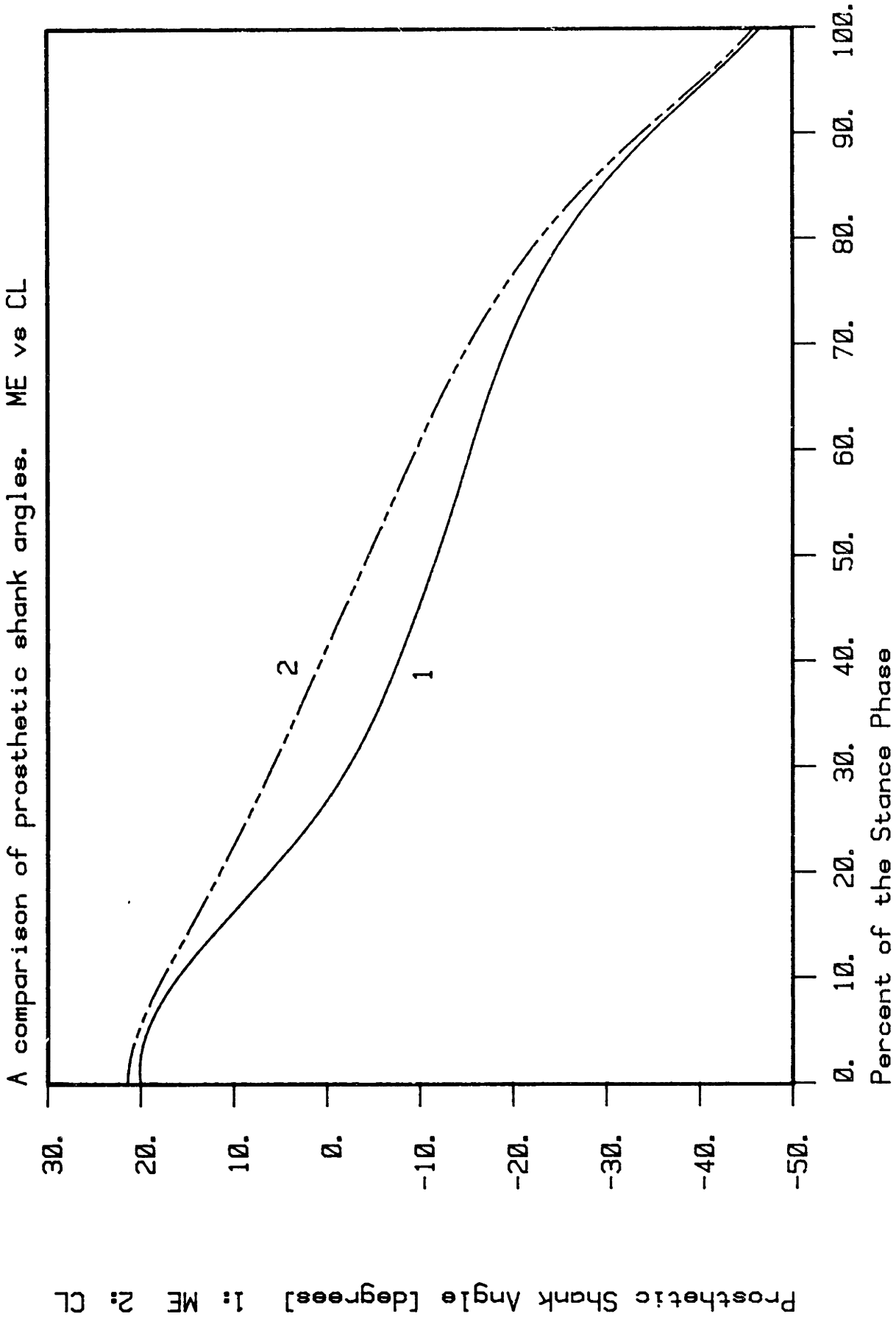


FIGURE IV-6

Typical Prosthetic Shank Angle Trajectories During Stance. A Comparison of ME vs CL Stance

Phase Knee Controllers. Run JL1427 vs JL2022.

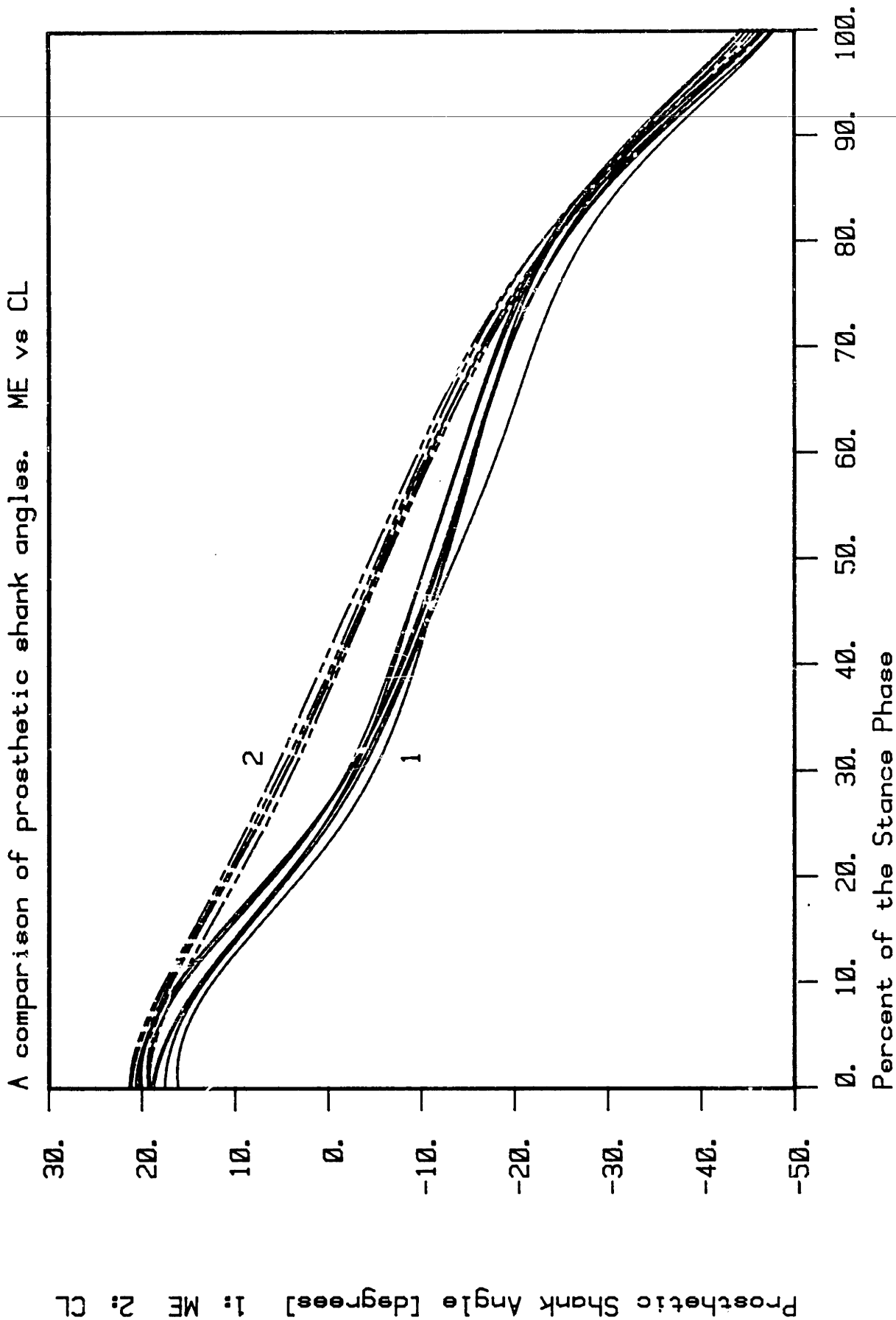


FIGURE IV-7

A Sample of Prosthetic Shank Angle Trajectories During Stance. A Comparison of ME vs CL Stance Phase Knee Controllers

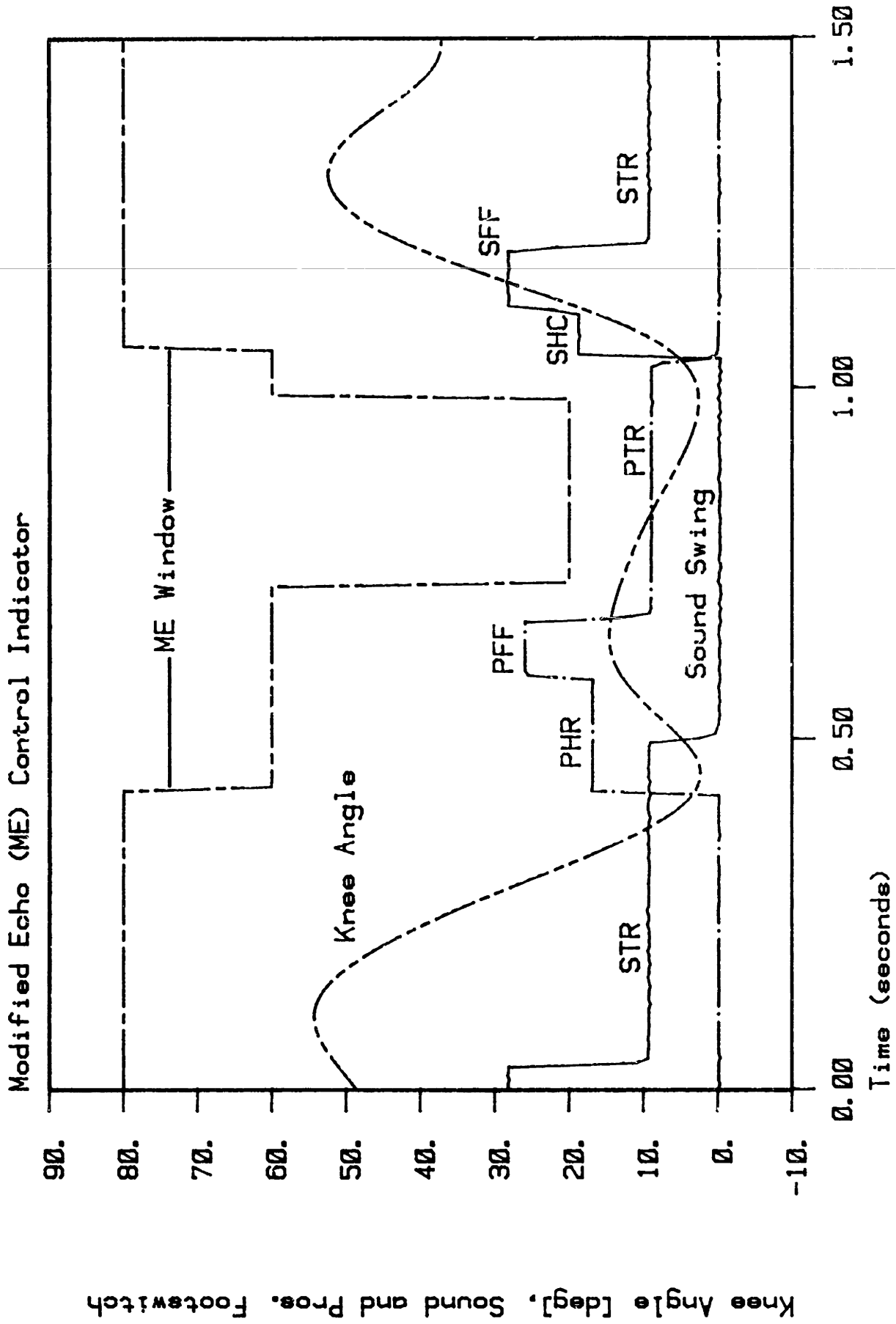


FIGURE IV-8

The Initiation and Termination of the ME Stance Phase Controller

#### IV-2.4 Foot placement timing - Figures IV-9, IV-10, IV-11, and IV-12

The subject was requested to walk at a normal comfortable pace. The cadence for this subject was an average of 110 steps per minute with the CL controller versus an average of 100 steps per minute with the ME controller. The major difference between these two controllers can be seen at PFF. In a very consistent manner the ME controller produces footflat which occurs approximately 33 percent sooner and whose duration is 27 percent shorter in time. Figure IV-12 shows that PTC occurs at 4 degrees and PHO occurs at -5 degrees independent of the controller used. This is related to shank angle movement (see Figure IV-6). Because the SACH foot provides no articulated ankle function and has a relatively fixed geometric shape near footflat, the relationship between footflat and shank angle is kinematic.

The sound leg timing is also affected by the controller used. This result, however, cannot be accurately determined by the sound leg foot switches. As was mentioned in Chapter III-6.2, the physical placement of the footswitches on the sole of the shoe causes an error between actual STO and measured STO. Sound leg foot placement timing was, therefore, inferred from the prosthetic foot/floor interaction forces, and the sound leg forces. The result is that STO is affected by the controller used. An average STO occurs at 38 percent of stance for the ME controller and at 20 percent of stance for the CL controller. Details of these results will be deferred until the sound leg forces and the prosthetic foot/floor reaction forces are discussed in sections (3.3 and 3.5).

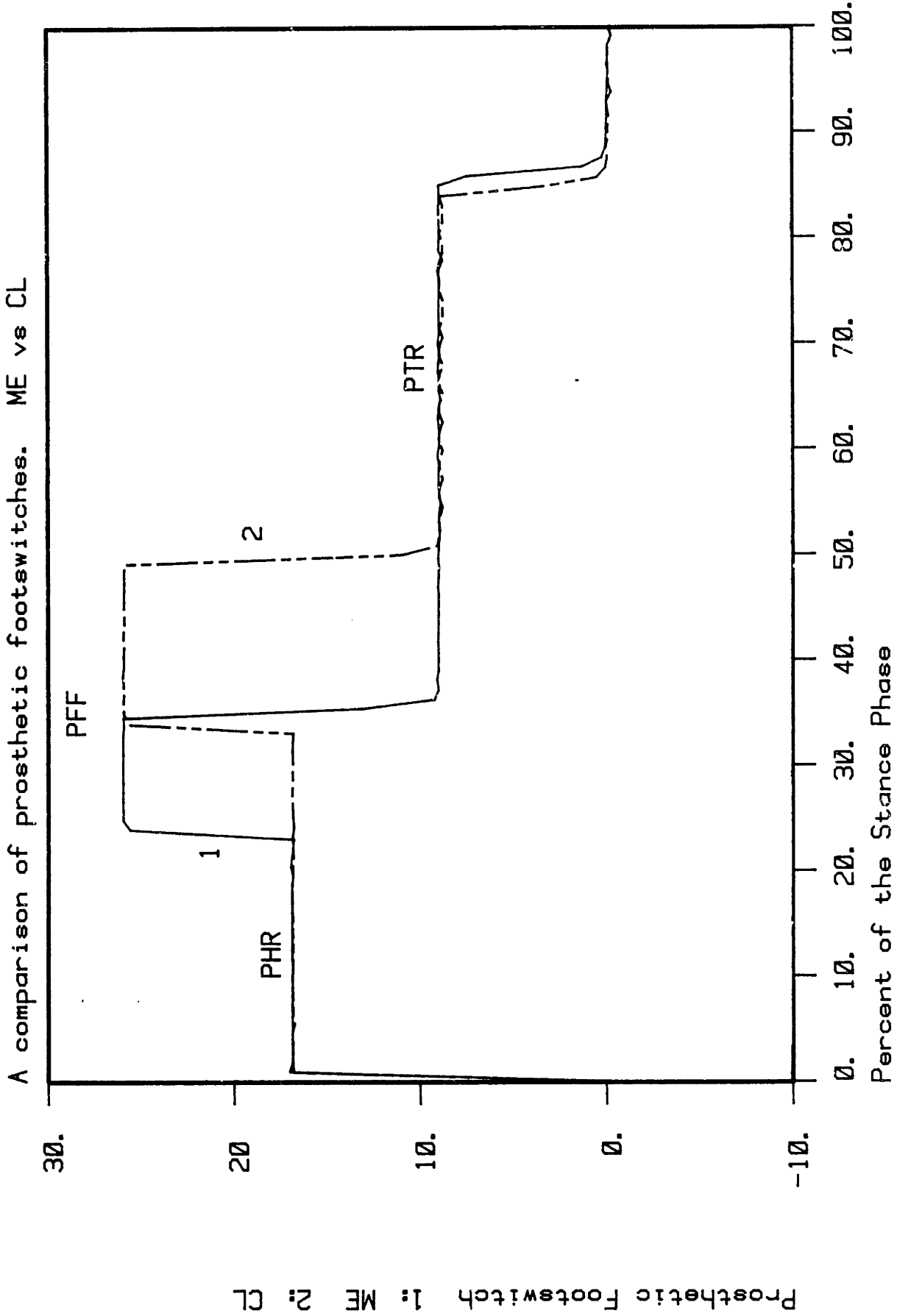


FIGURE IV-9

Typical Timing of Prosthetic and Sound Foot Placement During Stance. A Comparison of ME vs CL Stance Phase Knee Controllers. Run JLI427 vs. JLI2022



A comparison of prosthetic footswitches. ME vs CL

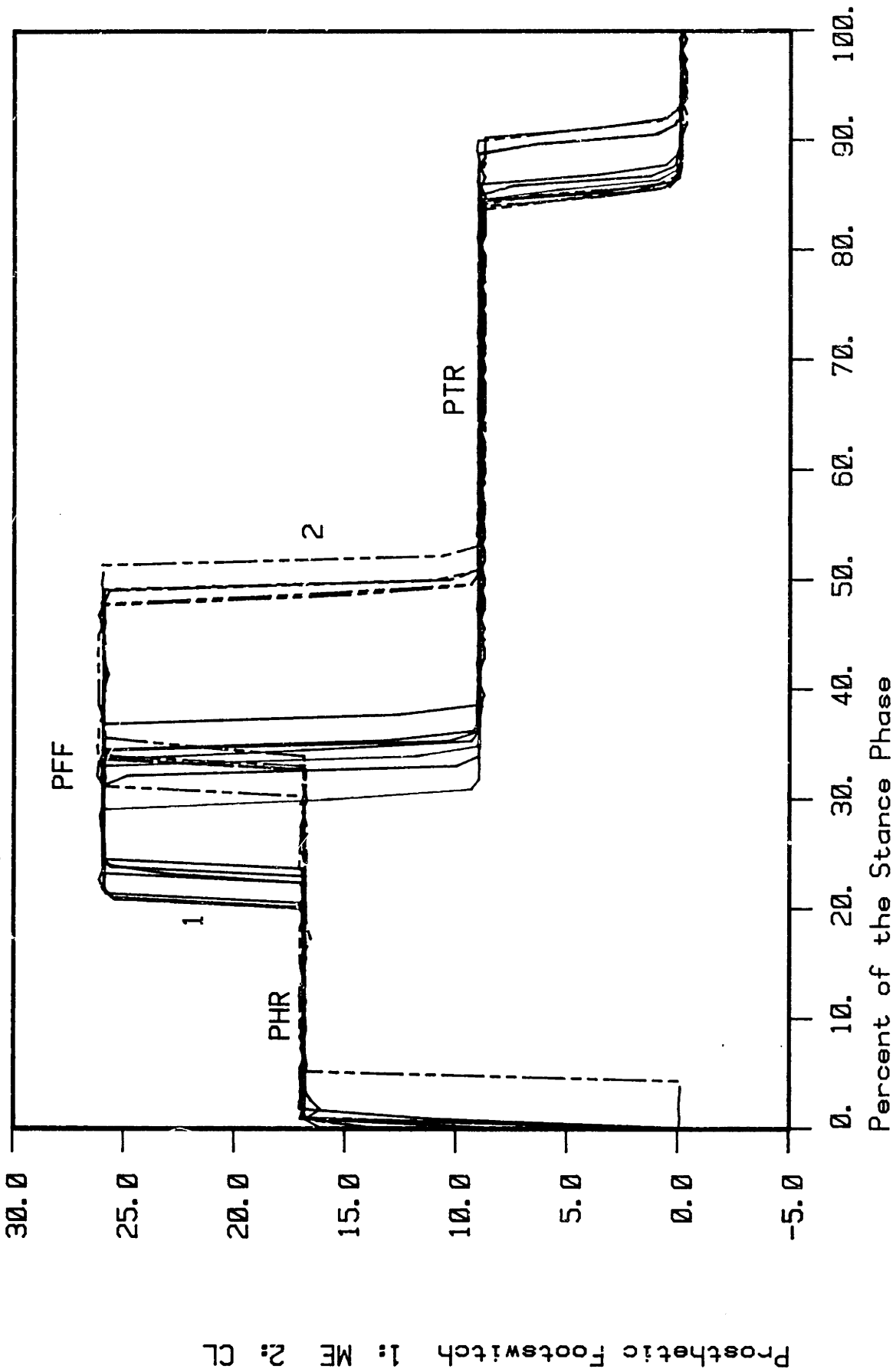


FIGURE IV-10

A Sample of Prosthetic Foot Placement Timings During Stance. A Comparison of ME vs CL Stance Phase Knee Controllers

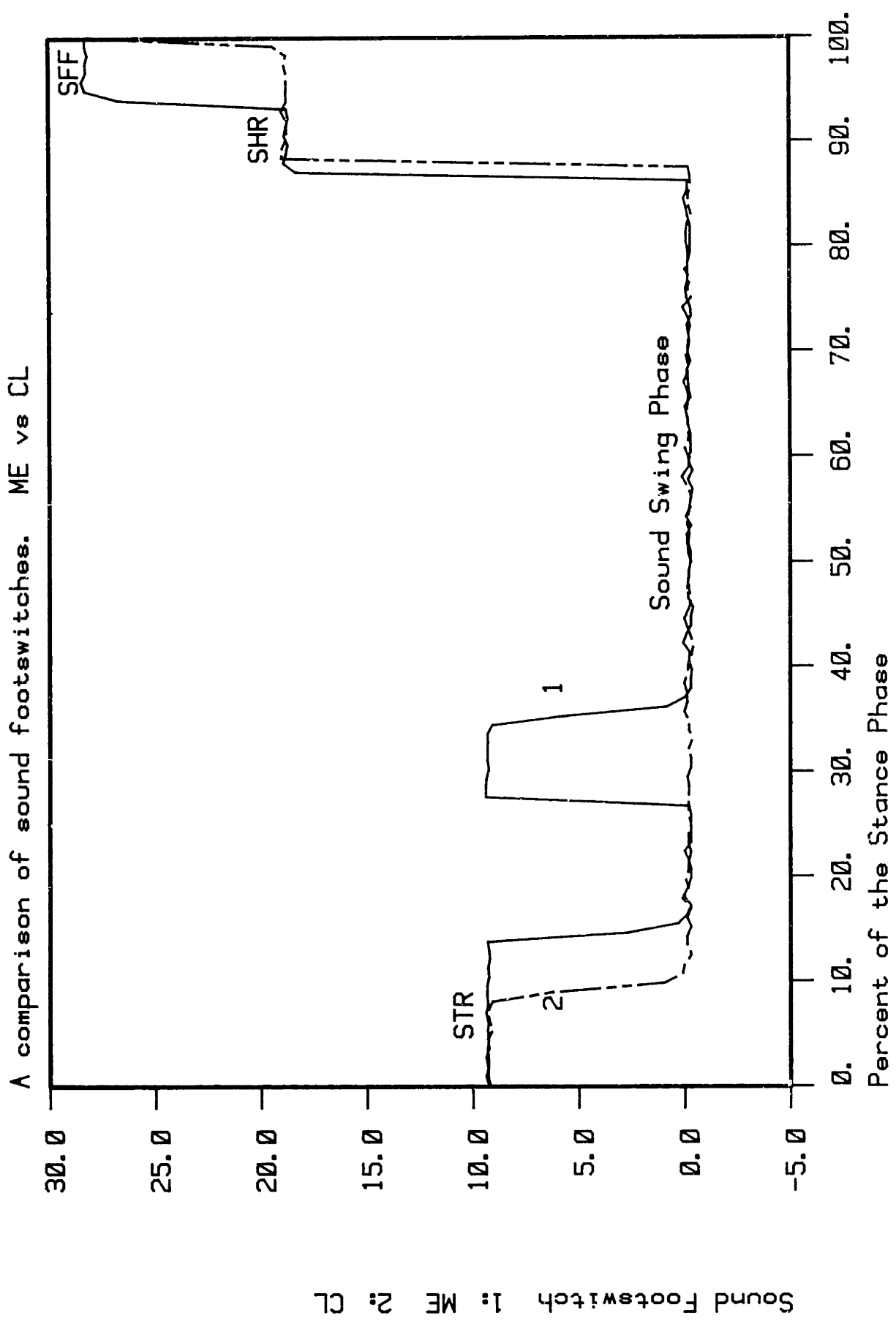


FIGURE IV-11

A Sample of Sound Foot Placement Timings During Stance. A Comparison of ME vs CL Stance Phase Knee Controllers

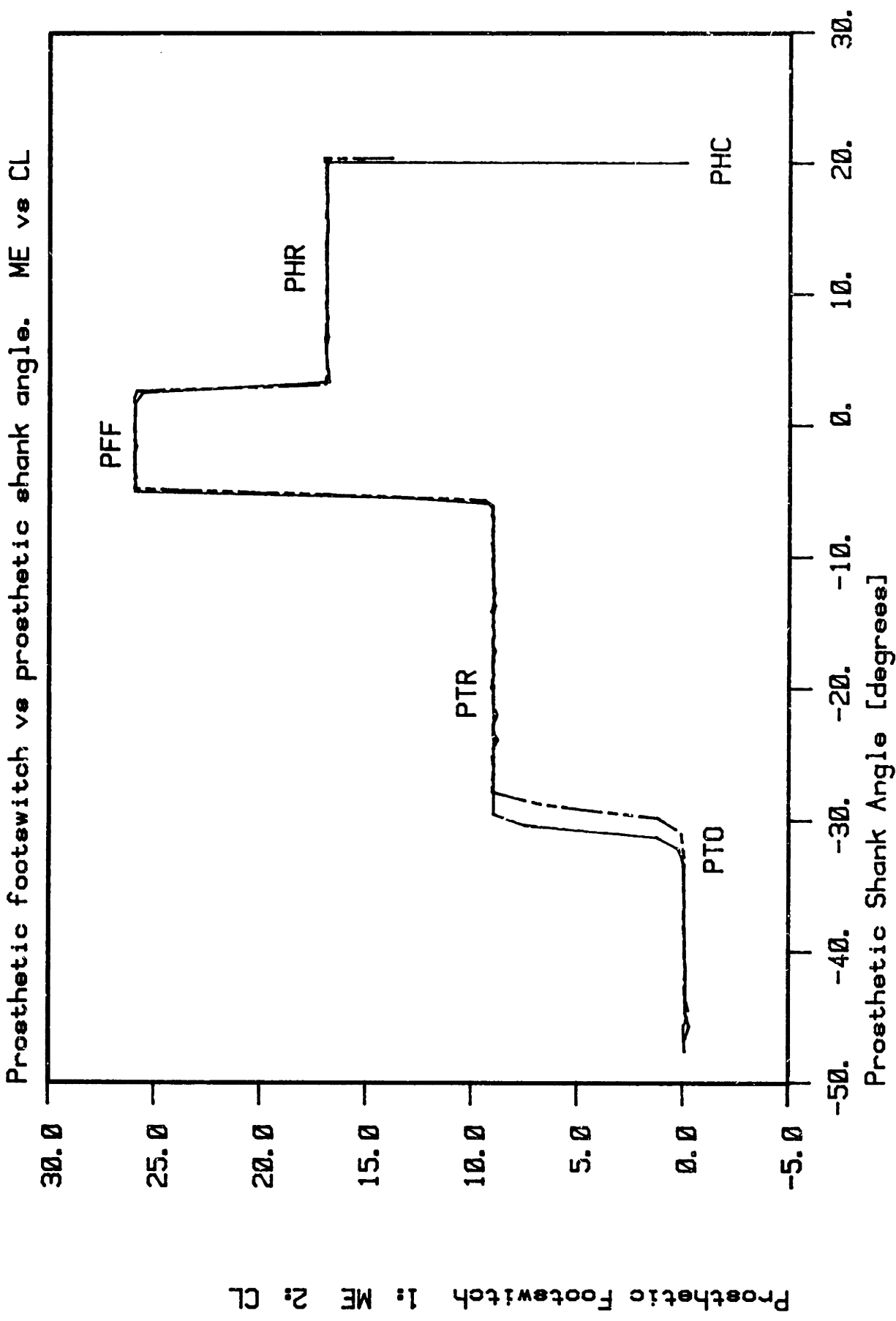


FIGURE IV-12

A Typical Prosthetic Footswitch Pattern as a Function Shank Angle. A Comparison of ME vs CL Stance Phase Knee Controllers. Run JL1497 vs JL1494

#### IV-2.5 Center of pressure - Figures IV-13, IV-14 and IV-15

The center of pressure in the forward direction is a locus of points representing the instantaneous position on the floor where a single force vector alone (no moments) can represent the loading between the SACH foot and the ground. As the SACH foot rolls forward during stance the center of pressure shows where the net load is on the floor and thus the SACH foot. This information should be correlated to the footswitch and shank angle information. Figure IV-13 shows a typical trajectory for each controller. Both curves show an initial period of small center of pressure change with time, followed by a period of rapid change, followed by another period of very small change with time and a final period following knee break of moderate change in the center of pressure. The most significant difference between the trajectories is the point in time when the center of pressure races forward. This occurs at PTC and reflects the differences in the timing of footflat initiation (see section 2.4 on foot placement timing).

An important ramification of the center of pressure movement can be seen by plotting it as a function of shank angle. As seen in Figures IV-14 and IV-15 there is little difference between the curves, thus indicating that an adequate model of the SACH foot is a rolling cam, a cam whose center of pressure is a simple algebraic function of shank angle. In addition, this implies at least for the two controllers and SACH foot tested, that the SACH foot geometry remains invariant under load. This cam is clearly shown in Figure IV-14 to be related to the heel and toe contact regions. In the prosthetic heel roll region, the center of pressure movement per shank angle rotation is small relative to the slope

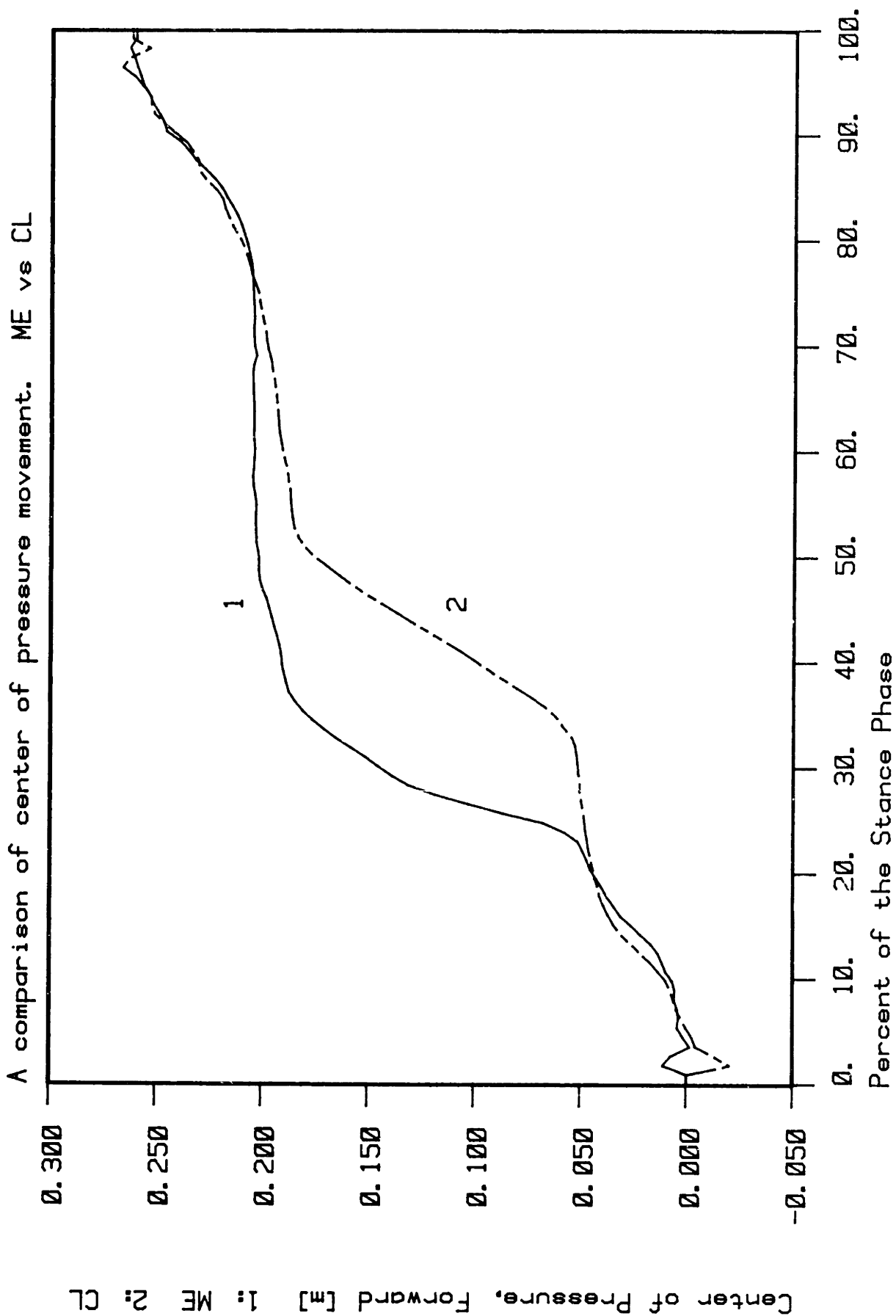


FIGURE IV-13

A Typical Center of Pressure Trajectory. A Comparison of ME vs CL Stance Phase Knee Controllers.  
Run JL1427 vs JL2022

A comparison of center of pressure vs shank angle profiles. ME vs CL

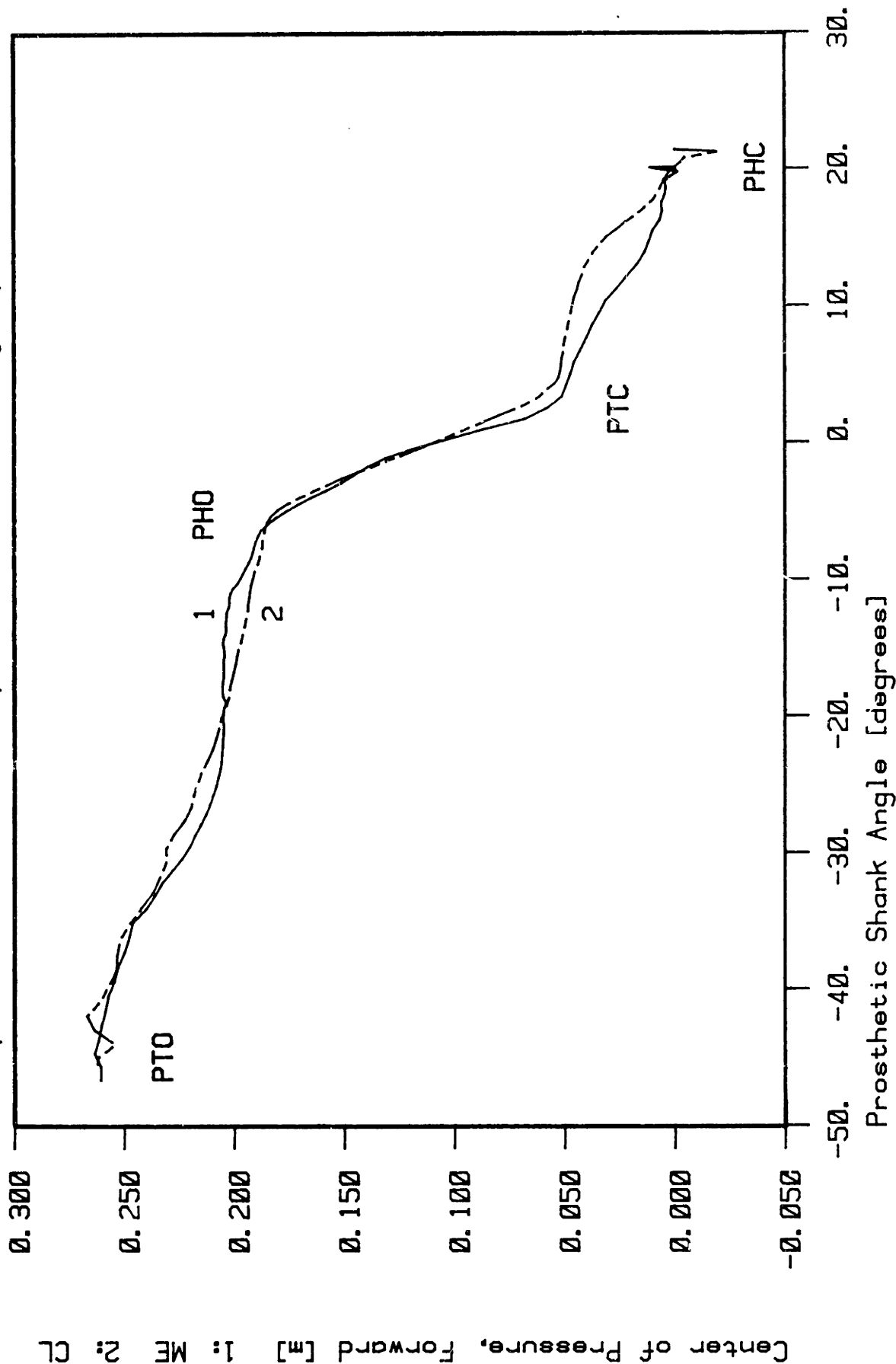
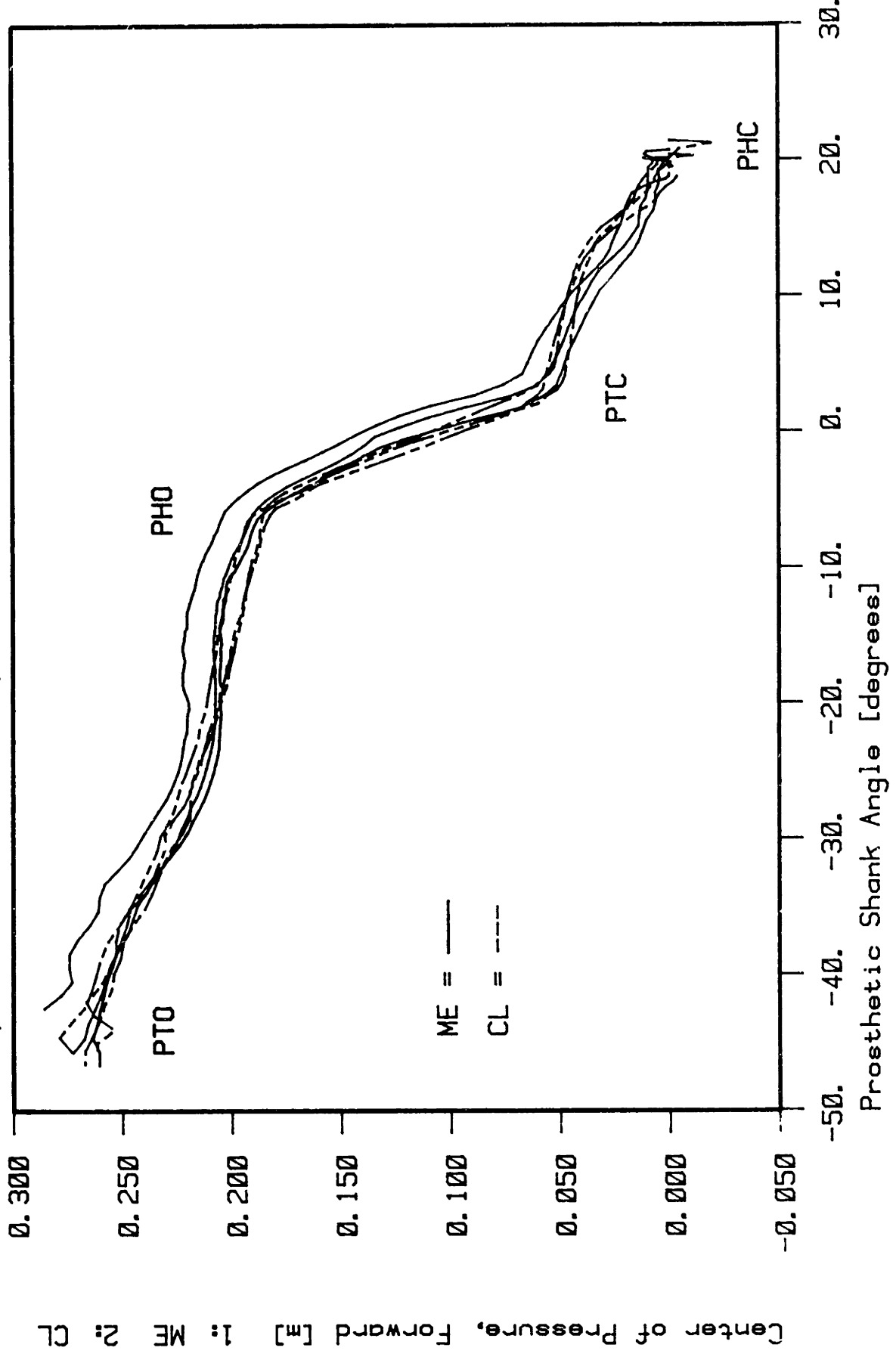


FIGURE IV-14

A Typical Center of Pressure vs Shank Angle. A Comparison of ME vs CL Stance Phase Knee Controllers.  
Run JL1427 vs JL2022

A comparison of center of pressure vs shank angle profiles. ME vs CL



Center of Pressure, Forward [m] 1: ME 2: CL

FIGURE IV-15

A Sample of Center of Pressure vs Shank Angles. A Comparison of ME vs CL Stance Phase Knee Controllers.

during PFF and similar to the slope during the prosthetic toe roll. This fact is used in the designer gait models discussed in Chapter V.

#### IV-2.6 Thigh (socket) angle - Figures IV-16 and IV-17

The measured socket angle trajectory, as discussed in Chapter II, is assumed to be equal to the thigh angle as defined by the position of femur.

The thigh angle, of course, is simply the sum of the shank and knee angle trajectories previously discussed. However, an important result is more evident by studying the thigh angle separately. At PHC both controllers produce the same initial thigh angle (approximately 23 degrees). For the CL controller with its zero knee angle up to knee break, the thigh angle equals the shank angle and extends from 23 degrees at PHC to -22 degrees at knee break. After knee break, however, the thigh angular velocity changes sign and the thigh flexes back up to -16 degrees at PTO. Under the ME controller, the thigh angle also extends after PHC but more slowly falling behind the CL controller thigh angle by an average of 7 degrees at mid footflat and remaining at that lag just past maximum knee flexion (33 percent of stance). After max knee flexion the thigh rotational velocity increases allowing the extending thigh to match the thigh angle for the CL controller at about SHC. After SHC the thigh angular velocity for the ME controller changes sign at 90 percent of stance, 5 percent after the CL controller case. As a result the thigh angle at PTO is 5 degrees more extended for the ME controller.



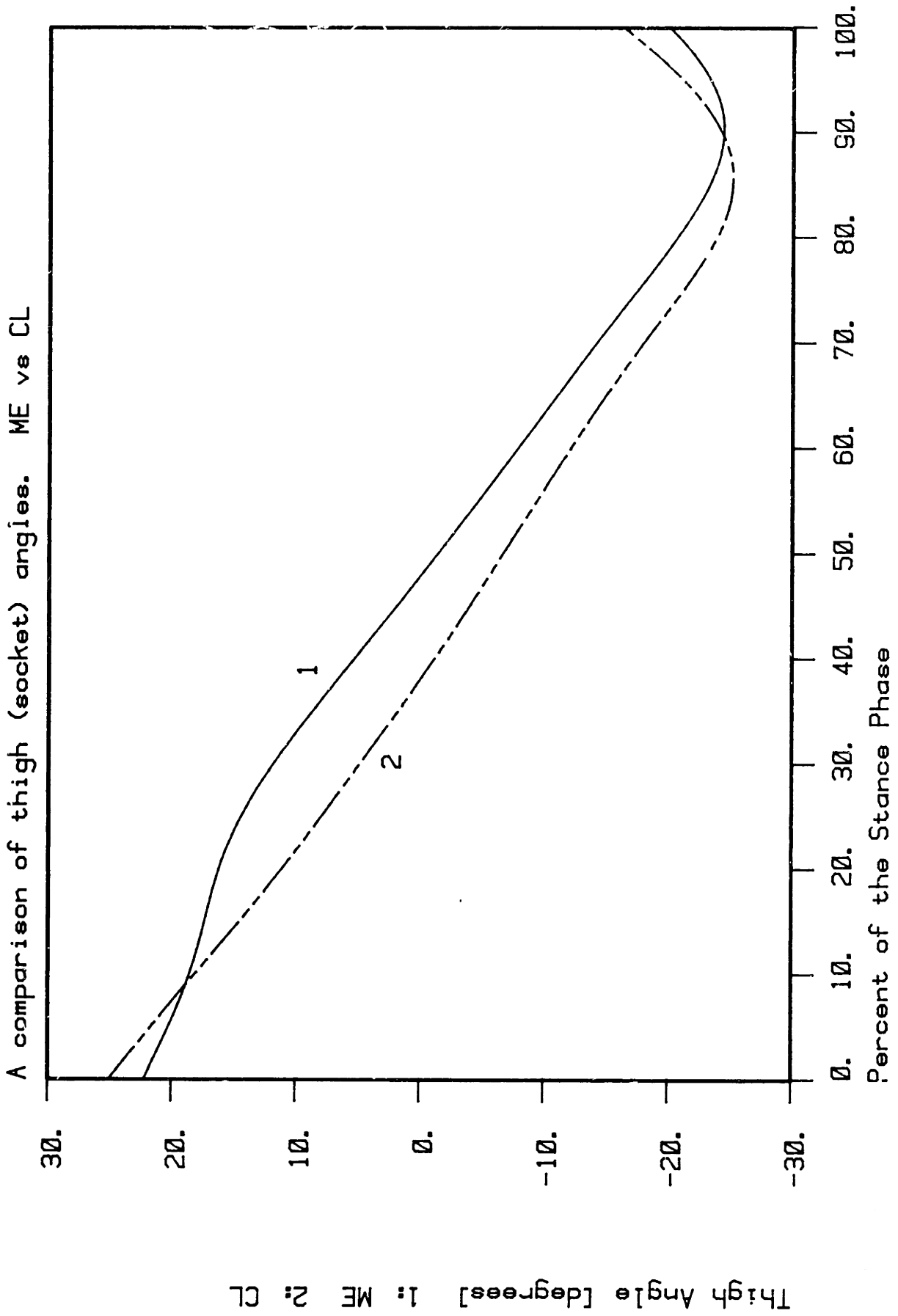


FIGURE IV-16

Typical Thigh (Socket) Angle Trajectories in Stance. A Comparison of ME vs CL Stance Phase Controllers.  
Run JL2024 vs JE2624

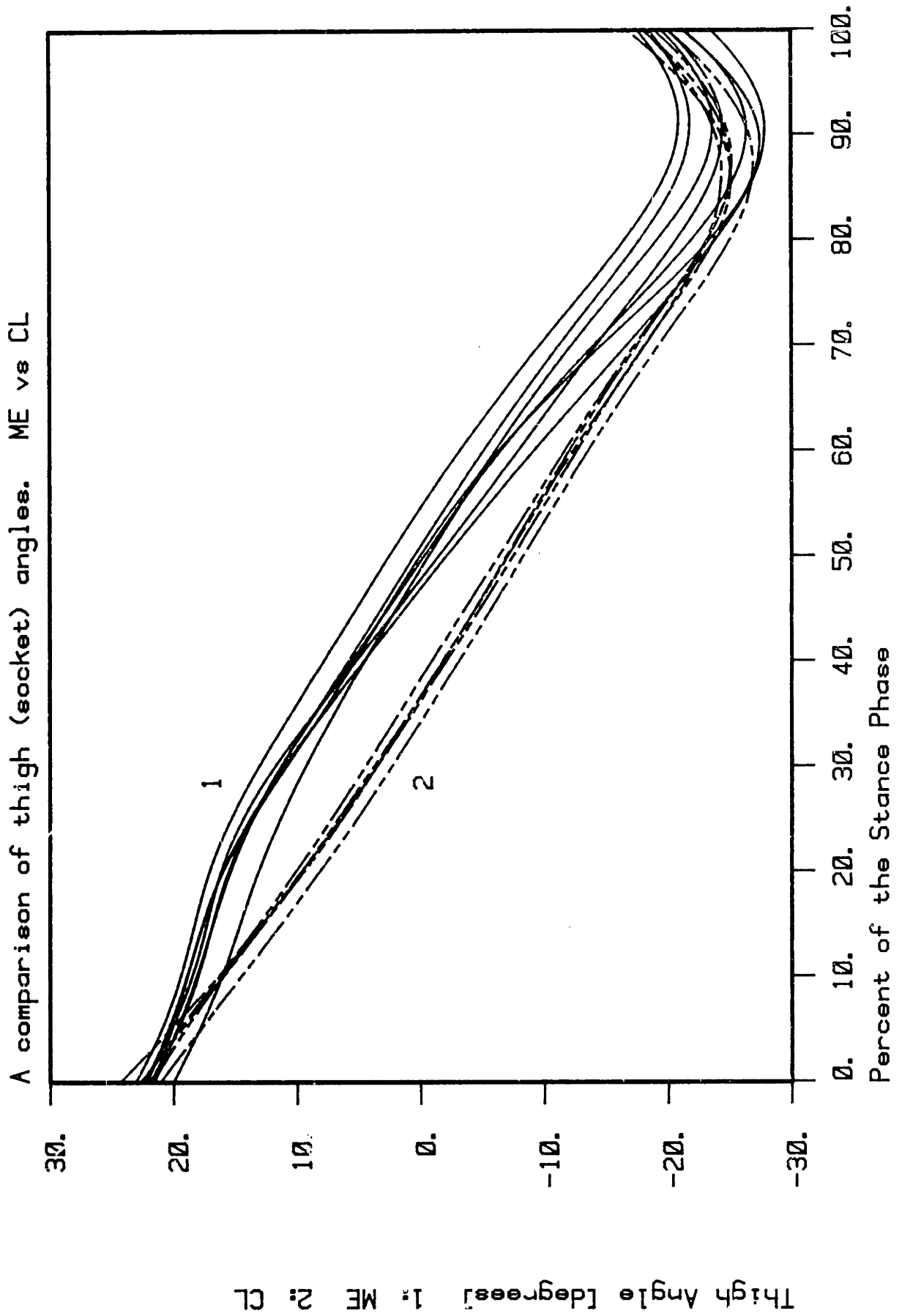


FIGURE IV-17

A Sample of Thigh (Socket) Angle Trajectories in Stance. A Comparison of ME vs CL Stance Phase Knee Controllers

A global result which can be seen by comparing the thigh and shank angles for the ME controller to the CL controller is that up to knee break, the nominal effective angle trajectory (defined as the angle with respect to vertical of the line connecting the hip to the center of pressure) is matched very closely by the CL controller and on average is also matched by the ME controller. Essentially, the shank angle lead is offset by a matching thigh angle lag. Thus the effective leg angle trajectory is similar for the two controllers. This implies that hip trajectories between the two controllers will also be similar. This may represent the amputee's effort to maintain his body c.g. motion in a fixed forward and vertical displacement pattern.

#### IV-2.7 Hip displacement

The hip displacement is really the displacement of the suction socket (see Chapter III-3). Thus the assumption of the femur remaining fixed to the motion of the socket applies for the following results.

##### IV-2.7.1 Forward displacement - Figure IV-18 and Figure IV-19

The difference between the forward hip trajectories of the two stance phase controllers at any instant is small (less than 5 percent) compared to the total forward displacement of the hip during stance. However, Figure IV-19 does show that a different pattern exists between the ME and CL stance phase knee controllers. During the first 33 percent of stance the knee is flexing up to its maximum 14 degrees. In addition, as shown in Figures IV-7 and IV-17, the shank and thigh angles lead and lag the similar segments with the CL controller. The net difference is that the forward displacement of the hip under ME control moves ahead of the CL

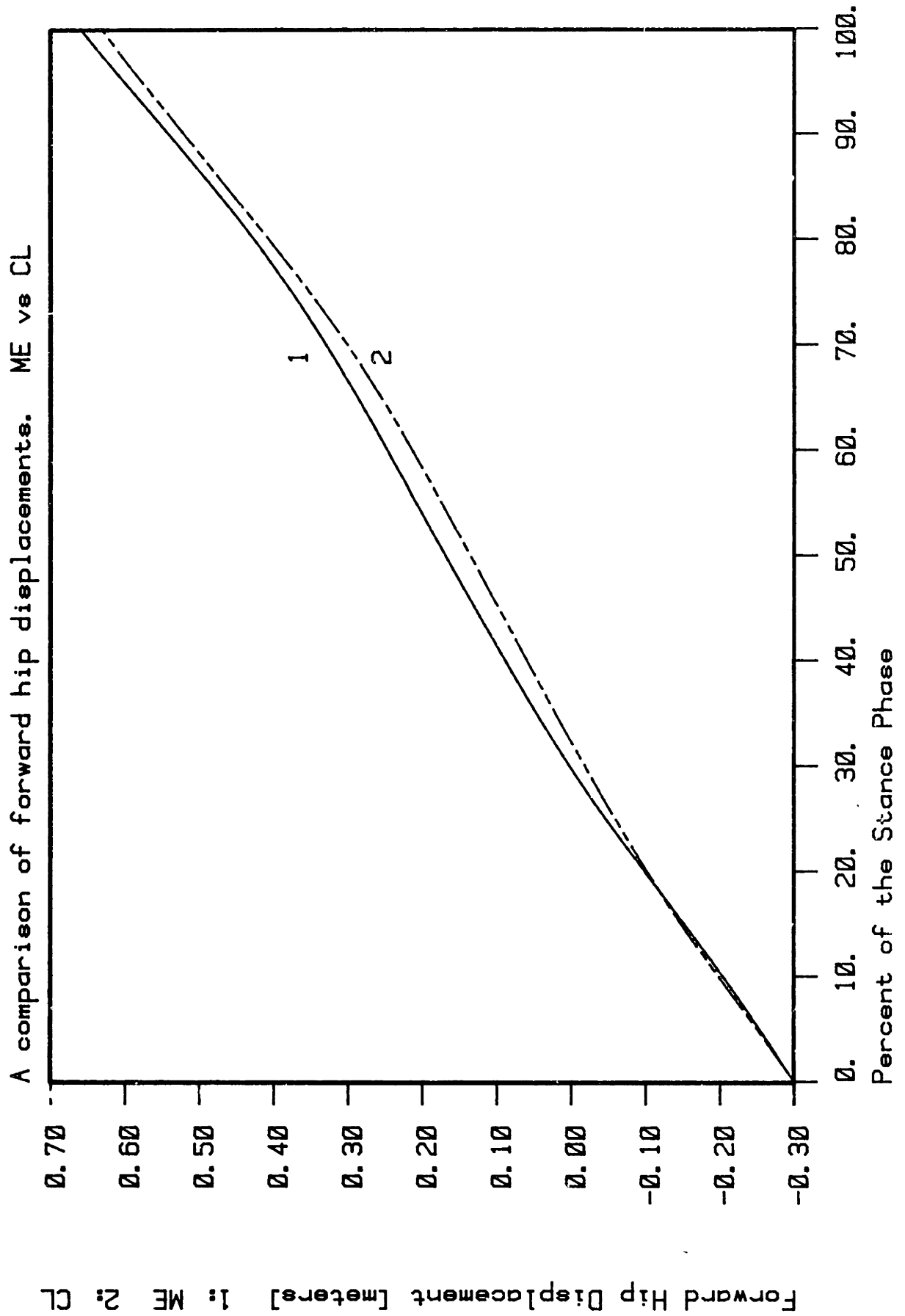


FIGURE IV-18

Typical Forward Hip Displacement Trajectories During Stance. A Comparison of ME vs CL Stance Phase Knee Controllers. Run JL1427 vs JL2022

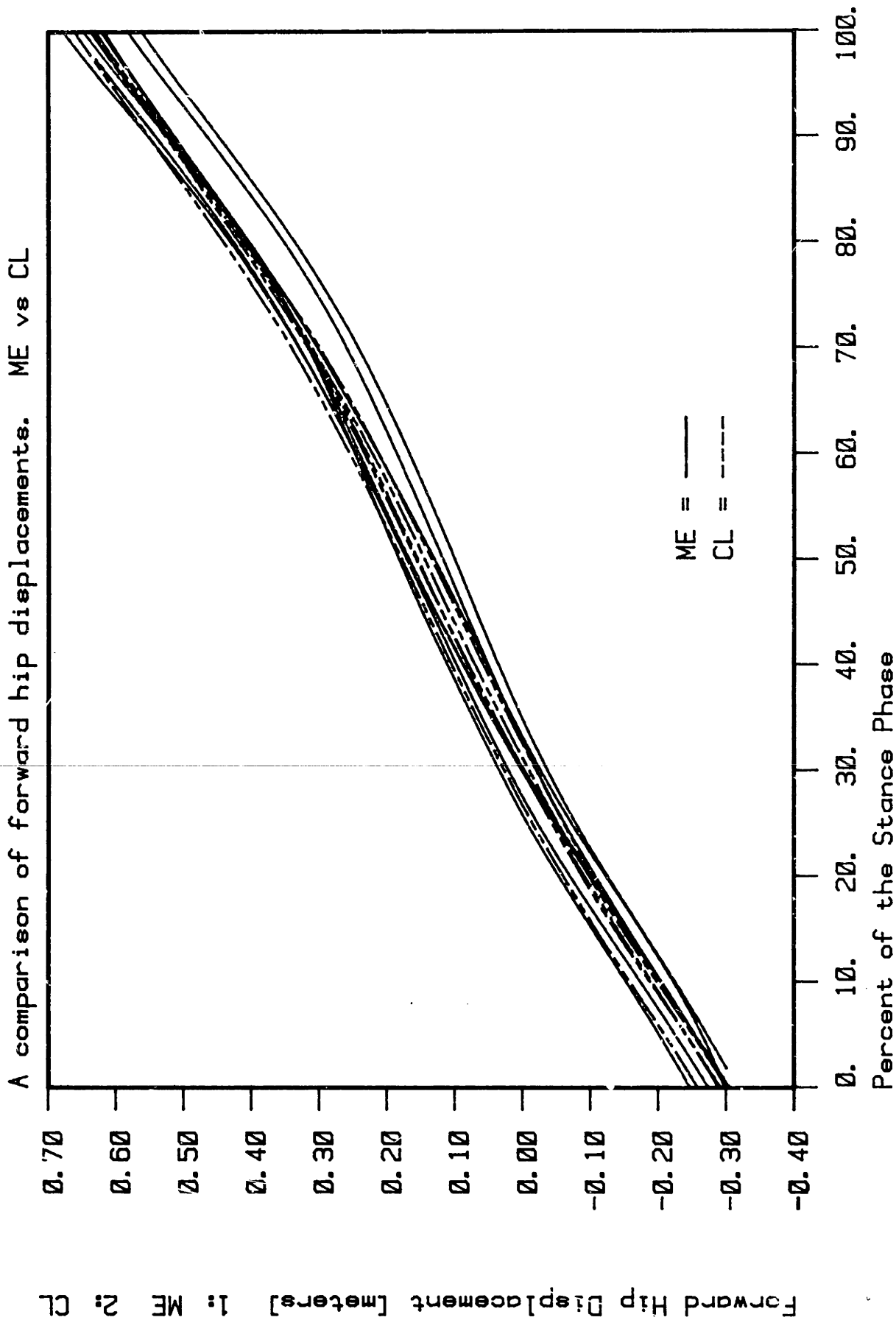


FIGURE IV-19

A Sample of Forward Hip Displacement Trajectories During Stance. A Comparison of ME vs CL Stance Phase Knee Controllers

controlled hip by approximately 2 cm. By SHC, however, CL controlled hip has moved up 1 cm but by PTO the ME controlled hip has moved ahead due to the larger thigh rotation after knee break.

#### IV-2.7.2 Vertical hip displacement - Figures IV-20 and IV-21

Vertical hip displacement is frequently discussed by the medical community in evaluating A/K amputee's gait. Abnormal vertical hip displacement (called vaulting in prosthetic stance, and hiking in prosthetic swing) is easily observed and is often held partially responsible for the higher energy consumption of A/K gait. As discussed in Chapter II one potential benefit of the ME controller is to eliminate or at least reduce vaulting.

Figure IV-20 and IV-21 show the vertical hip trajectories produced by the ME and CL stance phase knee controllers. The two controllers produce two distinctly different vertical trajectories. At PHC they are not measurably different but the ME controller profiles fall slightly below the CL case up until 30 percent of stance. At this point, the ME trajectory begins to move above the CL trajectory to higher vertical displacements. At 50 percent of stance when both curves are peaking (the hip is moving over the center of pressure) the approximate average height increase of the ME case over the CL case is 7 mm. By SHC the profiles are at the same value again but the ME trajectories have steeper negative slopes and by 90 percent of stance are 12 mm below the CL profiles. At PTO the ME profiles remain 12 mm's below the CL trajectories.

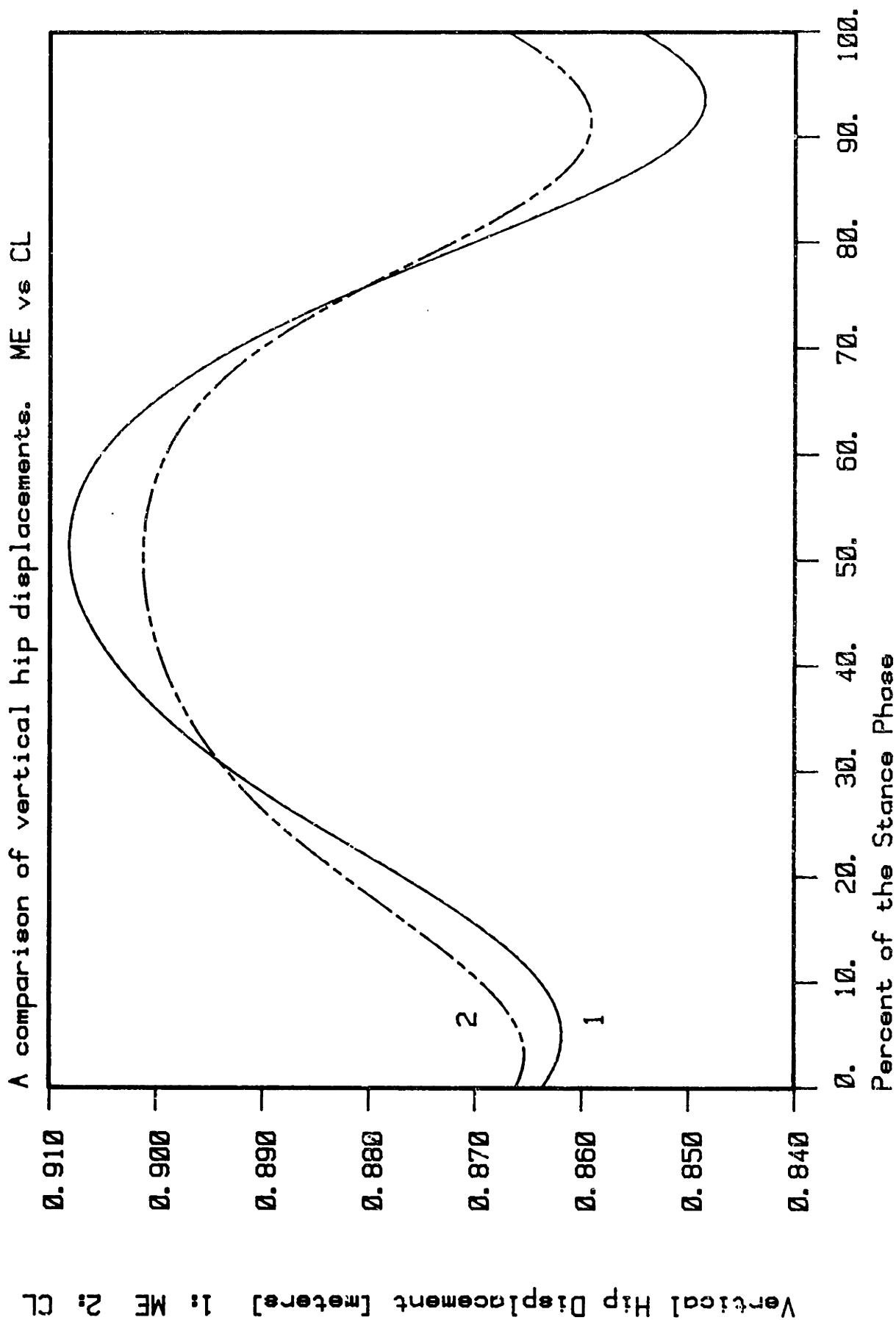
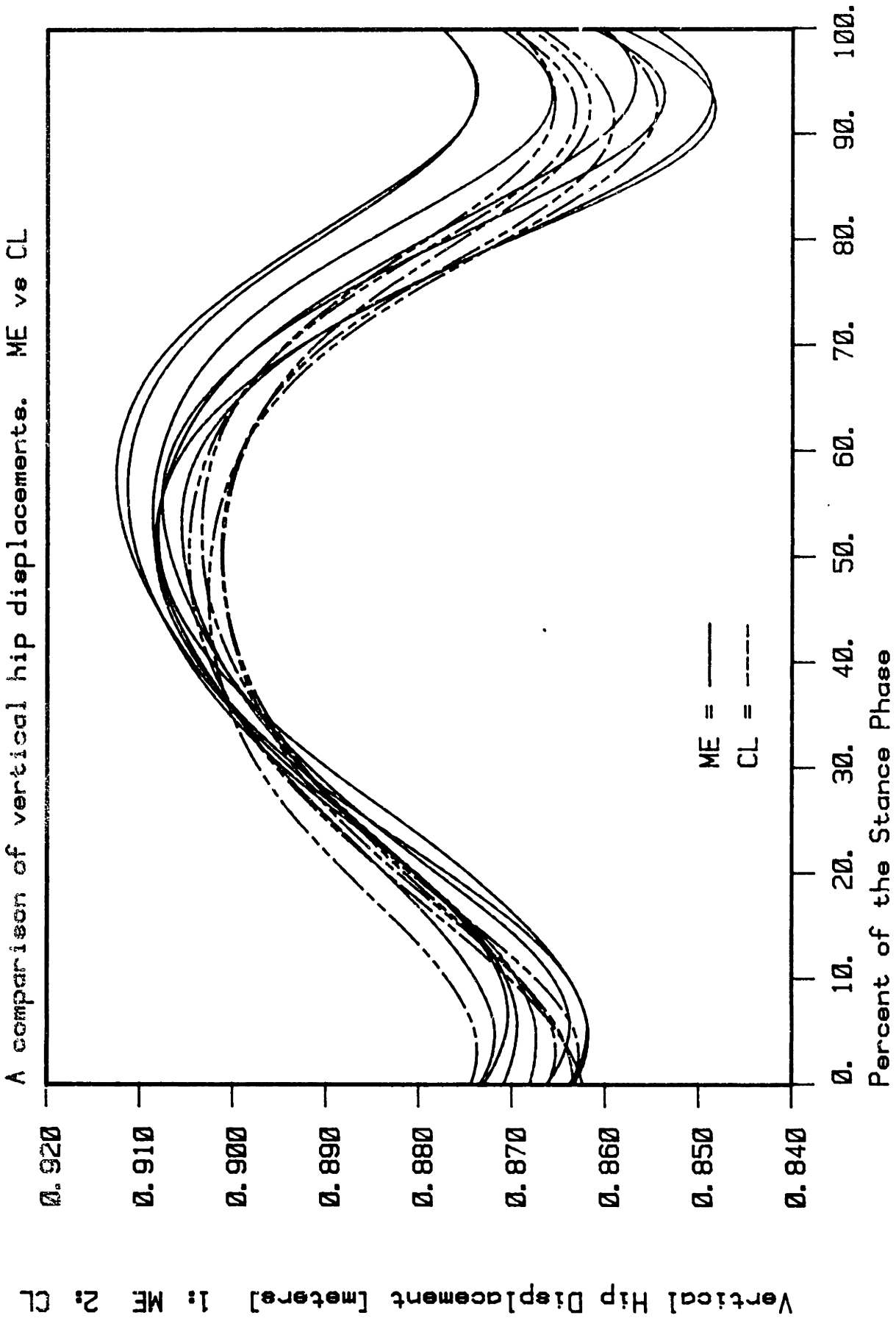


FIGURE IV-20

Typical Vertical Hip Displacement Trajectories During Stance. A Comparison of ME vs CL Stance Phase Knee Controllers. Run JL1427 vs JL1494.



FIGURES IV-21

A Sample of Vertical Hip Trajectories During Stance. A Comparison of ME vs CL Stance Phase Knee Controllers



The fact that the ME controlled prosthesis produces higher vertical hip displacements is a very unexpected result. To explain this an understanding of the underlying kinematics is necessary.

The vertical hip trajectories are a result of the subtle phasing of four competing kinematic factors. 1) the vertical height due to the rotation through the vertical of an imaginary pendulum defined from the hip to the point of rotation. 2) The effective length of that pendulum (the effective leg length, ELL) due to the change in the point of contact with ground due to the rolling SACH foot. 3) The effective length of that pendulum due to the change in knee angle. 4) The effective length of that pendulum due to compliance in the prosthesis. These four affects are summarized in Table IV-1. The compliance of the leg, at least during mid-stance, is probably small and is neglected. For the CL controller only the first two factors are important up to knee break, all three are important for the ME controller case.

There is, however, one additional constraint which reduces the degrees of freedom of the hip trajectories. As was previously shown (Chapter IV-2.4) there exists a kinematic relationship between shank angle and center of pressure. Therefore, as shown in Figure IV-22, the vertical displacement of the prosthetic knee as a function of shank angle is independent of the stance phase knee controller. Figure IV-22 also shows that there is only one maximum in the knee height trajectory and that it occurs at the non-zero shank angle of 16 degrees past vertical. This means, as can be seen in Figure IV-15, that the center of pressure is out under the toe section of the SACH foot. It also implies that the largest vertical hip displacement will occur if the thigh is vertical which means

Table IV-1: Kinematic Factors Affecting  
Vertical Hip Trajectories

1.	Rotation	Vertical hip displacement changes due to rotation of the ELL.
2.	CPM	Vertical hip displacement changes due to movement of the center of pressure.
3.	Knee Angle	Vertical hip displacement changes due to knee angle flexion.
4.	Compliance	Vertical hip displacement changes due to prosthesis compliance.

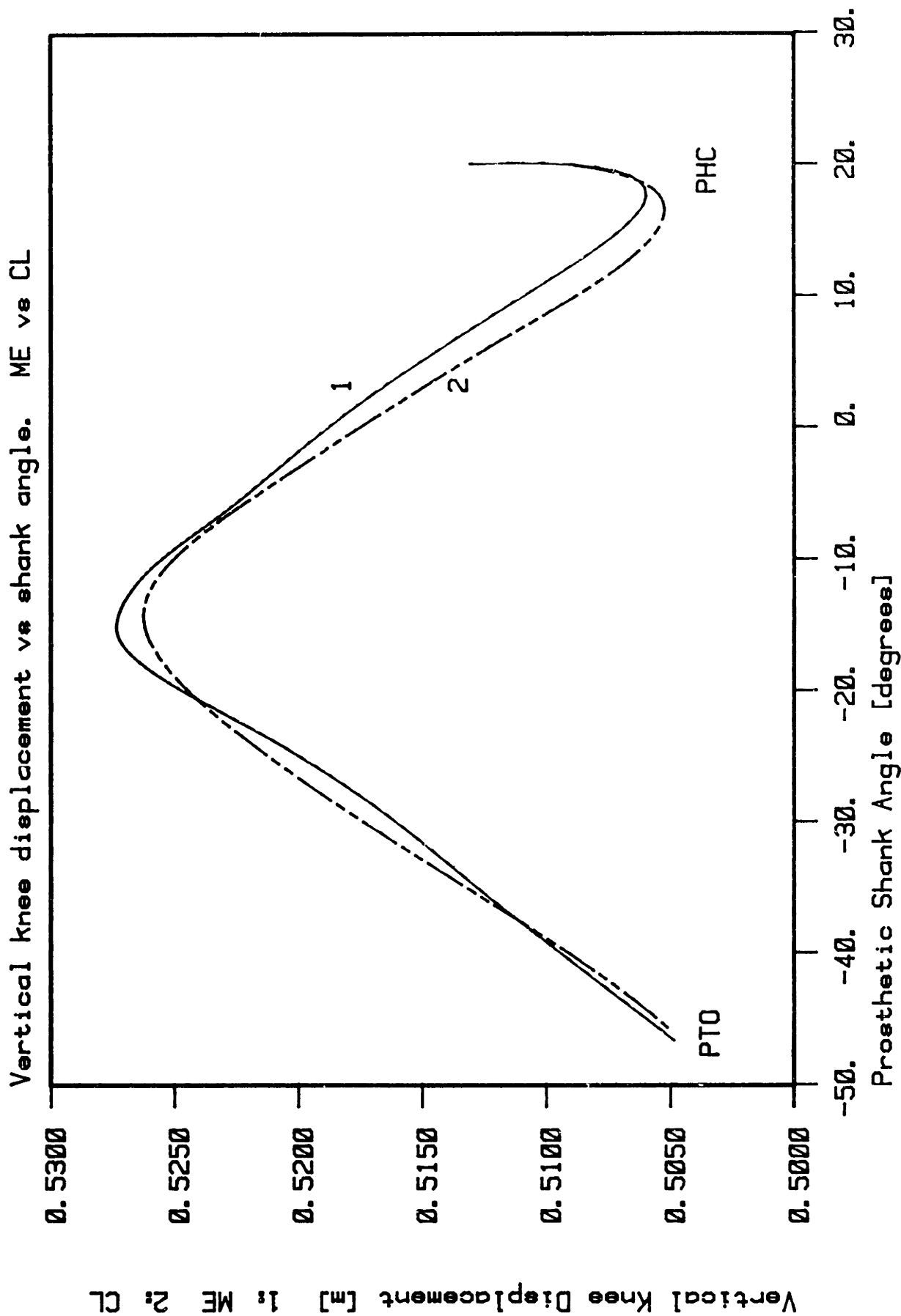


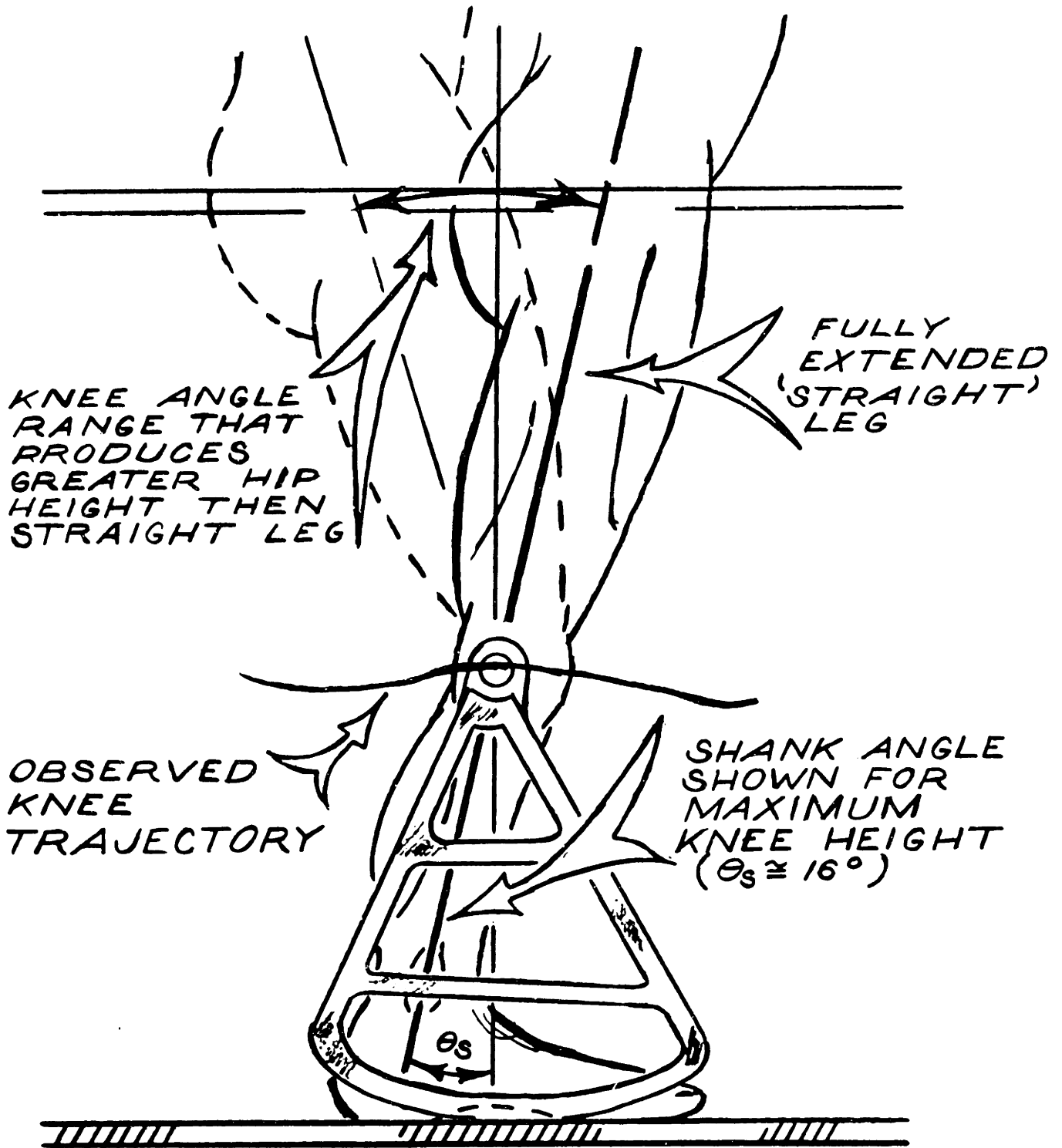
FIGURE IV-22

Typical Vertical Displacement of the Prosthetic Knee Joint as a Function of Shank Angle During Stance. A Comparison of ME vs CL Stance Phase Knee Controller. Run JL1427 vs JL1494

the knee angle must be at 16 degrees of flexion. Thus, as shown in Figure IV-23, any physiological amount (less than 32 degrees) of knee flexion as the shank rotates through the value of 16 degrees past vertical guarantees a higher hip displacement than would be produced with a knee angle of zero degrees (CL controller). However, this does not guarantee that this will be the highest point in the stance phase. There exists the possibility that the actual peak in the vertical hip trajectory occurs at some other shank angle due to the particular combination of cam profile and knee angle trajectory.

The possibility of the peak in the vertical hip trajectory occurring at a shank angle other than 16 degrees past vertical is explored in Figure IV-24. Indeed ME peak in the profile in the ME controller case occurs at close to 16 degrees past vertical (12 degrees). This implies that the "sharpness" of the peak in Figure IV-22 does indeed mean that the peak vertical hip trajectory is controlled by the SACH foot geometry. Figure IV-24 also shows that the CL controller produces the highest value in its trajectory at approximately 5 degrees past vertical. Thus any physiologically reasonable knee flexion angle implemented after 5 degrees past vertical will produce a vertical displacement trajectory with a peak value guaranteed to be greater than any produced with the zero angle CL controller.

In summary, the kinematics of the SACH foot used in this study dominates the vertical displacement of the hip. This will always be true unless the knee controller implemented violates the kinematic relationship between shank angle and center of pressure.



HIP HEIGHT QUESTION  
(STRAIGHT VERSUS FLEXED KNEE)

FIGURE IV-23

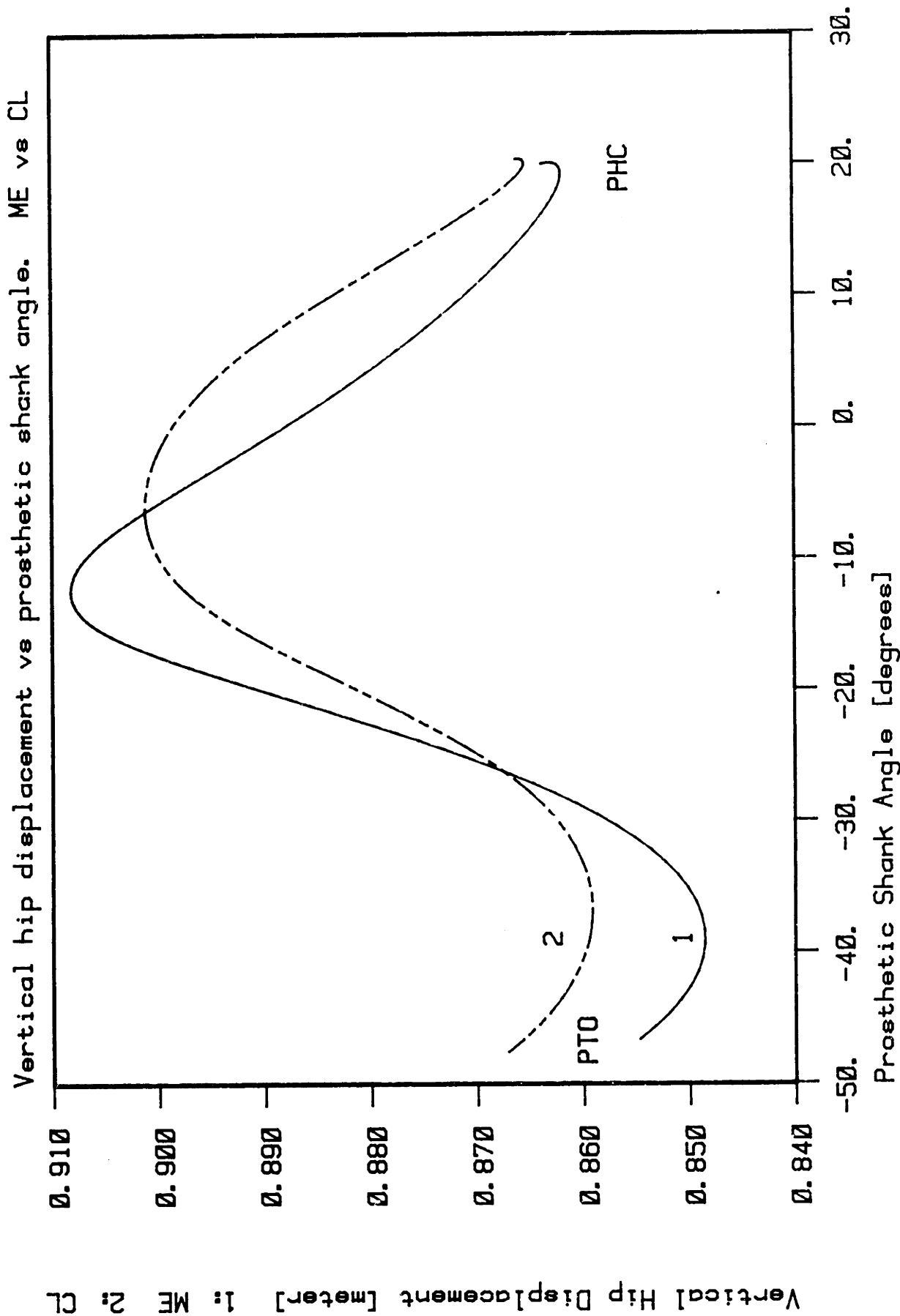


FIGURE IV-24

Typical Vertical Hip Displacements vs Shank Angle During Stance. A Comparison of ME vs CL Stance Phase Knee Controllers. Run JLI427 vs JLI494

## IV-2.8 Hip velocity

### IV-2.8.1 Forward velocity - Figure IV-25

Forward component of hip velocity is the single largest factor in determining the total kinetic energy. For this reason alone, it is an important variable to examine. However, as expected, the scatter in the velocity data is greater than for displacement data and this makes it more difficult to measure small differences between profiles. Nevertheless, useful trends were observed and are presented below.

The forward hip velocity profiles during the stance phase are similar but contain some differences as a function of each controller. During the initial rise in velocity as the body is being propelled forward by the sound leg (see Chapter V-4) there is a small but somewhat consistent result that the ME controller forward velocity trajectories peak later (at 20 percent instead of 10 percent) and at a lower amplitude (7 percent lower). This is followed by a decrease in velocity as the body climbs up the energy hill associated with the effective leg length angle approaching vertical. After vertical the body speeds up as the potential energy is converted back to kinetic. This continues until knee break (78 percent of stance, in the CL case and 83 percent of stance in the ME case). After SHC, the velocity profiles slow down due to the knee flexing to prepare for swing and due to the sound leg providing a restraining force (see Section 3.5 of this chapter).

A comparison of forward hip velocity. ME vs CL

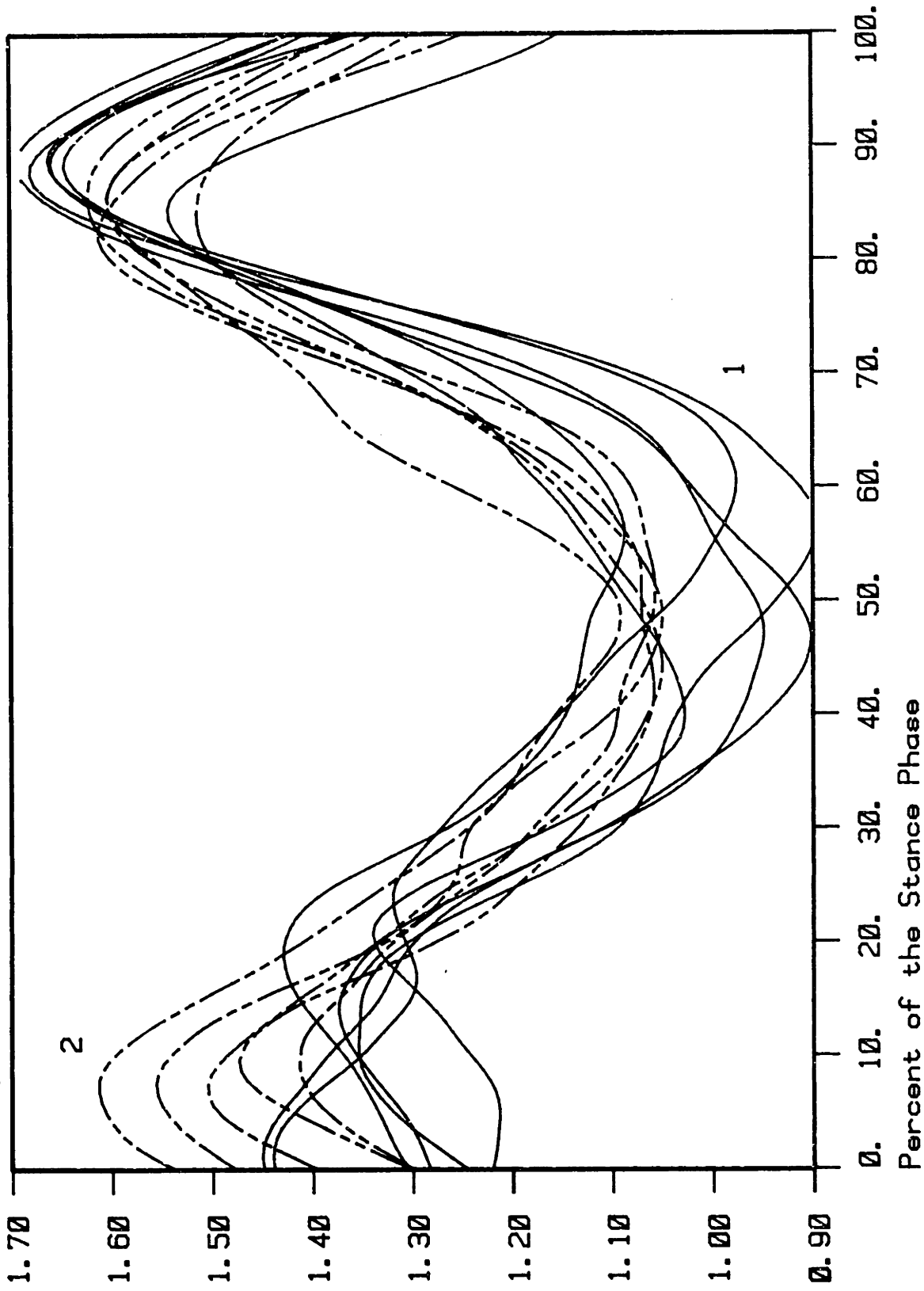


FIGURE IV-25

A Sample of Forward Hip Velocities During Stance. A Comparison of ME vs CL Stance Phase Knee Controllers

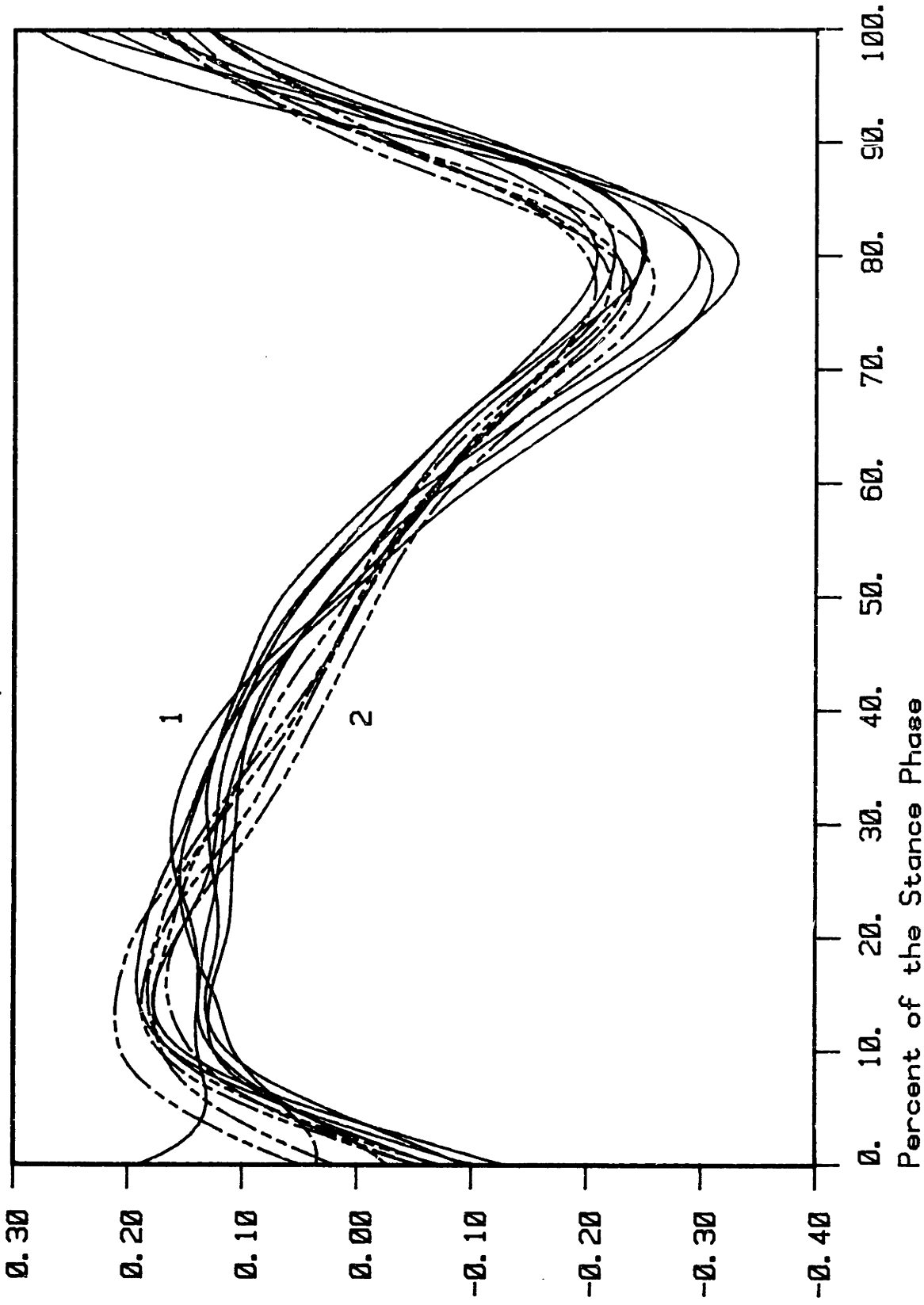


#### IV-2.8.2 Vertical hip velocity - Figure IV-26

The vertical velocity hip profiles show, as they should, a pattern consistent with the hip displacement profiles. During the first 5 percent of stance the magnitude of the hip velocity is getting smaller as the hip moves down. After 5 percent of stance the velocity changes sign and the hip starts to move up, accelerating until approximately 20 percent of stance. After 20 percent the acceleration is down but the body continues to move up with decreasing upward velocity as the hip displacement approaches the center of pressure position at 50 percent of stance (see Figure IV-2 and IV-3). The hip continues to accelerate down as the body passes over the center of pressure and begins to fall. The velocity is now downward. At knee break, the acceleration again reverses sign as the hip continues to fall down although at a slower rate. By 90 percent of stance, the hip velocity reverses, resulting in an upward movement of the hip. The hip accelerates upward through PTO.

As with the forward velocity, the scatter in the vertical velocity profiles makes it difficult to observe the differences caused by the two stance phase knee controllers. However, there is a separate and distinct pattern in the velocity profiles that can be observed for each controller. Up to 30 percent of stance the velocities for the CL controller are slightly larger in magnitude. This accounts for the vertical hip displacements in this region also being slightly higher. However, from 30 to 50 percent of stance the vertical velocities for the ME controller profiles are larger, and as a result, the vertical hip displacements rise above the CL case peaking at 50 percent of stance. From 50 to 90 percent of stance the ME velocity profiles fall below the CL case. This causes

A comparison of vertical hip velocities. ME vs CL



Vertical Hip Velocity [m/s] 1: ME 2: CL

FIGURE IV-26

A Sample of Vertical Hip Velocities During Stance. A Comparison of ME vs CL Stance Phase Knee Controllers

the vertical hip displacement to end up below the CL case right up to PTO even though during the last 10 percent of stance the ME velocity profiles do become larger in magnitude than the CL trajectories.

#### IV-2.9 Kinematics summary

Since the main focus of this thesis is to determine the relevant design and control issues in the stance phase of A/K amputee gait, it is, therefore, useful to summarize the main differences in the kinematics of stance phase gait as influenced by the changed design parameter (i.e. the stance phase knee controller). The implementation of ME control causes the following sequences of events to occur (see Figures IV-2 and IV-3). After PHC, the shank rotates rapidly forward causing footflat to occur sooner than for the CL controller. This has the consequence of moving the center of pressure forward of the shank and effectively lengthening the leg. While this also occurs under CL control, the knee flexion under ME control actually produces a longer effective leg length. As the shank rotates past vertical the knee is re-extended. The net result is that the hip joint moves through a higher peak in vertical displacement with the ME controller.

### IV-3 Dynamics and Power

The previous section described in detail the kinematics of the stance phase of A/K gait as a function of two stance phase controllers. This section will describe the joint torques, and forces acting on the amputee/prosthesis system which produced those kinematics.

#### IV-3.1 Prosthetic knee torque and power - Figures IV-27 thru IV-32

Ever since the first articulated knee joint, A/K prosthesis was used; amputees, physical therapists, prosthetists and A/K prosthesis designers have been concerned with knee torque, especially during the stance phase. It has always been the rule, that at PHC the prosthetic knee torque must be extensive so as to extend the knee into the hyperextension stops. In this configuration the prosthesis provides a stable pylon for the amputee and he maintains this stability up to knee break by keeping the knee torque extensive. In this thesis, the ME controller intentionally violates this rule by commanding the knee angle to flex during stance. The consequences of this control strategy are potentially large, and significantly different knee torques and powers are expected relative to those generated using the CL controller. Figure IV-27 compares prosthetic knee torques for the two knee controllers. Both controllers produce the same extensive knee torque at PHC, but diverge after that up to knee break where they reconverge ending at PTO with approximately equal flexive knee torques. During prosthetic heel roll (PHR) the CL controller produces a knee torque which moves toward zero. This corresponds to the c.g. load vector moving from behind the knee axis to ahead of it with decreasing assistance from the hip torque (see Chapter V-4). In Figures IV-31 and

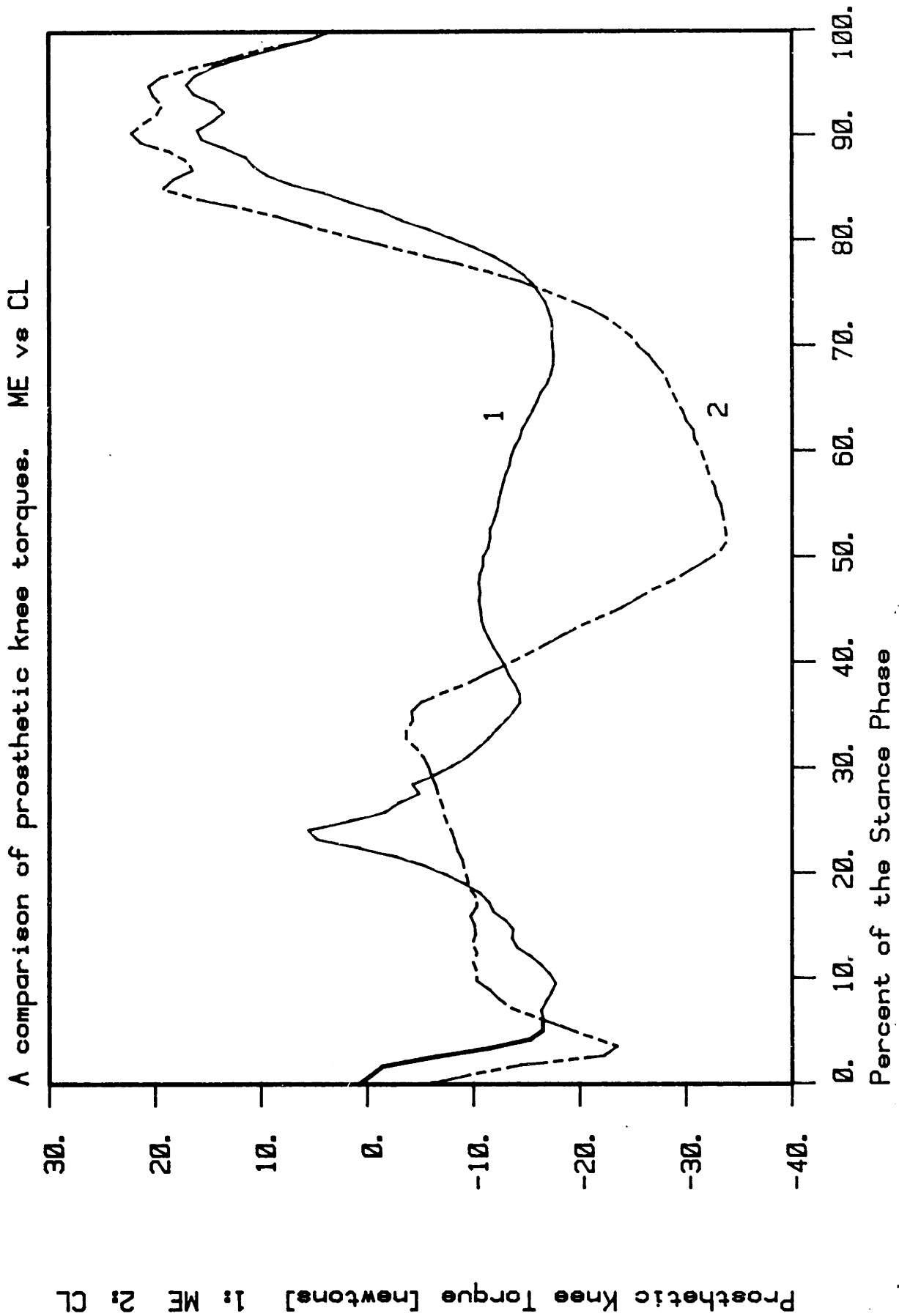


FIGURE IV-27

Typical Prosthetic Knee Torque Trajectories as Measured by TRACK During Stance. A Comparison of ME vs CL Stance Phase Knee Controllers. Run JL2004 vs JL1494

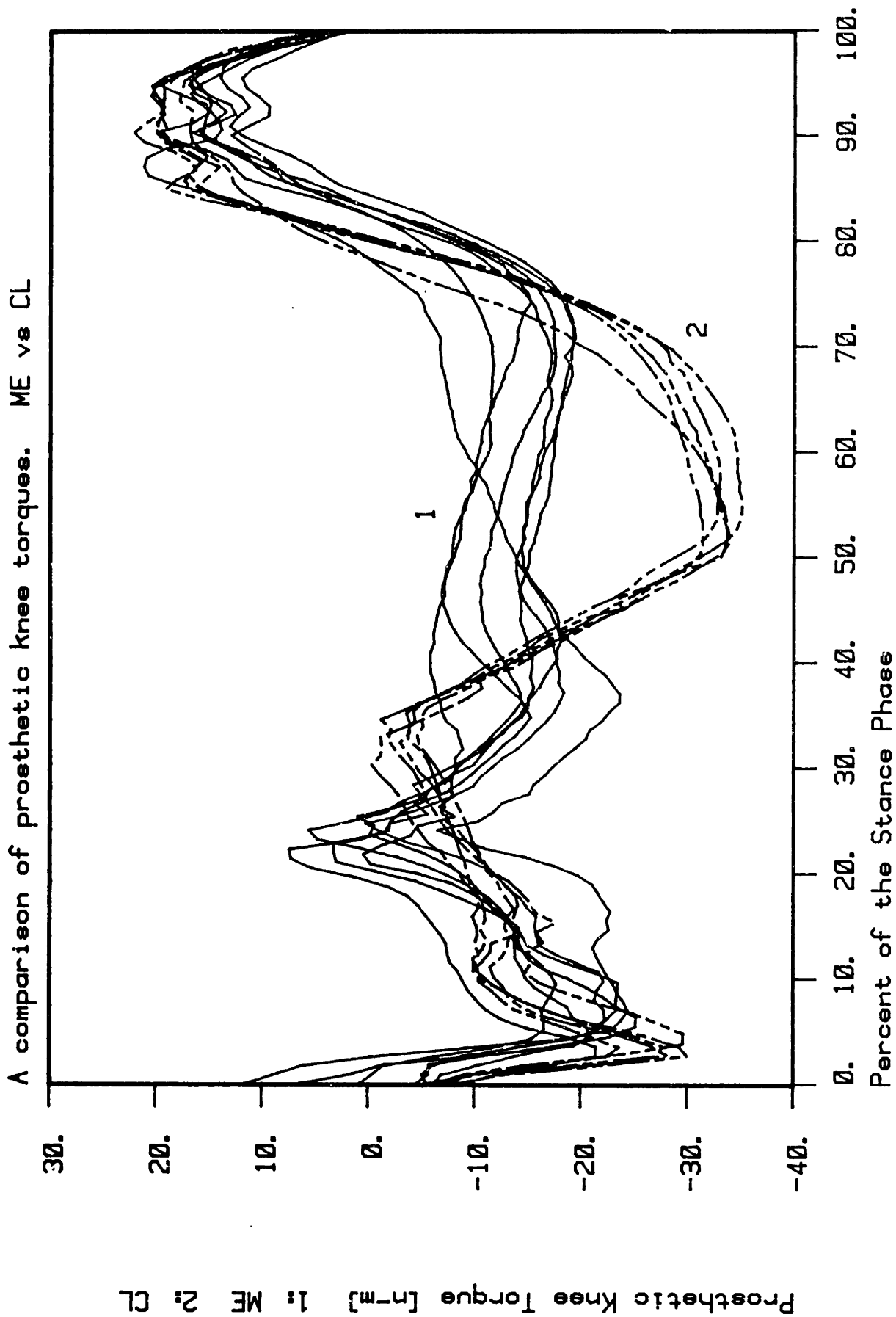


FIGURE IV-28

A Sample of Prosthetic Knee Torque Trajectories as Measured by TRACK During Stance. A Comparison of ME vs CL Stance Phase Knee Controllers.

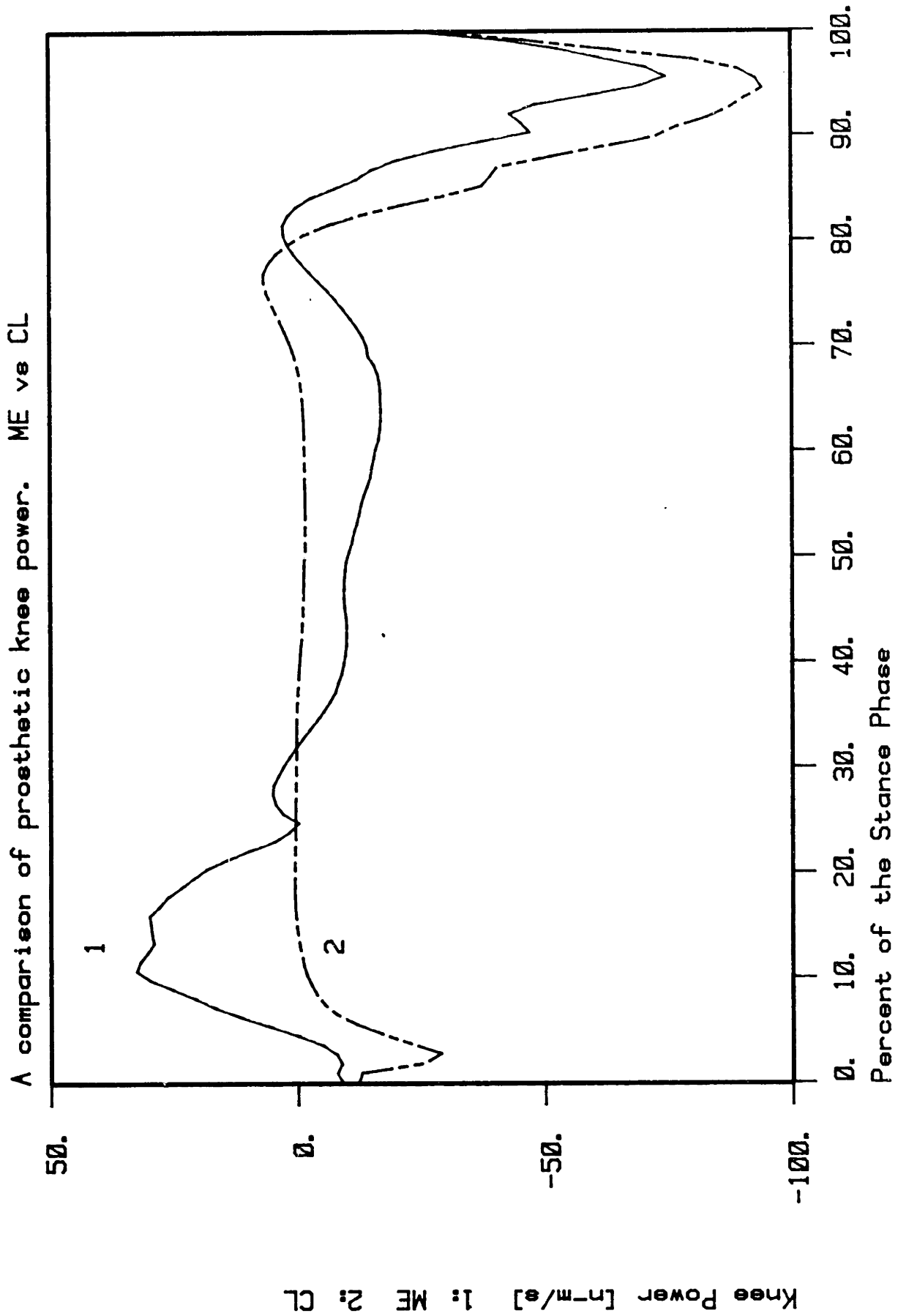
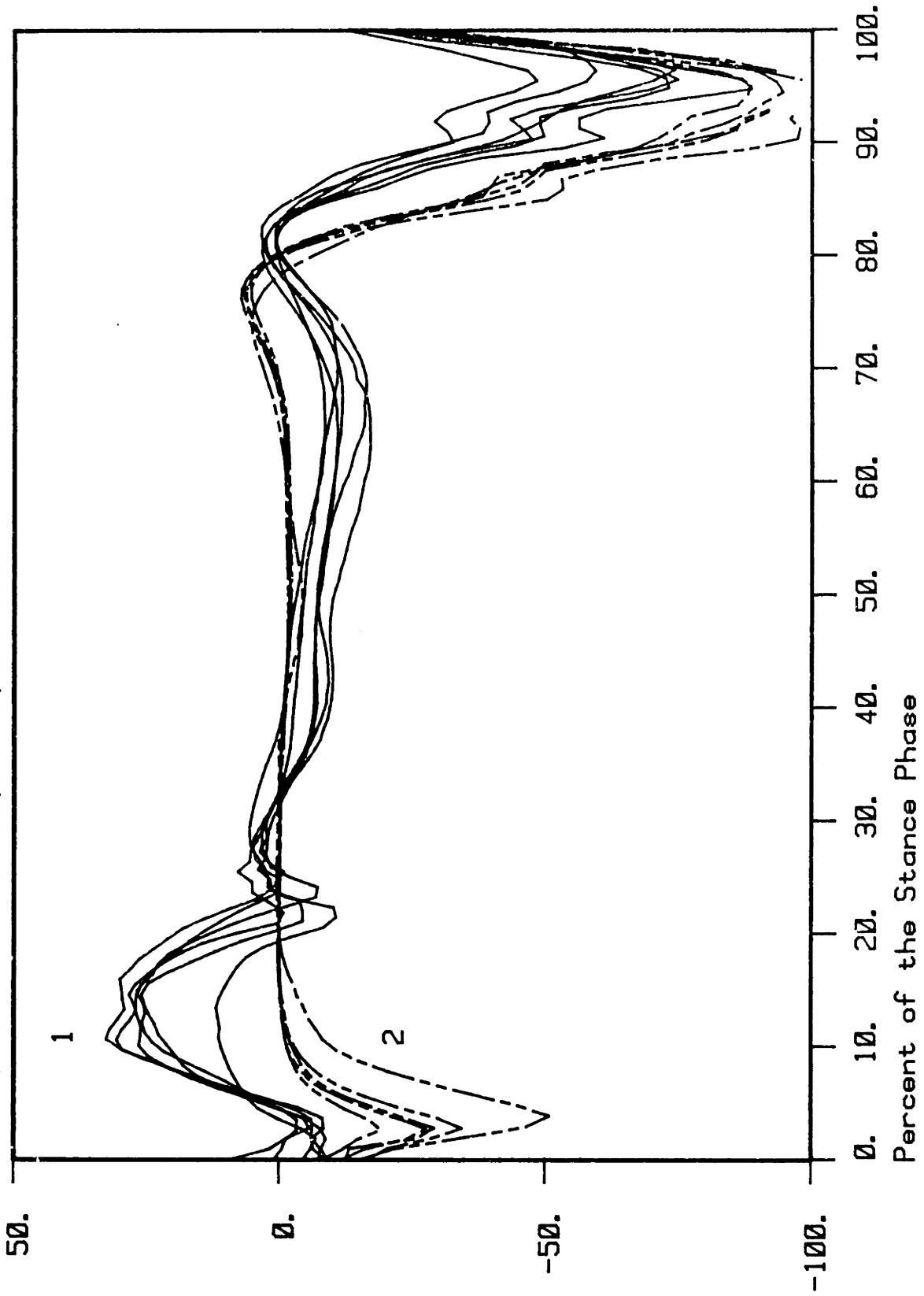


FIGURE IV-29

Typical Prosthetic Knee Power Trajectory as Measured by TRACK During Stance. A Comparison of ME vs CL Stance Phase Knee Controllers Run J11497 vs J11494

A comparison of knee power profiles. ME vs CL



Prosthetic Knee Power [n-m/s] 1: ME 2: CL

FIGURE IV-30

A Sample of Prosthetic Knee Power Trajectories as Measured by TRACK During Stance. A Comparison of ME vs CL Stance Phase Knee Controllers



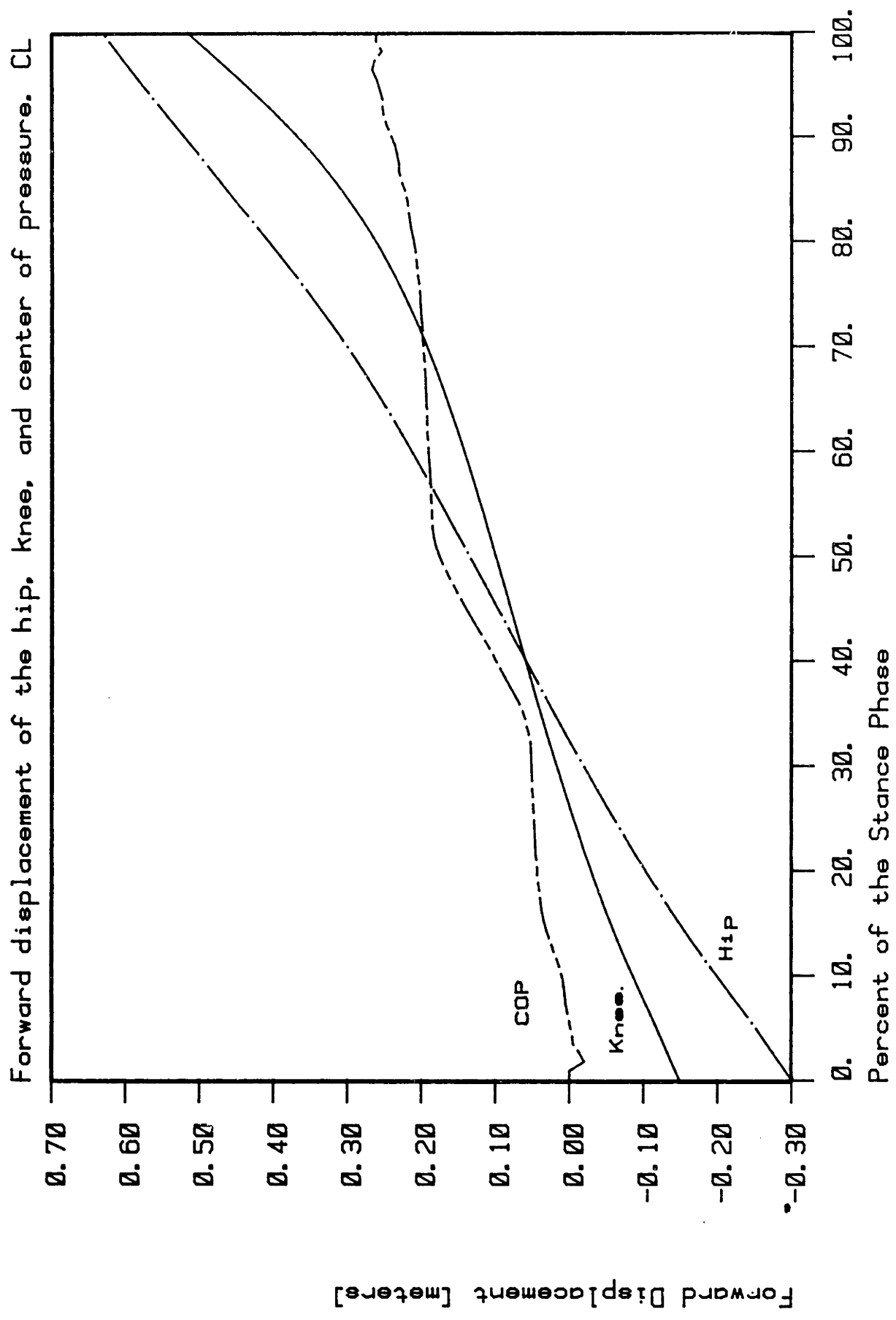


FIGURE IV-31

The Typical Kinematic Relationship that Exists Between Forward Hip, Knee, and Center of Pressure Position During Stance Under CL Control. Run J12022

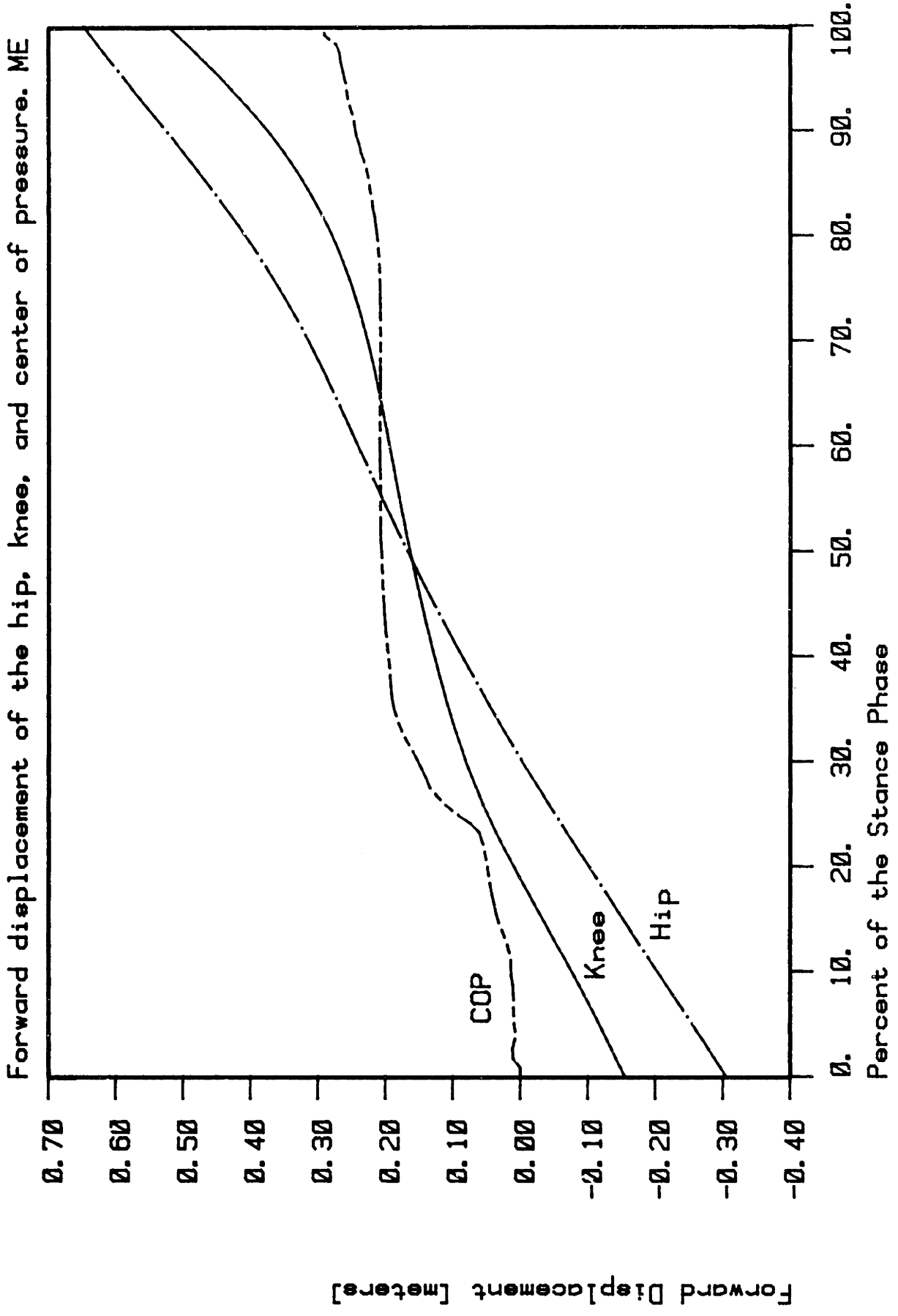


FIGURE IV-32

The Typical Kinematic Relationship that Exists Between Forward Hip, Knee, and Center of Pressure Position During Stance under ME Control. Run JL2024.

IV-32 the hip, knee and center of pressure displacement in the forward direction are all plotted against percent of stance to indicate the geometrical relationship between them. These demonstrate a purely static gravity load vectors effect on knee torque. As the body moves well ahead of the foot the system is self-stabilizing and in fact a large extensive knee torque is produced involuntarily. This, in fact, can be a problem because it must be overcome by the amputee applying a hip torque sufficiently large to produce a flexive knee torque which produces knee break right around SHC. After SHC the torque remains flexive (hip torque, sound leg forces are responsible) in order to initiate the swing phase. In contrast, during prosthetic heel roll the ME controller requires a prolonged extensive torque. This is due to amputee fighting against the flexing knee, trying to assure himself of a stable knee. This is, of course, unnecessary with an active controller such as the ME controller that can guarantee stability. In fact, as can be seen in Figure IV-30, power is consumed by the knee actuator to "fight" with the amputee.

The re-extension of the prosthetic knee joint under ME control is accomplished in a purely passive manner. The momentum vector, the gravitational loading vector, and near SHC the loading from the decelerating sound leg (see section on Sound Leg Forces) all tend to drive the knee into full extension and thus deliver power to the knee joint. However, the extensive prosthetic knee torque during this section of stance is as much as 75 percent less than the knee torque generated under CL control. This is due to the load vector being closer to the knee axis due to knee being flexed (see Figure IV-32). Thus from a purely static gravity load vector analysis, the ME controller would reduce the over

torque the CL controller shows before knee break. After SHC the two controllers are identical. The differences seen in prosthetic knee torque trajectories after SHC are due to the differences in initial conditions upon entering this last phase of stance.

#### IV-3.2 Hip torque and power - Figures IV-33, IV-34 and IV-35

The role of hip torque in A/K amputee gait has been explored for years due to its perceived importance in gait control. This will be explored in a general way in Section V, but first the role of hip torque in controlling knee torque during the stance phase will be studied as a function of the two stance phase knee controllers previously discussed.

The radical differences in prosthetic knee torque that were caused by the two stance phase knee controllers did not occur at the hip. This implies that hip torque and knee torque are not as closely related as traditionally thought. The two torque profiles are similar although some significant differences are evident.

The general shape of the profiles match those published by other researchers [12,38,47,118,120) with the traditional interpretation as follows. At PHC the amputee applies an extensive hip torque to insure the knee joint moves into and stays in against the hyperextension stops to prepare the prosthesis for stable weight bearing. The body is also being slowed down and hip extensive moment counterbalances this. During mid-stance the prosthesis is self-stabilizing and the hip torque values are low. Hip torque then becomes flexive to cause the knee to flex by overcoming the over self-stabilizing moment at the knee caused by the static load line (a vector from the body c.g. through the center of

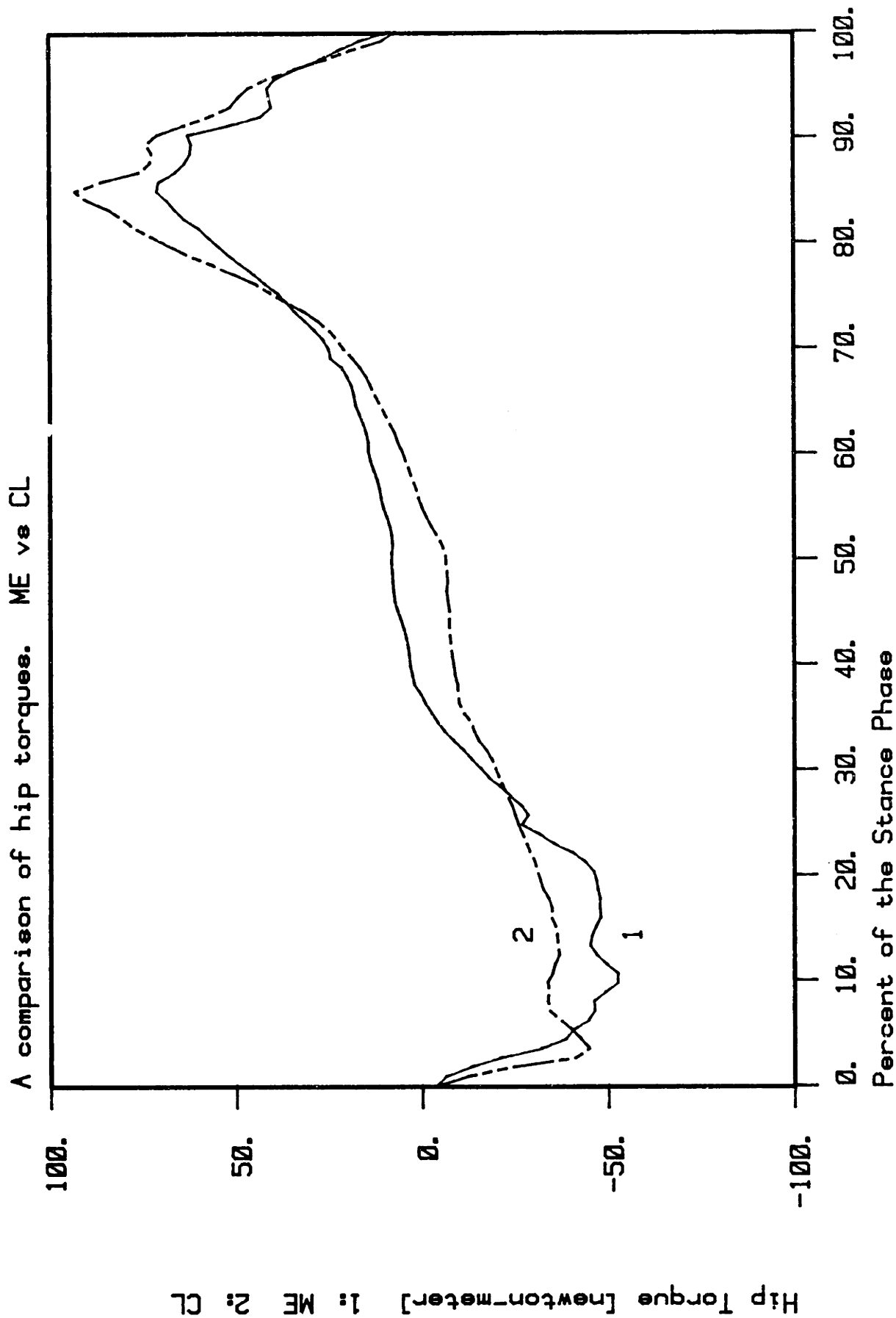
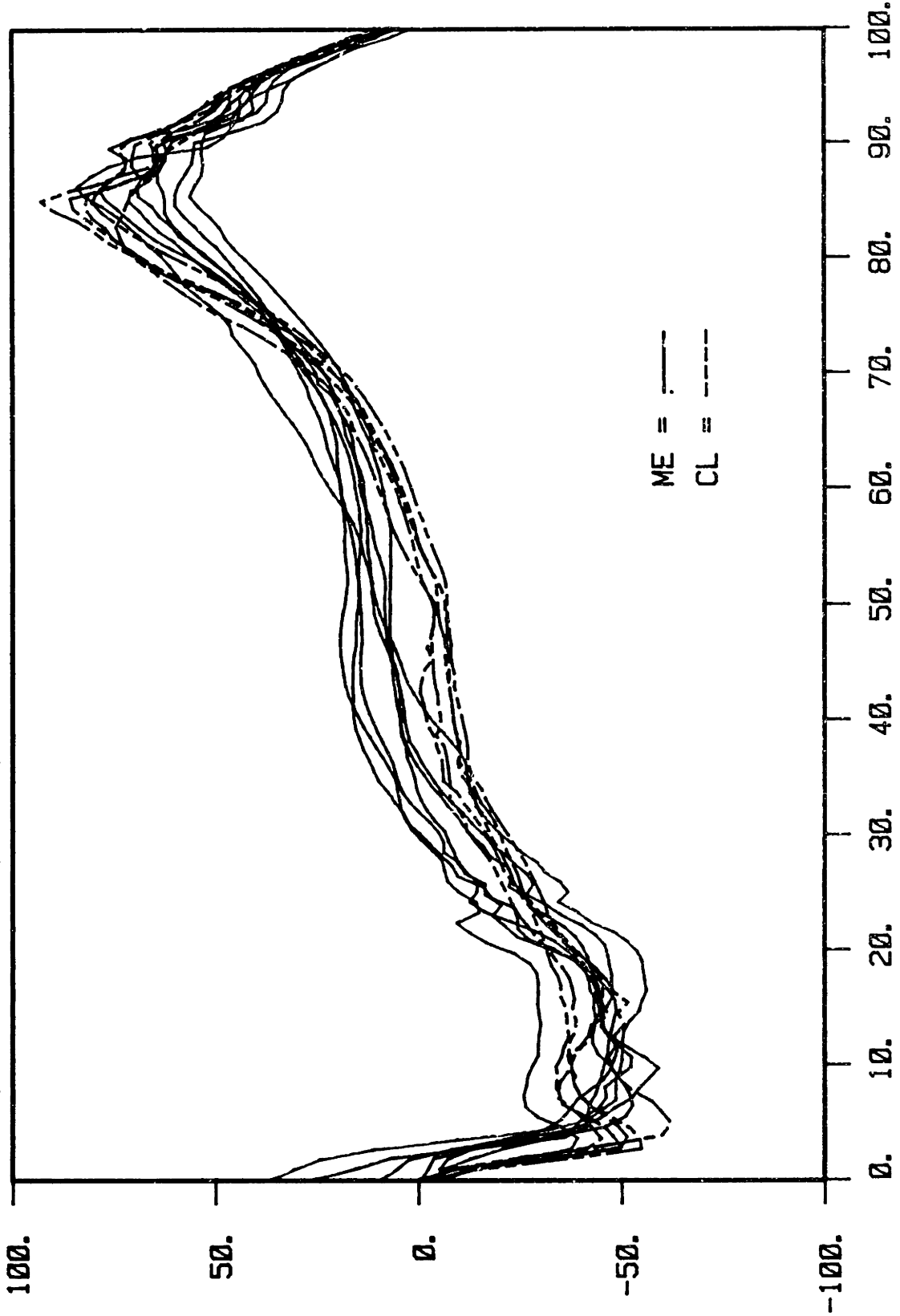


FIGURE IV-33

Typical Hip Torque Profiles on the Prosthetic Side During Stance. A Comparison of ME vs CL Stance Phase Controller. Run JL1427 vs JL1494

A comparison of hip torques. ME vs CL



Hip Torque [newton-meters] 1: ME 2: CL

Percent of the Stance Phase

FIGURE IV-34

A Sample Hip Torque Profiles on the Prosthetic Side During Stance. A Comparison of ME vs CL Stance Phase Controllers

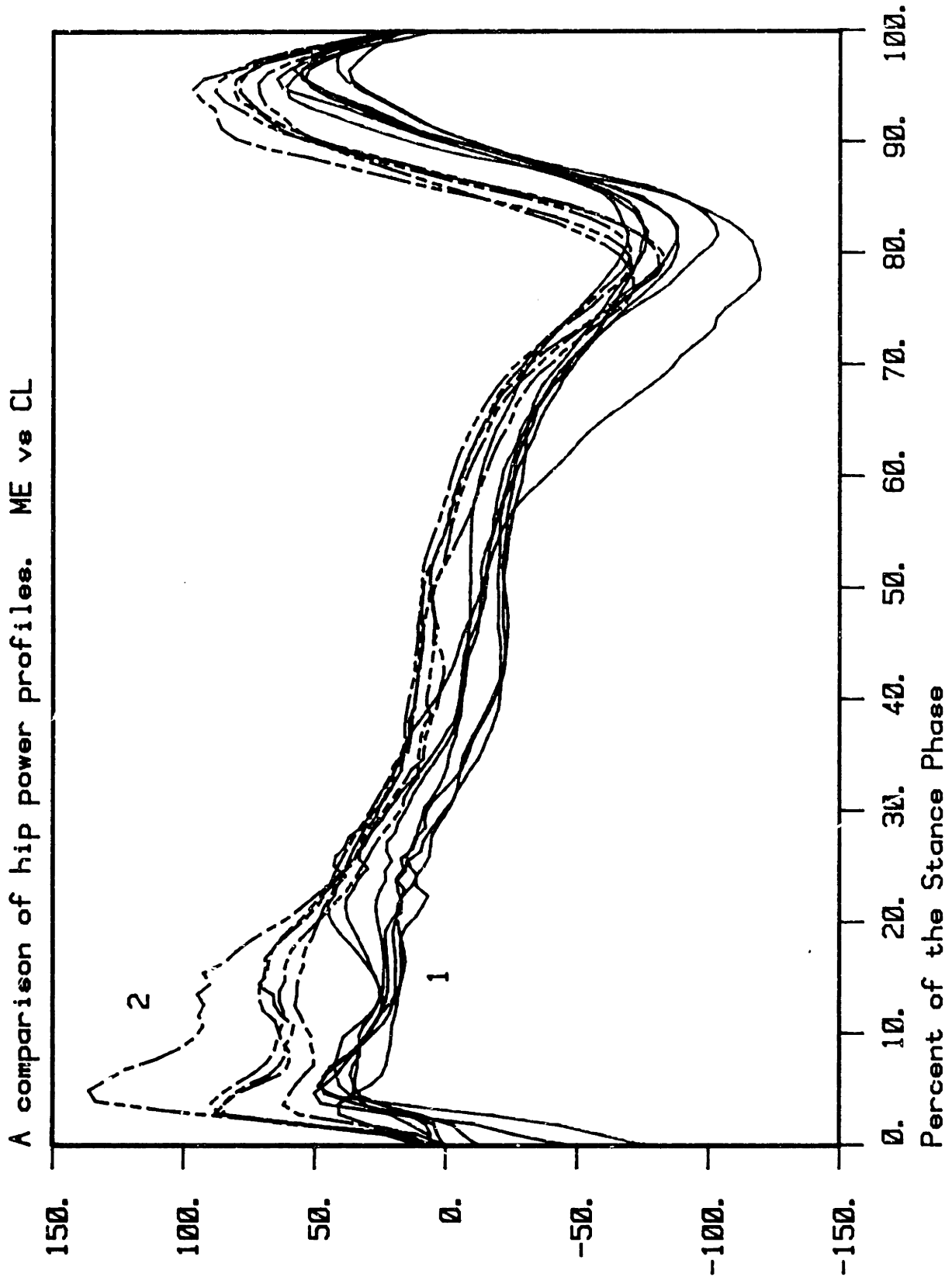


FIGURE IV-35

A Sample of Hip Power Profiles on the Prosthetic Side During Stance. A Comparison of ME vs CL Stance Phase Knee Controllers

pressure) being ahead of the knee axis. The hip torque remains flexive, rotating (flexing) the thigh preparing the whole leg for the swing phase.

The ME stance phase knee controller produces a hip torque trajectory that partially reflects the changes in the prosthetic knee torque profile as discussed in the last section. The fact that this is only partially true indicates some other external forces (e.g. sound push off forces) are also responsible for knee torque during double support. As discussed in the previous section and shown in Figure IV-28, the prosthetic knee torque profiles show a prolonged extensive torque as the amputee is fighting against the knee flexing. The ME controller hip torque profiles (see Figures IV-33 and IV-34) show this effect by remaining more extensive than in the CL case from approximately 10-25 percent of stance. The hip power profiles in this region of stance show a significantly lower value than the CL controlled counterparts. This is due to the reduced angular velocity of the thigh (see Figure IV-17). If, however, the power required at the knee is added to the hip power profiles, the result is equal to the hip power profiles produced under CL control.

After the prosthetic knee has reached maximum flexion (at 32 percent) and begins to re-extend, the hip torque profiles become slightly flexive as if the amputee wishes to prevent re-extension of the knee or perhaps he is attempting to move his body c.g. forward to compensate for being behind the axial line of the shank as the shank rotates underneath him. Under CL control, the hip profiles remain extensive, still trying to ensure knee lock up to 60 percent of stance.



The hip power also goes negative at maximum knee flexion indicating as with the knee power profiles that re-extension costs the amputee no mechanical work. In contrast the hip under CL control continues to produce work to maintain knee stability up to 60 percent of stance. At knee break the two hip torque and power profiles are equivalent. As break out continues, less hip torque and power are required to initiate the swing phase with the ME controller. This again illustrates the different initial conditions that exists at knee break for the two controllers.

### IV-3.3 Foot/Floor reaction forces

#### IV-3.3.1 Vertical reaction force - Figures IV-36 and IV-37

The vertical foot/floor reaction force trajectories under both stance phase knee controllers are shown in Figures IV-38 and IV-39. For the first 10 percent of stance the vertical loading is identical for the two controllers. From a kinematics perspective this is reasonable (although not guaranteed) since the knee has not significantly flexed and the thigh and shank angles are similar to those produced under CL control. After 10 percent, however, the knee flexes rapidly under ME control and the vertical loading rate drops close to zero. This continues until knee flexion slows down (approximately 24 percent of stance) as maximum knee flexion is approached, which is also when PTC occurs. The loading resumes its initial (pre-rapid knee flex) rate reaching an average maximum of approximately 720 newtons (an average of 7 percent over static weight) at maximum knee flexion. Under CL control, the loading rate simply continues to increase linearly until STO where an average maximum vertical load of approximately 710 newtons (6. percent over static weight) is observed.

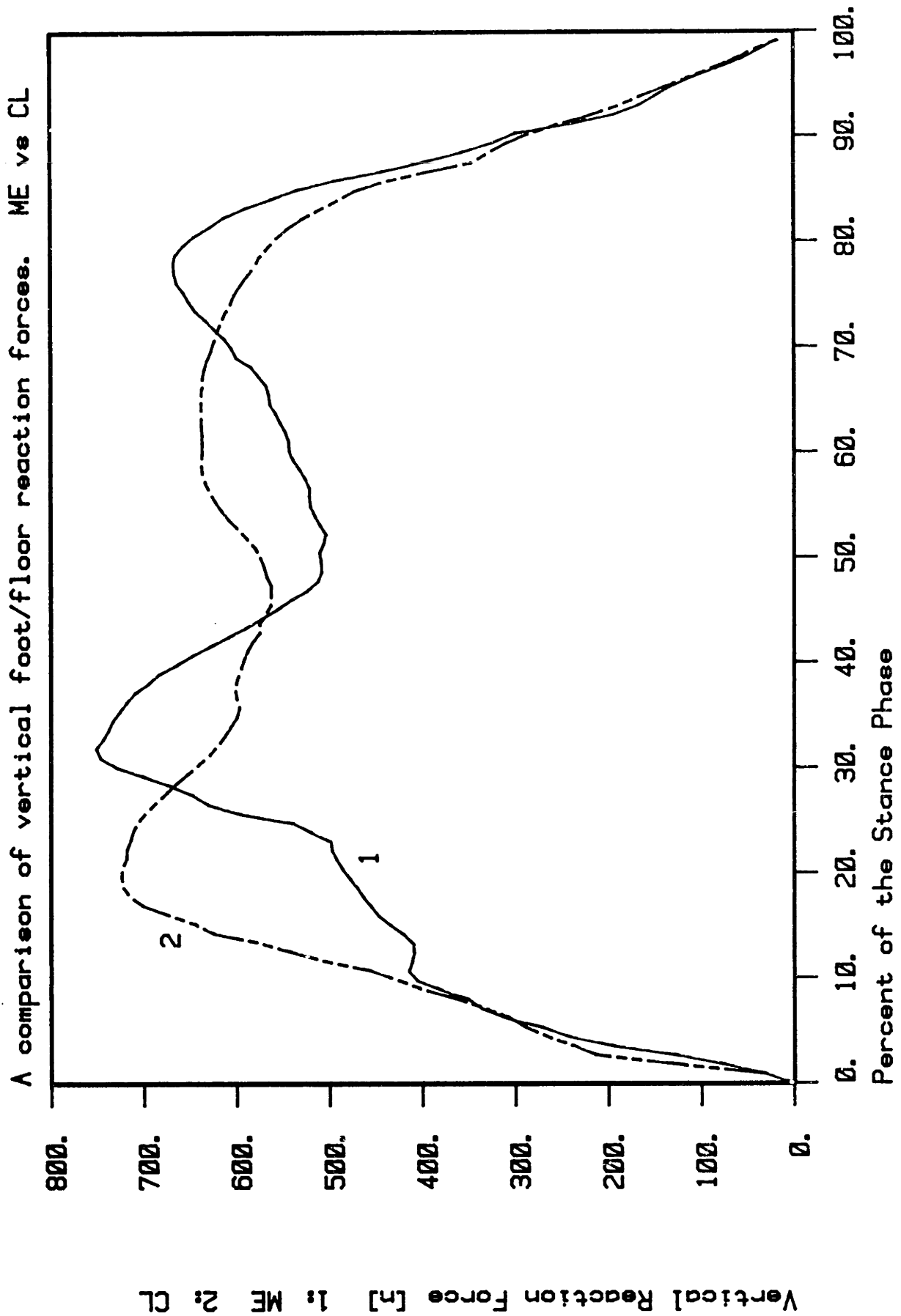


FIGURE IV-36

Typical Vertical Foot/Floor Reaction Trajectories. A Comparison of ME vs CL Stance Phase Knee Controller. Runs JL1427 vs JL2022.

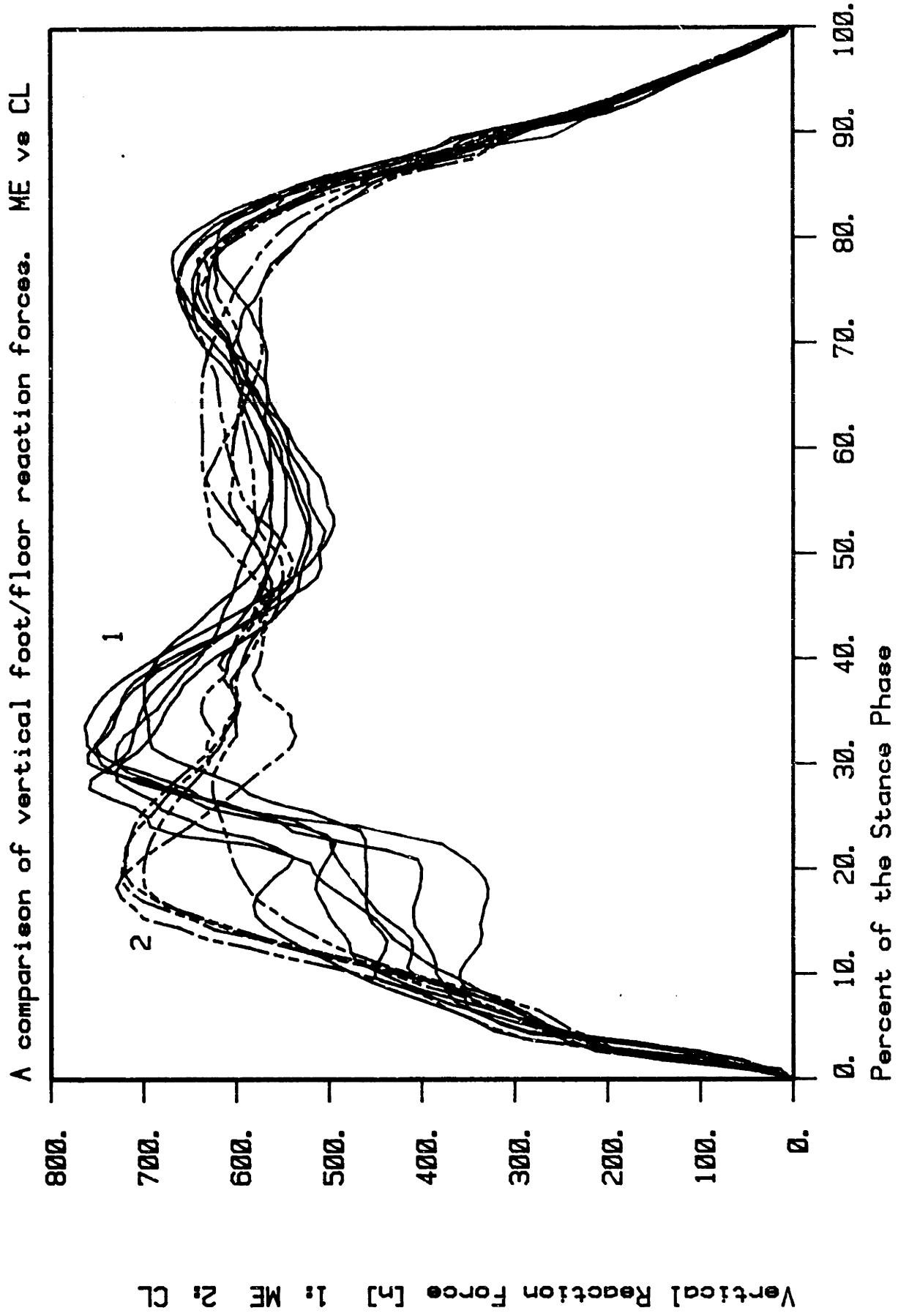


FIGURE IV-37

A Sample of Vertical Foot/Floor Reaction Trajectories. A Comparison of ME vs CL Stance Phase Knee Controllers

After peak loads occur both profiles fall off to below static body weight, where they remain relatively constant in value until SHC. The load profile for the ME controller does show a greater variation during this period (the period of knee extension) and this is probably related to the increased variation in vertical hip displacement profiles as shown earlier in Figure IV-21.

The final part of stance phase occurs after SHC. The vertical loads in both cases fall off quickly and approximately linearly as the sound leg assumes the load. Since the controllers are identical during this period and since it is reasonable to assume the sound leg dominates the load transfer rate, it is not surprising that the two vertical load profiles match despite entering this period of stance with different initial conditions.

#### IV-3.3.2 Anterior/Posterior reaction forces - Figures IV-38 and IV-39

The anterior/posterior (A/P) reaction force profiles as shown in Figures IV-38 and IV-39, differ significantly as a function of the two stance phase knee controllers. The general shape of both profiles is to brake or resist the falling body during the first half of stance and to provide a propulsive force during last half. However, the phasing of the braking forces and the magnitude of the propulsive forces clearly distinguishes the two controllers.

Close analysis of the A/P curves shows that both controllers produced A/P reaction force trajectories which peak and level out with the same histories as the vertical reaction force profiles. Thus, as with the vertical reaction force profiles, the A/P profiles for the ME controller

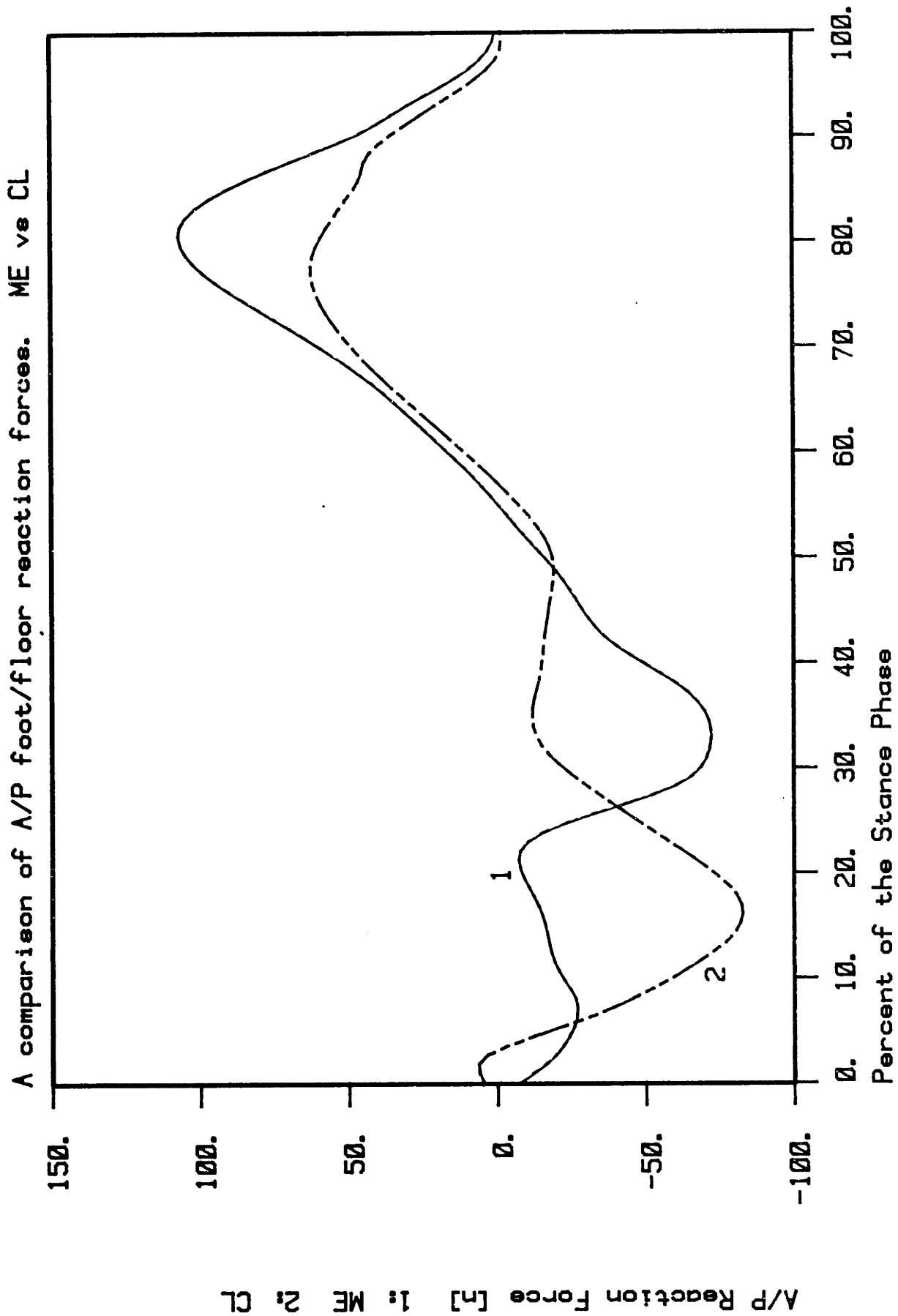


FIGURE IV-38

Typical A/P Foot/Floor Reaction Trajectories. A Comparison of ME vs CL Stance Phase Knee Controllers. Runs JL1427 vs JL2022

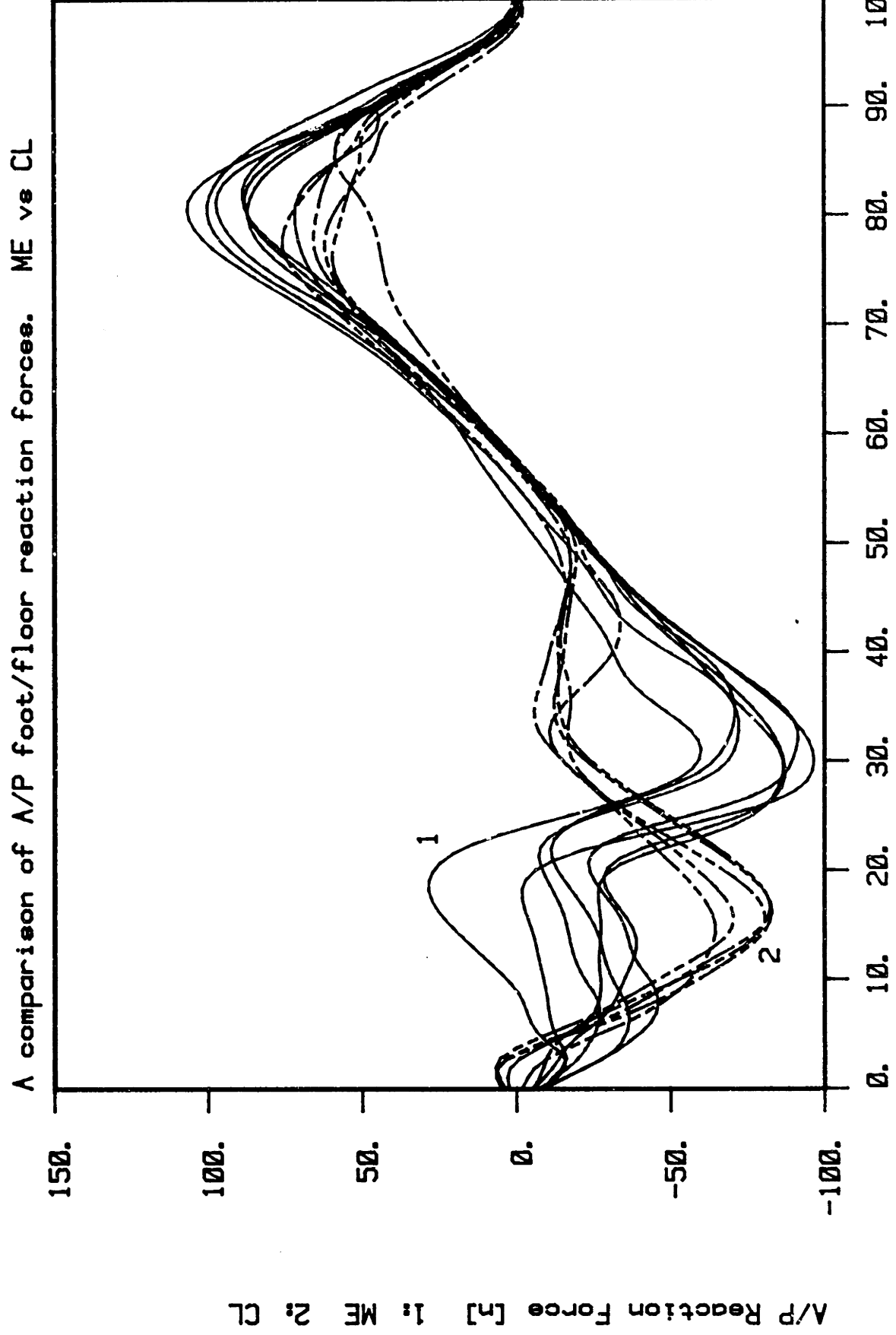


FIGURE IV-39

A Sample of A/P Reaction Force Trajectories. A Comparison of ME vs CL Stance Phase Knee Controllers

shows increasing braking force up until rapid knee flexion occurs at which point the A/P slope reverses and the force becomes smaller until PTC where the slope reverses again and the force builds up to a maximum of around 80 newtons at maximum knee flexion. The knee extends and the A/P force trajectory reverses sign approximately when the hip joint is nearly over the center of pressure (see Figure IV-32). As the knee continues to extend, propulsive reaction force of 100 newtons is recorded at knee break (40% larger than for CL controller). After knee break the A/P force returns to zero. For the CL controller the braking forces builds up a maximum of 80 newtons at STO then reduces in magnitude leveling off at near zero at PTC. It remains lower in value than for the ME case, changing sign when the hip joint is over the center of pressure (see Figure IV-31) and the hip torque changes sign (see Figure IV-34). A linear buildup in propulsive force is then seen up to knee break where a peak propulsive force of approximately 60 newtons is recorded. After knee break the A/P force returns to zero at PT0.

In summary, under ME control the peak foot/floor reaction forces during the first half of stance shifted from occurring at 22 to 34 percent of stance and the peak A/P reaction force in the second half of stance increased by 40 percent. This raises three important questions. 1. What is the mechanism which allows the maximum load to occur later in stance? 2. What is the mechanism which allows the peak prosthetic push-off force to increase by 40 percent? 3. What are the implications on stump loading? Exploration of questions 1 and 2 will be postponed until the section on sound leg forces. Question 3 will be considered subsequently.

#### IV-3.4 Stump loading

In this section a comparison of the saggital plane torques and axial loads acting on the distal end of the thigh as a function of stance phase knee controller are examined. This is done in order to compare the controller's effect on stump loading. While many factors account for a comfortable stump/socket interaction during gait, it is assumed for comparison purposes, that smaller torques or axial loads feel better to the amputee and cause less damage to the stump.

As discussed in the previous section, the peak vertical foot/floor reaction load is the same for both controllers, but occurs at a different time during stance. However, if the vertical reaction force profiles are plotted against thigh angle the peaks coincide (see Figure IV-40). Indeed, Figure IV-41 shows the actual distal axial loading on the thigh as a function of thigh angle for the two controllers and little difference is observed.

The knee torque is also assumed to have an effect on stump/socket comfort. The knee torque trajectories (see Figure IV-28) as a function of the two knee controllers were discussed in section 3.1 of this chapter. While the knee torque profiles for the ME controller are larger than the profiles for the CL case between 10 and 30 percent of stance, from 30 to 80 percent of stance they are smaller in magnitude. The stump loading due to the knee torque on average is lower under ME control.



A comparison of vert. rxn. force vs thigh angle. ME vs CL

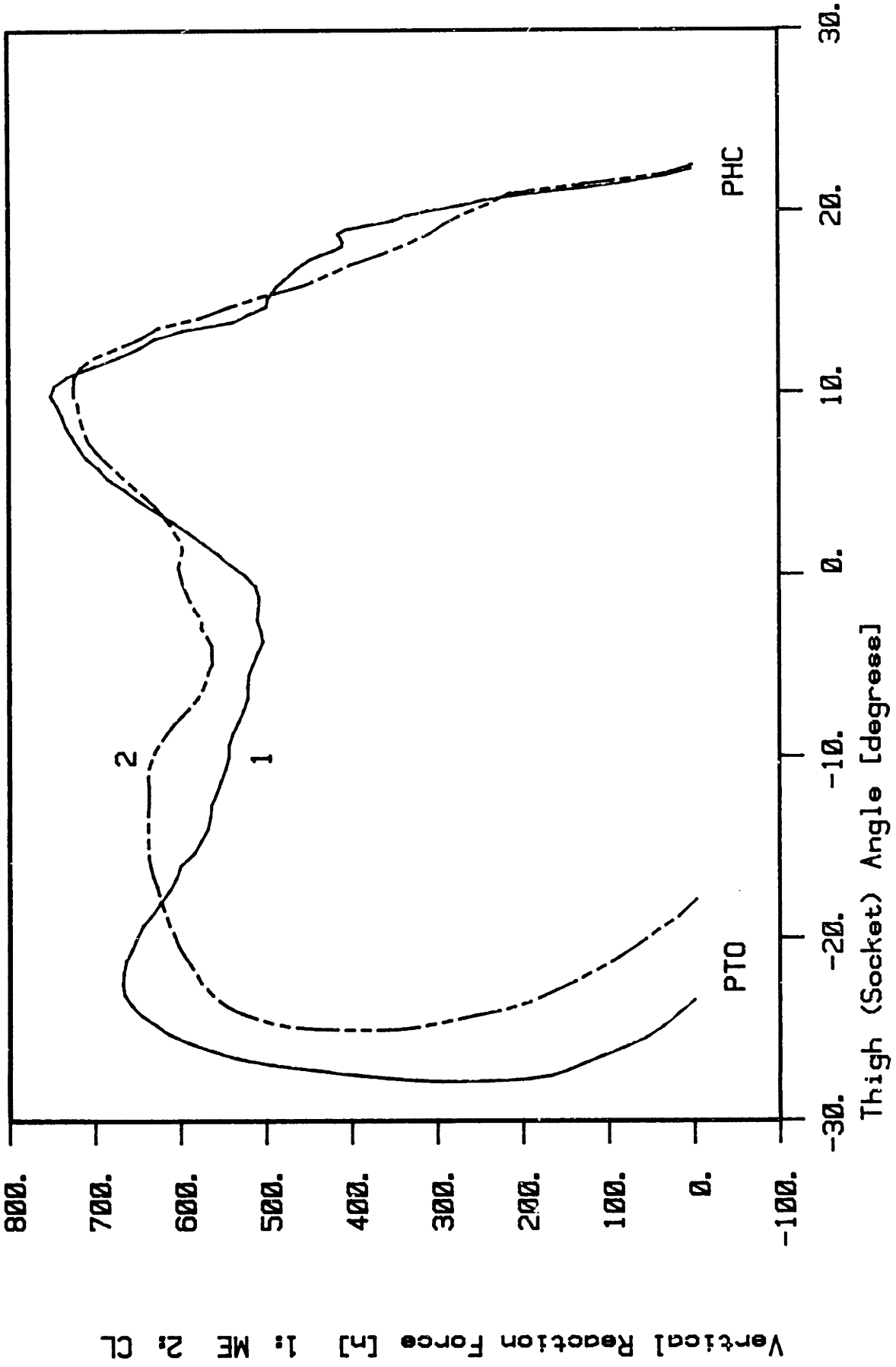


FIGURE IV-40

Typical Vertical Foot/Floor Reaction Forces as a Function of Thigh Angle. A Comparison of ME vs CL Stance Phase Knee Controller. Run JL1427 vs JL2022

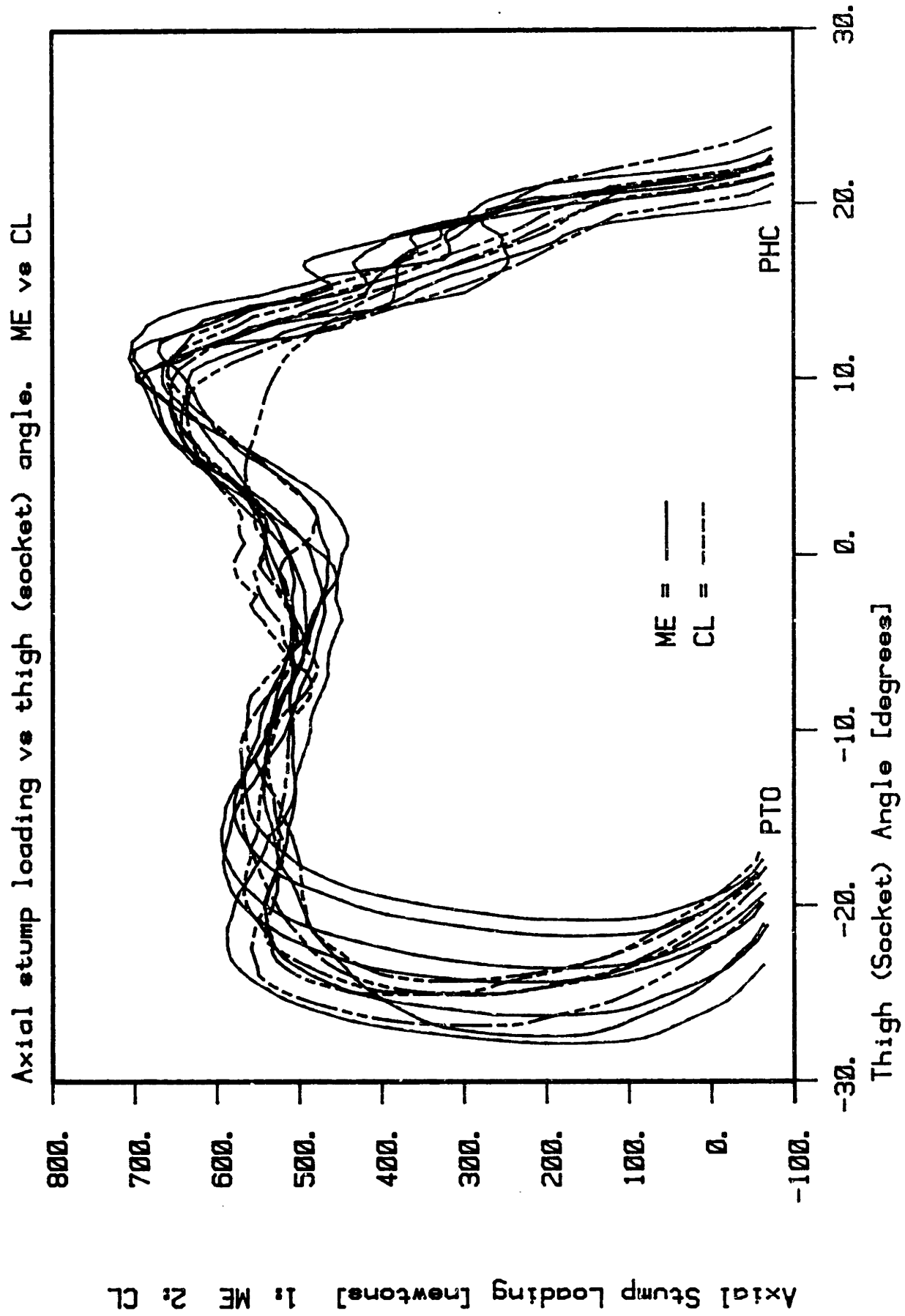


FIGURE IV-41

A Sample of Axial Loads on the Stump at the Knee as a Function of Thigh Angle During Stance. A Comparison of ME vs CL Stance Phase Knee Controllers

## IV-3.5 Sound leg forces - Figure IV-42

### IV-3.5.1 Vertical sound leg forces

The general shape of the vertical sound leg force profiles shown in Figure IV-42 is similar to published sound foot/floor reaction forceplate data (Cunningham [27], Eberhart [38]). (Note: The sound force as defined in this thesis is not the foot/floor reaction force of the sound leg but the effect of the sound leg on the prosthetic hip. Thus even after STO the sound leg will still affect the prosthetic side as a result of the gravitational and inertial properties of the sound leg.) At PHC the sound leg is pushing off and thus supporting the static weight of the body (670 newtons) plus the inertial effects of accelerating body up (approximately 330 newtons). After PHC the load is being transferred to the prosthetic leg and the sound leg forces show an approximately inverted load profile of the prosthetic leg. The sound leg force drops to approximately zero at STO. At SHC the sound leg catches the body as it comes off the prosthetic leg and the sound leg force quickly rises to full body weight plus the force due to accelerating the body up. Thus, the vertical sound leg force is a useful footswitch.

There is a significant difference in the sound leg forces as a function of the stance phase knee controller. The vertical sound leg forces and the vertical prosthetic foot/floor reaction forces shown in Figure IV-37 and IV-42 show how the load is being shared between the sound and prosthetic leg. Thus the delayed peak in the vertical reaction force under the ME controller is clearly related to the amputee remaining on his sound leg longer. This delay in reaching STO is a result of a halt in the

A comparison of vertical sound leg forces. ME vs CL

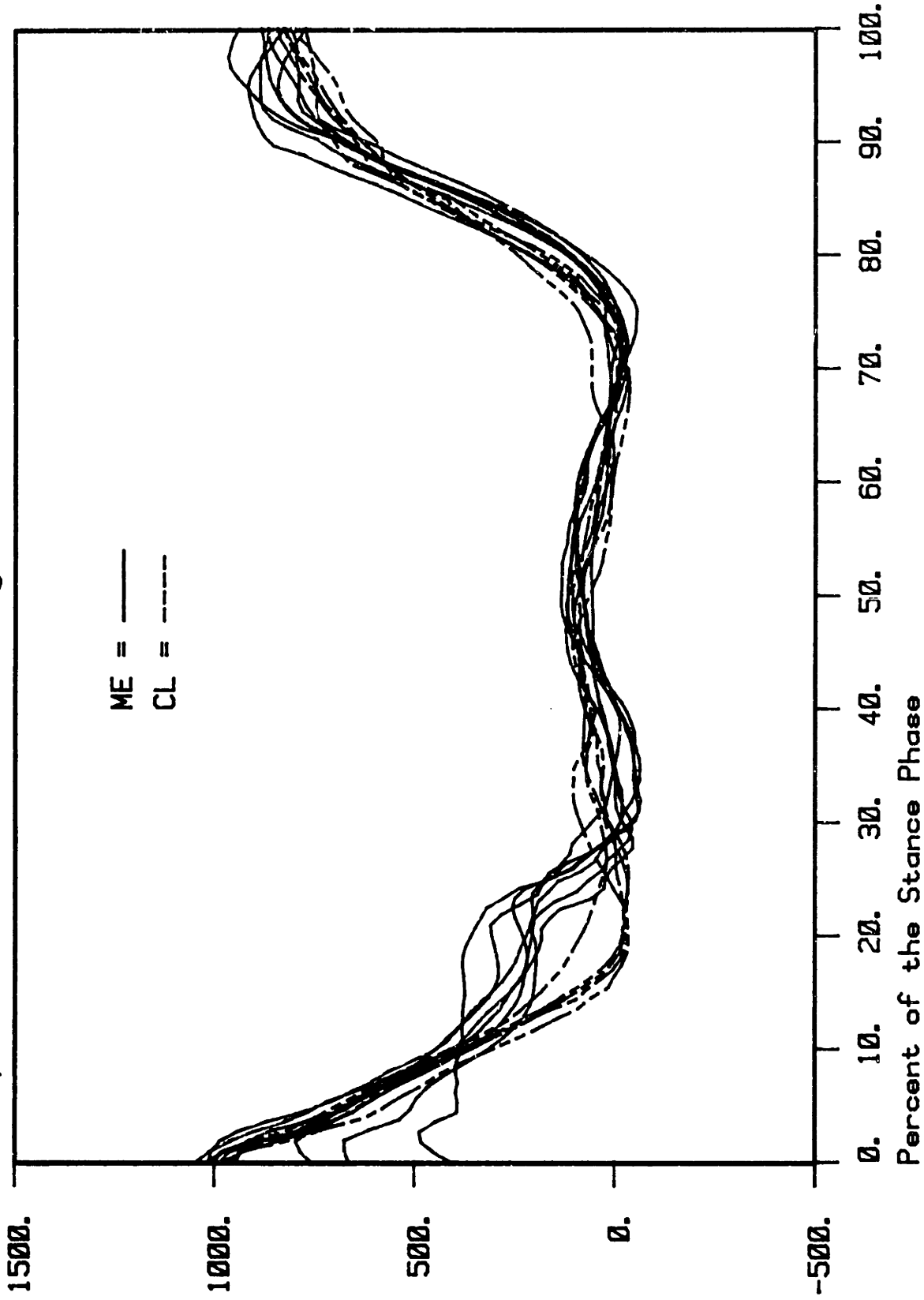


FIGURE IV-42

A Sample of Sound Leg Vertical Forces Applied at the Hip on the Prosthetic Side. A Comparison of ME vs CL Stance Phase Knee Controller

load transfer from the sound to prosthetic leg which occurs between 15 and 25 percent of stance. (Note in Figures IV-36 and IV-42 that the slope of the sound and prosthetic leg loads goes to approximately zero between 15 and 25 percent of stance.)

#### IV 3.5.2 Anterior/Posterior sound leg forces - Figure IV-43

The A/P sound leg force trajectory shown in Figure IV-43 is significantly different from published data (Eberhart [38], Cunningham [27]) on A/P sound leg foot/floor reaction forces. This is due to the significant energy levels of the sound thigh and shank as they are accelerated and decelerated during sound swing phase. This effect from an energy perspective has been reported by Bresler, Radcliffe and Berry [12] in 1957. While this makes it hard to compare foot/floor A/P reactions forces between the prosthetic and sound leg, it still provides a representation of the propulsive effect of the sound leg on prosthetic stance (see Chapter V-4).

The large amount of variation seen in the sound leg A/P force is due to the fact that the sound leg force is calculated from noisy acceleration data. Determining the acceleration at the hip is difficult due to the propagation of errors from measurements in the more distal links. This makes it difficult to use the A/P sound leg force to compare the effect of the two stance phase controller. Nevertheless, the general shapes of the curves are useful for understanding propulsion of the prosthetic leg during stance as affected by the sound leg. Up to approximately 15 percent of stance the sound leg propels the body forward as it pushes-off during the end of sound stance. As STO is reached the sound leg A/P force

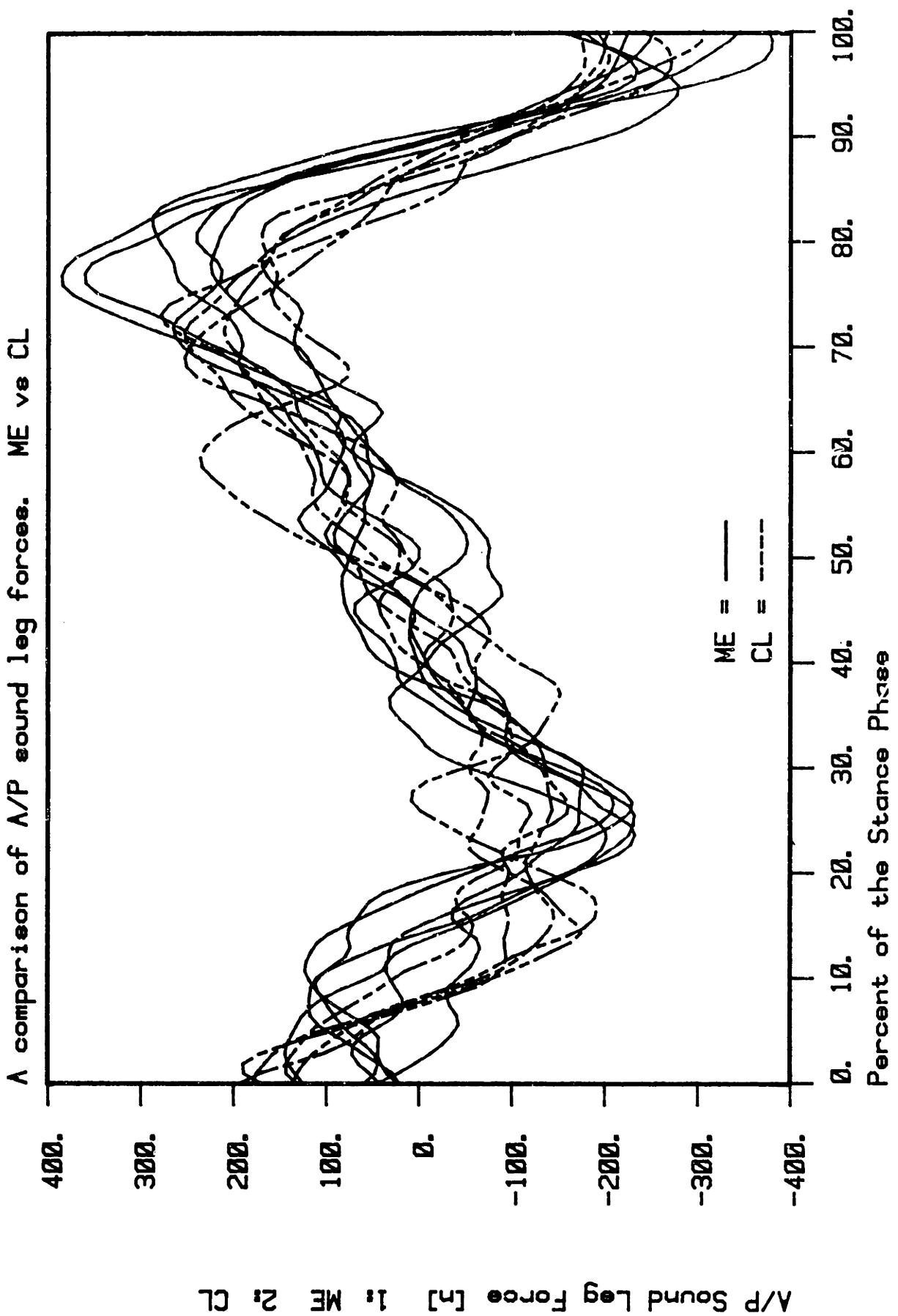


FIGURE IV-43

A Sample of Sound Leg A/P Forces Applied at the Hip on the Prosthetic Side. A Comparison of ME vs CL Stance Phase Knee Controllers

A/P Sound Leg Force [n] 1: ME 2: CL

goes negative indicating that as the sound leg is prepared (accelerated) into swing phase a pull back effect is seen by the prosthetic side. After 50 percent of stance, the sound swing leg begins to decelerate generating a positive sound leg A/P force. This is known as pull through (Bresler et al [10,12]). Soon after SHC, the sound leg A/P force goes negative as the sound leg breaks the forward motion of the body.

## V Designer Gait Modeling and Simulation

### V-1 Introduction

The purpose of this section is to determine the minimum set of factors necessary for simulating the stance phase of gait as represented by the data. This minimum set of factors or model should allow the designer to identify the real physical elements that are important to the gait process and thus be able to redesign the prosthesis and knee joint controller for improved performance during the stance phase of level walking.

The gait data discussed in Chapter 4 is a force and kinematic description of the amputee/prosthesis system. The kinematics represent the global movement of the LED segment attached to the prosthetic shank and the relative position of the thigh with respect to the shank as measured by a potentiometer. The dynamics are calculated from the foot/floor interaction forces measured by the forceplate and the geometry and mass distribution of the mass segments assumed to represent the amputee/prosthesis system from the hip on the prosthetic side to the floor (see Figures II-10 and II-12). Thus, the force and kinematic description contains no explicit representation of stiffness or damping characteristics that may exist in the amputee/prosthesis system. For example, the most distal segment in the inverse dynamic model used for the results presented in Chapter Four includes the shank and the SACH foot. The SACH foot is obviously compliant and, while its effect is accurately accounted for by the effect it has on the measured kinematics and forces, its contribution to those remains hidden.



(Note: There is an additional assumption that the deformation of the SACH foot does not significantly affect the assumed mass distribution of the segment. This is a very reasonable assumption given the maximum possible deformation of the SACH foot relative to the overall size of the shank is very small.)

To determine the hidden effect of actual physical stiffness, and damping has on the data, a model must be developed which either by explicit inclusion or exclusion of the dynamic element allows the interpretation of its effect.

## V-2 Role of SACH Foot

In Chapter IV the importance of the SACH foot geometry in determining the peak in the vertical hip displacement profiles during mid-stance (foot/flat) was demonstrated. In this section, this concept will be expanded to include the heel contact and toe break regions.

In Chapter IV-2.2, the vertical hip trajectory was described as being the result of the subtle phasing of four competing factors that are summarized in Table IV-1. This section will explore the relative importance of these four factors in the different periods of stance.

## V-2.1 Kinematics of prosthetic heel roll

Prosthetic heel roll (PHR) is defined as the time during stance from PHC to PTC. During this period, the vertical hip trajectory (see Figure IV-20) drops below its starting value at PHC before rising above this value at about 10 percent of stance. To explain this clearly, it is helpful to make the following observations. During the first 10 percent of stance the vertical hip trajectories for the two stance phase controllers are similar. In addition, the knee angle differences (see Figure IV-4) during this period are small. Therefore, during this period of stance assume that the knee angle effect on kinematics can be neglected. Therefore, the role of the SACH foot during this period can be accurately studied for both controllers by just studying the CL controller case.

The four kinematic factors affecting vertical hip displacement listed in Table IV-1 have been reduced to three by the elimination of knee angle. A further reduction is possible by looking at the effective leg length (ELL) during stance. The ELL is only affected by the CPM and compliance factors.

Figure V-1 shows the ELL trajectory during stance phase for CL run JL1494. From PHC to 13 percent of stance there is an approximately 2 cm change in the ELL. To determine the relative role of the compliance and CPM factor in causing this change, the following kinematic model is proposed.

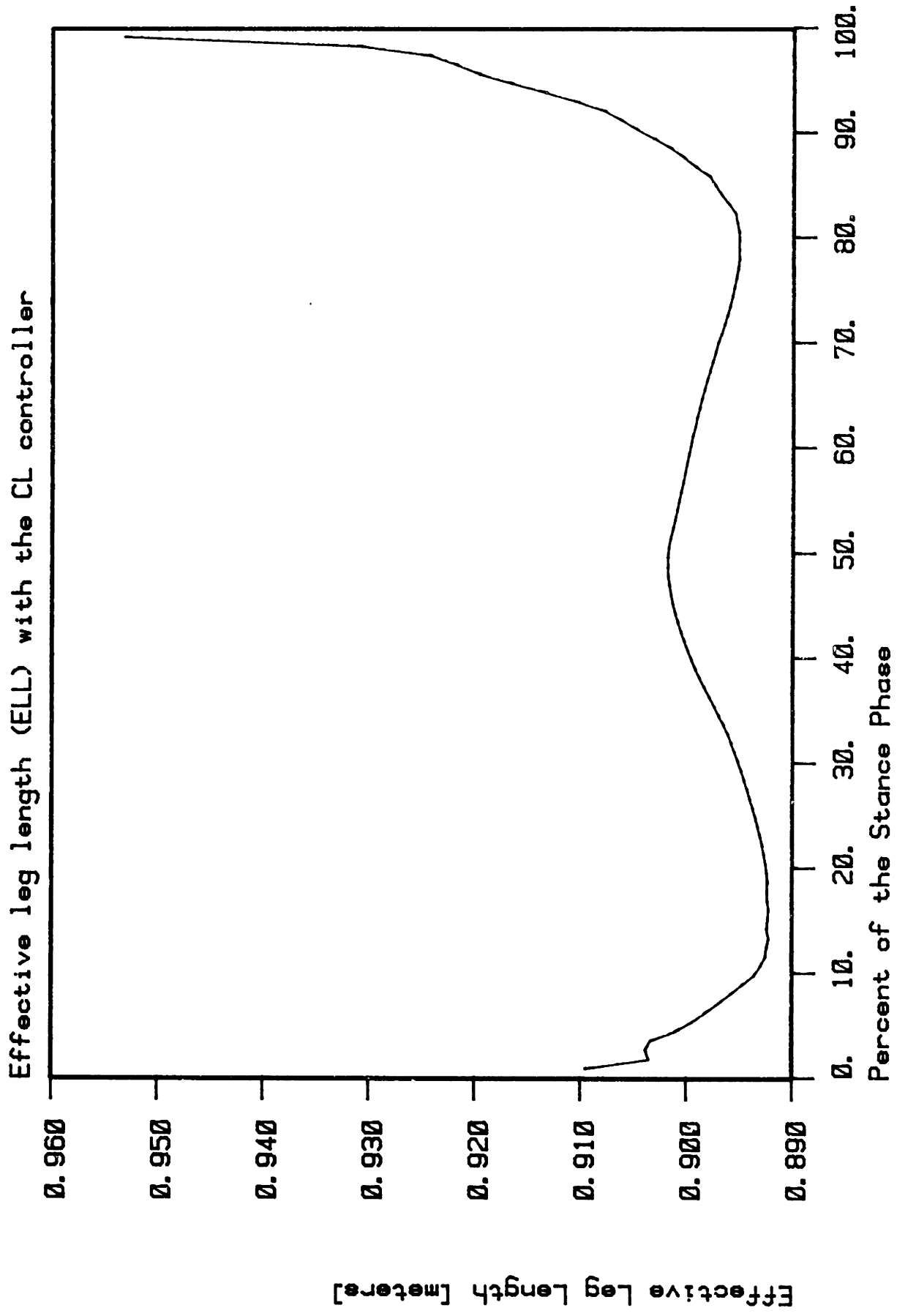


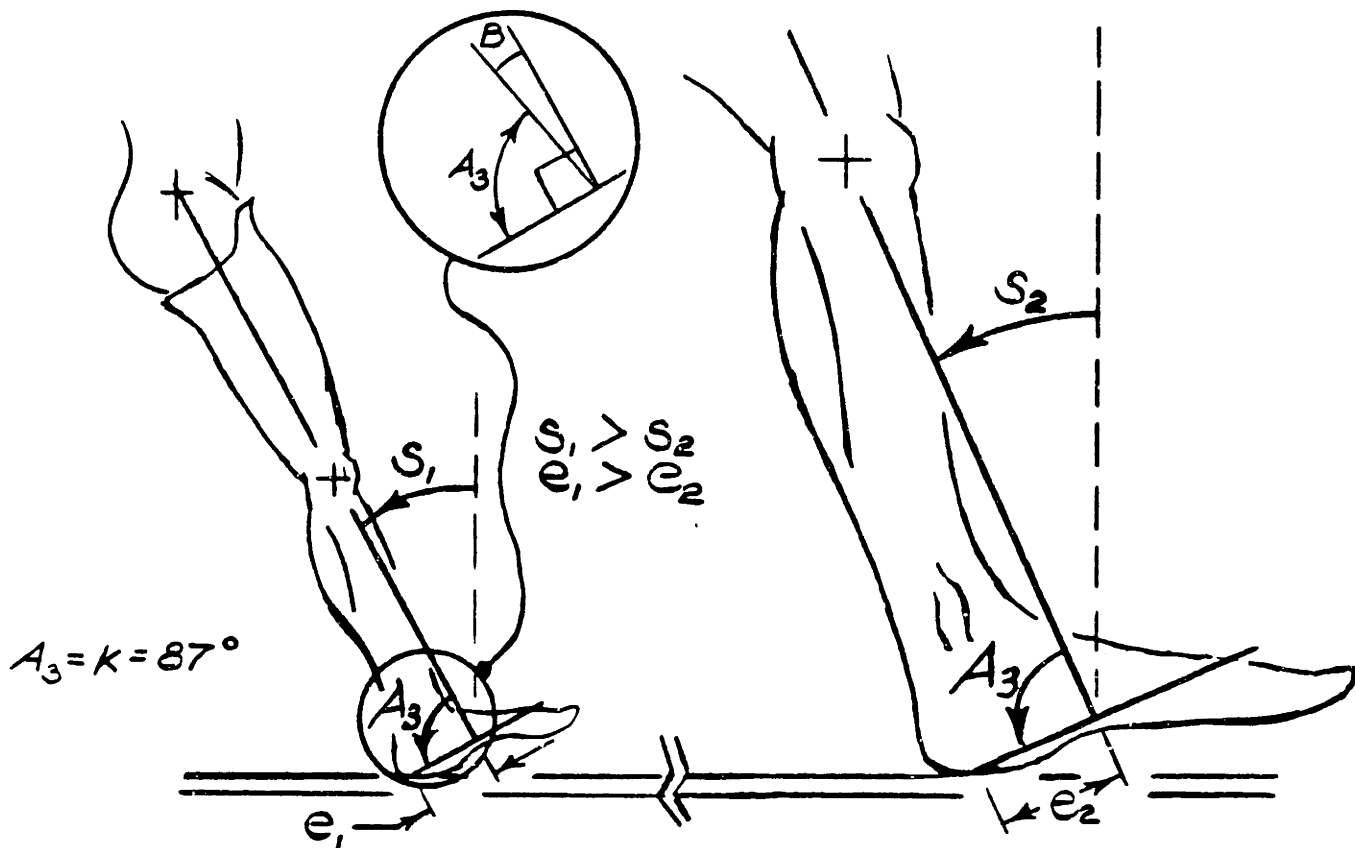
FIGURE V-1

A Typical ELL Trajectory During Stance with a CL Stance Phase Controller. Run JLI494.

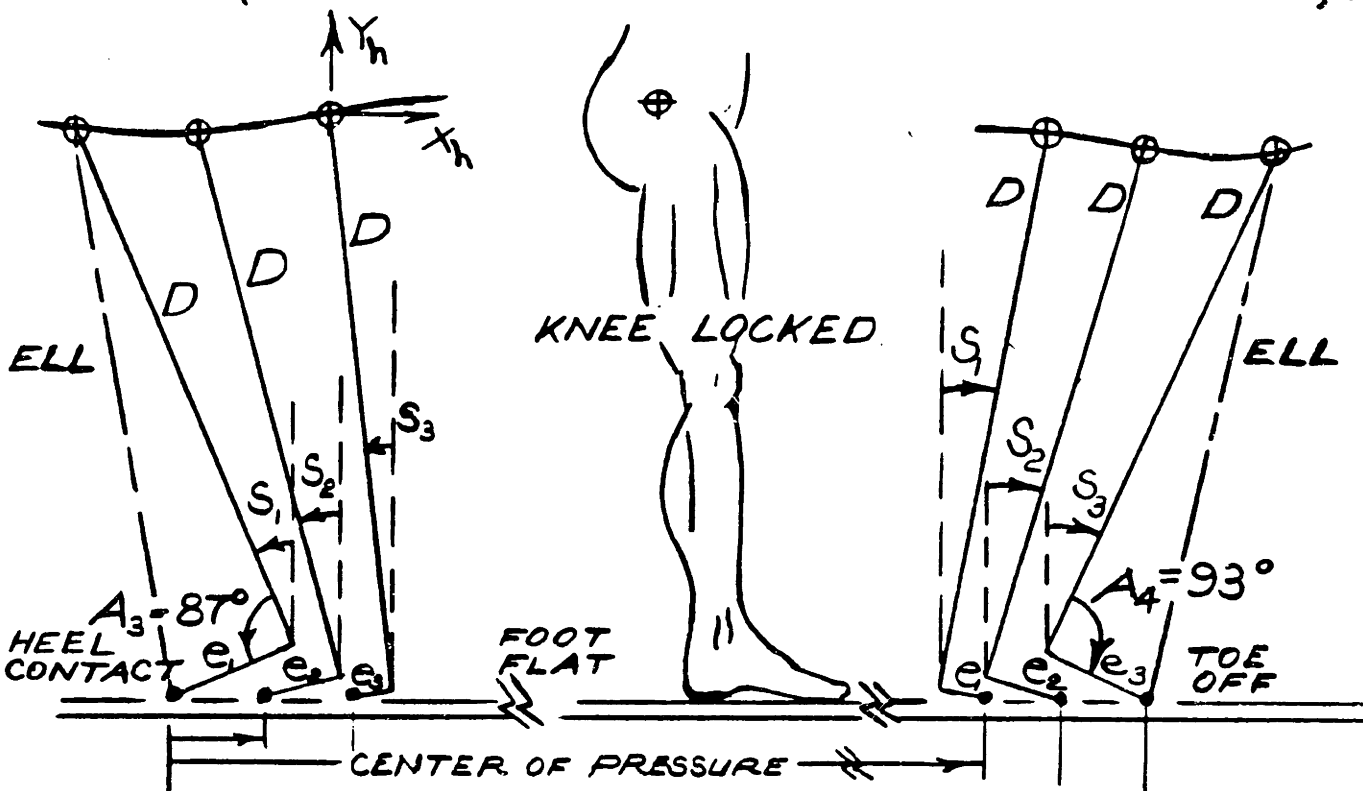
## V-2.2 Rigid model of SACH foot

In Section 2.4 the center of pressure in the forward direction was shown to be a kinematic function of shank angle. This fact can be used to model the SACH foot as a rigid rolling cam. The model is shown in Figure V-2. It consists of two rigid straight line segments. One is a line of constant length-D, representing the distance from the hip to the floor when the prosthesis is in static unloaded footflat. The second line segment is of variable length,  $e$ , representing the distance from the center of pressure to the line segment D at a constant angle,  $B$ . Line segment D represents the shank and its angle is measured with respect to the vertical as shown. Angle  $B$ , is defined to equal the shank angle at footflat.

The model can be initialized in many arbitrary ways. The method used was the following. The initial conditions were set by matching the model to the data at PHC. (This is useful since any compliant elements, if they exist, will not have deflected at that instant.) The initial conditions used are the CL controlled hip displacement,  $(X_h, Y_h)$ , and shank angle,  $S$ . The initial value of  $e$  was obtained as shown in Figure V-2. Subsequent values of  $e$  depend on shank angle. To determine an algebraic function relating  $e$  to shank angle an algebraic function was fit by hand to a typical center of pressure versus shank angle plot (see Figure V-3). Since shank angle,  $S$ , and  $B$  are known,  $D$  and  $ELL$  can be determined by simple trigonometry. See Appendix 1 for the details of the formulation and equations. Figure V-4 shows the approximate profile generated by this method.



$e_n$  LOCATES CENTER OF PRESSURE  
 (CHANGE  $e_n$  WITH EACH INCREMENT,  $\Delta S$ )



KINEMATICS OF THE SACH FOOT  
 FIGURE IV-2

A comparison of center of press. movement vs shank angle. ME vs CL

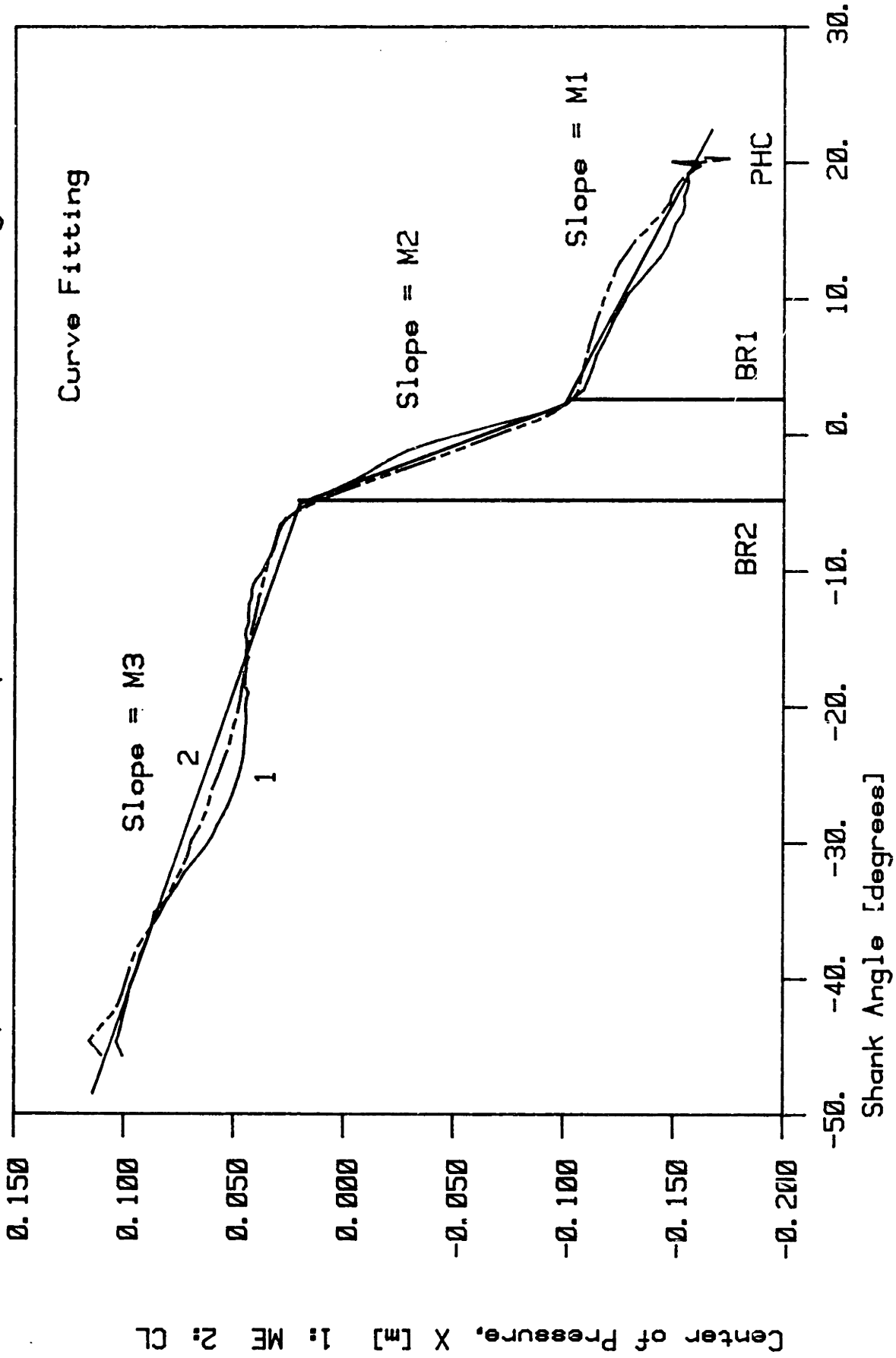
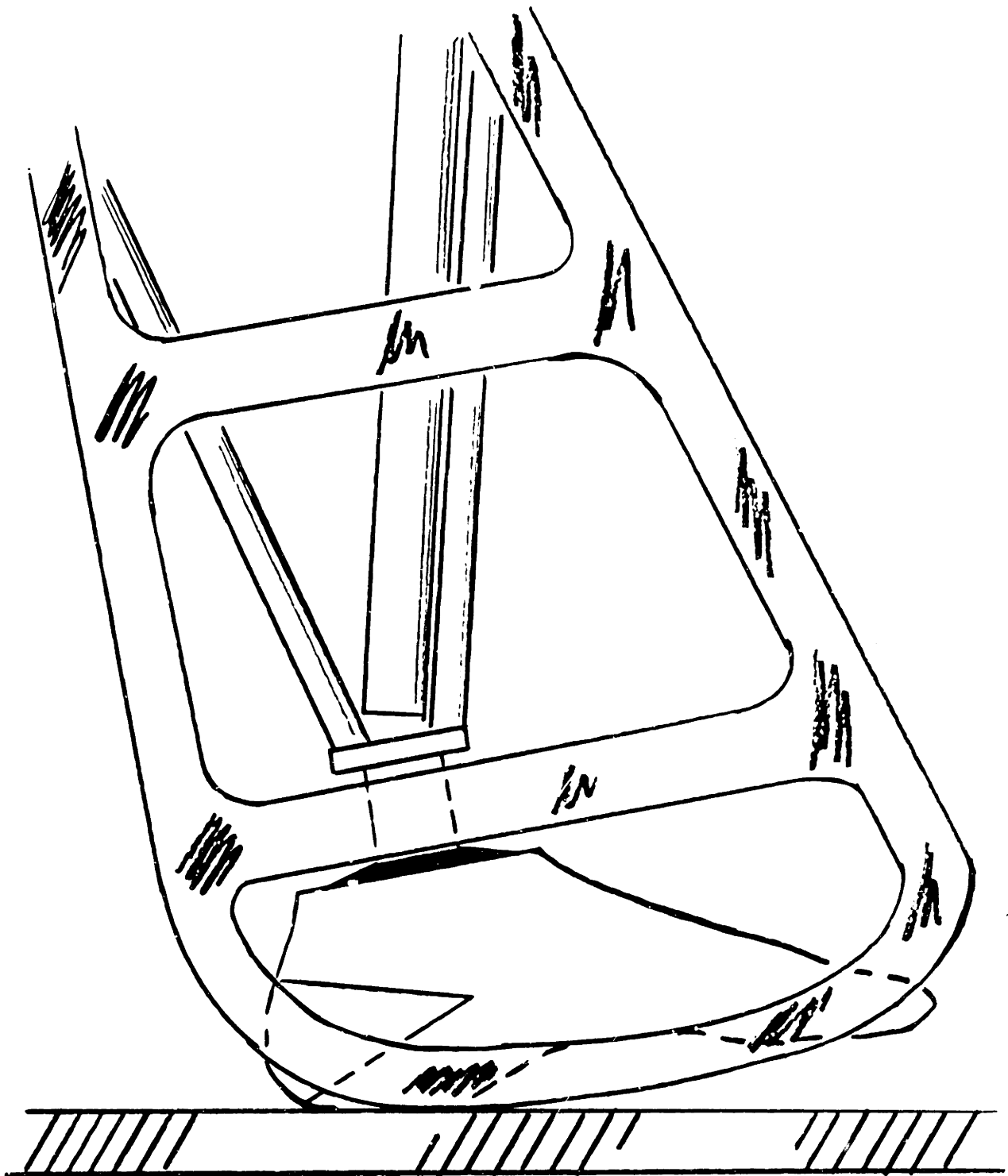


FIGURE V-3

Fitting Three Straight Lines to the Center of Pressure vs Shank Angle Data



SACH FOOT  
RIGID CAM PROFILE  
FIGURE V - 4

A comparison of the ELL as predicted by the model to the data is shown up to approximately PFF in Figure V-5. It is very clear that the initial shortening in the imaginary leg is not due to the SACH foot kinematics. At shank angle of 5 degrees or at about 13 percent stance the model's prediction of hip height is (2 cm) too high.

According to Table IV-1, the only factor left that could account for the observed leg shortening just after PHC is compliance in the prosthesis. It is clear that the most compliant element in the prosthesis is the SACH foot heel. The 2 cm leg length error shown in Figure V-5 is a very reasonable displacement for a SACH foot heel [108]. Therefore, in order to predict the ELL the SACH heel compliance must be measured and that level of complexity added to the model.

### V-2.3 SACH foot heel stiffness

The compliance (or the inverse which is stiffness) of the SACH foot with shoe was measured on an Instron testing machine. The details of the test are included in Appendix 2. Stiffnesses at three angles were measured and an exponential function was fit to the data by hand. This was done because while the SACH heel stiffness is linear with load at a given shank angle, the stiffness does change with angle. The results are shown in Figure V-6 as stiffness versus shank angle.

The measured stiffness was now used to calculate the deflection that would be produced when the kinematic model is loaded with the measured foot/floor vertical reaction force. The deflection can be calculated from equation (1).



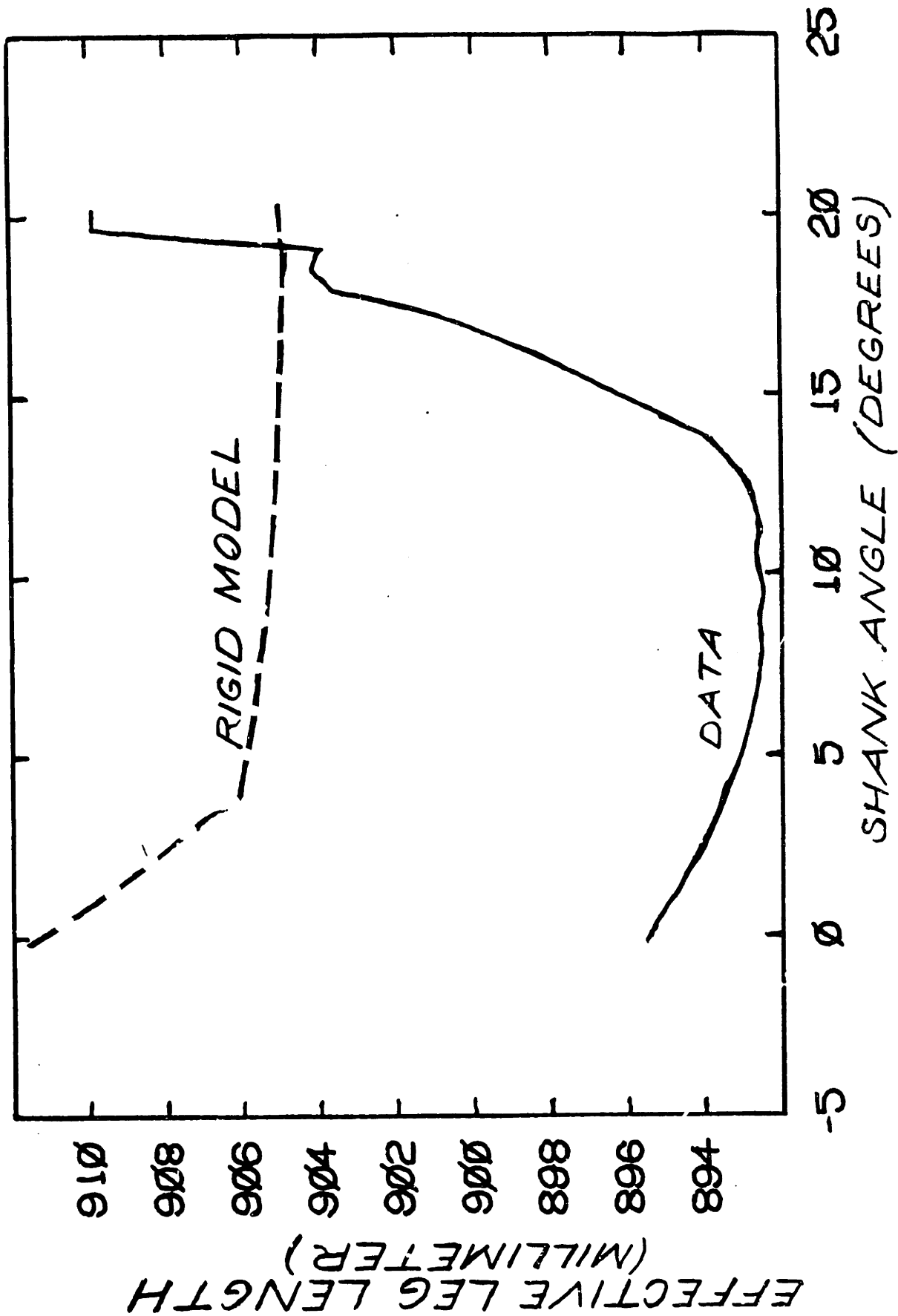


FIGURE IV-5

The ELL Versus Shank Angle. A Comparison of the Rigid SACH Foot Model to Data Produced by CL Stance Phase Controller

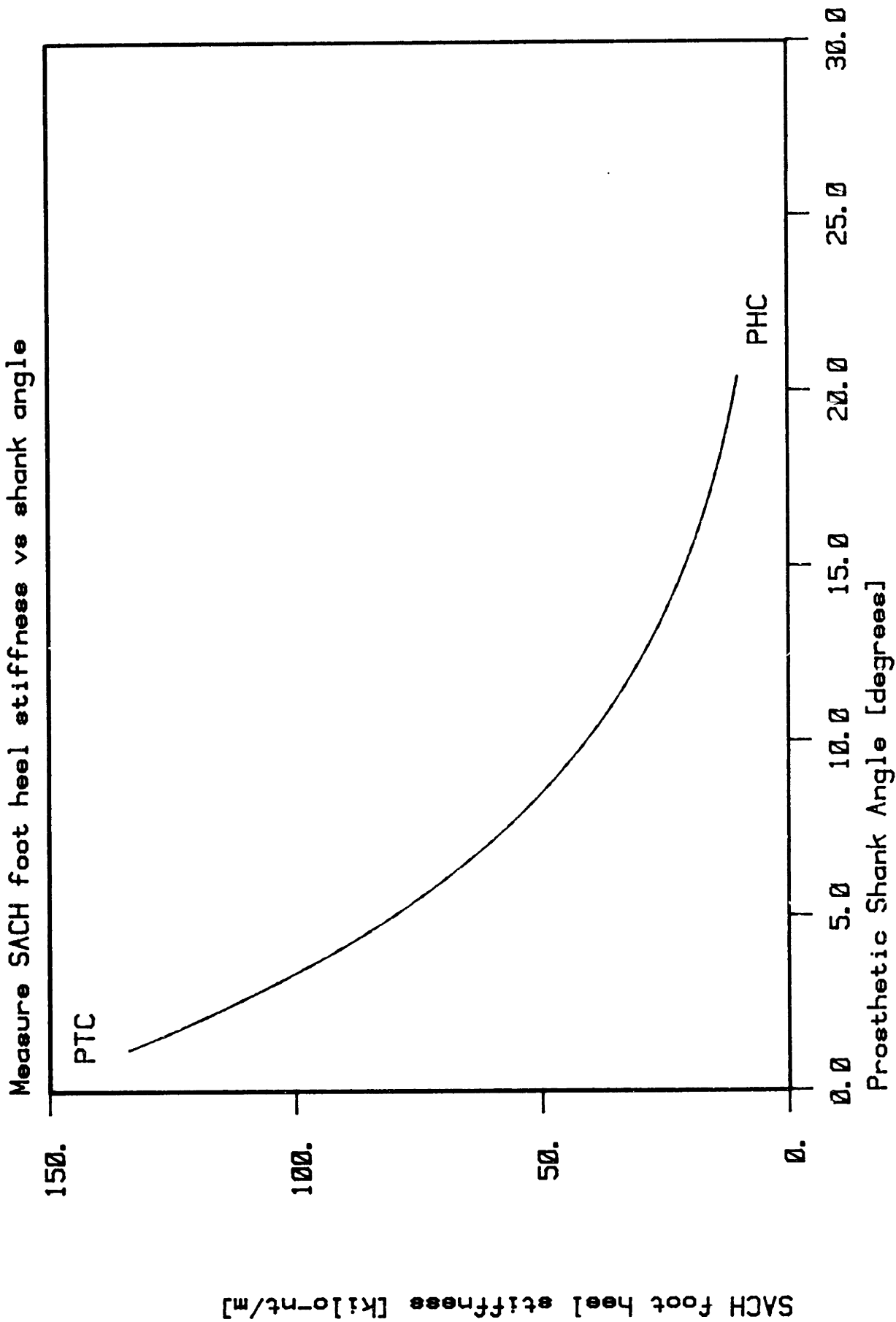


FIGURE V-6

Measured SACH Heel Stiffness as a Function of Shank Angle.

$$X = F/K \quad (1)$$

where  $F$  is the vertical reaction load as a function of shank angle,

$K$  is the measured SACH heel stiffness as a function of shank angle,

$X$  is the resultant displacement of the heel as a function of shank angle.

The result is shown in Figure V-7. The heel deflection of about 2.5 cm is quite reasonable. This suggests that the initial shortening of the ELL is due to SACH heel compliance. The role of the SACH foot in the first 13 percent of stance is thus to absorb the impact of heel contact by compressing under load and allow the hip trajectory to turn around from falling at the end of sound stance to rising in the beginning of prosthetic stance.

It appears that the most important factor from Table IV-1 controlling the kinematics of the first 13% of stance phase gait is SACH heel compliance.

### V-3 Dynamic Simulation of Gait

#### V-3.1 Introduction

The development of a dynamic model requires an explicit description of all relevant energy storing or dissipating elements in addition to the kinematic constraints. In Chapter IV-2.7.2 the kinematics of the SACH foot was shown to be important in predicting the peak in the vertical hip trajectory. In Chapter V-2.2 a kinematic model of conventional A/K gait

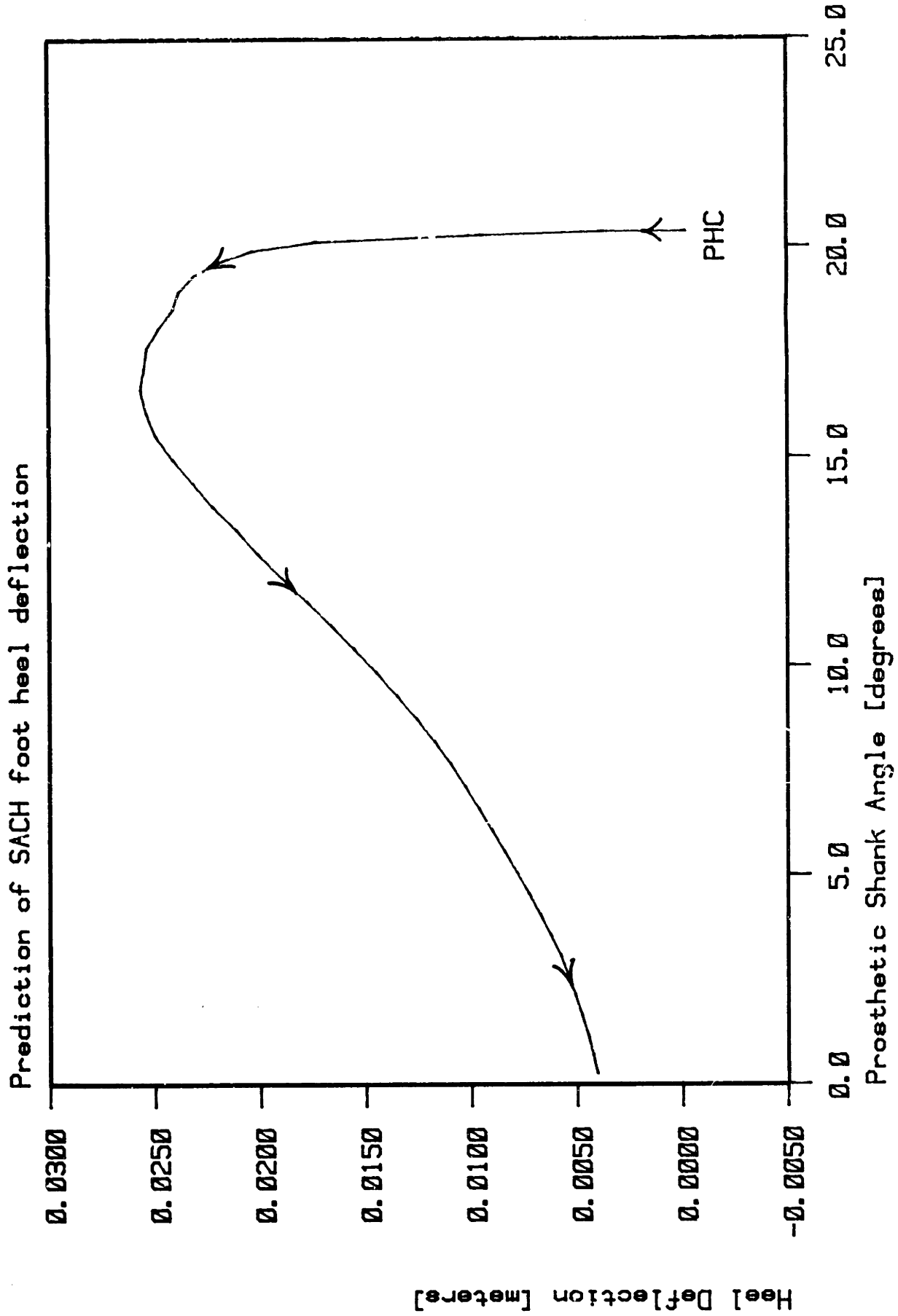


FIGURE V-7

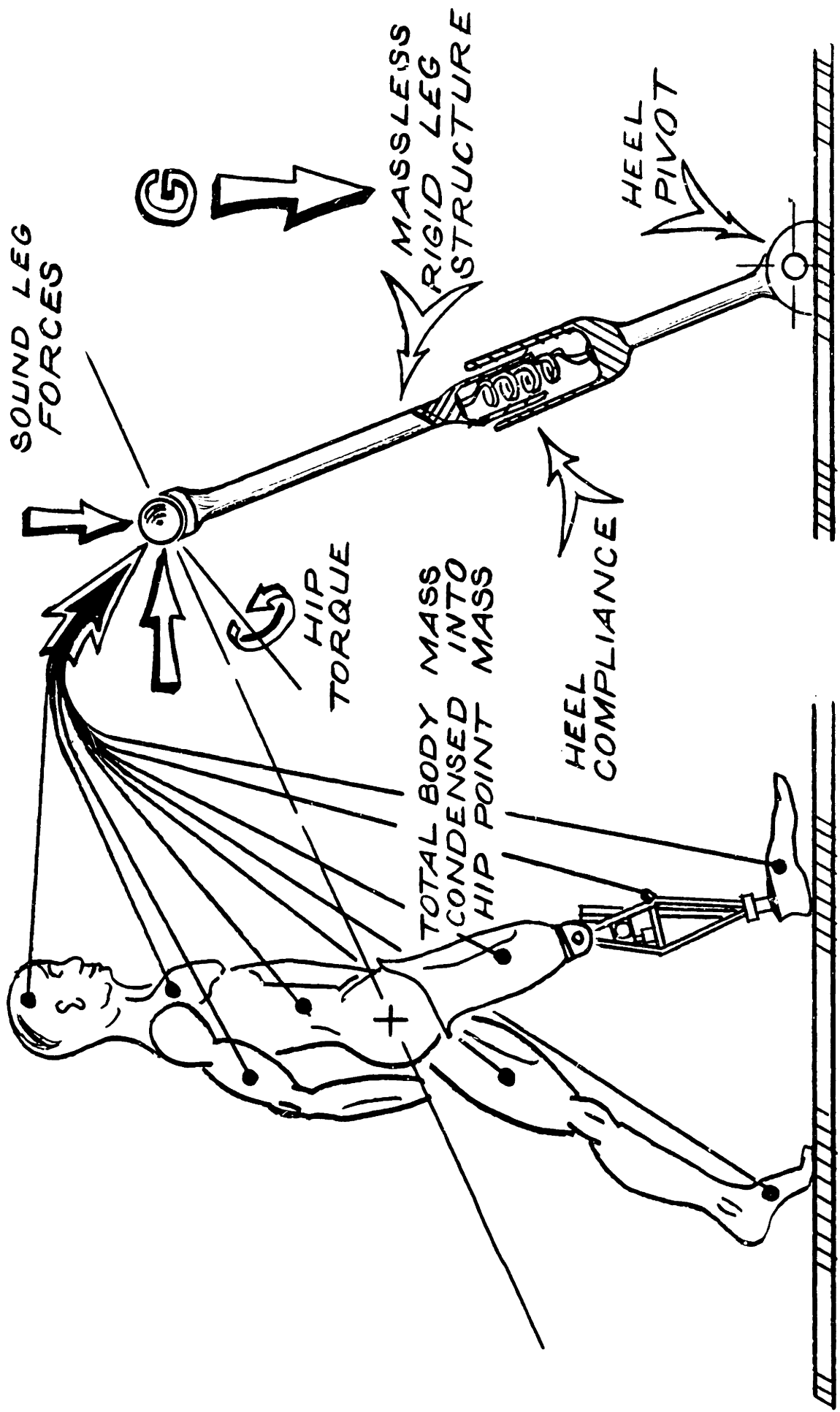
Predicted SACH Heel Deflection from Vertical Reaction Load Data as a Function of Shank Angle.  
Run JL1494.

was developed to show the effect of SACH foot geometry on ELL. This kinematic structure serves as the basis for the dynamic model.

### V-3.2 Dynamic simulation of heel compression

To make a stronger statement about the SACH foot in the beginning of stance a dynamic simulation of PHR is developed. To determine if heel compliance is a sufficient model, the dynamic elements required for the model are assumed to be SACH heel stiffness and the body as a point mass at the hip. The previous chapter indicated that SACH heel stiffness produced significant deflections relative to the observed change in height of the hip during the first 13 percent of stance. The fact that this result is based on actually measuring the stiffness of the SACH heel is a good reason for adding a spring to the model (at least during PHR). The body mass is clearly an important energy storage element. It is included as a point mass for the following reasons. 1) Bresler et al [10] showed that for normals the energy associated with the stance leg is small with respect to the energy of the body mass. 2) The rotational energy and kinematics of HAT (Head, Arms and Trunk) is small during stance phase of level walking (Zarrugh [120]). Since the c.g. is only several centimeters above the hips it appears to be a reasonable assumption to place the point mass of the entire body (HAT, sound swing leg, and prosthesis mass) at the hip.

To complete the model the kinematics of that SACH foot have to be added. Since it is not clear whether the cam profile is necessary in PHR model two simulations will be run. Model #1 uses a single point of rotation as shown in Figure V-8. Model #2 includes the cam profile of the



MODEL I  
 COMPLIANT HEEL-PIVOT MODEL  
 FIGURE IV-8

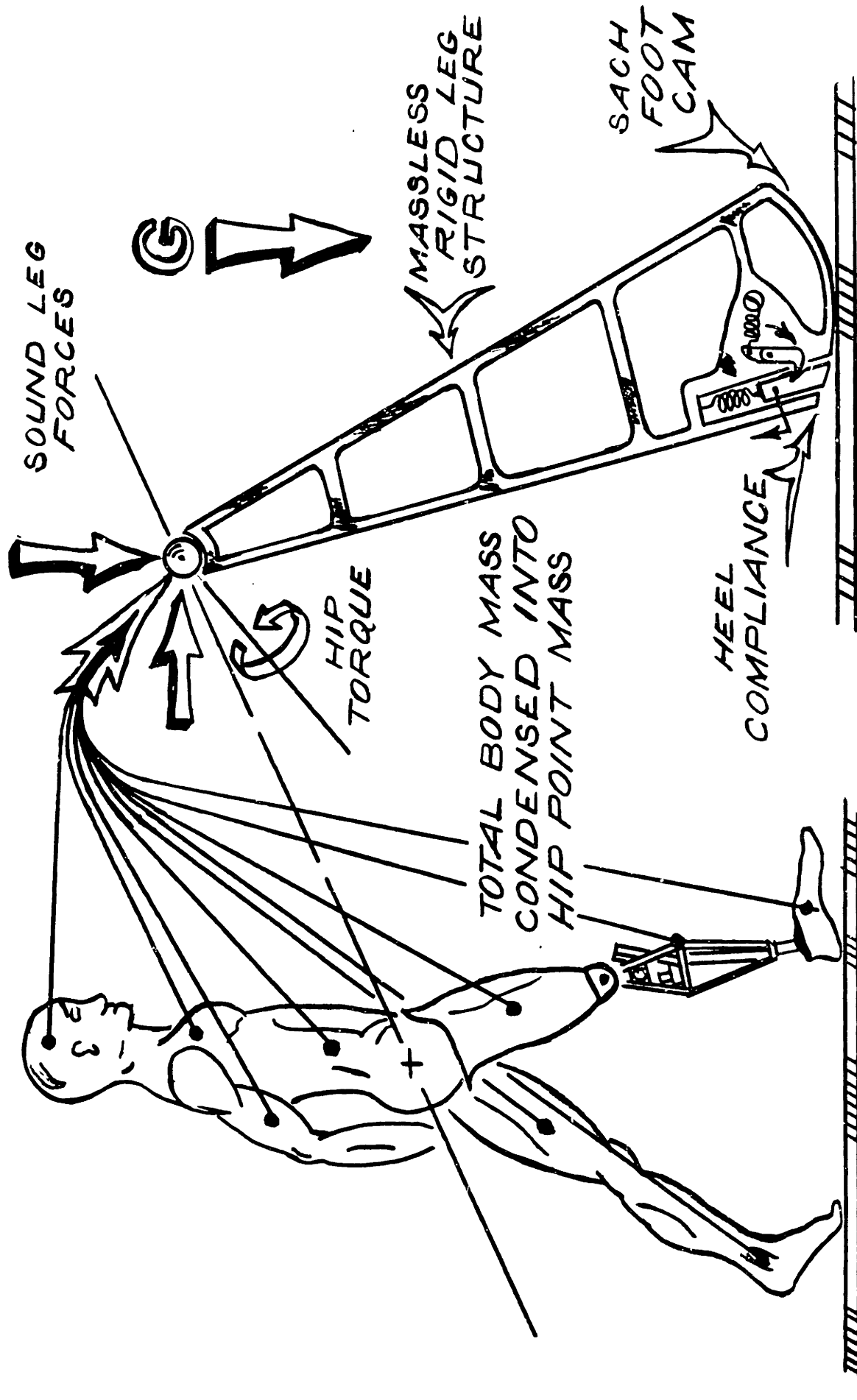
SACH foot as shown in Figure V-9. Note that the spring is aligned along the imaginary effective leg. This was done to match the orientation of the SACH foot to load used during SACH heel stiffness testing. The difference, however, is very small since the angle between the shank and the effective leg during PHR is less than four degrees.

During the stance phase of level walking, the only control the amputee has over the prosthesis is through his generation of force and torque at the hip, the force resulting from his sound leg and the sagittal torque is due to his hip muscles interacting with the torso and stump. This force and torque, therefore, represent the possible inputs to the model. Since they have been determined in Chapter IV, they can be used as inputs. The equations of motion and associated details are generated in Appendix 1. The equations were integrated using a fourth order Runge-Kutta technique.

Dynamic simulation of heel compression requires that the simulation run from PHC until full compression of the spring is reached (approximately 13 percent of stance (see Figure V-1)). When the spring has reached maximum deflection and the spring velocity goes to zero, the simulation region of heel compression is defined as ended.

#### Model #2

The simulation of Model #2 was run by assuming the spring is at its free length at PHC. The rest of the displacements were then matched to the initial conditions on vertical hip displacement, shank angle and measured initial values of  $e$ , and  $B$ . (This is identical to the kinematic model initialization described in Chapter V-2.2). The initial conditions



MODEL 2  
COMPLIANT HEEL-CAM FOOT MODEL  
FIGURE V-9



on velocity of the point mass (the model's hip joint) in the vertical and forward directions were set equal to the hip velocity data at PHC. For complete details of equations of motion, initializing etc., see Appendix 1.

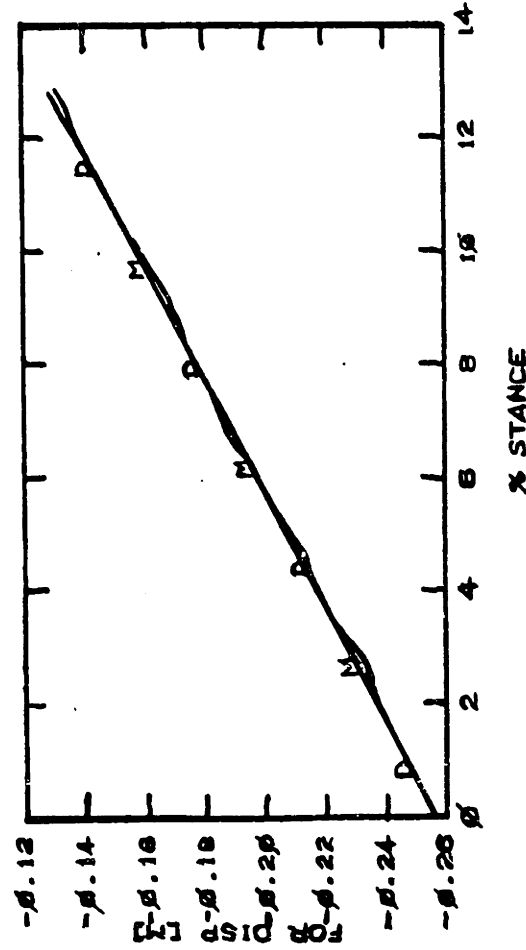
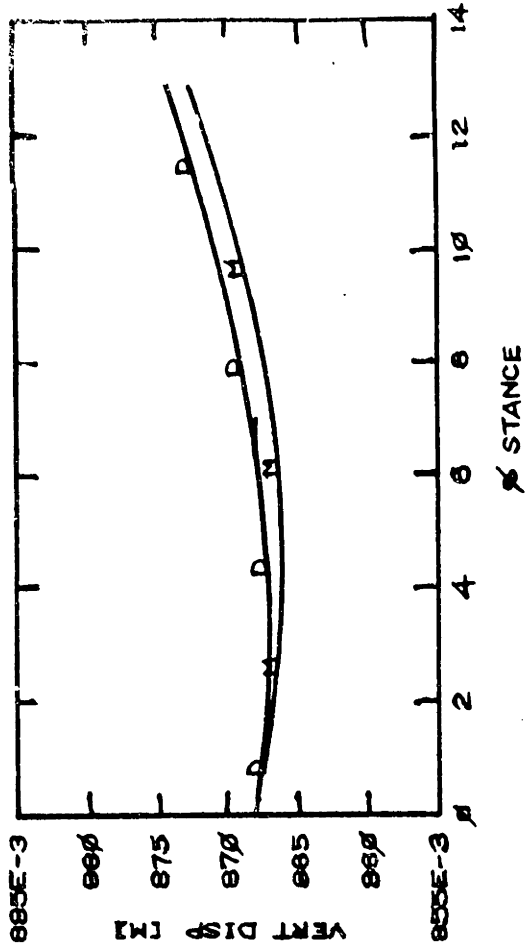
The results of the Model #2's hip joint displacement and velocity as compared to the data are shown in Figure V-10. The prediction of heel compression is very good. The vertical hip trajectory matches the data in magnitude, slope and phasing. The spring reaches maximum compression of 1.9 cm as was predicted necessary by the kinematic analysis of Chapter V-2.2. Maximum compression is reached at 13 percent of stance. This seems appropriate when compared to the effective leg length plot in Figure V-1.

The vertical velocity profile also matches the data with some 'overshoot' near the end of the simulation. This is probably a result of not including a small amount of damping in the SACH heel model. The SACH heel and/or the SACH heel shoe interface certainly have some damping which would help control energy exchange.

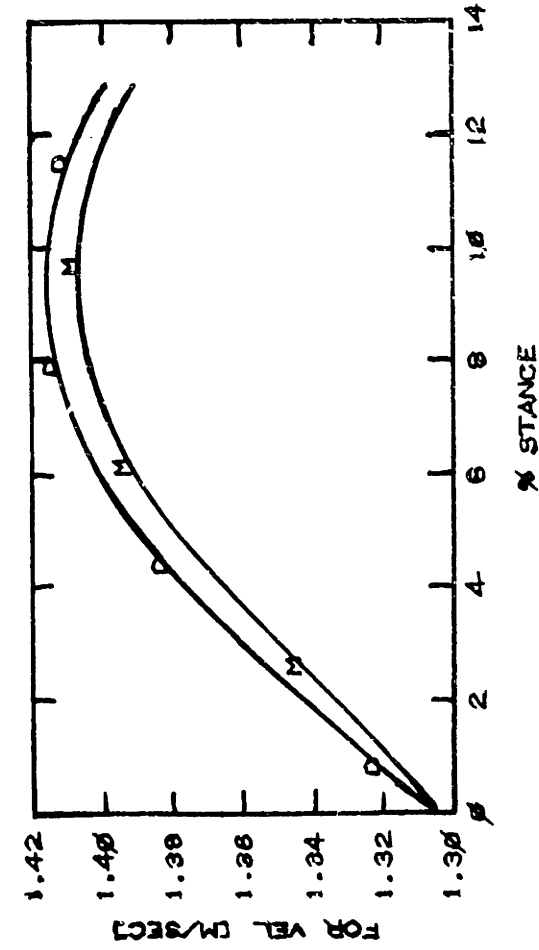
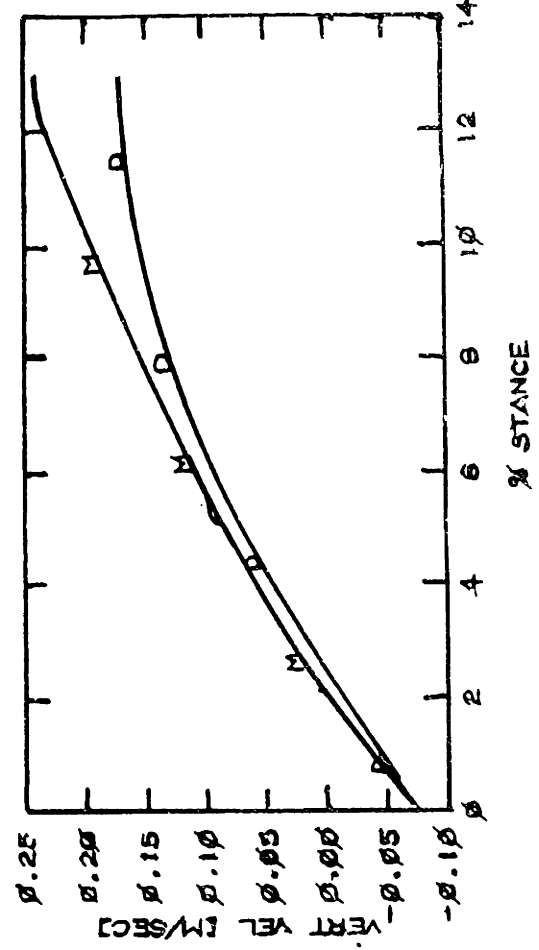
The forward displacement and velocity profiles also show good support for the compliant model during the first 13 percent of the stance phase.

#### Model #1

A simulation of SACH heel compression was also run with Model #1. Model #1 was initialized in a manner consistent with Model #2. The length of the leg was set equal to the equivalent leg length used for Model #2 at PHC. The rest of the initial conditions and inputs were identical to



D = DATA  
M = MODEL



Hip Displacements and Velocities During Heel Compression. A Comparison of Model versus Data

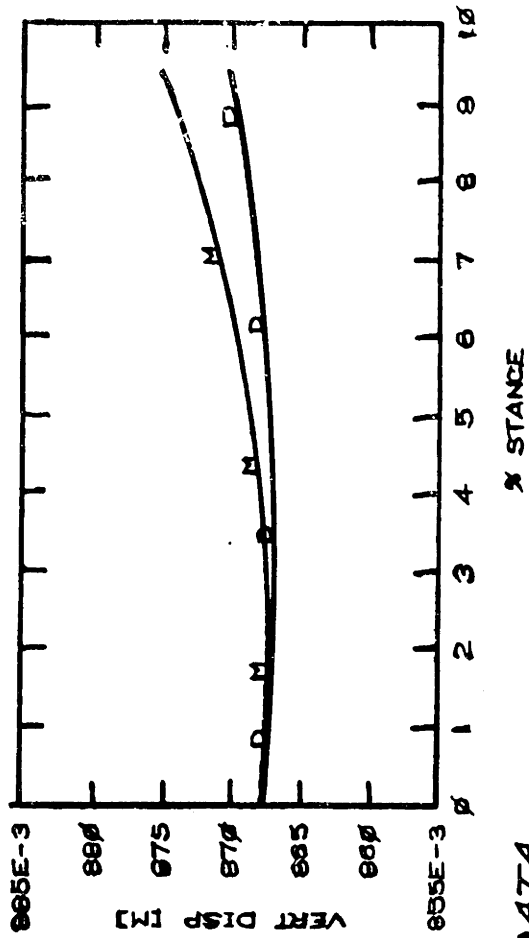
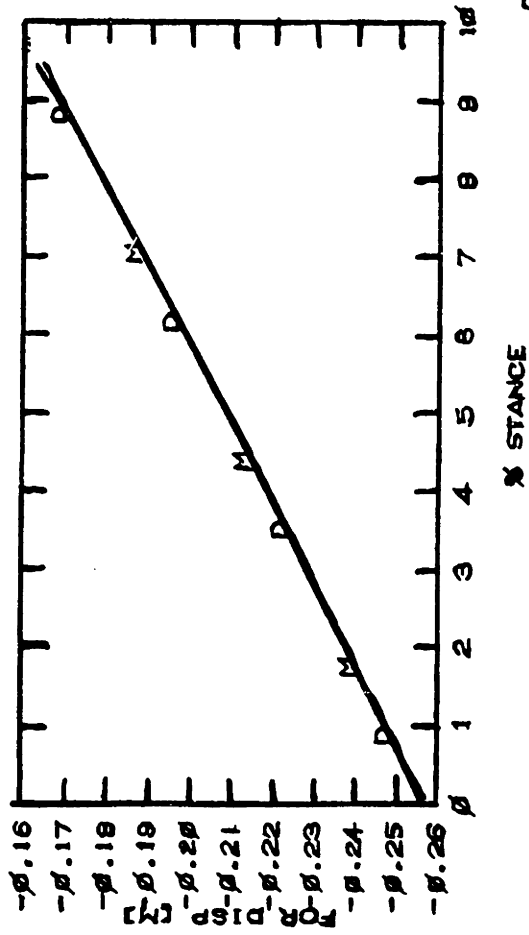
Model #2.

The results are shown briefly in Figures V-11 and V-12. Notice that the simulation ended at 9.5 percent of stance instead of 13 percent, and that the spring compressed only 15 mm instead of 19 mm. The vertical hip trajectory is also incorrect. It has started to diverge from the data by going too high (i.e. the spring has not compressed enough and has come to steady state too soon). Thus model #1 is less satisfactory in predicting the first 15 percent of stance phase of A/K gait. This is due to the effective leg length angle changing incorrectly due to the absence of center of pressure movement. Thus all the driving forces (ground leg force and the gravity body force) are producing the incorrect torque about the pivot point.

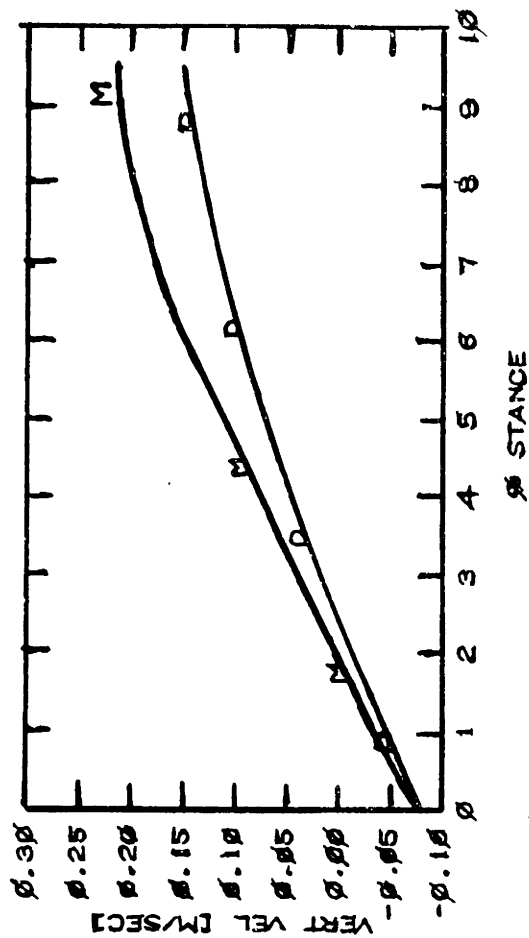
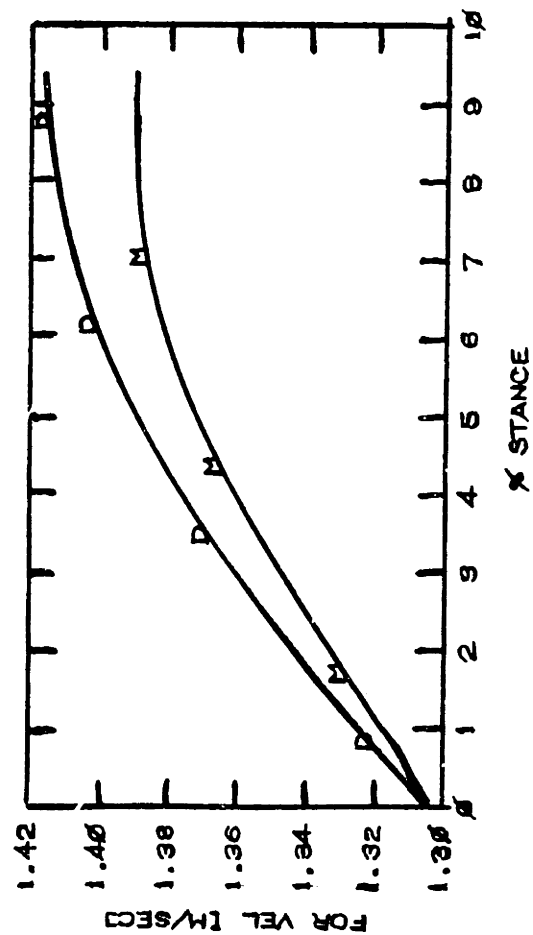
In summary, the first 13 percent of stance is adequately modeled for either stance phase knee controller with Model #2. The important elements of the the model are a point mass representation of the total body mass located at the hip, and a SACH foot with a well defined rolling cam geometry and compliant heel section.

### V-3.3 Dynamic simulation of the prosthetic stance phase - latching spring model

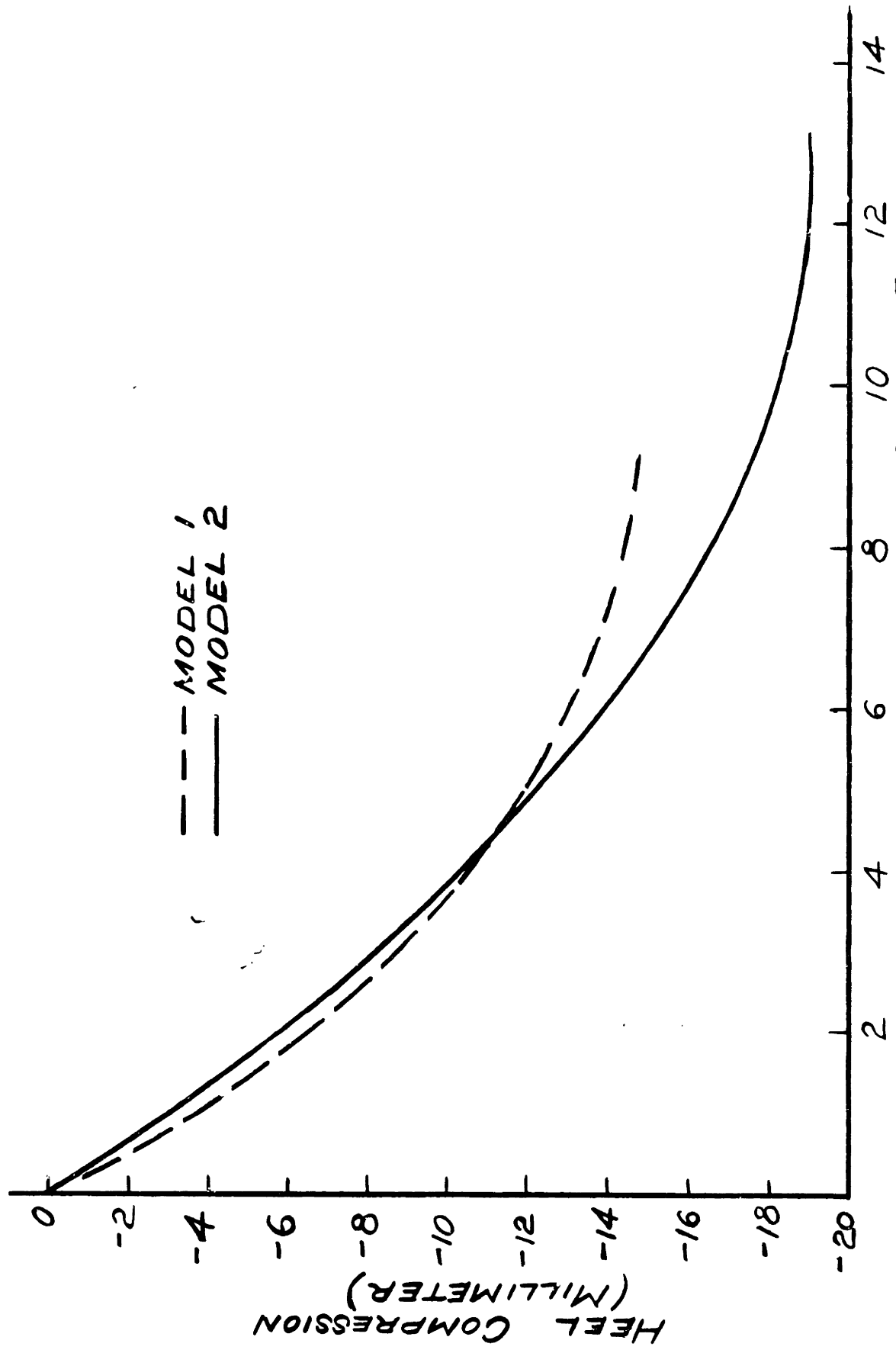
In the last section a good model for heel compression was developed. In Chapters IV-2.7.2 and V-2.2 a kinematic model for mid-stance was developed. In this section the dynamic simulation of heel compression will be extended through mid-stance by using the mid-stance rigid SACH foot cam model up to knee break. (Since both stance phase knee controllers are the same after knee break no attempt was made to model this part of stance).



D = DATA  
M = MODEL



Hip Displacements and Velocities During Heel Compression. A Comparison of Model 1 versus Data



HEEL COMPRESSION  
PERCENT OF STANCE  
FIGURE V-12

The rigid SACH foot dynamic model is identical to the compliant SACH foot dynamic model but without the spring (see Figure V-9). This simulation will proceed as in the dynamic heel compression simulation up to maximum heel compression, then the model is switched to the rigid SACH foot model to complete the simulation. This transition is accomplished in the following way. When the spring reaches full compression and the rate of compression goes to zero the model latches the spring at that deflection. The model now has one less degree of freedom and is equivalent kinematically to the rigid SACH foot model used in Chapter V-2.2.

Latching the heel spring at full deflection, however, does unfortunately change the energy in the system discontinuously. That is, all the energy stored in the spring is suddenly removed. The amount of energy removed can be calculated from the results of the heel compression simulation. The spring deflection at the end of heel compression was 2 cm and the value of stiffness was 28,000 newtons/meter. The energy stored in a linear spring is simply

$$E_s = \int f dx$$

where  $f$  = force in the spring

$x$  = the displacement of the spring

$dx$  = the differential displacement of spring

The energy stored in the model's heel spring during the simulation is 5 newton-meters. The average kinematic energy of the body is simply

$$E_b = .5 * m * v^{**2}$$

where  $m$ =body mass

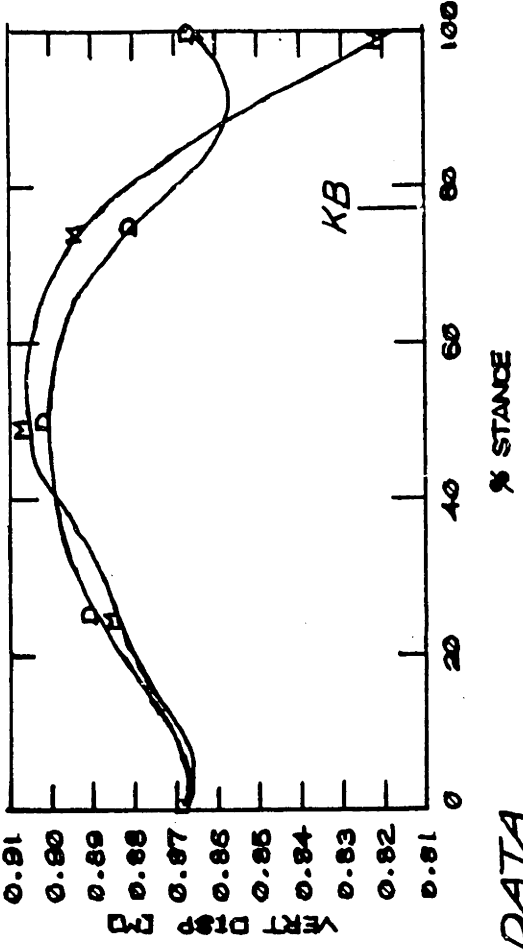
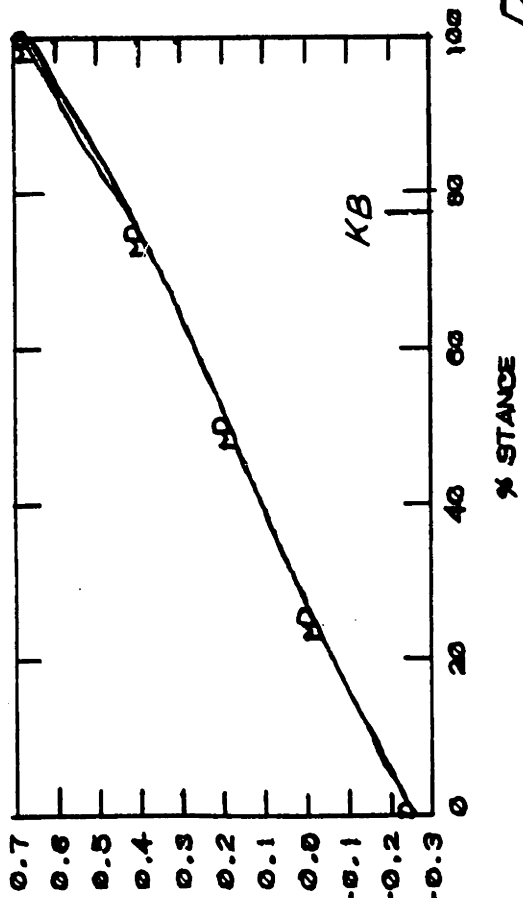
$v$ =average forward velocity

Therefore the average kinetic energy from data is 60 newton-meters. Thus the spring contains up to 8 percent of the average kinetic energy of the body. Thus, unless there is an unaccounted for mechanism like viscous damping in the SACH foot that normally dissipates this energy, then removing it arbitrarily may reduce the forward velocity in an inappropriate way. The alternative is to release the energy back into the system in some way. However, since the energy stored in the spring is relatively small compared to the average kinetic energy of the body, and since no dissipative effects are included in the model, it is assumed that simply latching the spring is a good representation of the energy exchange which occurs in the foot during stance.

#### V-3.3.1 Results simulation

Results of the dynamic simulation of stance phase with the latching spring model are shown in Figure V-13. In general the displacement and velocities at the hip are matched by the data up to knee break. After knee break, the model diverges from the data due to the neglected effect of knee angle.

The vertical displacement at the hip matches extremely well up to 20 percent of stance but because the center of pressure as a function of shank angle does not account for SACH foot compliance after maximum heel compression, some error is introduced.



*D = DATA*  
*KB = KNEE BREAK*  
*M = MODEL*

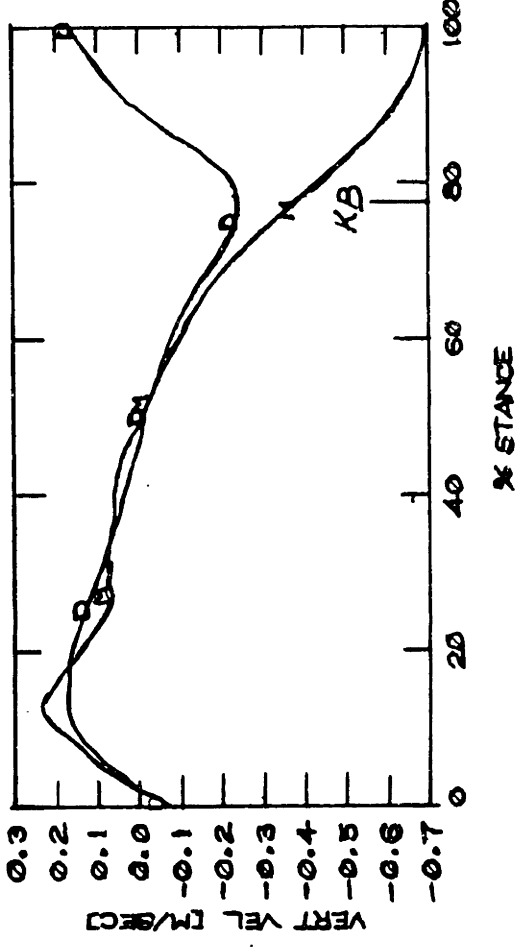
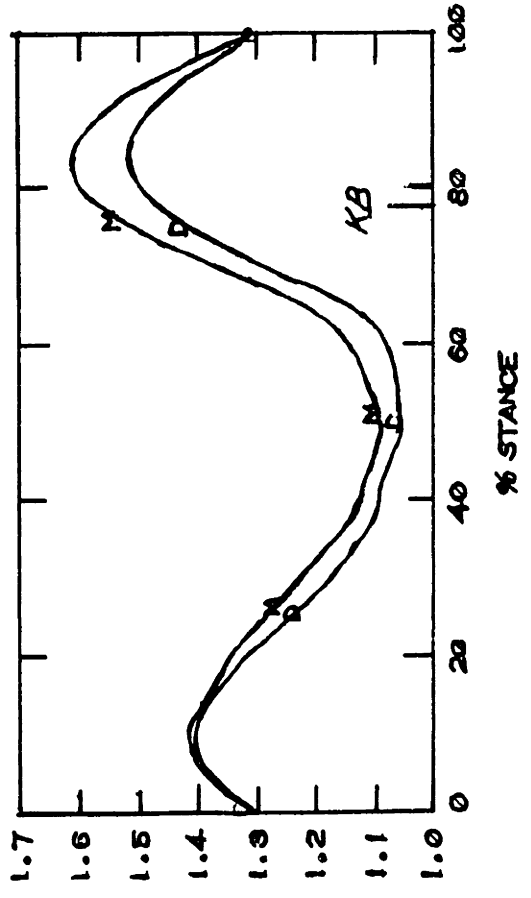


FIGURE V-13

Hip Displacement and Velocities During the Stance Phase of Level Walking with a CL Stance Phase Knee Controller. A Comparison of the Latching Spring Model Versus Data



In particular, as the simulation continues up to knee break, the vertical trajectory becomes too high because no toe break compliance was accounted for. The Otto Bock SACH foot used does have a stiff toe break but it does have some compliance.

The force and velocity profile gives some insights into energy flow during the stance phase. Up to 13 percent (heel compression), the energy that is being dumped into the spring is removing kinetic energy from the forward velocity so that it matches the data very well. After the model makes the transition into the rigid phase the forward velocity increases too much. This occurs despite the fact that the energy stored in the heel spring was just removed from the system. This argues for an energy dissipative mechanism in the SACH foot that dissipates most of the impact energy from PHC. One mechanism might be the SACH heel damping. While the damping ratio of the amputee on his SACH heel is probably quite low and thus not much energy is lost during heel compression, the damping ratio is quite high when the heel is unloaded at PHO because of its low inherent mass. Thus, the stored spring energy is just dissipated in the heel after the heel has lost contact with the ground (latching spring effect). In addition, there may be dissipative elements in the mid-stance region of the SACH foot. The neglected knee break allows too much forward velocity accumulation at the end of stance. This is due to the body falling over the leg rather than beginning to slow it down as the prosthesis leg flexes keeping the hip up and slowing down the forward rotation of hip. (See thigh angle data Figure IV-17.)

The hip vertical velocity is, of course, even more sensitive to errors in the SACH foot geometry and compliance than the vertical hip trajectory. Even so, on average the vertical velocity fits the data quite well up to knee break. It is clear that knee break allows the hip to climb back up as the thigh flexes for the same reason that the vertical hip trajectory during ME controlled stance is higher (See Section IV-2.8.2).

In summary, the latching spring model is a useful model of the stance phase of level walking up to knee break. The simple elements involved in the model makes it clear that SACH compliance and the SACH cam profile are very important during PHR. Also, energy equivalent to the amount stored in the SACH heel during PHR is dissipated and probably dissipated in the SACH heel. After PHR and up to knee break, SACH geometry is dominant. After knee break, the knee angle is assumed the dominant factor by deduction.

## V-4 Propulsion

### V-4.1 Introduction

The latching spring model of the stance phase of A/K gait provides the opportunity to compare the relative values of those sources of propulsion during the stance phase of level walking. The model shows explicitly that the sound leg, and hip torque act as inputs to the model. In addition, however, there exist a gravity term which can drive the system during gait (affects the momentum of the body c.g.). This propelling force will be labeled as a ballistic force, indicating while it affects the system it is not under the amputee's control and requires no work from him (i.e. he can fall over without even trying).

### V-4.2 Propulsion tests and results

To test the relative effect of sound leg forces, hip torque, and ballistic effects, the input conditions listed in Table V-1 were used in simulations with the spring latching model.

Table V-1 Propulsion Testing

Test #	Sound Leg Force (Fs)	Hip Torque (Th)	Ballistic Force	Figure V-14
1	on	on	on	A
2	on	off	on	B
3	off	on	on	C
4	off	off	on	D

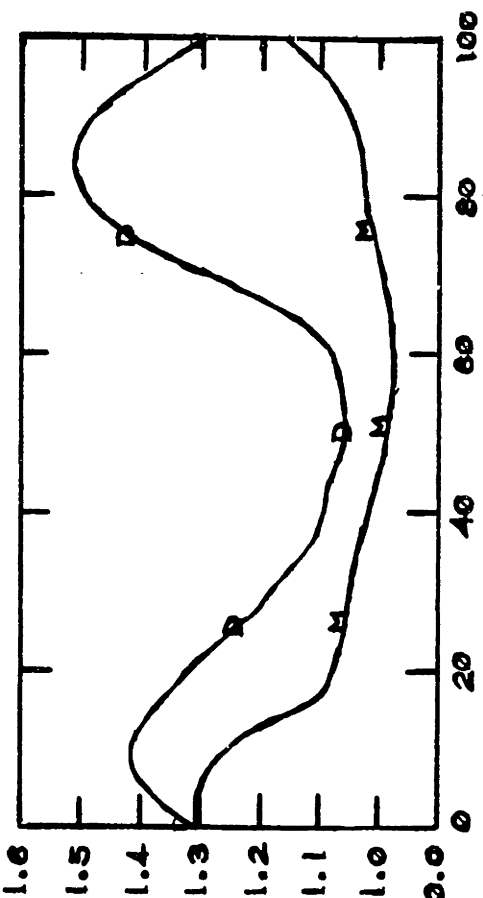
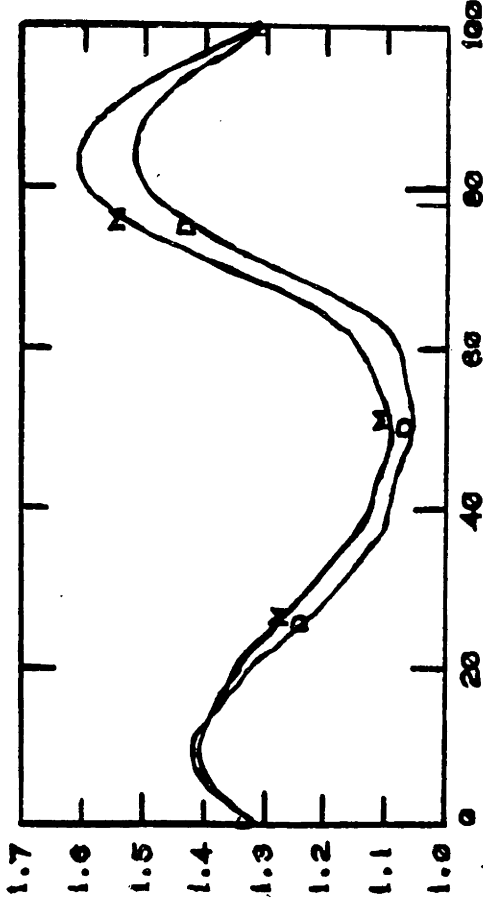
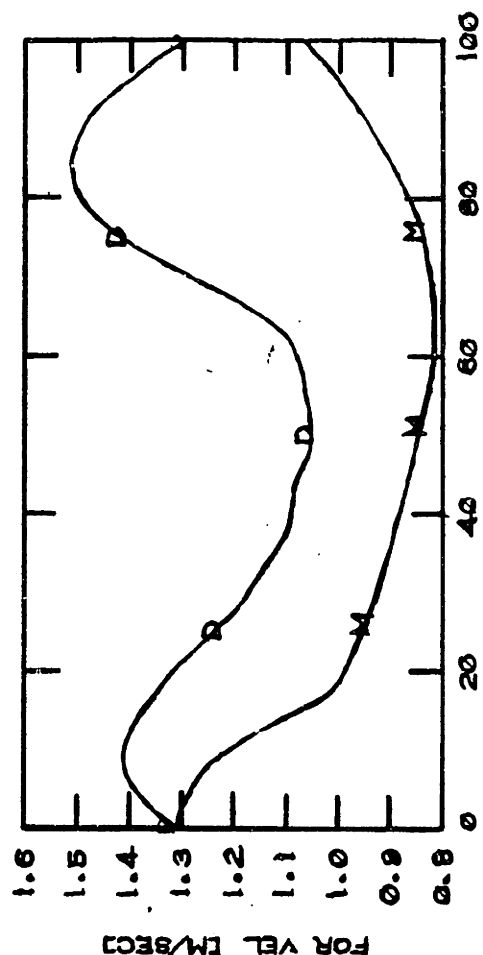
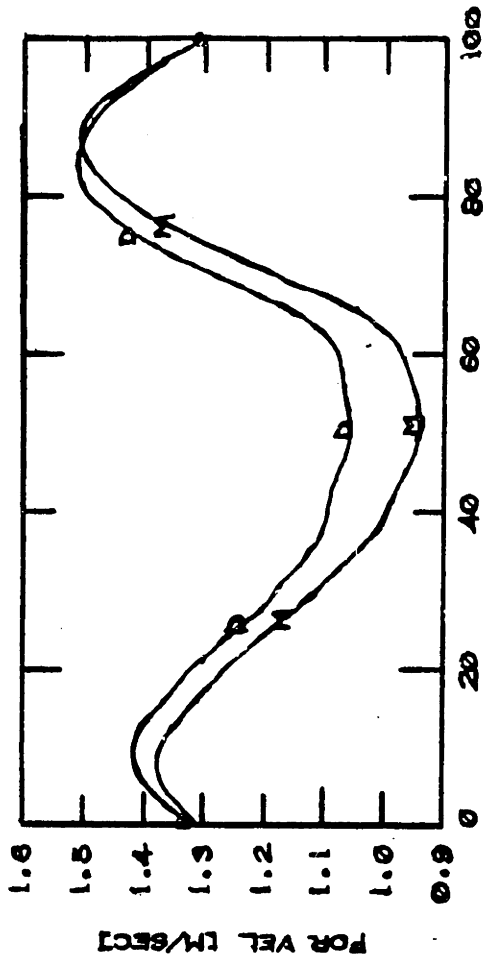


FIGURE V-14

Demonstrating the Effect that the Hip Torque and Sound Leg Forces have on Propulsion

The output variable which reflects propulsion is the forward velocity at the hip. Tests 1 - 4 are all presented in Figure V-14. It must be understood that running a simulation of stance phase gait without one of the inputs might produce flexive torques at the knee joint which would cause the leg to collapse. This is not allowed in the simulation and therefore knee stability has been isolated from propulsion. Note an alternative way of viewing the relative effects of these inputs is to plot their relative contribution during test 1. That is each term in the equation of motion (see equation (8) Appendix 1.2) is an angular acceleration term proportional to sound leg force, hip torque and gravity. These terms are plotted in Figure V-15.

The following general observation can be made from these 4 tests. Hip torque plays only a minor role in propelling the body forward. During double support, both at the beginning and end of stance, the sound leg forces dominate the propulsive nature of A/K gait. During single support ballistic effects and hip torque are important at the beginning, but the sound leg swing through pull effect is dominant at the end of single support.

ACCELERATION TERMS IN Eq. [8]; SECTION A-1.2  
 ACCELERATION DUE TO:

- .....  $F_y$  = VERTICAL SOUND LEG FORCES
- $F_x$  = HORIZONTAL SOUND LEG FORCES
- $G$  = GRAVITY
- $T_H$  = HIP TORQUE

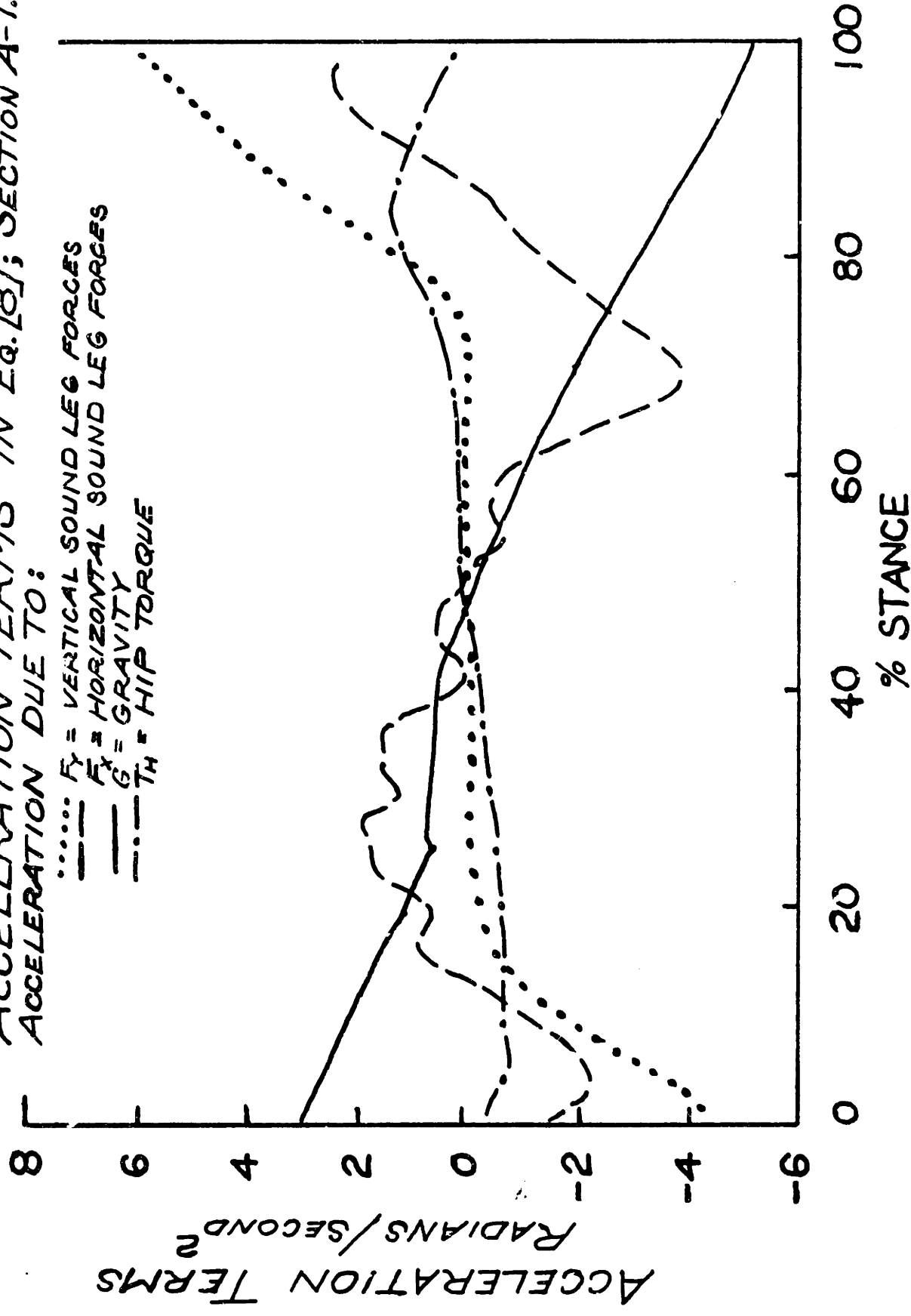


FIGURE V-15

The Relative Magnitude of the Terms in the Equation of Motion of the Spring Latch Model.

## VI Conclusions

### VI-1 Knee Control versus SACH Foot Design

The global purpose of this thesis was to determine the important factors affecting the design and control of above-knee prostheses during the stance phase of level walking. Toward that end, the single most important conclusion is that knee controller design and SACH foot design are completely mutually interdependent. Current conventional A/K prosthesis performance during stance is dominated by SACH foot design, not knee controller design. This is not an unexpected result in that prosthetists manipulate stance phase behavior by their choice of SACH foot (or ankle unit), SACH foot placement (alignment), socket alignment. The prosthetist has no real opportunity to manipulate the knee controller during stance, therefore, by adding the option of knee controller design, as in this study, additional decisions concerning the global behavior of the amputee/prosthesis system during stance have to be made. This study has shown that for at least one choice of stance phase knee controller, that SACH foot selection is still important. The fact that the vertical hip trajectory has a peak value which is higher for the ME stance phase controller was completely dominated by the stiffness and geometry of the SACH foot used.

As a result of this strong interplay, a study of the SACH foot's contribution to the prosthetic side hip trajectory was undertaken. Results of the heel compression model simulation strongly reinforce the idea that the behavior of the SACH foot at PHC is to absorb energy, simulating the function of normal ankle plantar flexing. Without the

normal knee function absorbing some of the energy, it is entirely incumbent on the SACH foot to reduce axial shank and stump loads. The subject, who is a young, active and experienced amputee had no reservations nor inability to fully utilize the prosthesis from a weight bearing perspective. Thus, the measured reaction forces from the amputee using the CL controller were normal in magnitude. Thus, the SACH foot's heel section appears to be providing the shock absorption that normals get from plantar flexion of the ankle and flexion of the knee. Thus, the question arises as to the appropriate amount of heel compliance the prosthetic foot should have when using the ME stance phase controller which provides knee flexion during stance.

While the question of the appropriate compliance and damping in the SACH heel as a function of the stance phase knee controller remains open for future research, it is clear that the stiff toe break in the SACH foot used did not allow for the different loading generated by the ME stance phase controller to affect the gait in a more beneficial manner (i.e. lower the peak in the vertical displacement trajectory of the hip). The fact that this SACH foot could be primarily modeled as a cam, while useful to the modeling process, seems inappropriate with this knee controller and an active amputee. Clearly, future stance phase knee controller design must consider the kinematic and dynamic characteristics of the SACH foot.



## VI-2 Person-Interactive Simulation

A second major conclusion is that person-interactive simulation is necessary. The aspects of A/K, level walking, stance phase are clearly shown in the results. Some of the amputee controlled variables that changed include: hip torque, cadence, foot-timing, and weight transfer from the sound to the prosthetic leg. Attempting to predict the changes observed in those variables without experimentation seems currently unrealistic. This is particularly true if one wants to make detailed enough predictions to assist the actual hardware design process.

The observation that changes in the prosthetic knee controller affect distal leg segments more than proximal also reinforces the need for person-interactive simulation. One of the results that led to this observation is the fact that while the vertical loading on the foot changed with knee controller, the vertical loading on the thigh did not. Apparently the amputee has some walking criterion to meet independent of disturbances that may act on the prosthesis system. The fact that distal segments accommodate disturbances more than proximal segments implies that this criterion places importance on the trajectory of the body c.g.. However, without a more complete and quantitative statement about this criteria, model predictions will be difficult and person-interactive simulation essential.

### VI-3 Hip Torque

The role of the torque produced from the hip on the prosthetic side up to knee break during the stance phase of level walking is to provide fine control over the prosthesis knee kinematics. The hip torque does not provide propulsion of the amputee in the sagittal plane. This implies that hip torque signifies amputee intent during this period. The following illustrates this conclusion. The hip torque does provide a small (relative to the torques produced by gravity and the sound leg forces) extensive torque (see Figure V-15) necessary to insure knee stability at PHC (i.e. the amputee is concerned with stability). During mid-stance, when stability is assured by the relative position of the body c.g. to the knee axis and center of pressure, the hip torque is relatively low (i.e. the amputee is not concerned with stability). At knee break, the flexive hip torque is large enough to cause the knee to buckle (i.e. the amputee wants to begin preparing the prosthesis for the swing phase). Thus a prosthesis designer should consider measuring and feeding back hip torque to a stance phase knee controller.

### VI-4 Designer Gait Modeling and Simulation

Designer gait modeling and simulation has been successful in improving the current understanding of the stance phase control of A/K prostheses. The ability to identify the role of specific parts of the prosthesis or to identify the role of specific amputee inputs to the prosthesis is a new and obviously very valuable tool to the prosthesis designer. The entire A/K prosthesis design process has been aided in a permanent way.

## REFERENCES

1. Agarwal, G.C., Gottlieb, C.L., "Compliance of the Human Ankle Joint", ASME Paper No. 77-WA/Bio.
2. Ahlen, A., Lanshammar, H., "Gait and Slip Analysis", Activity Report 1978-79, Department of Automatic Control and Systems Analysis, Teknikum Institute of Technology, Uppsala Univ.
3. Ahten, A., Lanshammar, H. "Analysis of Human Gait" Activity Report 1979/80, Department of Automatic Control and System Analysis, Teknikum, Institute of Technology, Uppsala Univ.
4. Antonsson, E.K., "The Derivation and Implementation of a Dynamic 3-D Linkage Analysis Technique", S.M. thesis, Dept. of Mech. Eng., MIT, May 1978.
5. Antonsson, E.K., "A Three-Dimensional Kinematic Acquisition and Intersegmental Dynamic Analysis System for Human Motion", Ph.D. Thesis, Dept. of Mech. Eng., MIT, Cambridge, MA., June 1982.
6. Appoldt, F.A., Bennett, L., Contini, R., "The Results of Slip Measurements in Above-Knee Suction Sockets", Bulletin of Prosthetics Research, 10-16, Fall 1968, pg 106-112.
7. Appoldt, F.A., Bennett, L. "A Preliminary Report on Dynamic Socket Pressures", Bulletin of Prosthetics Research 10-8, Fall, 1967.
8. Blinichikoff, J.J., Zverev, A.I., Filtering in the time and Frequency Domains, published by John Wiley and Sons, Inc. 1976.
9. Braune, W., and Fisher, O. "Über den Schwerpunkt des Menschlichen Körpers mit Rücksicht auf die Austrüstung des Deutschen Infanteristen. Abh. d. Math.-Phys. cl. d. k. Sach. Gesellsch. der Wiss., 26:561-672. 1889, in W. M. Krogman and F.E. Johnston, eds., Human Mechanics - Four Monographs, abridged, Wright-Patterson Air Force Base, Ohio, 1963 (AMRL-TDR-63-123).
10. Bresler, B., Berry, F.R., "Energy and Power in the Leg During Normal Level Walking", Prosthetic Devices Research Report, Univ. of California, Berkeley, Report Series 11, Issue 15, May 1951.
11. Bresler, B., Frankel, J.P. "The Forces and Moments in the Leg During Level Walking", Trans. of ASME, January 1959.
12. Bresler, B., Radcliffe, C.W., Berry, Jr., F.R., "Energy and Power in the Legs of Above-Knee Amputees During Normal Level Walking", Lower-Extremity Amputee Research Project, Inst. of Engineering Research, Univ. of California, Berkeley, Series 11, Issue 31, May 1957.

- 134-
13. Cappozzo, A., Leo, T., and Pedotti, A., "A General Computing Method for the Analysis of Human Locomotion", Journal of Biomechanics 8, 307-320, 1975.
  14. Cavagna, G.A., Thys, H., and Zamboni, A., "The Sources of External Work in Level Walking and Running", Journal of Physiology, 262, pg. 639-657, 1976.
  15. Cavagna, G.A., Margaria, R., "Mechanics of Walking", Journal of Applied Physiology, 21, pp 271-278, 1966.
  16. Chao, E.Y., Rim, K. "Application of Optimization Principles in Determining the Applied Moments in Human Leg Joints During Gait", Journal of Biomechanics, Vol 6, pp 497-510, 1973.
  17. Chan, G.D., "Foot-Ankle Prosthesis: A Kinematic and Dynamic Study of The SACH Foot", Project Report for Mech. Eng., Course 299, Univ. of California, Berkely, CA.
  18. Chow, C.K., Jacobson, D.H. "Studies of Human Locomotion via Optimal Programming", Mathematical Biosciences, 10, 239-306, American Elsevier Publishing Co., Inc., 1971.
  19. Conati, F., "Real Time Measurement of 3-D Multiple Rigid body Motion", S.M. Thesis, MIT, Cambridge, MA June 1977.
  20. Contini R., "Body Segment Parameters, Part II", Artificial Limbs, 16:1, 1-19, 1972.
  21. Contini, R., Rudolfs, J.D., Gage, H., Yatkaukas, A., "Functional Evaluation and Acceptability of the Henschke-Mauch Hydraulic Swing and Stance Control System", Report No. 1037-1, Research Div., New York Univ., School of Science and Engineering, NY, July 1964.
  22. Contini, R. "Henschke-Mauch 'Hydraulik' Swing Control System", Bulletin of Prosthetics Research, Fall 1970.
  23. Cortesi, S.S., "Above-Knee Prosthesis SC-75", Orthotics and Prosthetics, Vol. 29, No. 4 pp15-20, December 1975.
  24. Crowninshield, R.D., Johnston, R.C., Andrews, J.G., Brand, R.A., "A Biomechanical Investigation of the Human Hip", Journal of Biomechanics Vol. 11, pp 75-85, 1978.
  25. Crowninshield, R., Pope, M.H., Johnson, R.J., "An Analytical Model of the Knee", Journal of Biomechanics, Vol. 9, pp397-405, 1976.
  26. Crowninshield, R., Pope, M.H., Johnson, R., Miller, R., "The Impedence of the Human Knee Joint", Journal of Biomechanics, Vol 9 pp529-535, No. 8 1975.

27. Cunningham, D.M., "Components of Floor Reactions During Walking", Prosthetic Devices Research Project, Inst. of Engineering Research, University of California, Berkeley, Series 11, Issue 14, November 1950, Reissued October 1958.
28. Cvetinovic, M., Cvetkovic, V., "A Microcomputer Based Knee-Locking Control System", The Sixth International Symposium on the External Control of Human Extremities, p 451, Belgrade, Yugoslavia, Aug 28-Sept 2, 1978.
29. Daher, R.L. "Physical Response of SACH Feet Under Laboratory Testing", Bulletin of Prosthetics Research 10-23, pp4-50, Spring 1975.
30. Daher, R.L. and Heath, J.b., "Durability Testing of Artificial Feet in the Laboratory", Inter-Clinic Infor. Bull. 13(4):11-17, Jan 1974.
31. Daher, R.L., Nelson, P.J., Heath, J.b. Peteski, N. "Functional Evaluation of Artificial Feet by Load vs. Deflection Recordings", Inter-Clinic Infor. Bull. 13(4)3-7, Jan 1974.
32. Dempster, W.T., "Free-body Diagrams as an Approach to the Mechanics of Human Posture and Locomotion" in F.G. Evans, ed., Biomechanical Studies of the Musculoskeletal System, Springfield, Ill, Charles C. Thomas, 1961.
33. Donath, M., "Proportional EMG Control for Above-Knee Prostheses", S.M. and Mech. Eng. Thesis, Dept. of Mech. Eng., MIT, August, 1974.
34. Drillis, R., Contini, R., and Bluestein, M., "Body Segment Parameters: A Survey of Measurement Techniques", Artificial Limbs, 8:1, 44-66, 1967.
35. Drillis, R., Contini, R., Bluestein, M. "Body Segment Parameters a Swing of Measurement Techniques", Artificial Limbs, Vol 8, No. 1 pp 44-66, Spring 1964.
36. Dyck, W.R., Onyshko, S., Holeson, D.A., Winter, D.A., Quanburry, A.O., "A Voluntarily Controlled Electrohydraulic Above-Knee Prosthesis", Bulletin of Prosthetic Research, 10-23, Spring 1975.
37. Eberhart, H.D., Inman, V.T., and Bresler, B., "The Principle Elements in Human Locomotion," in: Klopsteg, P.E., and Wilson, P.D., Human Limbs and their Substitutes New York: Hafner Publishing Co., pp 437-471, 1968.
38. Eberhart, H.D., "Fundamental Studies of Human Locomotion and other Information Relating to Design of Artificial Limbs", Prosthetic Devices Research Project, Univ. of California, Berkeley, California, National Library of Medicine, WE172qN278F, 1947.
39. "Electromyographic Knee Control System", VAPC-Knee from V.A. Bulletin Fall 1975.

40. Elftman, H., "Basic Function of the Lower Limb", Bio-Medical Engineering, August 1967.
41. Fisher, L., Dewar, M., MacCoughlan, J., Chodera, J. "The Bouncy Knee and the BSK", Bioengineering Centre Report, Dept of Mech. Eng., Univ. College London, Roehampton, London, 1981.
42. Fisher, L.D., Dewar, M.E., MacCoughlan, J.J., Chodera, J.D., Marshall, L. "The Bouncy Knee and the Blotchford Stabilized Knee", Annual Report of the Bioengineering Centre, Univ. of London, Roehampton, London, 1982.
43. Flowers, W.C., "A Man-Interactive Simulator System for Above-Knee Prosthetics Studies", Ph.D. Thesis, Dept. of Mech. Eng., MIT, Cambridge, MA., August 1972.
44. Flowers, W.C., Mann, R.W., "An Electrohydraulic Knee-Torque Controller for a Prosthesis Simulator", Journal of Bioengineering, Vol 99, Series K, No. 1, Feb. 1977.
45. Fournier, A., Domlire, E., Coiffet, P. "Electrical Stimulation of Limbs Part III. Joint Position Control", Bulletin of Prosthetics Research, Veterans Administration, pp 5-24, spring 1976.
46. Frank, A.A. "An Approach to the Dynamic Analysis and Synthesis of Biped Locomotion Machines", Medical and Biological Engineering, Vol. 8, pp 465-476, Pergamon Press, 1970.
47. Frigo, D., Rodano, R., "Comparison Between the Reactive Moments at the Lower Limb Joints of Normal and Prosthetized Subjects", Proceedings of an IFAC Symposium on Control Aspects of Prosthetics and Orthotics, Ohio State Univ., May 7-9, 1982.
48. Garg, D.P., Ross, M.A., "Vertical Mode Human Body Vibration Transmissibility", IEEE Transactions on Systems, Man, and Cybernetics, Vol. SMC-6, No. 2, Feb. 1976.
49. Gottlieb, L.G., Agarwal, G.C., "Dependence of Human Ankle Compliance on Joint Angle", Journal of Biomechanics, Vol 11, pp 171-181, 1978.
50. Gore, T.A., Flynn, M., Stevens, J., "Measurement and Analysis of Hip Joint Movements", Eng. in Medicine, Vol. 8, No. 1, pp 21-25, Jan 1979.
51. Greene, P.R., McMahon, T.A., "Reflex Stiffness of Man's Anti-Gravity Muscles During Kneebends While Carrying Extra Weights", Journal of Biomechanics, Vol 12, pp 881-891, 1979, Pergamon Press Ltd.
52. Greenwood, R., Hopkins, A., "Muscle Responses During Sudden Falls in Man", Journal of Physiology, 254, pp 507-518, 1976.

53. Grieve, D.W., "Gait Patterns and Speed of Walking", Biomedical Engineering, March 1968.
54. Grimes, D.L., "An Active Multi-Mode Above-Knee Prosthesis Controller", Ph.D. Thesis, Dept. of Mech. Eng., MIT, Cambridge, MA June, 1979.
55. Grimes, Flowers, and Donath, "Feasibility of an Active Control Scheme for Above-Knee Prostheses", Journal of Biomechanical Engineering, Vol 99 Series K, No. 4, November 1977.
56. Hoo, C., Woo, L., Vitagliano, V., Freudenstein, F., "Analysis of Control-Mechanism Performance Criteria for an Above-Knee Leg Prosthesis", Proceedings of the Conference of Applications of Continuous System Simulation Languages, 1969.
57. Hemami, H., Jasiva, V.C., "On a Three-Link Model of the Dynamics Standing Up and Sitting Down", IEEE Trans. on Systems, Man, and Cybernetics, Vol CMC-8, No. 2, February 1978.
58. Hemami, H., Wall, III., C., Black, F.O., Golliday, Jr., G.L., "Single Inverted Pendulum Biped Experiments", Journal of Interdis. Model and Simulation, 2930 211-227, 1979.
59. Hermami, H., Weimer, F.C., Koozekanani, S.H., "Some Aspects of the Inverted Pendulum Problem for Modeling of Locomotion Systems", IEEE Transactions on Automatic Control, AC-18, pp658-661.
60. Hight, T.K., Piziali, R.L., Nagel, D.H., "A Dynamic, Nonlinear Finite Element Model of a Human Leg", Journal of Biomechanical Engineering, Vol 101, pp 176-184, August 1979.
61. Hirsch, A.E., White, L.A., "Mechanical Stiffness of Man's Lower Limbs", ASME, paper 65-WA/HUF-4, 1965.
62. Horn, G.W., "Electro-Control: An EMG-Controlled A/K Prosthesis", Med. and Biol. Engineering, Vol 10, pp 61-73, Pergamon Press, 1972.
63. Huang, C.T., Jackson, J.R., Moore, N.B., Fine, P.R., Kuhlemeier, K.V., Traugh, g.H., Saunders, P. "Amputation: Energy Cost of Ambulation", Archives of Physical Medicine in Rehabilitation, Vol 60, January 1979.
64. Inman, V.T., Ralston, H.J., Todd, F., "Human Walking", Pub. Williams and Wilkins, Baltimore, Md., 1981.
65. Jakobson, J.S., Kuzschekin, A.P., Kononov, E.V., "Methods of Designing and Results of Experimental Tests of Motorized Above-Knee Prosthesis", in supplement to the proceedings of The Sixth International Symposium on External Control of Human Extremities, Dubrovnik, Yugoslavia, Aug 28-Sept. 1, 1978.
66. Jira, R. "Stability Control of Knee Prosthesis", Univ. of Cal., Berkeley, Dept. of Mech. Eng., Ph.D. Thesis, Nov. 1978.

67. Judge, G., Fischer, L., "A Bouncy Knee for Above-Knee Amputees", Annual Report of the Biomechanical Research and Development Unit, Roehampton, London, 1978.
68. Judge, G. "Measurement of Knee Torque/Angle Characteristics During the Swing Phase of Gait", Biomechanical Research and Development Unit of the Department of Health and Social Security, Roehampton, London, Report 1977.
69. Judge, G., "Measurement of Knee Torque/Angle Characteristics During the Swing Phase of Gait", Biomechanical Research and Development Unit, Roehampton, London, Report 1978.
70. Judge, G.B., "Survey of Knee Mechanisms for Artificial Legs", Biomechanical Research and Development Unit, Roehampton Lane, London, Revised 1980.
71. Kato, I, Onozuka, T., Iida, S. "Clinical Testing of an Above-Knee Prosthesis with Myoelectric Control", The Sixth International Symposium on External Control of Human Extremities, Dubrovnik, Yugoslavia, Aug. 28-Sept 7, 1978.
72. Koozekanani, S.H., Stockwell, C.W., McGhee, R.B., Firoozmand, F., "On the Role of Dynamic Models in Quantitative Posturography", IEEE Transactions on Biomedical Engineering, Vol. BME-27, No. 10, Oct. 1980.
73. Larman, J.M., "Movement and the Mechanical Properties of the Intact Human Elbow Joint", Ph.D. Thesis, Dept. of Psychology, MIT, June 1980.
74. Lesh, M.D., Mansour, J.M., Simon, S.R., "A Gait Analysis Subsystem for Smoothing and Differentiation of Human Motion Data", Journal of Biomechanical Engineering, Vol. 101, August 1979.
75. Lord, Marilyn, Bioengineering Centre, Dept. of Mech. Eng., Univ. College, London, Roehampton Lane, London Tel.: 01-789-6500, ext. 266/260, Personal Communication.
76. Mauch, H.A., "Summary Report on Research and Development in the Field of Artificial Limbs", Bulletin of Prosthetics Research, Fall 1969.
77. McGhee, R.B., Koozekanani, S.H., Weimer, F.C., Rahmani, S., "Dynamic Modeling of Human Locomotion" Joint Automatic Control Conference, pp 405-413, June 1979.
78. McGhee, R.B., Tomovic, R., Yang, P.Y., MacLean, I., "An Experimental Study of a Sensor-Controlled External Knee Locking System", IEEE Transactions on Biomedical Engineering, Number 2, Vol. BME-25, March 1978.



79. McMahon, T.A., Greene, P.R., "The Influence of Track Compliance", Journal of Biomechanics, Vol. 12, No. 12, pp 893-904, Pergamon Press Ltd., 1979.
80. McMahon, T.A., Greene, P.R., "Fast Running Track", Scientific American, Dec 1978.
81. Marich, M. Prosthetists, NOPCO, Children's Hospital, Longwood, Boston, MA. Personal Communication.
82. Meyfarth, P.F., "Dynamic Response Plots and Design Charts for Third-Order Linear Systems", Research Memorandum, No. R.M. 7401-3, Dynamic Analysis and Control Lab., Dept. of Mech. Eng., MIT, Sept. 15, 1958.
83. Mochon, S. "Ballistic Walking: A Mathematical Model of Human Locomotion" Ph.D. Thesis, division of Applied Sciences, Harvard University, April 1979.
84. Moffatt, C.A., Harris, E.H., Haslam, E.T., "Experimental and Analytical Study of Dynamic Properties of the Human Leg", ASME Paper No. 69-BHF-4, Biomechanical and Human Factors Conference, June 12-13, 1969.
85. Morawski, J.M., "A Simple Model of Step Control in Biped Locomotion", Ieee Transactions of Biomedical Engineering, Vol. BME-25, No. 6, Nov. 1978.
86. Moskowitz, G., "Myoelectric Control of the Knee for Above-Knee Amputee", Bulletin of Prosthetic Research, pg. 299, Fall 1979.
87. Murray, M.P., Seireg, A., Scholz, R.C., "Center of Gravity, Center of Pressure, and Supportive Forces During Human Activities", Journal of Applied Physiology Vol, 23, No. 6., December 1967.
88. Myers, D.R., Moskowitz, G.D., "Myoelectric Pattern Recognition for Use in the Volitional Control of Above-Knee Prostheses", submitted to IEEE Trans. SMG
89. Nakamura, S., Sawamura, S. "HRC Adjustable Pneumatic Swing-Phase Control Knee", Prosthetics and Orthotics International 2, pp 137-142, 1978.
90. Nashner, L.M. "Fixed Patterns of Rapid Postural Responses Among Leg Muscles During Stance" Experimental Brain Research pp 813-24 1977.
91. Onyshko, S., Winter, D.A., "A Mathematical Model for the Dynamics of Human Locomotion", Journal of Biomechanics, 13, pp 361-368, 1980.
92. Pearson, K. "The Control of Walking", Scientific American, Dec. 1976.

93. Peizer, E., et al., "Human Locomotion", Bulletin of Prosthetics Research, Fall, 1969.
94. Peizer, E., "Work and Energy in Walking", Bulletin of Prosthetics Research, 10-8, Fall 1967.
95. Perry, J., "The Mechanics of Walking A Clinical Interpretation" Physical Therapy 47:778-801, 1967.
96. Piziali, R.L., Rastegar, J.C., Nagel, D.A., "Measurement of the Nonlinear, Coupled Stiffness Characteristics of the Human Knee, Journal of Biomechanics, Vol 10, pp 45-51, 1977.
97. Pope, M.H., Crowninshield, R., Miller, R., Johnson, R., "The Static and Dynamic Behavior of the Human Knee in Vivo", Journal of Biomechanics, Vol. 9, No. 7, pp. 449-452, 1976.
98. Radcliffe, C.W., "Biomechanical Design of an Improved Leg Prosthesis", Prosthetics Research Board National Research Council, Univ. of California, Berkeley, Series 11, Issue 33, Oct. 1957.
99. Radcliffe, C.W., "Locomotion and Lower-Limb Prosthetics", Bulletin of Prosthetics Research, 10-22, Fall 1974.
100. Radcliffe, C.W., Cunningham, D.M., Morris, J.M., Lamoreux, L., "Multi-Input Control of Knee Stability", Bulletin of Prosthetic Research Spring 1979.
101. Radcliffe, C.W., "Biomechanical Design of a Lower-Extremity Prosthesis", ASME No. 60-WA-305.
102. Rahmani, S., "An Experimental Study of Planar Models for Human Gait Utilizing on-line computer Analysis of Television and Force Plate Data", Ph.D. Thesis, Dept of Electrical Engineering, Ohio State Univ., June 1979.
103. Reswick, J., Perry, J., Antonelli, D., Su, N., Freeborn, C. "Preliminary Evaluation of the Vertical Acceleration Gait Analyzer (VAGA)", Proceedings of the Sixth International Symposium On External Control of Human Extremities, Derbrovnik, Yugoslavia, August 28-Sept 1, 1978.
104. Saunders, J.B. deC.M., Inman, V.T., Eberhart, H.D., "The Major Determinants in Normal and Pathological Gait", Journal of Bone and Joint Surgery, 35-A:543-558, July 1953.
105. Saxena, S.C., Mukhopadhyay, P., "A New approach to Central Above-Knee Prosthesis", Proceedings of the Conference on the Applications of Electronics in Medicine, London, England, pp 285, April 1976.
106. Siegler, S., Seliktar, R., Hyman, W., "Simulation of Human Gait with the Aid of a Simple Mechanical Model", Journal of Biomechanics, Vol. 15, No. 6, pp 415-425, 1982.

107. Smith, D.M., McCourt, P., "An Hydraulically Powered Prosthetic Knee Control Simulator", Annual Report the Biomechanical Research and Development Unit, Roehampton, London, 1978.
108. Standards and Specifications for Prosthetic Foot/Ankle Assemblies", Veterans Administration Prosthetics Center, N.Y., N.Y., June 1, 1973.
109. Tomovic, R., McGhee, R.B., "A Finite State Approach to the Synthesis of Bioengineering Control Systems", IEEE Transactions on Human Factors in Electronics, Vol. HFE-7, No. 2, June 1966.
110. Traugh, G.H., Corcoran, P.J., Reyes, R.L., "Energy Expenditure of Ambulation in Patients with Above-Knee Amputations", Archives of Physical Medicine and Rehabilitation, Vol. 56, Feb. 1975.
111. Wagner, E.M., Cartranis, J.G., "New Developments in Lower-Extremity Prostheses", Human Limbs and their Substitutes, McGraw-Hill, New York 1954.
112. Wallach, J., "Control Mechanism Performance Criteria for an Above-Knee Leg Prosthesis", Journal of Biomechanics, Vol. 3, pp 87-97, Pergamon Press, 1970.
113. White, B.F., Brown, D.W., Hundal, M., Johnson, R.J., Pope, M.H., "Knee Impedance Testing Machine", Medical Instrumentation Vol 13, No. 4, July-August 1979.
114. Wilson, Jr., A.B., Murphy, E.F., "Engineering Approaches to Limb Prosthetics and Orthotics", CRC Critical Reviews in Bioengineering pp 169-215, December, 1971.
115. Winter, D.A., Biomechanics of Human Movement, New York: Wiley-Interscience, John Wiley and Sons, 1979.
116. Winter, D.A., Sidwall, H.G., Hobson, D.A., "Measurement and Reduction of Noise in Kinematics of Locomotion", Journal of Biomechanics, 7, pp 157-159, 1974.
117. Winter, D.A., "Overall Principle of Lower Limb Support During Stance Phase of Gait" Journal of Biomechanics Vol. 13, pp 923-927, Pergamon Press Ltd., 1980.
118. Winter, D.A., Robertson, D.G.E., "Joint Torque and Energy Patterns in Normal Gait" Biol. Cybernetics 29, pp 137-142, 1978.
119. Winter, D.A., Quanbury, A.O., Hobson, D.A., Sidwall, H.G., Reimer, G., Trenholm, B.G., Steinke, T., and Shlosser, H., "Kinematics of Normal Locomotion -- A Statistical Study Based on Television Data", Journal of Biomechanics, 7, pp 479-486, 1974.
120. Zarrugh, M.Y., "Energy and Power in Human Walking", Ph.D. Thesis, Dept. of Mech. Eng., Univ. of California, Berkeley, Ca., June 1976.

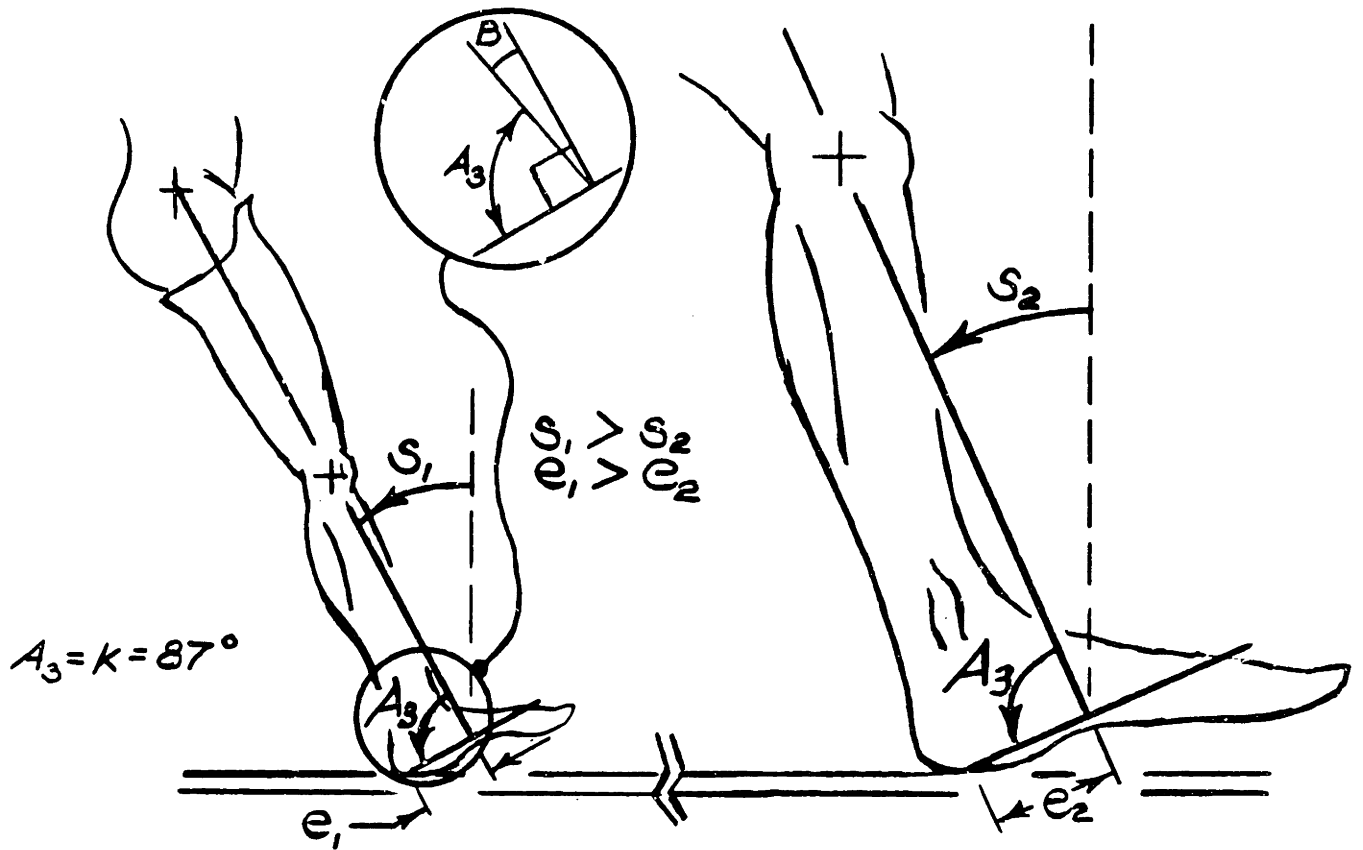
## APPENDIX 1 - DESIGNER GAIT MODELS

The general equations and flow of the simulations for the designer gait models are presented. Every detail of the simulator program is not included. The designer gait models are: SACH foot model, Model #1, and Model #2. The SACH foot model is a kinematic model of the cam geometry of the SACH foot. Model #1 is a compliant inverted pendulum rotating about a fixed point with a point body mass at the top. Model #2 is a compliant inverted pendulum during PHR and a rigid inverted pendulum during the rest of stance (latching spring model). It also has a point body mass at the top and the cam geometry of the SACH foot at the bottom.

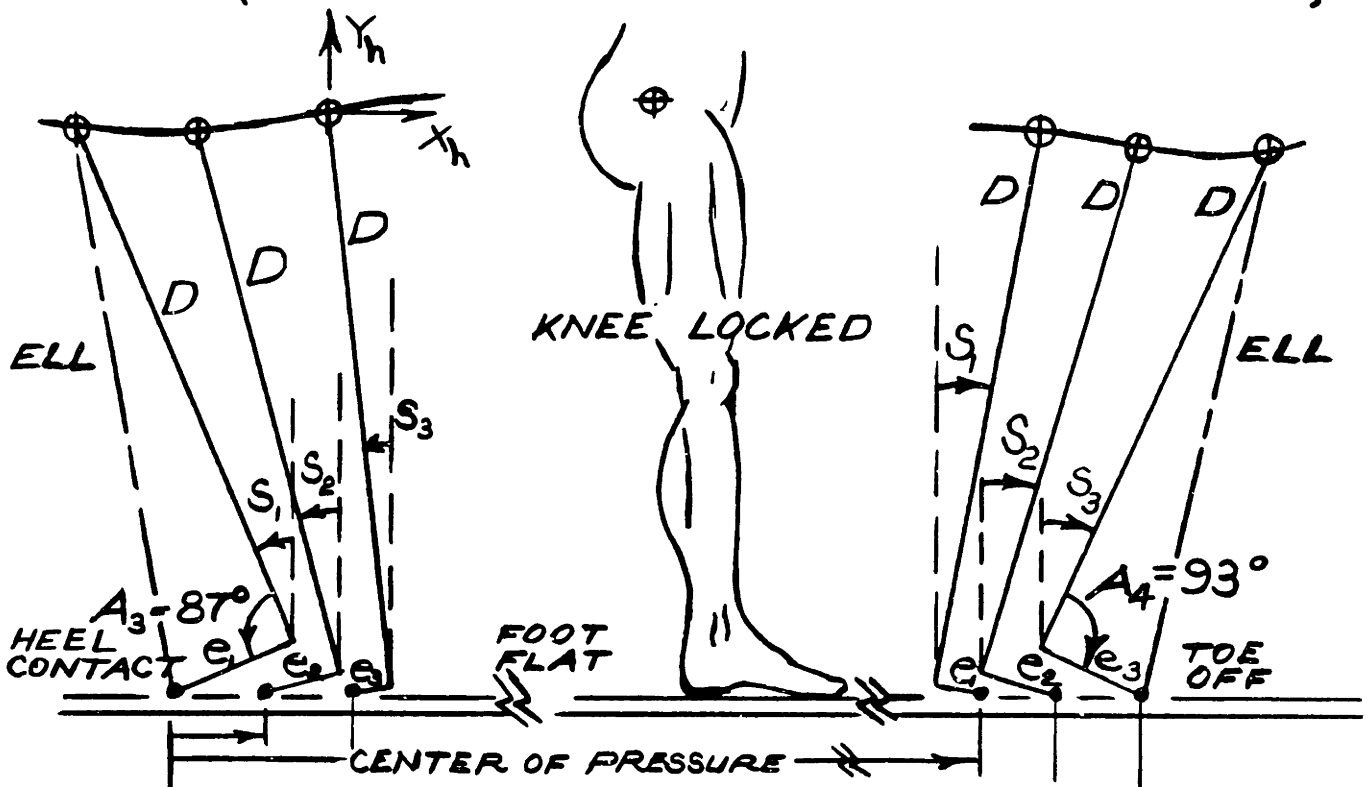
### A-1.1 Cam Geometry of the SACH Foot

The SACH foot cam effect is derived from the data showing that the forward motion of the center of pressure of the foot/floor reaction forces is related to the shank angle. This section uses that relationship as the basis for developing the kinematic relationship of the "locked Knee" prosthesis rolling over the SACH foot.

The process of determining the hip position as a function of shank angle is illustrated in Figure A-1.1. Two straight, massless line segments are used to represent the prosthesis. A line segment of constant length  $D$  is the length of the thigh and shank in their locked position. A second massless line segment  $e$ , of variable length represents the heel or toe of the SACH foot. At PHC, an initial value of  $e$ , and location of the hip are given by the data. This determines the initial shank angle,  $S$ . The angle,  $S$ , is then changed by a small amount, changing the location of



$e_n$  LOCATES CENTER OF PRESSURE  
(CHANGE  $e_n$  WITH EACH INCREMENT,  $\Delta S$ )



KINEMATICS OF THE SACH FOOT  
FIGURE A-11

the hip. a new location of the center of pressure is then determined from this new value of S. This requires a new foot length e to be calculated. Since leg length, D, and angle B are constant, the position of the hip is altered by this new value of e. The angle S is again changed by a small amount and the process repeats.

The detail of this process is contained in the following equations. They are all relatively simple trigonometric relationships obtained from Figure A-1.2.

The process is initialized by the shank angle, S, the hip position (Xh,Yh) at PHC an initial value for the heel length e, and the shank angle at foot flat B. Hip position and shank angle are obtained from the data and e is approximated by center of pressure movement up to footflat (approximately 6cm) (see Figure V-3). The shank angle at footflat is obtained from a plot of center of pressure versus shank angle (B=3.3 degrees).

Referring to Figure A-1.2 the following relationship applies. The initialization proceeds as follows:

An intermediate variable d is given by

$$d=e*\text{SIN}(S-B)/\text{COS}(S). \quad (1)$$

where \* indicates multiplication.

The length of the leg, D, is

$$D=(Yh/\text{COS}(S)) - d. \quad (2)$$

The effective leg length, ELL, is



$$ELL = (e + d - 2 * e * d * \sin(B))^{1/2} \quad (3)$$

and the angle of ELL with respect to vertical is

$$a = \cos^{-1}(Yh/ELL). \quad (4)$$

An intermediate angle, A2 is

$$A2 = \cos^{-1} [(ELL^2 + e^2 - D^2) / (2 * ELL * e)]. \quad (5)$$

Now that the model is initialized, a repetitive procedure for cam roll follows. First increment angle, a (a numerical decrease in value) and calculate a new value for the shank angle, S

$$S = \pi/2 + a + B - A2 \quad S > B \quad (6)$$

$$S = \pi/2 + a + B + A2. \quad S < B$$

Now calculate the new center of pressure, COP, location appropriate for this shank angle (see Figure V-3).

$$COP = M1 * S + COPINTER1 \quad \text{for } S > BR1$$

$$COP = M2 * S + COPINTER2 \quad BR2 < S < BR1 \quad (7)$$

$$COP = M3 * S + COPINTER3 \quad S < BR2$$

where M's COPINTER's and BR's are determined from Figure V-3 their values are:

$$M1 = -3.3 \times 10^{-3} \text{ Meter/Degree}$$

$$M2 = -1.38 \times 10^{-2} \text{ Meter/Degree}$$

$$M3 = -1.96 \times 10^{-3} \text{ Meter/Degree}$$

$$BR1 = 3.3 \text{ Degrees}$$



$$BR2 = -5.7 \text{ Degrees}$$

and the intercepts are

$$COPINTER1 = COPPHC - M1 * SPHC \quad (8)$$

where COPPHC is the center of pressure at PHC which is defined as zero, and SPHC is the shank angle at PHC

$$COPINTER2 = COP2 - M2 * BR1$$

where

$$COP2 = M1 * BR1 + COPINTER1,$$

and

$$COPINTER3 = COP3 - M3 * BR2$$

where

$$COP3 = M2 * BR2 + COPINTER2.$$

Now that the new COP position has been determined, determine the new heel length (or toe length), e,

$$e = e_{old} - (COP_{new} - COP_{old}) / \cos(B - S) \quad S > B \quad (9)$$

$$e = e_{old} + (COP_{new} - COP_{old}) / \cos(B - S) \quad S < B$$

where  $e_{old}$  is the previous value of e

$COP_{new}$  and  $COP_{old}$  are the current and old values of COP respectively and thus a new equivalent (or effective) leg length, ELL, can be calculated.

$$ELL = (e^2 + D^2 - 2 * e * D * \sin(B))^{1/2} \quad S > B \quad (10)$$

$$ELL = (e^2 + D^2 + 2 * e * D * \sin(B))^{1/2} \quad S < B.$$

The intermediate length, d, is now

$$d = -e * \sin(B - S) / \cos(S) \quad S > B \quad (11)$$

$$d = -e * \sin(S - B) / \cos(S) \quad S < B$$

and A2 is recalculated by

$$A2 = \cos^{-1}((ELL^2 + e^2 - D^2) / (2 * ELL * e)) \quad (12)$$

and the new ELL angle, a, is

$$a = S - \pi/2 - B + A2 \quad S > B \quad (13)$$

$$a = S + \pi/2 - B - A2 \quad S < B$$

calculate the new hip position

$$Y_h = ELL * \cos(a) \quad (14)$$

$$X_h = -ELL * \sin(a) + COP \quad (15)$$

The process has completed one cycle. Repeat by incrementing angle, a, and returning to equation (6).

## A-1.2 Equations of Motion for Model #1

The structure and equations of motion for Model #1 are presented. The motivation for this model is presented in Chapter V. Figure A-1.3 shows the basic structure and energy storage elements for the model as well as a free body diagram. Model #1 has two degrees of freedom that include:

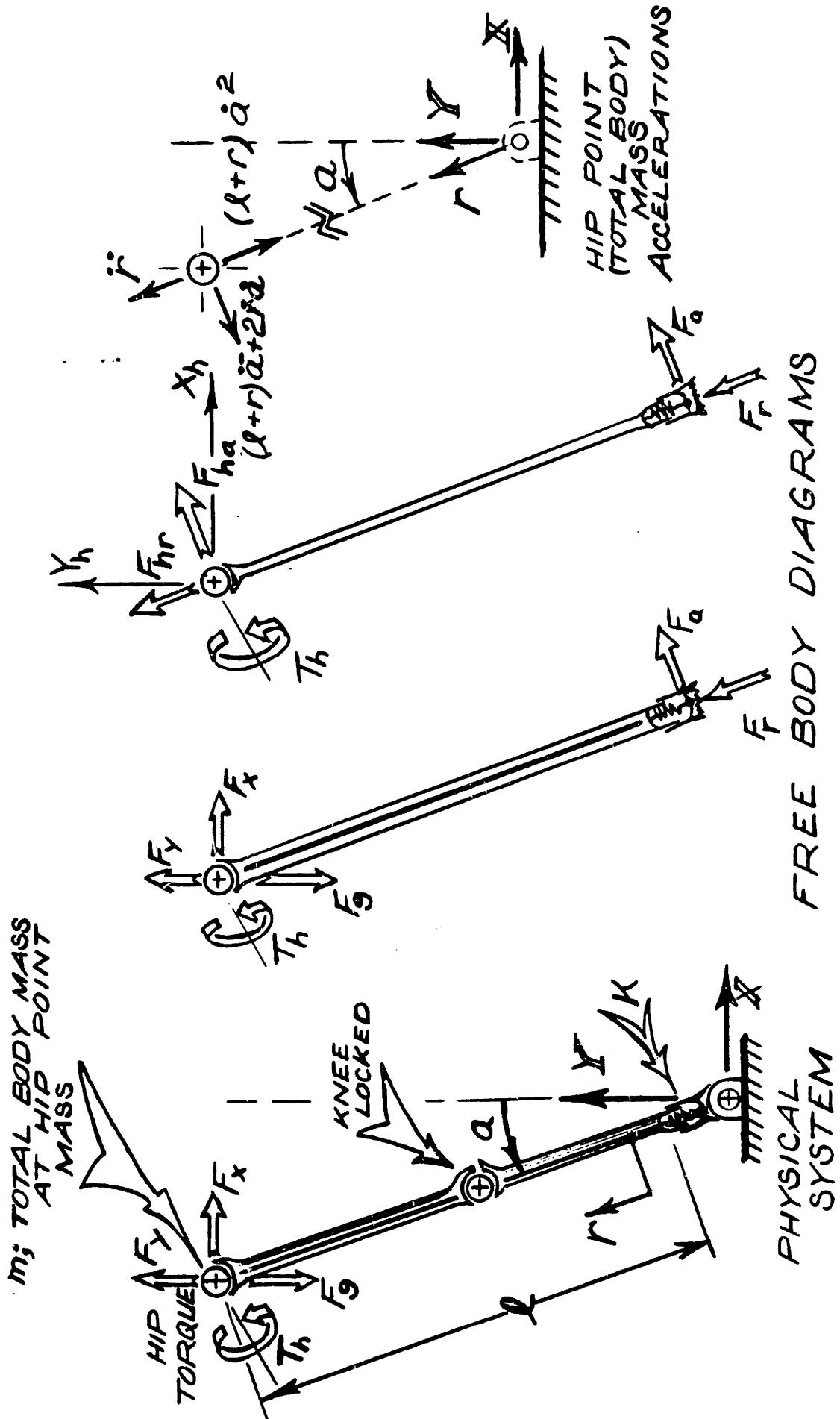
- 1) rotation from vertical,  $\alpha$ , positive angles BTDC,
- 2) displacement of spring along axis of pendulum,  $r$ .

The model has two energy storage elements that include:

- 1) a point mass,  $m$ , representing the mass of the amputee and his prosthesis and is located at the top of the pendulum at a location representing the hip;
- 2) a spring representing the heel stiffness of the SACH foot,  $K$ .

The model has four inputs or driving functions that include:

- 1) the constant body force due to gravity,  $F_g$ ;
- 2) a vertical force representing the sound leg contribution at the hip,  $F_y$ ;
- 3) a horizontal force representing the sound leg contribution at the hip,  $F_x$ ;
- 4) a torque representing the amputee's saggital plane hip torque,  $T_h$ .



MODEL 1 DETAILS  
FIGURE A-1.3

The model has one geometric constraint which is the pendulum of length  $r$  plus  $l$  which rotates without friction about a fixed point.

The equations of motion are developed in the following equations.

The forces,  $F_x$ ,  $F_y$ ,  $F_g$  can be defined in terms of the  $(r, a)$  coordinate system by the following transformation.

$$\begin{bmatrix} F_{ha} \\ F_{hr} \end{bmatrix} = \begin{bmatrix} \cos(a) & \sin(a) \\ -\sin(a) & \cos(a) \end{bmatrix} \begin{bmatrix} F_x \\ F_y - F_g \end{bmatrix} \quad (1)$$

Now apply Newton's Laws to the free body diagram.

Summing forces in the  $r$ -direction yields

$$F_r - F_g \cos(a) + F_y \cos(a) - F_x \sin(a) = m(\ddot{r} - (1+r)\dot{a}^2) \quad (2)$$

Summing forces in the direction perpendicular to  $r$  yields

$$F_a - F_g \sin(a) + F_y \sin(a) + F_x \cos(a) = -m(2\dot{r}\dot{a} + (1+r)\ddot{a}) \quad (3)$$

where  $\dot{\quad}$  = the first derivative with respect to time

$\ddot{\quad}$  = the second derivative with respect to time

$m$  = the total body mass including the prosthesis

Summing the torques about the hip, (note that the inertia equals zero) yields

$$T_h + F_a(1+r) = 0. \quad (4)$$

Rearranging equation 4

$$F_a = -T_h / (1+r) \quad (5)$$

Note that equation (5) implies that dynamic load line will pass through the shaft of the pendulum unless a hip torque is present. This is a simple way of viewing the amputee's control over knee stability through hip torque control.

The constitutive law for a spring provides:

$$F_r = -K(a) * r \quad (6)$$

where  $K(a)$  show the stiffness of the heelspring depends on the angle,  $a$ . Substituting equations (5) and (6) into equations (2) and (3) and rearranging to solve for the accelerations explicitly the following equations of motion are obtained.

$$\ddot{r} = (m(1+r)\dot{a}^2 - F_g \cos(a) - K(a)r + F_y \cos(a) - F_x \sin(a)) / m \quad (7)$$

$$\ddot{a} = (-2(r+1)\dot{r}\dot{a} + F_g(1+r)\sin(a) - F_y(1+r)\sin(a) - F_x(1+r)\cos(a) + T_h) / m(1+r)^2 \quad (8)$$

Equations (7) and (8) can be numerically integrated if the initial conditions on the state variables  $a$ ,  $r$ ,  $\dot{a}$  and  $\dot{r}$  are determined and if the inputs  $F_x$ ,  $F_y$ ,  $F_g$  and  $T_h$  are known. Except for  $F_g$ , which is simply the mass times the acceleration due to gravity, the inputs are provided by the data and the inverse dynamics model (see Chapters II and IV). The initial conditions are determined from the hip displacement and velocity data at PHC.

At PHC the spring is at its free length which is defined as zero, so the initial condition on  $r$  is

$$r_{ic}=0. \quad (9)$$

Since the total length of the leg (hip to contact point) is known, then the initial condition on angle  $a$  is

$$a_{ic}=\cos^{-1} (Y_{hd}/(l+r_{ic})) \quad (10)$$

where  $Y_{hd}$  = the height of the hip above the ground at PHC according to the data. With the initial conditions on the displacements known the initial conditions on the velocities can be determined. The initial condition on the axial velocity is

$$\dot{r}_{ic}=\dot{Y}_{hd}\cos(a_{ic})-\dot{X}_{hd}\sin(a_{ic}) \quad (11)$$

and on the angular velocity is

$$\dot{a}_{ic}=-((\dot{X}_{hd}\cos(a_{ic})+\dot{Y}_{hd}\sin(a_{ic})))/(l+r_{ic})) \quad (12)$$

where  $\dot{X}_{hd}$ =the forward velocity of the hip at PHC according to the data

$\dot{Y}_{hd}$ =the vertical velocity of the hip at PHC according to the data.

The values for the parameters are

$$l=.89 \text{ meters}$$

$$m=68.2 \text{ Kg}$$

The relationship for  $K$ , the stiffness comes from Appendix 2 and is

repeated here

$$K=157,000e^{-\frac{a}{a_0}} \quad (13)$$

where  $a$  is in radians.

The hip displacement can be calculated by

$$X_h = -(1+r) \cdot \text{SIN}(a) \quad (14)$$

$$Y_h = (1+r) \cdot \text{COS}(a) \quad (15)$$

The vertical hip velocity can be determined from

$$\dot{X}_h = -(1+r) \text{COS}(a) \cdot \dot{a} - \dot{r} \cdot \text{SIN}(a) \quad (16)$$

$$\dot{Y}_h = -(1+r) \dot{a} \cdot \text{SIN}(a) + \dot{r} \cdot \text{COS}(a) \quad (17)$$

### A-1.3 Equations of Motion for Model #2 and Latching Spring Model

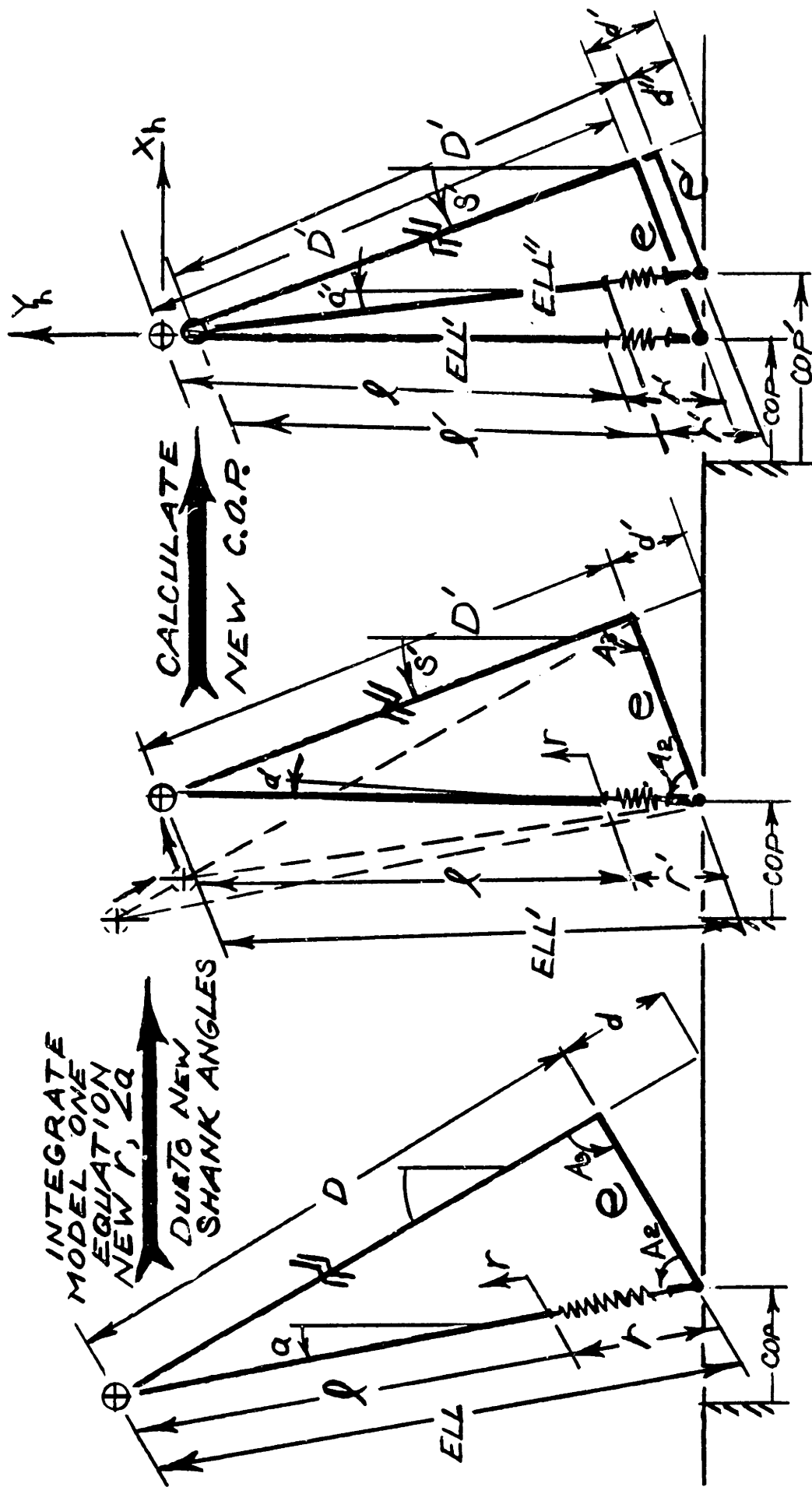
Model #2 is identical to Model #1 except the kinematics of the SACH foot are added. The Latching Spring Model is equivalent to Model #2 during the heel compression portion of stance phase and equivalent to a dynamic version of the SACH foot cam kinematic model presented in A-1.1. Therefore, Model #1's equations can be used by adding the kinematic constraint of the SACH cam foot during heel compression. After heel compression the model's equations will change, reflecting the loss of the energy storage element  $K$ . The same description that was used for describing the forward progress of the hip in A-1.1 applies here except that now the changes in shank angle,  $S$ , results from integration of the equations of motion rather than just an arbitrary increment. In addition, during the time that a new value of  $S$  is being determined, a new value of



the effective leg length,  $\bar{ELL}$ , is also being determined (see Figure A-1.4). End of heel compression is defined by spring compression rate going to zero. At this point the spring is latched at its current length. The equations of motion degenerate to a one degree of freedom rigid inverted pendulum. The simulation then proceeds until the data driving the model ends at PT0. Note, knee break is not modeled.

The flow to this process can be described as follows.

1. Problem is initialized by data  $Y_{hd}$ ,  $S$ ,  $e$ ,  $\dot{X}_{hd}$ ,  $\dot{Y}_{hd}$  providing starting values for  $r, a, \dot{r}, \dot{a}$ .
2. Find new real leg length,  $D$ .
3. Find new shank angle,  $S$ .
4. Find new COP location.
5. Find new  $e$ .
6. Find new  $ELL$ ,  $X_h$ ,  $Y_h$  the output states.
7. Find new  $d$  and  $A2$ .
8. Find new initial conditions  $a$ ,  $\dot{a}$ ,  $\dot{r}$  ( $r$  is left unchanged).
9. Integrate for one more time step, the compliant inverted pendulum equations producing new  $a$ ,  $r$ ,  $\dot{a}$ ,  $\dot{r}$ .
10. If  $r=0$  go to step 12.
11. Return to step 2.



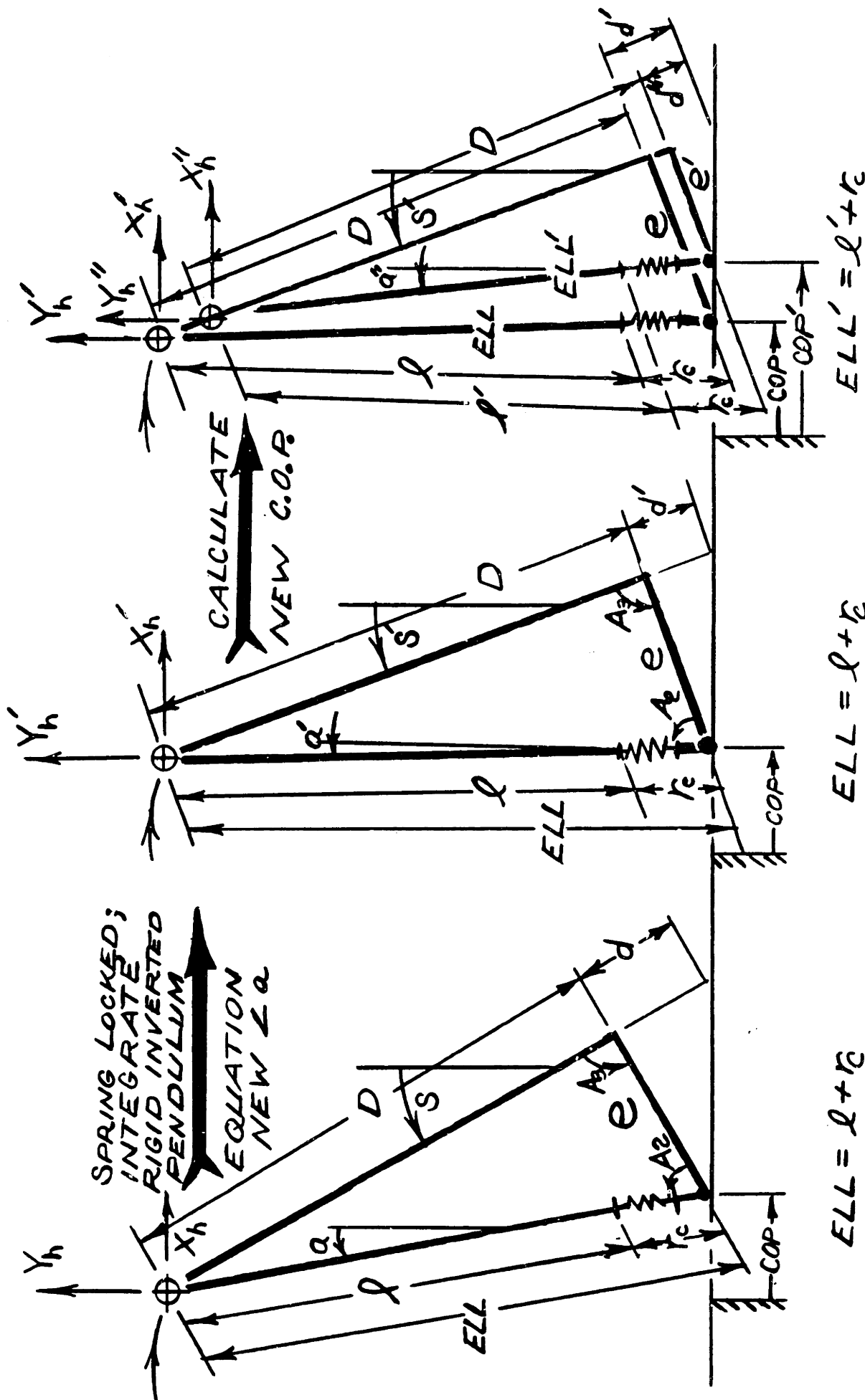
$ELL = L + r$        $ELL' = L' + r'$        $ELL'' = L'' + r''$

COMPLIANT INVERTED PENDULUM WITH CAM

FIGURE A-1.4

12. Set spring length,  $r$ , equal to its current value,  $r_c$ .
13. Find new shank angle,  $S$ .
14. Find new COP location.
15. Find new  $e$ .
16. Find new ELL,  $X_h$ ,  $Y_h$  the output states.
17. Find new  $d$ , and  $A_2$ .
18. Find new initial conditions on  $a$ , and  $\dot{a}$ .
19. Integrate, for one more time step, the rigid inverted pendulum equations.
20. Find new,  $a$  and  $\dot{a}$ .
21. If input data has ended STOP.
22. Return to step 13.

For equations of motions for compliant inverted pendulum see Model #1. For the rigid inverted pendulum model the equations are developed below. All of the assumptions are identical to the compliant case except that the pendulum is rigid which reduces the degrees of freedom to one, the angle of the leg with respect to vertical. The simple inverted pendulum equation is (see Figure A-1.5):



$ELL = \ell + e_c$        $ELL' = \ell' + e'_c$   
**RIGID INVERTED PENDULUM WITH CAM**  
**FIGURE A-1.5**

$$\begin{aligned} \ddot{a} &= G * \text{SIN}(a) / \text{ELL} \\ &+ Th / (M * \text{ELL}^2) \\ &- Fx * \text{COS}(a) / (M * \text{ELL}) \\ &- Fy * \text{SIN}(a) / (M * \text{ELL}) \end{aligned} \quad (1)$$

where G = acceleration due to gravity.

ELL= effective leg length, distance from hip  
to point of contract, includes compliant  
element effect on length

Th= hip torque input

Fx= horizontal sound leg force input

Fy= vertical leg force input

Initialization of Model #2 is a combination of the initialization process for Model #1 plus the process for the rigid cam model. It proceeds as follows.

At PHC assume spring length, r, is zero.

$$ric=0 \quad (2)$$

Given the heel length, e, (see cam model), shank angle, s, and the shank angle at foot flat, B

$$d=e * \text{SIN}(S-B) / \text{COS}(S). \quad (3)$$

Given vertical displacement hip at PHC,  $Y_{hd}$ , then the real leg length,  $D$ , is

$$D=(Y_{hd}/\cos(S))-d \quad (4)$$

and the effective leg length,  $ELL$ , is

$$ELL=1+ric=(e^2+D^2-2*e*D*\sin(B))^{\frac{1}{2}} \quad (5)$$

where 1 is the  $ELL$  at PHC since  $ric=0$ .

The initial condition on  $a$  is, therefore,

$$a=\cos^{-1}(Y_{hd}/ELL). \quad (6)$$

Intermediate angle,  $A2$  is

$$A2=\cos^{-1}((ELL^2+e^2-D^2)/(2*ELL*e)). \quad (7)$$

The initial conditions on  $\dot{a}$  and  $\dot{r}$  are

$$\dot{a}=-(\dot{X}_{hd}*\cos(a)+\dot{Y}_{hd}*\sin(a))/(ELL) \quad (8)$$

$$\dot{r}=\dot{Y}_{hd}*\cos(a)-\dot{X}_{hd}*\sin(a) \quad (9)$$

the output trajectory of the hip is defined by

$$X_h=-ELL*\sin(a)+COP \quad (10)$$

$$Y_h=ELL*\cos(a) \quad (11)$$

$$\dot{X}_h=-ELL*\cos(a)*\dot{a}-\dot{r}*\sin(a) \quad (12)$$

and

$$\dot{Y}_h = -ELL \cdot \dot{a} \cdot \sin(a) + \dot{r} \cdot \cos(a). \quad (13)$$

Now integrate the compliant inverted pendulum equations (equations (7) and (8) in A-1.2 for one time step. This produces new values for  $a$ ,  $r$ ,  $\dot{a}$ , and  $\dot{r}$ , thus update the "triangle" shown in Figure A-1.4.

$$ELL = l + r \quad (14)$$

$$D = (ELL^2 + e^2 - 2 \cdot ELL \cdot e \cdot \cos(A2))^{1/2} \quad (15)$$

The new shank angle,  $S$ , and change in center of pressure, COP, and heel length,  $e$ , are calculated using equations 6, 7, 8, and 9 in A-1.1. Thus, the new leg length  $l$  is calculated with the length of spring remaining fixed.

$$l = (e^2 + D^2 - 2e \cdot D \cdot \sin(B)) - r \quad S > B \quad (16)$$

$$l = (e^2 + D^2 + 2e \cdot D \cdot \sin(B)) - r \quad S < B$$

and the new ELL is

$$ELL = l + r. \quad (17)$$

The new value for  $d$ ,  $A2$ ,  $a$ ,  $X_h$ ,  $Y_h$  are calculated using equations 11, 12, 13, 14, and 15 from A-1.1.

The new geometry means the equations have to be reinitialize. The spring length remains the same but  $\dot{a}$ , and  $\dot{r}$  change. The new values are given by

$$\begin{aligned} \dot{r} = \dot{r}_{\text{new}} = & \dot{r}_{\text{old}} * \text{COS}(a_{\text{new}} - a_{\text{old}}) \\ & + (l_{\text{old}} + r) \dot{a}_{\text{old}} * \text{SIN}(a_{\text{new}} - a_{\text{old}}) \end{aligned} \quad (18)$$

$$\begin{aligned} \dot{a} = \dot{a}_{\text{new}} = & (-\dot{r}_{\text{old}} * \text{SIN}(a_{\text{new}} - a_{\text{old}}) + \\ & + (l_{\text{old}} + r) \dot{a}_{\text{old}} * \text{COS}(a_{\text{new}} - a_{\text{old}}) \end{aligned} \quad (19)$$

where old is value of the states before cam kinematics structure changed the geometry after the last time step, and new is the current value.

The equations are then integrated again producing new values of  $a$ ,  $r$ ,  $\dot{a}$ ,  $\dot{r}$  and the process returns to equation (10).

If, however,  $\dot{r} = 0$  then spring latch is assumed to have occurred. Then  $r$  is permanently defined as its current length  $r_c = r$  where  $r_c$  is the length of the latched spring. The cam model in A-1.1 can now be used directly to compute new values of  $e$ ,  $d$ ,  $A_2$ ,  $a$ ,  $X_h$ ,  $Y_h$ . The only additional information needed is how to reinitialize  $\dot{a}$  to integrate the rigid inverted pendulum equation. This is done by taking the component of the old velocity vector which is no longer perpendicular to the pendulum due to the cam profile and use the component of the velocity vector that is perpendicular to the pendulum. This means that part of the energy is thrown away due to the inability of the rigid pendulum model to compress along its length. Thus the reinitialization of  $\dot{a}$  is

$$\dot{a} = (l_{\text{old}} + r_c) \dot{a}_{\text{old}} * \text{COS}(a_{\text{new}} - a_{\text{old}}) / (l_{\text{new}} + r_c) \quad (20)$$

The output states,  $X_h$ ,  $Y_h$ ,  $\dot{X}_h$ , and  $\dot{Y}_h$  are

$$X_h = -(l + r_c) * \text{SIN}(a) + \text{COP} \quad (21)$$

$$Y_h = (l + r_c) * \text{COS}(a) \quad (22)$$



$$\dot{X}_h = -(1+rc) \cdot \dot{a} \cdot \cos(a) \quad (23)$$

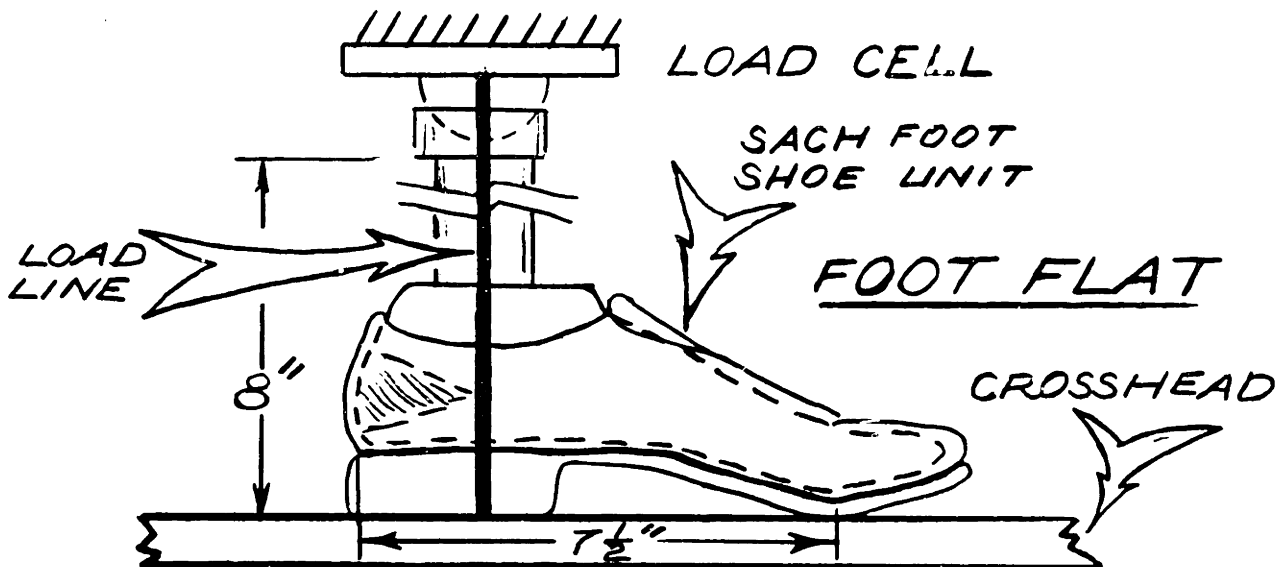
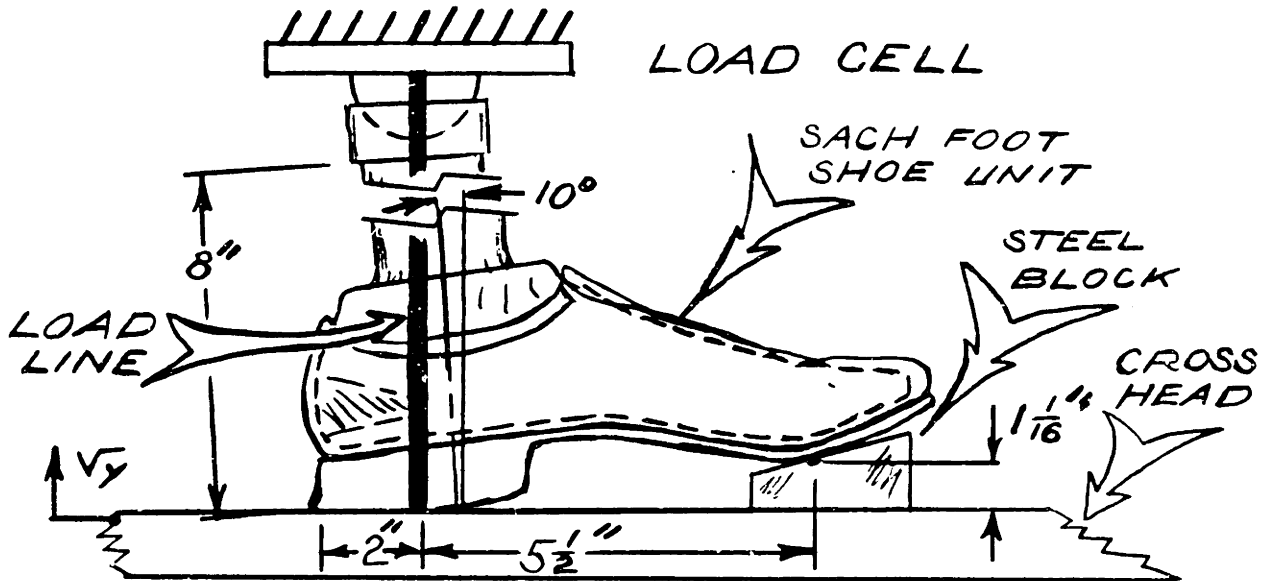
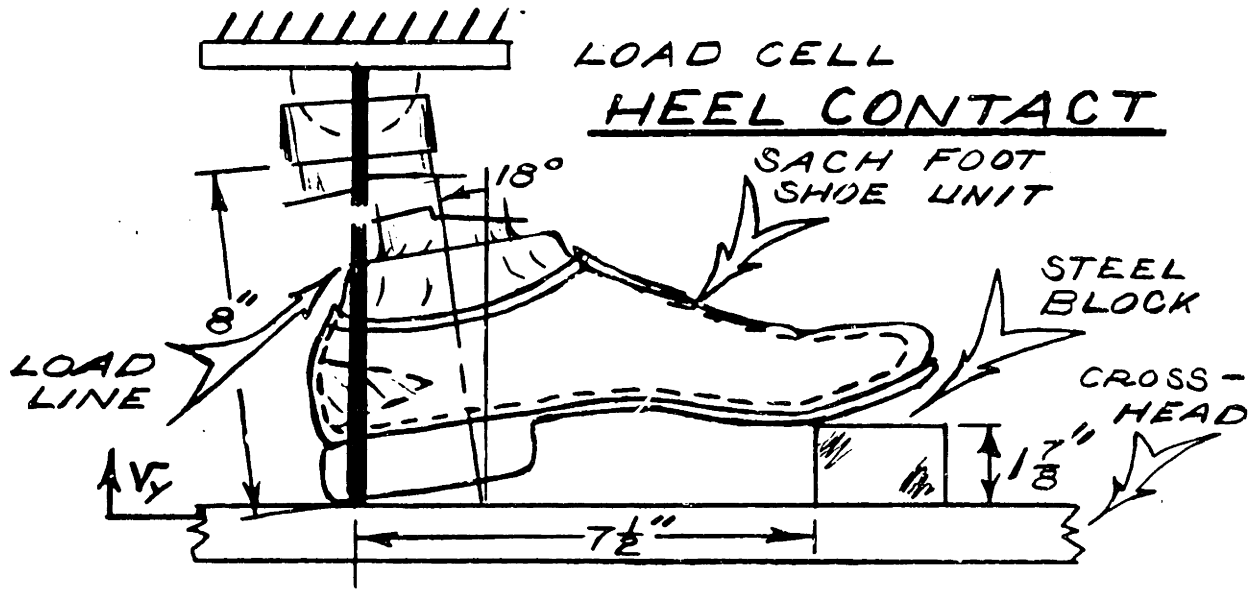
$$\dot{Y}_h = -(1+rc) \cdot \dot{a} \cdot \sin(a) \quad (24)$$

## APPENDIX 2 - SACH HEEL STIFFNESS TESTING

An Otto Bock, Pedilan, Size 11, SACH foot with soft heel was tested on an Instron testing machine. The SACH foot was inside a hard soled shoe. The SACH foot was nine months old but only had 24 hours of use. The test was made with the shoe at three different angles with a vertical load being applied through a ball and socket joint so no moment would be applied to the Instron's load cell. The angles of the foot were roughly set so that the vertical load would go through the back edge of the heel, mid-heel, and the front edge of the heel. The final angle was simply the foot in foot flat (see Figure A-2.1). The foot was loaded at a quasi-static rate of .03 inches/minute. The maximum load applied exceeded the peak dynamic load the foot would see at those three angles. This was determined by plotting vertical reaction force versus shank angle. The results are that the heel stiffness is linear at each angle up to the maximum load applied, but the value for the stiffness changes with angle (see Table A-2.1).

Table A-2.1 Heel Stiffness Values as a Function of Shank Angle

Shank Angle [deg] BTDC	Stiffness [nt/m] (lbf/in)
18	24,000 (140)
10	43,000 (250)
Foot flat	157,000 (900)



SACH FOOT HEEL STIFFNESS TESTING  
FIGURE A-2.1

An exponential function relating stiffness, K, to shank angle, S, can be fit to the three points in Table A-2.1. The function is of the form

$$K=K_0 * e^{-\frac{S}{b}}$$

where  $K_0$  is a free scaling parameter

S is the shank angle

b is the "decay" constant

At foot flat  $S=0$ , therefore

$$K_0=157,000 \text{ newton/meter}$$

with one parameter remaining, b, and two points remaining; it is arbitrary which is used. Using  $S=10$  degrees the the value of b is

$$b=7.7 \text{ degrees or } .13 \text{ radians.}$$

APPENDIX - 3 INVERSE DYNAMIC MODEL PARAMETERS

PARAMETERS FROM THE BODY (Winter [115])

5.6 MASS1, MASS OF SHANK INCLUDING FOOT [KG]

6.3 MASS2, MASS OF THIGH [KG]

61.4 MASS3, MASS OF TOTAL BODY - PROSTHETIC LEG [KG]

INERT1(3), INERTIA OF SHANK W/ FOOT [KG-M\*\*2]

.12 Ixx

.001 Iyy

.12 Izz

INERT2(3), INERTIA OF THIGH (INC. SOCKET AND TURNTABLE)

.076 Ixx

.015 Iyy

.076 Izz

GEOMETRY PARAMETERS FOR SHANK AND THIGH FOR PROGRAM FORTOR.FTN

VECTOR FROM CG OF SHANK TO KNEE AXIS IN METERS

0. X COMPONENT

.25 Y COMPONENT

0. Z COMPONENT

VECTOR FROM CG OF THIGH TO HIP AXIS IN METERS

0. X COMPONENT

.191 Y COMPONENT

0. Z COMPONENT

VECTOR FROM CG OF THIGH TO KNEE AXIS IN METERS

0. X COMPONENT

-.191 Y COMPONENT

0. Z COMPONENT

VECTOR FORM FROM ORIGIN OF BCS1 (array segment origin)

TO C.G. OF SHANK IN METERS

0. X COMPONENT

.09 Y COMPONENT

.041 Z COMPONENT

#### APPENDIX 4 - LED ARRAY

The rigid LED array was machined out of a Plexiglas sheet to the dimensions shown in Figure A-4.1.

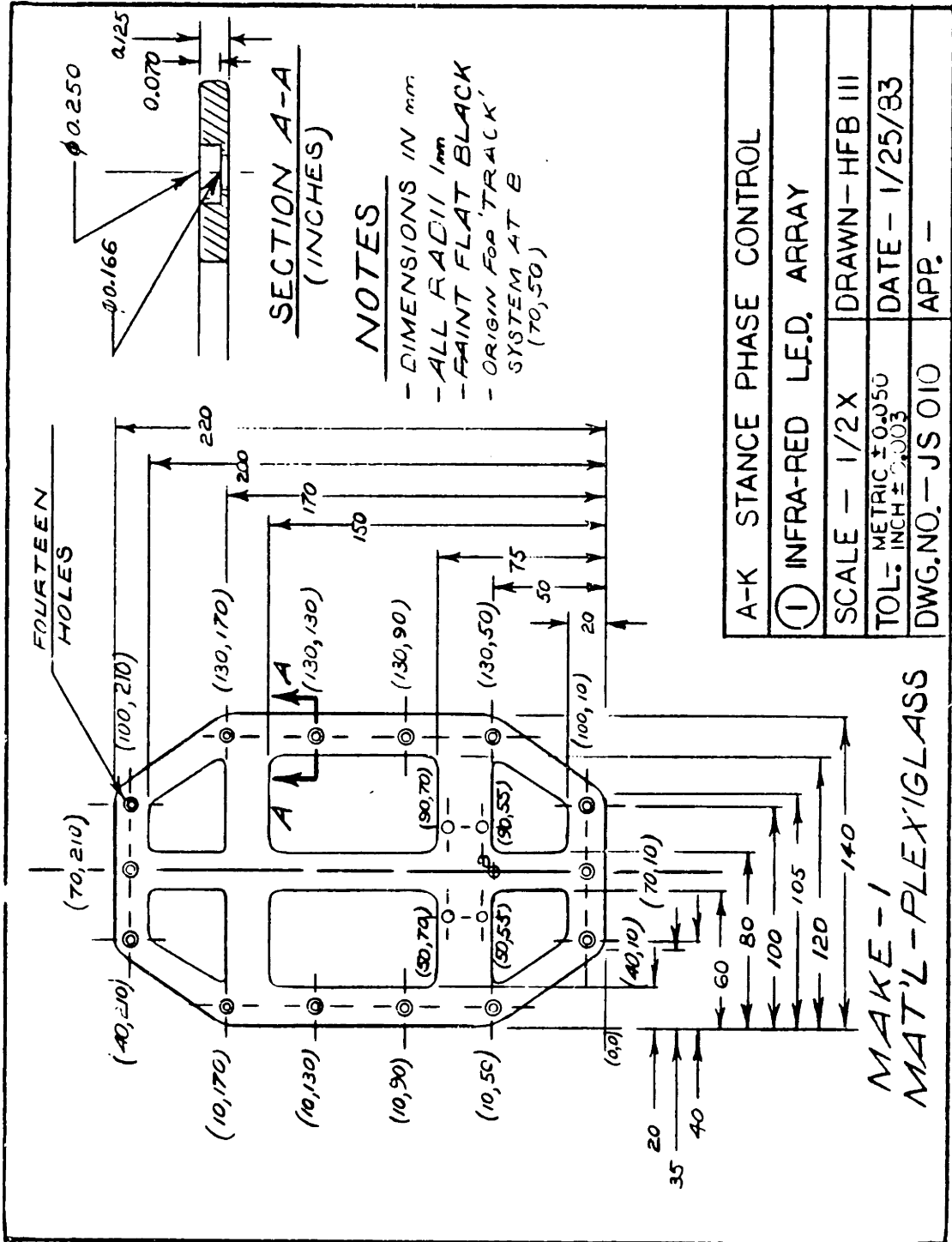


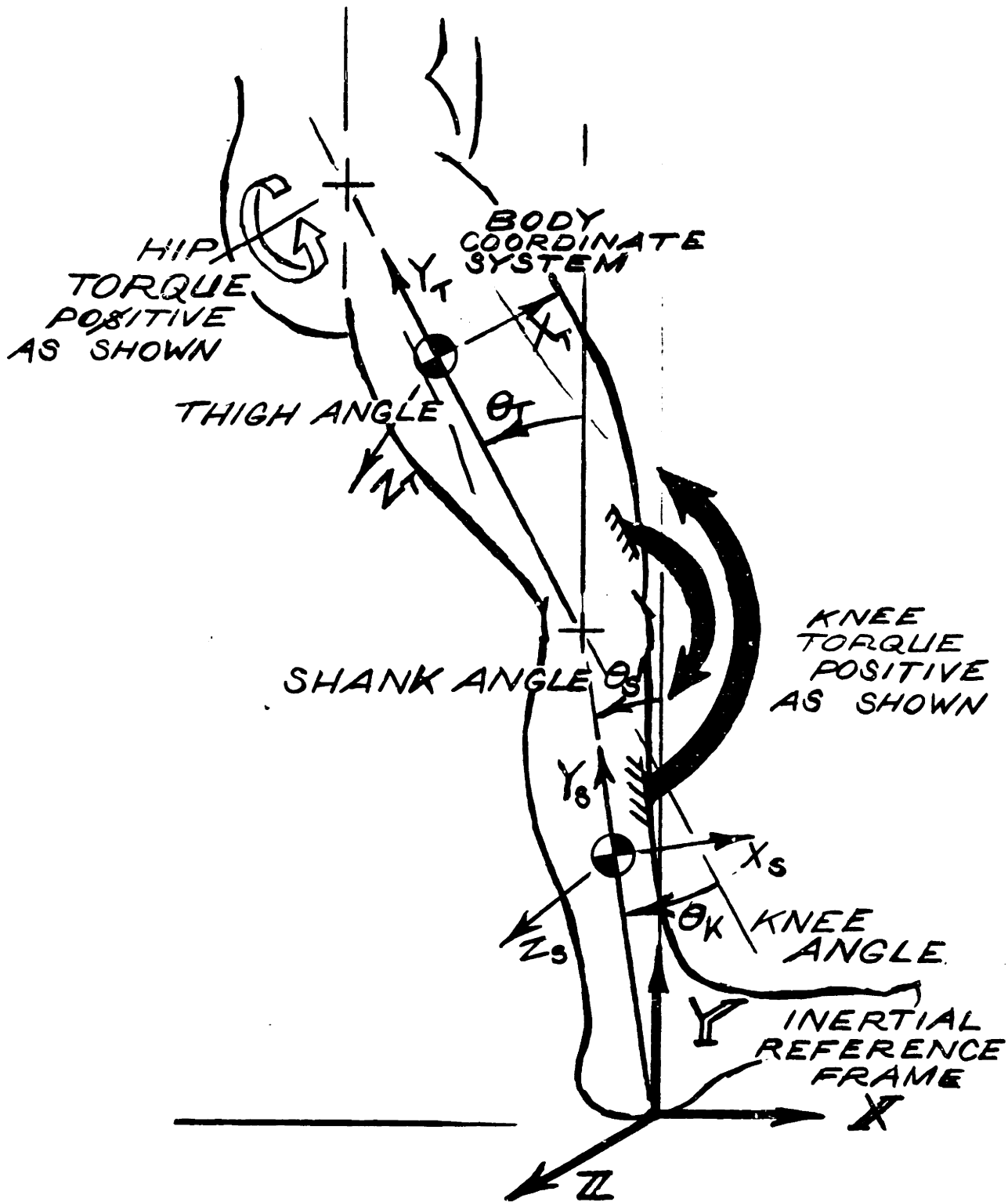
FIGURE A-4.1

Infra-Red LED Array



## APPENDIX 5 - SIGN CONVENTION

The sign convention shown in Figure A-5.1 was used for the inverse dynamic model and the designer gait models.



**SIGN CONVENTION**  
FIGURE A-5.1

APPENDIX 6 - DATA FILE NOMENCLATURE

All the data of the locomotion trials (runs) presented in this thesis are stored under the following filename format. Each filename is six characters long. The first four characters are the month and day of the run. The last digits represents the actual data run on that day. The fifth digit is an internal processing number. For example, filename JL1427 is the seventh run during which data was collected on July 14. JL1020 is the 10th run on July 10.

Run or Filename	Stance Phase Controller Type
JE1921	CL
JE2624	CL
JL1020	ME
JL1427	ME
JL1429	ME
JL1494	CL
JL2009	ME
JL2022	CL
JL2024	ME
AG0301	CL
AG0304	ME
AG0328	ME

APPENDIX 7 - DATA ACQUISITION AND PROCESSING PARAMETERS

EXPERIMENTAL TRACK PARAMETERS:

SAMPLING PARAMETERS:

Sampling frequency= 157.50  
Total number of frames = 236: 1.50 seconds of data  
Segment file name = STEIN1: 14 channels, 1 segments

Camera positions:	X	Y	Z [Meters]	AX	AY	AZ [Degrees]
Camera 1	0.000	0.000	0.000	0.000	-26.000	0.000
Camera 2	3.353	0.000	0.000	0.000	26.000	0.000

Camera calibration factors: Camera 1 Camera 2  
Focal distance (SU) 2315.16 2295.02

PROCESSING PARAMETERS:

Forceplate scale factors: X Y Z [Newtons/Volt]  
2.00E+01 1.00E+02 1.00E+01

Skew ray max error= 10 [Selspot Units], Errmax= 5.00 %

Data Smoothing: Interpolation Low-pass (Stein) Filter

Raw Selspot None None

3-D Selspot None None

BCS Selspot Yes 5.0 Hz Cutoff

Derivative None Available None

Forceplate None Available 20.0 Hz Cutoff (no filtering on  
vertical reaction force and center of pressure movement in X and Z  
directions)

Global axes origin: ( 1.695,-0.617, 3.466) [meters]

Approximate data processing time: 2[min] 21[sec]

Filtering of the transducers from the prosthesis simulator is done by  
the program FLTAUT which is presented in Appendix 8.

APPENDIX 8 - LOW PASS (STEIN) FILTER PROGRAM LISTING

CC

C  
C PROGRAM FLTAUT FLTAUT.FTN

C BY  
C JEFFREY L. STEIN  
C 22-JUL-82  
C 11-AUG-82  
C 01-SEP-82  
C 27-OCT-82

CC

C This program will read a user selected file of standard form and  
C filter all the rows of that file. The cutoff frequency for each row  
C of the file is user selectable. The default values listed for .SID  
C files are the filter cutoff frequencies used for the data coming  
C from the prosthesis simulator.

CC

C  
C DIMENSION PARAM(20),ISPECS(10),DATA(15,300),  
C 1DATAI(300),DATAO(300),ZA(4),FLT(15),IFLTRW(15),ITE(30)  
C DIMENSION A(10),B(10),C(10),GRAF(2,10),CF(10)  
C LOGICAL\*1 COMENT(80),NAMFIL(18),ROWNAM(10,20)  
C DATA LU,LU1,LU2,LR,LW/9,10,11,5,5/  
C DATA NS,ILOCK/3,0/  
C DATA DATAI,DATAO/600\*0./

C  
C DEFAULT FILTER VALUES FOR THE THE FIRST 15 ROWS OF THE DATA FILE

C  
C DATA IFLTRW/1,2,3,4,5,6,7,8,9,10,11,12,13,14,15/  
C DATA FLT/0.,10.,5.,5.,10.,10.,10.,0.,0.,0.,10.,7.,10.,7.,0./

C  
C WRITE(LW,1003)  
1003 FORMAT(/1X,'Double pass 3rd order linear filter')

C  
C 2 CONTINUE

C  
C GET THE FILE NAME

C  
105 FORMAT(A)  
CALL STRING('SK1:XXX000.111;0',NAMFIL)  
WRITE(LW,10)7  
10 FORMAT(/1X,'Enter >9< char file name to be filtered'/1X,  
1'SK1:\*\*\*\*\*.\*\*\*',/,'\$SK1:',A,\$)  
READ(LR,20)(NAMFIL(I),I=5,14)  
20 FORMAT(10A)

C  
C IF THE FILE IS A EXT EXTENSION THEN CHANGE THE DEFAULT FILTERING

C IF THE FILE IS A .PWR EXTENSION THEN CHANGE THE DEFAULT FLTERING.  
C IF THE FILE IS A .SID EXTENSION THEN CHANGE THE DEFAULT FILTERING.

C  
IF(NAMFIL(12).EQ.'E'.OR.NAMFIL(12).EQ.'e')GO TO 23

23 GO TO 26  
CONTINUE  
FLT(1)=0.  
FLT(2)=0.  
FLT(3)=0.  
FLT(4)=5.  
FLT(5)=5.  
FLT(6)=5.  
FLT(7)=5.  
FLT(8)=5.  
FLT(9)=5.  
FLT(10)=0.  
FLT(11)=5.  
FLT(12)=5.  
FLT(13)=0.  
FLT(14)=0.  
FLT(15)=5.

C  
GO TO 24  
26 CONTINUE

C  
C CHECK FOR .PWR FILES  
C

IF(NAMFIL(12).EQ.'P'.OR.NAMFIL(12).EQ.'p')GO TO 25  
GO TO 28

C  
25 CONTINUE  
FLT(1)=0.  
FLT(2)=10.  
FLT(3)=10.  
FLT(4)=10.  
FLT(5)=10.  
FLT(6)=5.  
FLT(7)=5.  
FLT(8)=10.  
FLT(9)=10.  
FLT(10)=0.  
FLT(11)=20.  
FLT(12)=5.  
FLT(13)=0.  
FLT(14)=0.  
FLT(15)=0.

C  
C CHECK FOR .SID FILES (files from the simulator system used in the  
C inverse dynamic model)

C  
28 CONTINUE  
IF(NAMFIL(12).EQ.'S'.OR.NAMFIL(12).EQ.'s')GO TO 27  
GO TO 24

```
27      CONTINUE
        FLT(1)=0.
        FLT(2)=10.
        FLT(3)=5.
        FLT(4)=5.
        FLT(5)=0.
        FLT(6)=5.
        FLT(7)=5.
        FLT(8)=0.
        FLT(9)=20.
        FLT(10)=0.
        FLT(11)=5.
        FLT(12)=5.
        FLT(13)=5.
        FLT(14)=0.
        FLT(15)=0.
C
C 24      CONTINUE
C
C GET THE DATA FROM THE FILE- SUPPLY NAME AND LU ONLY SUB RETURNS
C ISPECS,DATA,PARAM,COMENT
C
C      CALL RXFILE(NAMFIL,ISPECS,PARAM,CF,ROWNAM,COMENT,DATA,LU)
C
C      NPTS=ISPECS(3)
C      NROW=ISPECS(4)
C      NCOL=ISPECS(5)
C      NPARAM=ISPECS(6)
C
C
C PRINT FILE NAME
C
C      WRITE(LW,106)(NAMFIL(I),I=1,17)
106     FORMAT(/1X,17A)
C
C PRINT FILE SPECS
C
C      WRITE(LW,110)ISPECS
110     FORMAT(/1X,'FILE SPECIFICATIONS ARE',/1X,10I4)
C
C PRINT OUT COMMENT
C
C      WRITE(LW,15)(COMENT(J),J=1,40)
15      FORMAT(/1X,40A)
C
C PRINT OUT PARAMETER VALUES
C
C      WRITE(LW,220)(PARAM(J),J=1,NPARAM)
220     FORMAT(/1X,'THE PARAMETERS ARE',20(/1X,G10.4))
C
C SINCE PARAM(5-20) ARE TO BE USED TO INDICATE FILTERING ZERO
C OUT OLD VALUES IN PARAM
C
```

```
DO 237 I=5,20
PARAM(I)=0.
237 CONTINUE
C
1 CONTINUE
C
C PRINT OUT NAMES OF DATA ROWS
C
IF(NAMFIL(12).EQ.'S')GO TO 150
GO TO 200
150 CONTINUE
C
WRITE(LW,251)
251 FORMAT(/1X,'Row order is.....',/1X,
1' 1= TIME',/1X,' 2= ACL',/1X,' 3= SPOS',/1X,' 4= SVEL',/1X,
2' 5= SFSW',/1X,' 6= PPOS',/1X,' 7= PVEL',/1X,' 8= PFSW',/1X,
3' 9= ACTUATOR TORQUE',/1X,'10= STOCNTRL',/1X,
4'11= PROS. ACCELERATION',/1X,'12= CALC. PROS. VEL',/1X,
5'13= CALC. PROS. ACCELERATION')
C
GO TO 201
200 CONTINUE
C
CALL PRTROW(ROWNAM,NROW)
201 CONTINUE
C
C DISPLAY ROWS AND CUTOFF FREQUENCIES
C
WRITE(LW,300)IFLTRW,FLT,7
300 FORMAT(/1X,'The default filtering is....',/1X,
1' ROW =',15I4,/1X,
1'CUTOFF FREQ (Hz) =',1X,15F4.0,/,
3'$Do you want to change it? [Y/N]:',$,A)
C
READ(LR,105)IANS
IF(IANS.NE.'Y'.AND.IANS.NE.'y')go to 350
307 CONTINUE
WRITE(LW,301)7
301 FORMAT(/1X,'Enter row #i,FREQ (Hz),ROW #j,FREQ,...etc',
1/1X,'Enter as integers!!',
2/,'$ROW#=#,FREQ Hz=',$,A)
READ(LR,302)ITE
302 FORMAT(30I)
C
C DETERMINE # OF ROWS THAT WERE REQUESTED TO BE CHANGED
C
ILOCK=0
DO 303 I=1,29
IF(ITE(I).EQ.0.AND.ITE(I+1).EQ.0.AND.ILOCK.EQ.0)GO TO 304
GO TO 303
304 CONTINUE
NFLT=I/2
ILOCK=1
```



```
303 CONTINUE
C
  II=-1
  DO 305 I=1,NFLT
    II=II+2
305 FLT(ITE(II))=FLOAT(ITE(II+1))
C
  WRITE(LW,306)IFLTRW,FLT,7
306 FORMAT(/1X,'The NEW filtering is....',/1X,
1'      ROW =',15I4,/1X,
1'CUTOFF FREQ (Hz) =',1X,15F4.0,/,
3'$Do you want to change it? [Y/N]:',$,A)
C
  READ(LR,105)IANS
  IF(IANS.EQ.'Y'.OR.IANS.EQ.'y')GO TO 307
350 CONTINUE
C
  ISTART=1
  ISTOP=NPTS
  FREQ=PARAM(2)
  PERIOD=1./FREQ
C
C PUT DATA INTO INPUT VECTOR
C
  DO 414 IROW=1,NROW
C
C SKIP FILTERING IF CUTOFF LESS THAN .1
C
  IF(FLT(IROW).LT..1)GO TO 414
C
  DO 415 J=1,NPTS
  DATAI(J)=DATA(IROW,J)
415 CONTINUE
C
  TW=.1
  Z=.8
  CUTOFF=FLT(IROW)
  CALL LPDES1(CUTOFF,ZA,TW,Z)
  CALL FIDFDP(DATAI,DATAO,ZA,PERIOD,NPTS)
C
C WRITE OUT FILE
C
  DO 420 J=1,NPTS
  DATA(IROW,J)=DATAO(J)
420 CONTINUE
C
C PUT CUTOFF FREQUENCY FOR ROWS 1-15
C
  PARAM(5+IROW)=CUTOFF
C
414 CONTINUE
C
```

```

WRITE(LW,416)7
416  FORMAT(/,'$Do you wish to RE-filter the same data? [Y/N]:',$,A)
      READ(LR,105)IANS
      IF(IANS.NE.'Y')GO TO 500
      GO TO 1
500  CONTINUE
      CALL STRING('FILTERED DATA',COMENT(41))

```

```

C
C  CHANGE # OF PARAMETER TO 20
C
      ISPECS(6)=20

```

```

C
C  OPTIONAL FILE NAME
C

```

```

WRITE(LW,418)NAMFIL,7
418  FORMAT(/1X,'The filtered file name is...',18A,/,
1'$Do you wish to CHANGE it. [Y/N]?',$,A)
      READ(LR,105)IANS
      IF(IANS.NE.'Y')GO TO 423
      WRITE(LW,422)7
422  FORMAT(/1X,'Enter new file name',/1x,'SK1:*****.***',/,
1'$SK1:',$,A)
      READ(LR,424)(NAMFIL(I),I=5,14)
424  FORMAT(10A)
423  CONTINUE
      CALL WXFILE(NAMFIL,ISPECS,PARAM,CF,ROWNAM,COMENT,DATA,LU)

```

```

C
      WRITE(LW,417)7
417  FORMAT(/,'$Do you wish to filter another FILE. [Y/N]?',$,A)
      READ(LR,105)IANS
      IF(IANS.EQ.'Y')GO TO 2

```

```

C
      STOP
      END

```

CC

```

C
C
C  PROGRAM LPDES1                LPDES1.FTN
C
C  BY
C
C  JEFFREY L. STEIN
C
C  25-AUG-82

```

CC

```

C
C
C  THIS SUBROUTINE WILL CALCULATE THE COEFFICIENTS OF THE FOLLOWING FILTER
C  EQUATION
C
C          A3*YDDDOT+A2*YDDOT+A1*YDOT+A0=X
C
C  WHERE Y IS THE FILTERED OUTPUT

```

```

C           X IS THE INFILTRATED INPUT
C
CCCCCCCCCCCCCCCCCCCCCCCCCCCCCCCCCCCCCCCCCCCCCCCCCCCCCCCCCCCCCCCC
C
C           AO IS SET =1.
C
C           INPUTS TO THE SUB ARE
C
C               DESIRED CUTOFF FREQUENCY
C               TAU*WC SEE MEYFARTH 1958 MEMORANDUM FROM LSDC
C               ZETA   DAMPING, SEE "   "   "   "
C
C           OUTPUTS ARE
C               THE COEFFICIENTS A1,A2,A3 IN ARRAY A
C               WHERE A(1)=A1 ETC
C
CCCCCCCCCCCCCCCCCCCCCCCCCCCCCCCCCCCCCCCCCCCCCCCCCCCCCCCCCCCCCCCC
C

```

```

SUBROUTINE LPDES1(WC,A,TW,Z)
DIMENSION A(1)
WR=WC*2.*3.141592
AO=1.
A(1)=(TW+2.*Z)*(1./WR)
A(2)=(2.*Z*TW+1.)*(1./WR)**2
A(3)=TW*(1./WR)**3

```

```

C
C           RETURN
C           END
CCCCCCCCCCCCCCCCCCCCCCCCCCCCCCCCCCCCCCCCCCCCCCCCCCCCCCCCCCCCCCCC
C

```

```

C           PROGRAM FIDFDP           FIDFDP.FTN
C
C           BY
C
C           JEFFREY L. STEIN
C

```

```

CCCCCCCCCCCCCCCCCCCCCCCCCCCCCCCCCCCCCCCCCCCCCCCCCCCCCCCCCCCCCCCC
C

```

```

C           THIS IS A FINITE DIFFERENCE APPROXIMATION OF THE FOLLOWING DIFFERENTIAL
C           EQUATION

```

$$A3*YDDDOT+A2*YDDOT+A1*YDOT=X$$

```

C           WHERE THE COEFFICIENTS MUST BE PREVIOUSLY CALCULATE BY USING
C           SUBROUTINE LPDES1.FTN
C

```

```

C           THE DATA IS FILTERED IN TWO DIRECTIONS
C

```

```

CCCCCCCCCCCCCCCCCCCCCCCCCCCCCCCCCCCCCCCCCCCCCCCCCCCCCCCCCCCCCCCC
C

```

```

C           INPUTS ARE
C               DATAI -INPUT DATA ARRAY
C               DT -TIME STEP USED IN COLLECTING DATA
C               A AN ARRAY WITH COEFFICIENTS
C

```

```
C           A(1)=A1
C           ETC
C           NPTS - THE NUMBER OF POINTS IN THE INPUT DATA ARRAY
C
C           OUTPUT IS
C           DATAO -OUPUT DATA ARRAY
C
CCCCCCCCCCCCCCCCCCCCCCCCCCCCCCCCCCCCCCCCCCCCCCCCCCCCCCCCCCCC
C
C           SUBROUTINE FIDFDP(DATAI,DATAO,A,DT,NPTS)
C
C           DIMENSION A(1),DATAI(1),DATAO(1),Y(4)
C
C           INITIALIZE THE Y VECTOR
C
C           Y(4)=CURRENT FILTERED OUTPUT
C           Y(3)=PREVIOUS " "
C           Y(2)=2ND PREVIOUS " "
C           Y(1)=3RD " " "
C
C           DO 10 I=1,4
10          Y(I)=DATAI(1)
C
C           DEFINE SOME COEFFICIENTS
C
C           B3=A(3)/(DT**3)
C           B2=A(2)/(DT**2)
C           B1=A(1)/DT
C           AA=B3+B2+B1+1.
C
C           FILTER EQUATION IN FINITE DIFFERENCE FORM
C
C           DO 20 N=1,NPTS
C
C           Y(4)=(DATAI(N)
1            +B3*(3.*Y(3)-3.*Y(2)+Y(1))
2            +B2*(2.*Y(3)-Y(2))
3            +B1*Y(3))
4            /AA
C
C           SWAPP VALUE IN Y
C           Y(3) GET THE VALUE IN Y(4)
C
C           DO 30 J=1,3
30          Y(J)=Y(J+1)
C
C           PUT FIRST PASS OUTPUT IN Y(4) IN DATA INPUT ARRAY
C
C           DATAI(N)=Y(4)
C
C           CONTINUE
20
C
C
```

```
C SECOND PASS
C
C REINITIALIZE THE OUTPUT ARRAY FOR THE FIRST THREE POINTS
C
      DO 40 I=1,3
40    Y(I)=DATAI(NPTS)
C
C RUN FILTER AGAIN WITH DATA IN REVERSE DIRECTION
C
      DO 50 N=NPTS,1,-1
      Y(4)=(DATAI(N)
1      +B3*(3.*Y(3)-3.*Y(2)+Y(1))
2      +B2*(2.*Y(3)-Y(2))
3      +B1*Y(3))
4      /AA
C
C SWAPP DATA
C
      DO 60 I=1,3
60    Y(I)=Y(I+1)
C
C ENTER OUTPUT INTO OUTPUT DATA ARRAY
C
      DATAO(N)=Y(4)
C
50    CONTINUE
C
      RETURN
      END
```

APPENDIX 9 - CONTROL AND DATA ACQUISITION PROGRAM LISTING

```

CCCCCCCCCCCCCCCCCCCCCCCCCCCCCCCCCCCCCCCCCCCCCCCCCCCCCCCCCCCCCCCC
C
C          PROGRAM STANCE          STANCE.FOR          C
C          BY          C
C          JEFFREY L. STEIN          C
C          24-JUN-82          C
C          C
CCCCCCCCCCCCCCCCCCCCCCCCCCCCCCCCCCCCCCCCCCCCCCCCCCCCCCCCCCCCCCCC
C This program provides for Modified Darling swing phase and
C and modified Grimes modified echo control for the stance phase.
C The basic control structure in the completion routine
C is taken from Don Grimes MTRANS.FOR program.
C This program thus controls only one locomotion mode
C which is level walking. Two functional modes are employed.
C They are the swing and stance phase. Checks for transitions to
C these functional modes are made at every interrupt. A
C supplementary mode for standing still is included. Standing still
C is defined as no functional mode change in one second (user
C selectable). If the
C amputee is in prosthetic swing no change is implemented. If the
C amputee is in prosthetic stance the prosthesis is commanded to
C extend to full extension at a slow rate.
C
C The swing phase is identical to SWING.FOR AND SWTRK.FOR programs.
C The stance phase is user selectable to be either conventional
C lockup as in SWING.FOR AND SWTRK.FOR or active modified echo
C control as in MTRANS.FOR.
C
C This program is a data collection program as well. A user
C selectable sampling period, (selected by the TRACK3 SYSTEM
C or by the hand held sampling connected to the simulator control
C box) writes data from the simulators transducers to a file
C selected by the user. A maximum of 300 points of data is
C allowed. At the default sampling frequency of 157.5 Hz that
C is slightly less than 2 seconds worth of data. The default
C sampling frequency comes from the TRACK3 SYSTEMS limited
C ability to pick an arbitrary sampling frequency. The
C simulator should be sampled above 120 Hz. for good stable
C performance.
C
C Data is read in to a direct access unformatted file while
C the completion routine is not being serviced. The file is
C of standard form (see NEWFILE.FOR). Some parameters and
C a user supplied comment and row names are written into the
C the file header.
C
C          THIS PROGRAM CONTROLS THE HYDRAULIC PROSTHESIS TO BEHAVE          C
C          IN A PURELY PASSIVE MODE. THE DAMPING TORQUE AT THE          C
C          KNEE AXIS IS APPROXIMATELY          C

```

```
C          TOR=B(ANGLE)XVEL.X VFL. C
C      IN THIS PROGRAM THERE ARE 4 DAMPING COEFFICIENTS. C
C      THE PROGRAM SELECTS A DAMPING COEFFICIENT BASED ON C
C      THE SIGN OF THE VELOCITY TERM (WHETHER FLEXIVE OR EXTENSIVE) C
C      AND THE KNEE ANGLE. C
C      IMPORTANT VARIABLES AND THEIR DEFAULT VALUE C
C      C
C      FREQ=SAMPLING FREQUENCY (157.5 HZ) C
C      BES =DAMPING FACTOR FOR THE END OF STANCE C
C          (SUGGESTED VALUE 0.000002) C
C      BMIN=MIN DAMPING OF SYSTEM. USED FOR TOE CLEARANCE AT THE C
C          THE BEGINNING OF SWING AND FOR SWING THROUGH IN C
C          IN MIDSWING. C
C          (SUGGESTED VALUE 0.0 ) C
C      BHR =DAMPING FACTOR TO CONTROL HEEL RISE C
C          (SUGGESTED VALUE 0.0001 ) C
C      BFE =DAMPING FACTOR FOR END OF SWING C
C          (SUGGESTED VALUE 0.0003 ) C
C      C
C      AES=ANGLE INDICATING THE BEGINNING OF THE END OF STANCE C
C          (SUGGESTED VALUE 1340 (0 DEG.) ) C
C      ATC=ANGLE INDICATING THE END OF STANCE (THE BEGINNING OF C
C          TOE CLEARANCE) C
C          (SUGGESTED VALUE 700 (35 DEG.)) C
C      AHR=ANGLE INDICATING THE BEGINNING OF HEEL RISE C
C          (SUGGESTED VALUE (70 DEG.)) C
C      AFE=ANGLE INDICATING THE BEGINNING OF FULL EXTENSION C
C          (SUGGESTED VALUE 1720 (15 DEG.)) C
C      C
C      FOR FLEXIVE VELOCITIES: C
C      IF(ATC>ANGLE>AES)THEN C
C      B=BES*(ATC - ANGLE) + BMIN C
C      IF(AHR>ANGLE>ATC)THEN C
C      B=BMIN C
C      IF(ANGLE>AHR)THEN C
C      B=BHR*(ANGLE-AHR) + BMIN C
C      FOR EXTENSIVE VELOCITIES: C
C      IF(ANGLE>AFE)THEN C
C      B=BMIN C
C      IF(ANGLE<AFE)THEN C
C      B=BFE*(AFE-ANGLE) + BMIN C
C      C
C      Some other important variables C
C      C
C      IECHO-Flag for active stance C
C          active stance=1 C
C          lockup stance=0 C
C      IFM-Functional mode indicator C
C          1=stance C
C          2=swing C
```

ISSPOS - Sound Leg storing indicator  
 0=not storing  
 2=storing

FOR THIS PROGRAM:

A/D CHANNEL	PARAMETER	IBUF
0	PROS. AXIAL LOAD CELL	1
1	SOUND POSITION	2
2	SOUND VELOCITY	3
3	SOUND FOOTSWITCH	4
4	PROSTHESIS POSITION	5
5	PROSTHESIS VELOCITY	6
6	PROSTHESIS FOOTSWITCH	7
7	PROSTHESIS TORQUE	8

DIGITAL OUTPUT 8 CONTROLS THE READY LED ON THE SAMPLE SWITCH  
 DIGITAL OUTPUT 9 IS CLEARED SO THE TORQUE LOOP IS CLOSED.  
 DIGITAL OUTPUT 10 CARRIES A SQUARE WAVE.

SWING SHOULD PROVIDE AN ADEQUATE (MODIFIED DARLING) SWING  
 PHASE CONTROL SCHEME FOR LEVEL WALKING.  
 DIGITAL OUTPUT 9 IS HIGH DURING SWING SO THE TORQUE  
 LOOP IS CLOSED.  
 DIGITAL OUTPUT 9 IS LOW DURING STANCE WHILE A POSITION  
 LOOP CONTROLS THE PROSTHESIS.  
 DIGITAL OUTPUT 10 CARRIES A SQUARE WAVE.

SERVO AMP INPUT-- LEG WILL EXTEND IF DA1 IS +

TORQUE SIGN

FLEXIVE = +

EXTENSIVE = -

PROSTHETIC ANGLE SIGN [RAW & CONVERTED]

FULL EXTENSION=0

INCREASING FLEXION = LARGER POS ANGLE

PROS VEL [RAW & CONVERTED]

FLEXIVE = +

EXTENSIVE = -

SOUND ANGLE SIGN [RAW]

FULL EXTENSION=0

INCREASING FLEXION = LARGER NEG ANGLE

SOUND ANGLE SIGN [CONVERTED]

NOTE: BECAUSE OF CLIBRATION FACTORS

SOUND ANGLE SIGN FOR SPOS IS

FLEXIVE = +

SOUND VEL [RAW]

FLEXIVE = -

EXTENSIVE = +







```

      CALL SCCA(ICTRLC)
C
C READ CALIBRATION FACTORS FOR POS AND VEL
C
      OPEN(UNIT=35,NAME='DLO:CALBRA.DAT',TYPE='OLD')
      READ(35,3)CF
3     FORMAT(10(G10.3,/))
      CLOSE(UNIT=35)
C CALIBRATION FACTORS
      ALCCF=CF(1)
      SPOSCF=CF(2)
      SVELCF=CF(3)
      PPOSCF=CF(5)
      PVELCF=CF(6)
C
C DEFAULT STANCE PHASE CONTROL PARAMETERS
C
      ERRMAX=1./STIFF
      ILEAD=IFIX(TMLEAD*FREQ)
      MINALC=IFIX((CNTRSH/(-CF(1)))*2047.)
      IFMSTP=IFIX(FMTIM*FREQ)
      ISSSTP=IFIX(SSTIM*FREQ)
      ISTOSP=IFIX(STOTIM*FREQ)
      INOSTP=IFIX(RNOSTM*FREQ)
      MAXSTP=IFIX(CADMIN*FREQ)
      MINSTP=IFIX(CADMAX*FREQ)
C
C DEFAULT SWING PHASE CONTROL PARAMETERS
C
      BES=.000002
      BMIN=0.
      BHR=.0001
      BFE=.0003
C
      AES=0.
      ATC=35.
      AHR=70.
      AFE=15.
C
C
      TYPE *, ' '
      TYPE *, '          Program ECHO/STANCE/SWING/TRACK'
      TYPE 110
110  FORMAT(//1X,'This program will control the leg to be a passive'
1, /1X,'swing phase unit with lockup in stance or an active '
1, /1X,'modified echo control in stance. Swing phase is a'
2, /1X,'modified darling swing phase controller. In addition'
3, /1X,'data will be stored in a user entered file after'
3, /1X,'sampling initiated by the track system or the'
4, /1X,'hand held switch has been completed.'
5, /1X, //, 1X, 'Remember to set offset on the

```

6posthetic and sound angles!!!')

C  
C PUT THE NAMES OF THE DATA (A/D CHANNELS) INTO NAM  
C SCOPY PUTS 9 CHARACTERS IN NAM(1,10) TO NAM(9,1)

C CALL SCOPY('FRAME # ',NAM(1,1),9)

C  
C NOW IT PUTS IN AT NAM(1,2) TO NAM(9,2)

C  
C CALL SCOPY('PROS LOAD',NAM(1,2),9)  
C CALL SCOPY('SOUND POS',NAM(1,3),9)  
C CALL SCOPY('SOUND VEL',NAM(1,4),9)  
C CALL SCOPY('SOUND FSW',NAM(1,5),9)  
C CALL SCOPY('PROS. POS',NAM(1,6),9)  
C CALL SCOPY('PROS. VEL',NAM(1,7),9)  
C CALL SCOPY('PROS. FSW',NAM(1,8),9)  
C CALL SCOPY('PROS. TOR',NAM(1,9),9)  
C CALL SCOPY('STO CNTRL',NAM(1,10),9)

C  
C PUT GENERAL FILE NAME INTO NAMFIL

C CALL SCOPY('RK1:NEWFILE.RAW',NAMFIL,14)

C  
C PUT IN PARAMETER NAMES MUST BE A MAX OF 9 CHARACTERS!

C  
C CALL SCOPY('# FRAMES ',PARNAM(1,1),9)  
C CALL SCOPY('SAMP FREQ',PARNAM(1,2),9)  
C CALL SCOPY('EOS DAMP ',PARNAM(1,3),9)  
C CALL SCOPY('TC+ST DAM',PARNAM(1,4),9)  
C CALL SCOPY('H.R. DAMP',PARNAM(1,5),9)  
C CALL SCOPY('FEXT DAMP',PARNAM(1,6),9)  
C CALL SCOPY('EOS ANGLE',PARNAM(1,7),9)  
C CALL SCOPY('TC ANGLE ',PARNAM(1,8),9)  
C CALL SCOPY('HR ANGLE ',PARNAM(1,9),9)  
C CALL SCOPY('FEXT ANGL ',PARNAM(1,10),9)

C  
C AUTOMATIC FILE NAMING

C  
WRITE(LW,616)7  
616 FORMAT(/,'\$Do you want automatic file naming? (Y/N)',\$,A)  
READ(LR,617)IANS  
617 FORMAT(A1)  
IF(IANS.NE.'Y')GO TO 618  
IAUTO=1  
WRITE(LW,619)7  
619 FORMAT(/1x,'Enter a 4 character date in the following form',/1x,  
1'MonthDay',A,\$)  
READ(LR,621)(NAMFIL(I),I=5,8)  
621 FORMAT(4A1)  
618 CONTINUE

C

```

C*****
C
C LOOP POINT! ALL STATEMENT ABOVE ARE ONLY EXECUTED ONCE!
C
C*****
C
2      CONTINUE
      ILAG=0
      IFM=2
      IECHO=0
      ISTND=0
      INOST=0
      IOALC=0
      ICNT=0
      Istor=1

C
C SET DIGITAL OUTPUT REGISTER TO ZERO
C
C      CALL LDO(0)
C
C TURN OFF THE READY LED ON THE SAMPLE SWITCH
C
C      CALL BITSET(8)
C
C READ DIGITAL OUTPUT REGISTER AND DISPLAY THE 9TH BIT IN THE FRONT
C PANEL LED 'S
C
C      CALL RDOBIT(IX,9)
C      CALL LEDSP(IX)
C
C      JKL=0
C      ICMF1=0
C      INTCT=1

C
C INITIALIZE IBUF
C
C      DO 10 I=1,8
C          IBUF(I)=2048
10     CONTINUE
C
C RUN NUMBER MANIPULATION
C      NEXT=NRUN+1
C
C      WRITE(LW,957)NEXT,7
957    FORMAT(/,'$The next run will be run #',I2,1X,
1' . Do you want to alter it? (Y/N)',$,A)
      READ(LR,958)IANS
958    FORMAT(A)
      IF(ICTRLC.NE.0)STOP 'VIA DOUBLE CONTROL/C'
      IF(IANS.NE.'Y')GO TO 959
      WRITE(LW,961)7

```

```

-202-
961  FORMAT(/1X,'ENTER A NUMBER FOR THE NEXT RUN',/,'$RUN #=',$,A)
      ACCEPT *,NEXT
      NRUN=NEXT-1
      IF(ICTRLC.NE.0)STOP 'VIA DOUBLE CONTROL/C'
959  CONTINUE
C
C  WRITE OUT CALIBRATION FACTORS
C
      WRITE(LW,614)(CF(I),I=1,8)
614  FORMAT(/1X,'Calibration factors for the control loops are
      1...'//1X,
      2'Axial load cell = ',F8.3,' [Newtons/volt]'/,1X,
      3'Sound position = ',F8.3,' [Degrees/volt]'/,1X,
      4'Sound velocity = ',F8.3,' [Radians/sec/volt]'/,1X,
      5'Sound foot switch= ',F8.3,' [Unitless]'/,1X,
      6'Pros. position = ',F8.3,' [Degrees/volt]'/,1X,
      7'Pros. velocity = ',F8.3,' [Radians/sec/volt]'/,1X,
      8'Pros. foot switch= ',F8.3,' [Unitless]'/,1X,
      9'Pros. torque = ',F8.3,' [Newton-meter/volt]')
C
C  SET SAMPLING FREQUENCY
C
      WRITE(LW,941)FREQ,7
941  FORMAT(/,
      1'$Do you want to change the current sampling freq of'
      2,1X,F5.1,'Hz? (Y/N)',A,$)
      ACCEPT 13,IANS
13   FORMAT(A2)
      IF(ICTRLC.NE.0)STOP 'VIA DOUBLE CONTROL/C'
      IF(IANS.EQ.'Y')GO TO 213
      GO TO 114
213  CONTINUE
      WRITE(LW,942)7
942  FORMAT(/,'$Enter sampling frequency...' ,A,$)
      ACCEPT *,FREQ
114  CONTINUE
C
C  SELECT STANCE PHASE CONTROLLER
C
      WRITE(LW,800)7
800  FORMAT(/,'$Do you want active echo control in stance phase?
      1[Y/N]:' ,$,A)
      READ(LR,801)IANS
801  FORMAT(A)
      IF(ICTRLC.NE.0)STOP 'VIA DOUBLE CONTROL/C'
      IF(IANS.EQ.'Y')IECHO=1
      IF(IANS.NE.'Y')IECHO=0
      IF(IECHO.NE.1)GO TO 850
      WRITE(LW,945)7
945  FORMAT(/,'$Do you want to adjust any of the stance phase control
      1 parameters? [Y/N]:' ,$,A)

```

READ(LR,958)IANS  
IF(ICTRLC.NE.0)STOP 'VIA DOUBLE CONTROL/C'  
IF(IANS.NE.'Y')GO TO 850

C  
C WRITE OUT MENU

C  
821 CONTINUE  
WRITE(LW,803)STIFF,TMLEAD,CNTRSH,ANGTOL,FMTIM,SSTIM,STOTIM,  
1RNOSTM,CADMIN,CADMAX,MAXSIG,7  
803 FORMAT(/1X,'STANCE PHASE CONTROL PARAMETERS',  
1/1X,'Enter parameter # of the parameter to be changed',  
2//1X,'Param #',2X,'Present Value',2X,'Description',  
3/1X,' <CR>',T25,'No [more] changes',  
4/1X,' 1',T11,F10.4,T25,  
6 'Position loop resp. faster=larger',  
5/1X,' 2',T11,F10.4,T25,  
6 'Lead in secs of the stored pos. traj.',  
6/1X,' 3',T11,F10.4,T25,  
6 'Contact threshold of ALC in Newtons',  
7/1X,' 4',T11,F10.4,T25,  
6 'Amount sound angle allowed to change/sample [deg]',  
8/1X,' 5',T11,F10.4,T25,  
6 'Time [sec] between functional mode changes',  
9/1X,' 6',T11,F10.4,T25,  
6 'Time [sec] to STAND STILL MODE',  
1/1X,' 7',T11,F10.4,T25,  
6 'Time [sec] minimum sound position storing time',  
2/1X,' 8',T11,F10.4,T25,  
6 'Time [sec] to wait before start storing again',  
3/1X,' 9',T11,F10.4,T25,  
6 'Time [sec] minimum cadence, pros. heel to pros. heel',  
4/1X,' 10',T11,F10.4,T25,  
6 'Time [sec] maximum cadence, pros. heel to pros. heel',  
5/1X,' 11',T11,I10,T25,  
6 'Max signal allowed to servo amp',  
6/1X,' 12',T25,'Return all values to their default values',  
6//'\$PARAMETER #=',\$,A)

C  
READ(LR,804)IPARCG  
804 FORMAT(I)  
IF(IPARCG.EQ.0)GO TO 850

C  
C GO TO PARAMETER THAT NEEDS CHANGING

C  
GO TO(811,812,813,814,815,816,817,818,819,820,822,823)IPARCG  
811 CONTINUE  
WRITE(LW,831)7  
831 FORMAT(/1X,'Enter the new stiffness factor. [fp]',/,  
1'\$STIFFNES=',\$,A)  
READ(LR,841)STIFF  
841 FORMAT(F10.3)

ERRMAX=1./STIFF  
GO TO 821

C  
812 CONTINUE  
WRITE(LW,832)7  
832 FORMAT(/1X,'Enter the new TIME LEAD FACTOR in seconds',/,  
1'\$LEAD TIME=',\$,A)  
READ(LR,841)TMLEAD  
ILEAD=IFIX(TMLEAD\*FREQ)  
GO TO 821

C  
813 CONTINUE  
WRITE(LW,833)7  
833 FORMAT(/1X,'Enter the new threshold contact force in Newtons'  
1./,'\$FORCE=',\$,A)  
READ(LR,841)CNTRSH

C  
C NOTE: -CF(1)\*2 REPRESENTS THE MAXIMUM FORCE. REMEMBER THAT ALC IS  
C OFFSET. THUS 0 NEWTONS =-1 VOLT = UNITS, WHILE MAX FORCE = +1  
C VOLTS = 4095 UNITS.  
C NOTE: CALIBRATION FACTOR IS NEGATIVE SO THE SIGN IS CHANGED FOR THIS  
C PROGRAM

C  
MINALC=IFIX((CNTRSH/(-CF(1)))\*2047.)  
GO TO 821

C  
814 CONTINUE  
WRITE(LW,834)7  
834 FORMAT(/1X,'Enter the new ANGLE tolerance in Degrees.',/,  
1'\$ANGLE=',\$,A)  
READ(LR,841)ANGTOL  
GO TO 821

C  
815 CONTINUE  
WRITE(LW,835)7  
835 FORMAT(/1X,'Enter the Function mode transition time in sec.',  
2/,'\$TIME=',\$,A)  
READ(LR,841)FMTIM  
IFMSTP=IFIX(FMTIM\*FREQ)  
GO TO 821

C  
816 CONTINUE  
WRITE(LW,836)7  
836 FORMAT(/1X,'Enter the new Stand Still time in secs.',  
1/,'\$TIME=',\$,A)  
READ(LR,841)SSTIM  
ISSSTP=IFIX(SSTIM\*FREQ)  
GO TO 821

C  
817 CONTINUE  
WRITE(LW,837)7



```
837  FORMAT(/1X,'Enter the new minimum storage of SPOS in secs',  
1/,'$TIME=',$,A)  
      READ(LR,841)STOTIM  
      ISTOSP=IFIX(STOTIM*FREQ)  
      GO TO 821
```

C

```
818  CONTINUE  
      WRITE(LW,838)7  
838  FORMAT(/1X,'Enter the new minimum time before restarting to  
1store, secs.'/, '$TIME=',$,A)  
      READ(LR,841)RNOSTM  
      INOSTP=IFIX(RNOSTM*FREQ)  
      GO TO 821
```

C

```
819  CONTINUE  
      WRITE(LW,839)7  
839  FORMAT(/1X,'Enter the minimum Cadence time in secs',  
1/,'$TIME=',$,A)  
      READ(LR,841)CADMIN  
      MAXSTP=IFIX(CADMIN*FREQ)  
      GO TO 821
```

C

```
820  CONTINUE  
      WRITE(LW,840)7  
840  FORMAT(/1X,'Enter the maximum Cadence time in secs',  
1/,'$TIME=',$,A)  
      READ(LR,841)CADMAX  
      MINSTP=IFIX(CADMAX*FREQ)  
      GO TO 821
```

C

```
822  CONTINUE  
      WRITE(LW,843)7  
843  FORMAT(/1X,'Enter the maximum signal allowed to servo amp.'/,1X,  
1'An integer value, 0 < MAXSIG < 2048',/, '$MAXSIG=',$,A)  
      READ(LR,842)MAXSIG  
842  FORMAT(I)  
      GO TO 821
```

C

C DEFAULT VALUES OF STANCE PHASE PARAMETERS

C

```
823  CONTINUE  
      STIFF=.01  
      ERRMAX=1./STIFF  
      TMLEAD=.0733  
      ILEAD=IFIX(TMLEAD*FREQ)  
      CNTRSH=10.  
      MINALC=IFIX((CNTRSH/(-CF(1)))*2047.)  
      ANGTOL=3.5  
      FMTIM=.260  
      IFMSTP=IFIX(FMTIM*FREQ)  
      SSTIM=1.5
```

```

ISSSTP=IFIX(SSTIM*FREQ)
STOTIM=.75
ISTOSP=IFIX(STOTIM*FREQ)
RNOSTM=.125
INOSTP=IFIX(RNOSTM*FREQ)
CADMIN=1.5
MAXSTP=IFIX(CADMIN*FREQ)
CADMAX=.93
MINSTP=IFIX(CADMAX*FREQ)
MAXSIG=500
GO TO 821

```

C  
850

CONTINUE

C  
C

```

C INITIALIZE DAMPING FACTORS AND TRANSITIONAL
C DAMPING ANGLES FOR SWING PHASE

```

C  
C  
C

17

```

CONTINUE
WRITE(LW,943)7

```

943

```

FORMAT(/,'$Do you want to change the current transition
1 damping angles? (Y/N)',A,$)
ACCEPT 111, IANS

```

111

```

FORMAT(A2)
IF(ICTRLC.NE.0)STOP 'VIA DOUBLE CONTROL/C'
IF(IANS.EQ.'Y')GO TO 15
GO TO 115

```

15

```

CONTINUE
TYPE *, 'WHICH OF THE TRANSITION ANGLES DO YOU WANT TO CHANGE?'
TYPE *, '      1....NO CHANGES'
TYPE *, '      2....INITIATE KNEE FLEX, CURRENT VALUE= '
1, AES, 'DEGREES'
TYPE *, '      3....INITIATE TOE CLEARANCE, CURRENT VALUE= '
1, ATC, 'DEGREES'
TYPE *, '      4....INITIATE HEEL RISE, CURRENT VALUE= '
1, AHR, 'DEGREES'
TYPE *, '      5....INITIATE FULL EXTENSION, CURRENT VALUE= '
1, AFE, 'DEGREES'
TYPE *, '      6....CHANGE ALL ANGLES TO DEFAULT THE VALUES'
ACCEPT *, ICHGE
GO TO (115,112,122,132,142,152) ICHGE

```

C

112

```

CONTINUE
TYPE *, 'ENTER THE NEW KNEE FLEX ANGLE IN DEG.' 'S'
ACCEPT *, AES
GO TO 30

```

122

```

CONTINUE
TYPE *, 'ENTER THE NEW TOE CLEARANCE ANGLE IN DEG.' 'S'
ACCEPT *, ATC

```

```
GO TO 30
132 CONTINUE
TYPE *, 'ENTER THE NEW HEEL RISE ANGLE IN DEG.' 'S'
ACCEPT *, AHR
GO TO 30
142 CONTINUE
TYPE *, 'ENTER THE NEW END OF SWING ANGLE IN DEG.' 'S'
ACCEPT *, AFE
GO TO 30
152 CONTINUE
AES=0.
ATC=35.
AHR=70.
AFE=15.
30 CONTINUE
TYPE *, 'DO YOU WANT TO MAKE ANY MORE CHANGES?(Y/N)'
ACCEPT 31, IANS
31 FORMAT(A2)
IF(IANS.EQ.'Y')GO TO 15
C
115 CONTINUE
C
WRITE(LW,944)7
944 FORMAT(/,'$Do you want to change the current damping
1 values? (Y/N)',A,$)
ACCEPT 113, IANS
113 FORMAT(A2)
IF(ICTRLC.NE.0)STOP 'VIA DOUBLE CONTROL/C'
IF(IANS.EQ.'Y')GO TO 200
GO TO 18
200 CONTINUE
TYPE 3000, BES, BMIN, BHR, BFE
3000 FORMAT(' WHICH DAMPING FACTORS DO YOU WANT TO CHANGE?',/,
1' 1....NO CHANGES',/,
1' 2....END OF STANCE, CURRENT VALUE=',1X,F10.7,/,
1' 3....TOE CLEARANCE AND MID SWING, CURRENT VALUE='
1,1X,F10.7,/,
1' 4....HEEL RISE, CURRENT VALUE=',1X,F10.7,/,
1' 5....END OF SWING, CURRENT VALUE=',1X,F10.7,/,
1' 6....CHANGE ALL DAMPING VALUES TO THE DEFAULT VALUES',
1/)
ACCEPT *, ICHGE
GO TO (18,5,6,7,8,9) ICHGE
5 CONTINUE
TYPE *, 'ENTER NEW END OF STANCE DAMPING COEFFICIENT'
ACCEPT *, BES
GO TO 16
6 CONTINUE
TYPE *, ' TYPE IN NEW MID SWING DAMPING COEFFICIENT'
ACCEPT *, BMIN
GO TO 16
```

```

7      CONTINUE
      TYPE *, 'ENTER NEW HEEL RISE DAMPING COEFFICIENT'
      ACCEPT *, BHR
      GO TO 16
8      CONTINUE
      TYPE *, 'ENTER NEW END OF SWING DAMING COEFFICIENT'
      ACCEPT *, BFE
      GO TO 16
9      CONTINUE
      BES=.000002
      BMIN=0.
      BHR=.0001
      BFE=.0003
16     CONTINUE
      TYPE *, 'DO YOU WANT TO MAKE ANY MORE CHANGES?(Y/N)'
      ACCEPT 4, IANS
4      FORMAT(A2)
      IF(IANS.EQ.'Y')GO TO 200
18     CONTINUE
C
      TYPE *, ' '
      TYPE *, 'CONTROL LOOPS ACTIVE!!!!.....'
      TYPE *, ' '
      TYPE *, 'READY TO TAKE FIRST SET OF DATA'
      TYPE *, 'REMEMBER: Front panel switches = "173000 for TRACK
      initiated sampling'
      WRITE(LW,477)7
477    FORMAT(/1X,'      ALC          SPOS          SVEL          SFSW          PPOS
      1      PVEL      PFSW          TORQ',A)
C      SET POS FEEDFORWARD PATH TO ZERO
C
      CALL DASCL(0,1.,IVAL)
      CALL DATWO(IVAL)
C
      PRESET=1.E6/FREQ
C
      CALL SETR(1,1,PRESET,ICMF1,INTCT,CONPL)
C
C      TURN ON THE SAMPLE SWITCH READY LED
C
      CALL BITCLR(8)
C
C
C      THE WAY TO EXIT THE TIMING LOOP
C
1      CONTINUE
      CALL READSW(NBIT)
      CALL READDI(IBIT)
C      IBIT<0 SAMPLE
C      IBIT=0 NO SAMPLING BUT CONTROL LOOPS ACTIVE
C      IBIT>0 CONTROL LOOPS DOWN

```

```
C NBIT>0 CONTROL LOOPS DOWN
C NBIT=-2554 ="173006 WHICH IS THE BOOT ADDRESS, THE MUTLI-METER WILL
C BE DISPLAYED. THIS MUST BE REMOVED BY
C CHANGING ANY FRONT PANEL SWITCH EXCEPT SWITCH #15
C LIMIT THE NUMBER OF FRAMES TO BE TAKEN
C
C     IF(NFRAME.GE.300)GO TO 913
C
C MAKE SURE IBIT IS STABLE
C
C     DO 688 IDELAY=1,100
C     ADELAY=ADELAY*1.
C688  CONTINUE
C
C     IF(NBIT)695,50,50
695  IF(IBIT)700,701,50
C
C SAMPLING
700  CONTINUE
C     IDATA=1
C     NEWDAT=1
C
C TURN OFF READY LED
C
C     CALL BITSET(8)
C     GO TO 1
C NO SAMPLING
913  CONTINUE
C     IDATA=0
C     WRITE(LW,937)
937  FORMAT(/1X,'MAXIMUM AMOUNT OF DATA HAS BEEN COLLECTED',
C     1/1X,'SAMPLING HAS BEEN TERMINATED!!!!')
701  CONTINUE
C
C IF TRACK SYSTEM IS NOT SAMPING OR IS FINISHED SAMPLING
C THEN IBIT WILL = 0
C
C     IDATA=0
C     NFRAME=0
C
C IF NOT SAMPLING AND IF NEW DATA IS AVAILABE TO BE PUT IN A FILE THEN
C
C     IF(NEWDAT.EQ.1)GO TO 704
C     IF(ICTRLC.NE.0)GO TO 78
C
C IF SYSTEM IS IN "173006 GET LARGE MULTIMETER DISPLAY
C
C     IF(NBIT.EQ."173006)GO TO 1
C     IF(NBIT.EQ."173007)GO TO 890
C     DO 978 I=2,8
C     CALL ADSCL(IBUF(I),TARRAY(I))
```

```
      ARRAY(I)=TARRAY(I)*CF(I)
978  CONTINUE
      ARRAY(1)=(FLOAT(IBUF(1))/2047.)*-CF(1)
      WRITE(LW,1000)TOP,ARRAY
      WRITE(LW,1000)BOT,ARRAY
1000  FORMAT(1X,3A1,1F4.0,1X,1F5.1,1X,1F4.0,1X,1F3.0,1X,1F5.1,
          11X,1F4.0,1X,1F3.0,1X,1F5.1)
      WRITE(LW,20)UP
20    FORMAT(1X,4A1)
      GO TO 1
890  CONTINUE
      WRITE(LW,1003)CADTIM,ANGNRM,SPOSMX,ACF,OFFSET,ERROR,IERROR,
          1PPOS,SPOS
1003  FORMAT(1X,' CADTIM  ANGNRM  SPOSMX      ACF  OFFSET
          1ERROR IERROR      PPOS      SPOS',
          2/1X,6(F8.3,1X),1I5,1X,2(F8.3,1X))
      WRITE(LW,20)UP
      GO TO 1
704  CONTINUE
C
C  RESET NEW DATA FLAG
C
      NEWDAT=0
C
C  INCREMENT RUN #
C
      NRUN=NRUN+1
C
C  GET FILE NAME
C
705  CONTINUE
C
C  ERASE SCREEN AND RETURN CURSOR TO HOME POSITION
C
      WRITE(LW,469)ERASE,HOME
469  FORMAT(1X,4A1,3A1)
C
C  CHECK FOR AUTO FILE NAMING
C
      IF(IAUTO.EQ.1)GO TO 622
      WRITE(LW,470)NRUN,NTOT,(NAMFIL(I),I=5,10),7
470  FORMAT(/1X,'THAT WAS RUN NUMBER ',I2,/1X,
          1I3,1X,'DATA POINTS WERE COLLECTED',/1X,
          2'The previous filename used was...',6A,//,
          2' Enter a 6 character FILENAME',/1X,'RK1:*****.RAW' /,
          3'$RK1:',$,A,$)
      READ(LR,501)(NAMFIL(I),I=5,10)
501  FORMAT(6A)
      GO TO 633
C
C  AUTO FILE NAMING
```

```
C
622 CONTINUE
    IF(NRUN.GE.10)GO TO 636
    CALL SCOPY('0',NAMFIL(9),14)
    ENCODE(1,634,NAMFIL(10))NRUN
634 FORMAT(I)
    GO TO 635
636 CONTINUE
    ENCODE(2,626,NAMFIL(9))NRUN
626 FORMAT(I2)
635 CONTINUE
    WRITE(LW,627)NRUN,NTOT,(NAMFIL(I),I=1,14),7
627 FORMAT(/1X,'THAT WAS RUN NUMBER ',I2,/1X,
    1I3,1X,'DATA POINTS WERE COLLECTED',//
    21X,'The autofile name is',3x,14A1,/
    3'$Do you wish to alter it? (Y/N)',2A1,$)
    READ(LR,628)IANS
628 FORMAT(A1)
    IF(IANS.NE.'Y')GO TO 633
    WRITE(LW,629)7
629 FORMAT(/1X,'Enter a 6 character file name',
    1/1X,'RK1:*****.RAW',/,'$RK1:',A,$)
    READ(LR,631)(NAMFIL(I),I=5,10)
631 FORMAT(6A1)
633 CONTINUE
C
C TEST FOR A VALID FILENAME--IT MUST BE SIX ALPHANUMERIC CHARC.
C
    IFFLAG=0
    DO 1150 I=5,10
    IF(NAMFIL(I).LT."60.OR.(NAMFIL(I)).GE."72.AND.NAMFIL(I).LE."100)
    1.OR.(NAMFIL(I)).GE."133.AND.NAMFIL(I).LE."140)
    2.OR.(NAMFIL(I)).GE."173))IFFLAG=1
1150 CONTINUE
C
C IF FILE NAME STARTS WITH AN E[XIT] STOP CLOCK AND RETURN TO BEGINNING
C
    IF(NAMFIL(5).EQ."105)GO TO 50
C
C SEE IF A DOUBLE CONTROL/C HAS BEEN ISSUED
C
    IF(ICTRLC.NE.0)GO TO 78
C
C CHECK FOR PROPER FILE NAME
C
    IF(IFFLAG.EQ.0)GO TO 83
    TYPE *,' '
    TYPE *,'INVALID FILE NAME--IT MUST BE SIX ALPHANUMERIC CHAR.'
    GO TO 705
C
83 CONTINUE
```

```
WRITE(LW,471)7
471  FORMAT(/1X,'***ENTER UP TO A 40 CHARACTER COMMENT***',A,$)
      READ(LR,502)COMENT
502  FORMAT(40A)
      IF(ICTRLC.NE.0)GO TO 78
C
C  SET MATRIX SIZE 7 ROWS FOR A/D DATA AND 300 DATA POINTS MAX
C
      NROW=10
      NCOL=300
C  NPTS = THE ACTUAL NUMBER OF DATA POINTS TAKEN
      NPTS=NTOT
      IF(NPTS.GT.300)NPTS=300
C  NPARAM = THE NUMBER OF PARAMETERS TO BE STORED IN FILE
C
      NPARAM=10
C
C  LAST TWO FILE SPECS
C  NIORR INDIATES THE DATA IS IN INTEGER FORM
C  NSTD TELLS OTHER PROGRAMS THAT THIS IS A STANDARD FILE
      NIORR=1
      NSTD=1
C
C  SET FILE SIZE
C
      NREC=NROW+5
C
C  NUMBER OF WORDS IN RECORD = NUMBER OF COLUMNS IN MATRIX
C  SINCE INTERGERS ARE BEING WRITTEN
C
      NWRD=NCOL
C
C  CREATE FILE--DIRECT ACCESS,UNFORMATTED
      CALL ASSIGN(1,NAMFIL,14,'NEW')
      DEFINE FILE 1(NREC,NCOL,U,IR)
C
C  WRITE INTO THE FIRST RECORD THE FILE SPECS
C
      WRITE(1'1)NREC,NWRD,NPTS,NROW,NCOL,NPARAM,NIORR,NSTD
C
C  WRITE DATA IN TO RECORDS 2-NROW+1
C
      DO 510 I=1,NROW
      WRITE(1'I+1')(IA(I,J),J=1,NCOL)
510  CONTINUE
C
C  WRITE PARAMETERS INTO NROW+2 RECORD
C
      RNTOT=FLOAT(NTOT)
      PARAM(1)=RNTOT
      PARAM(2)=FREQ
```



```
PARAM(3)=BES
PARAM(4)=BMIN
PARAM(5)=BHR
PARAM(6)=BFE
PARAM(7)=AES
PARAM(8)=ATC
PARAM(9)=AHR
PARAM(10)=AFE
WRITE(1'NROW+2')(PARAM(I),I=1,NPARAM)
C
C WRITE ROW NAMES INTO THE SECOND TO LAST RECORD
C
C WRITE(i'NROW+3)((NAM(J,I),J=1,10),I=1,NROW)
C
C WRITE PARAMETER NAMES INTO NROW+4
C
C WRITE(1'NROW+4)((PARNAM(J,I),J=1,10),I=1,NPARAM)
C
C WRITE THE COMMENTS INTO THE LAST RECORD
C
C WRITE(1'NREC)COMENT
C
C CALL CLOSE(1)
C
C REINITIALIZE DATA ARRAY
C
C DO 603 I=1,NROW
C DO 604 J=1,NCOL
C IA(I,J)=0
604 CONTINUE
603 CONTINUE
C
C NTOT=0
C
C WRITE(LW,473)
473 FORMAT(/IX,'READY TO TAKE NEW DATA',/)
TYPE *,'REMEMBER: Front panel switches = "173000 for TRACK
initiated sampling'
C
C TURN ON READY LED
C
C CALL BITCLR(8)
C WRITE(LW,477)7
C
C GO TO 1
C
C 50 CONTINUE
C
C IF THE PROGRAM HAS BEEN QUIT, IT PRINTS OUT IBUF,
C THEN THE CLOCK IS STOPPED AND RTS IS ALSO SHUT DOWN
C CALL BRAKE
```

```

C
C IF CLOCK IS STOPPED BY AN E AS FIRST LETTER IN NAMFIL
C PRESERVE NRUN
C

```

```

        IF(NAMFIL(5).EQ."105)NRUN=NRUN-1
        TYPE 60,IBUF
60      FORMAT(/1X,'IBUF=' ,/,8I5)
C

```

```

        TYPE *,' '
        TYPE *,'CONTROL LOOPS DOWN!!!!'
        TYPE *,' '
        GO TO 2

```

```

78      CONTINUE
        CALL BRAKE

```

```

        WRITE(LW,79)7
79      FORMAT(/1X,'USER INITIATED ABORT VIA DOUBLE CONTROL/C!!!!',
1//1X,'ALL SYSTEMS SHUT DOWN!!!!',A,/)
        STOP
        END

```

```

CCCCCCCCCCCCCCCCCCCCCCCCCCCCCCCCCCCCCCCCCCCCCCCCCCCCCCCCCCCC
CCCCCCCCCCCCCCCCCCCCCCCCCCCCCCCCCCCCCCCCCCCCCCCCCCCCCCCCCCCC
CCCCCCCCCCCCCCCCCCCCCCCCCCCCCCCCCCCCCCCCCCCCCCCCCCCCCCCCCCCC
CCCCCCCCCCCCCCCCCCCCCCCCCCCCCCCCCCCCCCCCCCCCCCCCCCCCCCCCCCCC

```

```

C
C THIS COMPLETION ROUTINE IS THE CONTROL LOOP
C
C

```

```

        SUBROUTINE CONPL

```

```

C
        COMMON IA(10,320),NFRAME,NTOT,IDATA,IBUF(8),INTCT,BES,
        1BMIN,BHR,BFE,AES,ATC,AHR,AFE,PPOSCF,PVELCF,SPOSCF,
        2ISTART,IFM,ILAG,IECHO,IFMSTP,MINALC,ISFSW,ISHFSW,ISTFSW,
        3ISFFSW,IPFSW,IPHFSW,IPTFSW,IPFFSW,ISSSTP,ISTND,INOST,
        4INOSTP,ILEAD,IOALC,MAXSTP,MINSTP,ANGTOL,ERRMAX,SSPOS(250),
        5ICNT,FREQ,ISTOSP,STIFF,ERROR,IERROR,CADTIM,ANGNRM,SPOSMX,
        6ACF,OFFSET,SPOS,PPOS,CF(10),ISTOR,MAXSIG

```

```

C
C THIS ALLOWS SET TO RETURN TO CONPL THE NEXT TIME THE CLOCK OVERFLOWS
C

```

```

        INTCT=1

```

```

C
C THIS IS FOR THE SQARE WAVE OUT ON DIGITAL OUTPUT 10
C

```

```

        CALL BITCNG(10,IDUMMY)

```

```

C
C GO SAMPLE CHANNELS 0-7 ONCE
C

```

```

        CALL LPS(IBUF,8,0,1,0)

```

```

C
C IF COLLECT DATA FLAG IS SET THEN PUT CONTENTS OF IBUF INTO MEMORY

```



C  
 C GO TO LAST FUNCTIONAL MODE IMPLEMENTED AND THEN CHECK TO SEE IF YOU  
 C SHOULD STAY THERE. NOTE: ON THE VERY FIRST TIME THE "LAST"  
 C FUNCTINAL MODE IS THE DEFAULTED VALUE OF IFM, WHICH IS 2 OR SWING  
 C PHASE.

C GO TO(100,200)IFM

C  
 C  
 C .....

C 100 CONTINUE

C  
 C  
 C CCC

C MODIFIED ACTIVE ECHO CONTROLLER FOR THE STANCE PHASE

C  
 C CCC

C  
 C  
 C FUNCTIONAL MODE ONE  
 C STANCE, LEVEL WALKING

C  
 C CCC

C CHECK FOR TRANSITIONS

C CCC

C IFMTIM MSECONDS AFTER LAST FUNCTIONAL MODE TRANSITION?  
 C DEFAULT IFMTIM=260 MSEC

C IF(ILAG.LT.IFMSTP)GO TO 150

C IF IN DOUBLE SUPPORT AND TORQUE IS FLEXIVE, GO TO SWING CONTROL  
 C TORQUE IS FLEXIVE MEANS THAT THE LOAD CELL IS BEING STRETCHED.  
 C THAT IS THE EXTERNAL LOADS ARE NO LONGER FORCING THE LEG INTO  
 C THE ENDSTOP. THE ENDSTOP OF COURSE IF THE LOAD CELL ITSELF.  
 C NOTE: THE LOAD CELL DOES NOT READ THE NET TORQUE ABOUT THE KNEE.

C  
 C IF (IBUF(1).GT.MINALC ! IF (PROSTHESIS IS ON GROUND  
 C 1.AND.IBUF(4).LT.ISFSW ! AND SOUND FOOT IS ON GROUND  
 C 2.AND.IBUF(8).LT.2048) ! AND ACT. TORQUE IS FLEXIVE)  
 C 1 GO TO 225 ! GO TO SWING CONTROL

C IF AXIAL LOAD CELL IS BELOW MIN AND SOUND FOOTSWITCH IS HIGH,  
 C GO TO SWING CONTROL

C IF (IBUF(1).LT.MINALC ! IF (POSTHESIS IF OFF GROUND

```

1.AND.IBUF(4).LT.ISFSW)           ! AND SOUND FOOT IS ON GROUND)
2GO TO 225                         ! GO TO SWING CONTROL
CCCCCCCCCCCCCCCCCCCCCCCCCCCCCCCCCCCCCCCCCCCCCCCCCCCCCCCCCCCC
C FOR SELF TESTING PURPOSES
C IF(IBUF(7).GT.IPSW.AND.IBUF(4).LT.ISFSW)GO TO 225
CCCCCCCCCCCCCCCCCCCCCCCCCCCCCCCCCCCCCCCCCCCCCCCCCCCCCCCCCCCC
C
C STILL IN SAME FUNCTIONAL MODE
C
GO TO 150
C
C
C END OF TRANSITION CHECKS
C
CCCCCCCCCCCCCCCCCCCCCCCCCCCCCCCCCCCCCCCCCCCCCCCCCCCCCCCCCCCC
C
C FIRST SAMPLE IN STANCE PHASE AFTER SWING PHASE
C AS A FUNCTION MODE CHANGE FROM SWING TO STANCE OCCURS FOR THE
C FIRST TIME IN LEVEL WALKING, THE TRANSITION DELAY COUNTER IS
C INITIALIZED.
CCCCCCCCCCCCCCCCCCCCCCCCCCCCCCCCCCCCCCCCCCCCCCCCCCCCCCCCCCCC
125 ILAG=0
C
C SET THE FIRST TWO LIGHT ON THE DIGITAL OUTPUT PANEL TO INDICATE
C IN STANCE PHASE
C
CALL BITSET(0)
CALL BITSET(1)
C
C STORE CADENCE TIMER
NSAMPS=ICNT
C
C INITIALIZE CADENCE TIMER
ICNT=0
C
C INITIALIZE THE RECALL COUNTER
IRECL=1
C
C OPEN THE TORQUE FEEDBACK LOOP BY SETTING DIGITAL OUTPUT #9
CALL BITSET(9)
C
C SET FEEDFORWARD PATH GAIN TO +1 VOLT
C
CALL DAONE(2458)
C
C
C SET CADENCE WINDOW
C NOTE: THESE CADENCE # CORRESPOND TO THE # OF SAMPLE PERIODS
C THAT HAVE PASSED SINCE IN ONE COMPLETE WALKING CYCLE. (I.E.
C ICNT GETS RESET EVERY FIRST TIME BACK INTO THE PROSTHETIC STANCE
C PHASE) PROSTHETIC HEEL CONTACT TO PROSTHETIC HEEL CONTACT

```

```
C  DEFAULT CADence MINimum = 1.5 seconds [CADMIN*FREQ=MAXSTP]
C      CADence MAXimum = .933 seconds [CADMAX*FREQ=MINSTP]
C      IF(NSAMPS.GT.MAXSTP)NSAMPS=MAXSTP
C      IF(NSAMPS.LT.MINSTP)NSAMPS=MINSTP
C
C  CADENCE TIME IN SECONDS
C
C      CADTIM=FLOAT(NSAMPS)/FREQ
C
C  DETERMINE FROM CHART ON PAGE 60 GRIMES Ph.D. THESIS
C  THAT THE MAX ANGLE IN STANCE OF NORMALS AS A FUNCTION OF CADENCE
C  IS =(45. DEG/SEC)/CADANCE TIME +(-22.5 DEG)
C  WHERE TIME DEFINE AS CADENCE. THE TIME TO
C  COMPLETE A WALKING CYCLE (HEEL CONTACT TO SAME HEEL CONTACT)
C
C
C  NORMALS MAX STANCE KNEE ANGLE IN DEGREES
C
C      ANGNRM=(45./CADTIM)-22.5
C
C  ANGLE CORRECTION FACTOR
C  NORMALIZES SOUND POSITION TRAJECTORY TO HAVE THE SAME MAX KNEE ANGLE
C  FOR A NORMAL
C
C      DIFF=SPOSMX-SSPOS(1)
C      IF(DIFF.LT.1.)DIFF=1
C      ACF=ANGNRM/DIFF
C
C  AS A SAFTEY (IN GENERAL ACF < 1.)
C
C      IF(ACF.GT.2.)ACF=2.
C
C  MATCH THE INITIAL CONDITION ON SOUND POS TO PROS. POS
C  I.E. PPOS[CURRENT VALUE]=SSPOS(1)*ACF + OFFSET
C
C      OFFSET=PPOS-SSPOS(1)*ACF
C
C      GO TO 160
CCCCCCCCCCCCCCCCCCCCCCCCCCCCCCCCCCCCCCCCCCCCCCCCCCCCCCCCCCCC
C  SUBSEQUENT CALLS TO STANCE FUNCTIONAL MODE PROCESS BELOW ONLY
C
CCCCCCCCCCCCCCCCCCCCCCCCCCCCCCCCCCCCCCCCCCCCCCCCCCCCCCCCCCCC
150  CONTINUE
C
C  REJECT LARGE TRANSIENTS
C
C      CHECK=ABS(SSPOS(IRECL+ILEAD)-SSPOS(IRECL+ILEAD-1))
C      IF(CHECK*ACF.GT.ANGTOL)SSPOS(IRECL+ILEAD)=SSPOS(IRECL+ILEAD-1)
C
160  CONTINUE
```

```
C
C THE DESIRED SOUND POSITION TO FOLLOW IS ...REFPOS
C REFPOS=RECORDED SPOS * CORRECTED MAGNITUDE (NORMALIZED TO NORMALS) +
C OFFSET DUE TO PPOS AND SPOS NOT HAVING THE SAME REFERENCE VALUE.
C PPOS VALUE IS ASSUMED CORRECT
C
      REFPOS=SSPOS(IRECL+ILEAD)*ACF+OFFSET
C
C DETERMINE ERROR SIGNAL
C WHERE ERROR=SOUND POSITION REFERENCE - PROS POS FEEDBACK
C
      ERROR=STIFF*(REFPOS-PPOS)
C
C
C STAND STILL CONDITIONS?
C DEFAULT=1 SECOND
      IF(ILAG.GE.ISSSTP)ISTND=1
C
C D/A OUTPUTS
C POSITION COMMAND SIGNAL
      CALL IDOR(1,"170422",-1,IACT)
C
C ERRMAX = MAXIMUM EXPECTED VALUE OF THE VARIABLE ERROR
C NOTE THE LARGER ERRMAX THE SLOWER THE RESPONSE OF THE
C MANIPULATOR
C
      CALL DASCL(ERROR,1.,IERROR)
C
C IF SO THEN LEG WILL SLOWLY EXTEND TO FULL EXTENSION
C
      IF(ISTND.EQ.1)IERROR=2036
C
C PROVIDE A CEILING ON THE CONTROL SIGNAL
C
      IF(IERROR.LT.2047-MAXSIG)GO TO 185
      GO TO 186
185  CONTINUE
      IERROR=2047-MAXSIG
C
C TURN ON DO# 7
C
      CALL BITSET(7)
      GO TO 189
186  IF(IERROR.GT.2047+MAXSIG)GO TO 187
      GO TO 188
187  CONTINUE
      IERROR=2048+MAXSIG
      CALL BITSET(7)
      GO TO 189
188  CONTINUE
      CALL BITCLR(7)
```





```
C STILL IN THE SAME FUNCTIONAL MODE
C
C GO TO 250
C
C FIRST TIME IN SWING
C INITIALIZE TRANSITION DELAY COUNTER
C
225 ILAG=0
C
C FIRST TIME IN SWING
C CLOSE THE TORQUE FEEDBACK LOOP BY CLEARING DIGITAL OUTPUT #9
C
C CALL BITCLR(9)
C
C SET FEEDFORWARD PATH IN POSITION = 0 VOLTS
C
C CALL DATWO(2048)
C
CCCCCCCCCCCCCCCCCCCCCCCCCCCCCCCCCCCCCCCCCCCCCCCCCCCCCCCCCCCC
C
CCCCCCCCCCCCCCCCCCCCCCCCCCCCCCCCCCCCCCCCCCCCCCCCCCCCCCCCCCCC
C
250 CONTINUE
C
C
C SWING PHASE CONTROLLER
C
C CHECK FOR THE SIGN OF THE VELOCITY
C POSTIVE=FLEXIVE
C NEGATIVE=EXTENSIVE
C
C ASSUME A FLEXIVE VELOCITY STATE ONLY WHEN FLEXION PVEL >.023
C .023 COMES FROM D.G. (EQUALED 2000 IN OFFSET BINARY WITH SIGN
C CHANGE)
C THIS INSURES THAT DURING STANCE WHEN PVEL IS APPROX. ZERO, THAT
C END OF SWING DAMPING WILL STAY IN EFFECT. THUS THE FIRST 35
C DEGREES OF FLEXION DURING STANCE IS CONTROLLED WITH BFE.
C
C IF(IBUF(6).GT.2060)GO TO 20
C IF(PVEL.GT..023*PVELCF)GO TO 20
C IF(PVEL.GT.-.001)GO TO 20
C
C SWING THROUGH DAMPING
C
C IF(PPOS.GT.AFE)GO TO 400
C GO TO 401
400 CONTINUE
C B=BMIN
C CALL SETDO(3)
401 CONTINUE
C
```

```
C END OF SWING DAMPING
C
      IF(PPOS.LE.AFE)GO TO 402
      GO TO 403
402  CONTINUE
      B=BFE*(AFE-PPOS)+BMIN
      CALL SETDO(4)
403  CONTINUE
      GO TO 25
C
20  CONTINUE
C
C END OF STANCE DAMPING
C
      IF(PPOS.GE.AES.AND.PPOS.LT.ATC)GO TO 301
      GO TO 300
301  CONTINUE
      B=BES*(ATC-PPOS)+BMIN
      CALL SETDO(0)
300  CONTINUE
C
C TOE CLEARANCE DAMPING
C
      IF(PPOS.GE.ATC.AND.PPOS.LT.AHR)GO TO 302
      GO TO 303
302  CONTINUE
      B=BMIN
      CALL SETDO(1)
303  CONTINUE
C
C HEEL RISE DAMPING
C
      IF(PPOS.GE.AHR)GO TO 304
      GO TO 305
304  CONTINUE
      B=BHR*(PPOS-AHR)+BMIN
      CALL SETDO(2)
305  CONTINUE
C
25  CONTINUE
C
      D=409.6/(1.+B*ABS(FLOAT(IBUF(6))-2048)))
      IDAMP=2048-IFIX(D)
C
C PUT OUT DAMPING SIGNAL OF DA 1
C
      CALL DAONE(IDAMP)
C
C IF IN CONVENTION CONTROL THEN RETURN
C
      IF(IECHO.EQ.0)RETURN
```



CC

C  
C IF(IBUF(4).LT.ISFSW)GO TO 710 ! IF( SOUND FOOT CONTACT OCCURS)  
C ! THEN START STORING SOUND POS

C  
C ONCE STORAGE HAS BEGUN STORE FOR AT LEAST .75 SECONDS  
C IF STORAGE BEGINS, STORE FOR AT LEAST 750 MS THIS INSURE THAT EVEN  
C IF THE ABOVE TWO CRITERIA ARE NOT MET THEN THE STORAGE WILL CONTINUE  
C ONCE STARTED UNTIL .75 SECONDS THIS IS BECAUSE IF KNEE FLEXES RIGHT  
C BEFORE SOUND HEEL CONTACT ONE WANTS TO START STORING. IF IT STARTS  
C TO EXTEND AGAIN STILL BEFORE SOUND HEEL CONTACT THEN DESPITE BOTH  
C OF THE ABOVE IF. STATMENTS BEING FALSE STORING WILL CONTINUE BECAUSE  
C OF TIMER. (FOR AT LEAST .75 SECONDS)

C  
C IF(ISTOR.GT.1.AND.ISTOR.LT.ISTOSP)GO TO 710

C  
C THE STORGE WILL NOT START AGAIN UNTIL INOST IS INCREMENTED TO INOSTP  
C STEPS  
C OR RNOSTM SECONDS DEFAULT=125MSEC  
C THIS IS TO KEEP STORAGE FROM STARTING DURING THE HEEL RISE PORTION OF  
C SOUND SWING WHEN CRITERIA #1 FOR STORING SOUND POSITION WOULD BE MET

C  
C 705 IF(ISTOR.NE.1)INOST=0  
C INOST=INOST+1

C INITIALIZE THE STORAGE COUNTER  
C ISTORE=1

C  
C IF NOT STORING CLR DIGITAL OUPUT LIGHT 6  
C AND SET SOUND LEG POSITION STORING INDICATOR TO 0

C  
C ISSPOS=0  
C CALL BITCLR(6)  
C GO TO 720

C  
C INITIALIZE THE MAXIMUM STANCE PHASE FLEXION STORED  
C VALUE WHEN STORAGE BEGINS

C  
C 710 IF(ISTOR.EQ.1)GO TO 711  
C GO TO 712

C  
C 711 CONTINUE  
C SPOSMX=SPOS

C  
C LIGHT DIGITAL OUTPUT LIGHT 6 TO INDICATE STORING SOUND LEG PROFILE  
C ALSO SET SOUND LEG STORING INDICATOR TO 2

C  
C ISSPOS=2  
C CALL BITSET(6)

C  
C 712 CONTINUE

C  
C STORE SOUND POSITION

```
C
      SSPOS(ISTOR)=SPOS
C
C LOOK FOR IMAX ONLY IN FIRST PART OF POSITION (I.E. WANT THE PEAK
C ANLGE OF THE SOUND KNEE AS IT FLEXES DURING MID STANCE NOT THE
C LARGE KNEE ANGLE THAT RESULTS AS SWING IS INITIATED.
C THEREFORE LOOK FOR IMAX UP UNTIL
C THE PROSTHESIS CONTACTS THE FLOOR AS MEASURED BY THE AXIAL LOAD CELL
C THIS HAPPENS BEFORE THE SOUND KNEE BEGINS TO FLEX AGAIN INITIATING
C SWING.
C
C
      IF(IBUF(1).GT.MINALC)GO TO 715
CCCCCCCCCCCCCCCCCCCCCCCCCCCCCCCCCCCCCCCC
C SELFTESTING
C      IF(IBUF(7).LT.IPFSW)GO TO 715
CCCCCCCCCCCCCCCCCCCCCCCCCCCCCCCCCCCCCCCC
      IF(SPOS.GT.SPOSMX)SPOSMX=SPOS
C
C IF AT THE END OF SSPOS, STAY PUT DO NOT INCREMENT STORAGE COUNTER
C
715 IF(ISTOR.EQ.250)GO TO 720
C INCREMENT THE STORAGE COUNTER
      ISTOP=ISTOP+1
C
720 CONTINUE
C
C INCREMENT THE FUNCTIONAL MODE TRANSITION DELAY COUNTER
C
      IF(ILAG.LT.3000)ILAG=ILAG+1
C
C STORE THE OLD PROSTHETIC FOOTSWITCH VALUE
C
      IOPFS=IBUF(7)
C
C RESET FOOTSWITCH TIMER IF THE SOUND FOOTSWITCH VALUE IS DIFFERENT
C THAN THE OLD VALUE (I.E. A SWITCH HAS OPENED OR CLOSED)
C THIS ALLOWS THE PROGRAM TO KNOW HOW LONG IT HAS BEEN SINCE A SOUND
C FOOTSWITCH CHANGED HAS OCCURRED.
C
      IF(IABS(IBUF(4)-IOSFS).GT.300)ISLAG=0
      ISLAG=ISLAG+1
C
C STORE THE OLD SOUND FOOTSWITCH VALUE
C
      IOSFS=IBUF(4)
C
      IOALC=IBUF(1)
C
      RETURN
      END
```